CARDIOLOGY JOURNAL

Impact Factor: 1.743

May 2020, Vol. 27, No. 3, pp. 225–328 www.cardiologyjournal.org

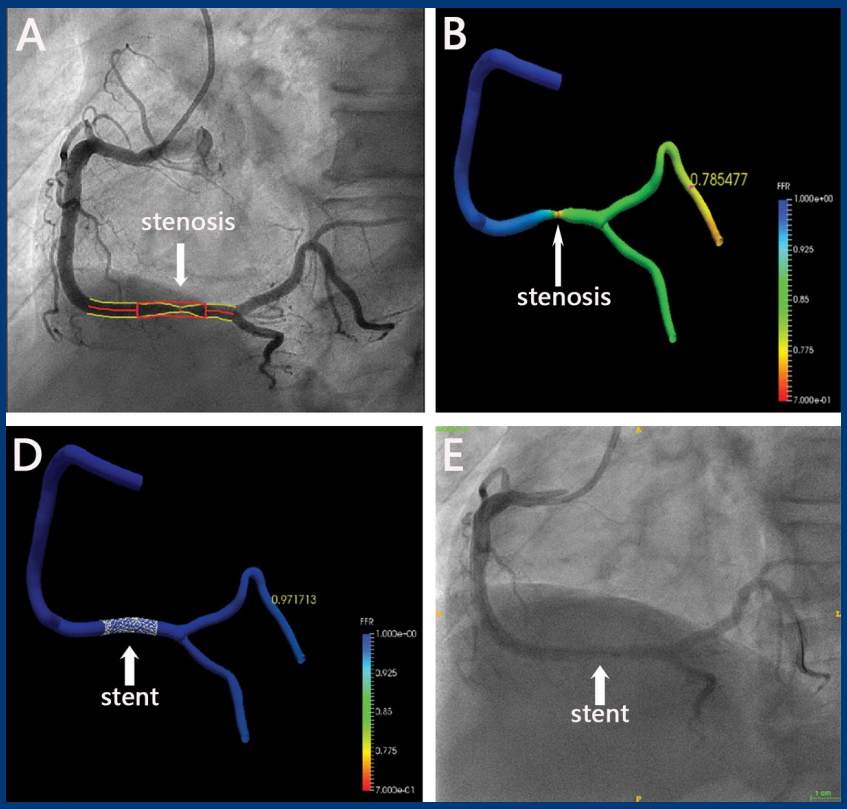

Fang-Yang Huang et al., see figure legend on page 319

ISSN 1897–5593

VIA MEDICA

CARDIOLOGY JOURNAL

www.cardiologyjournal.org

CARDIOLOGY JOURNAL

www.cardiologyjournal.org

"Cardiology Journal", a bimonthly publication, is an official journal of the Working Groups on Cardiac Rehabilitation and Exercise Physiology, Congenital and Valvular Heart Disease, Echocardiography, Experimental Cardiology, Heart Diseases in Women, Heart Failure, Heart Rhythm, Invasive Cardiology, Noninvasive Electrocardiology and Telemedicine, Pediatric Cardiology and Resuscitation and Intensive Care of the Polish Cardiac Society.

This journal is edited under the auspices of the International Society of Holter and Noninvasive Electrocardiology.

Cardiology Journal (ISSN 1897-5593) is published 6 times a year by VM Media sp. z o.o. VM Group sp.k.

Subscription rates: Paper subscription, 6 issues incl. package and postage institutional — 270 euro. The above prices are inclusive of regular postage costs. Payment should be made to: VM Media sp. z o.o. VM Group sp.k., Grupa Via Medica, Bank BGŻ Paribas SA account number: 15 1600 1303 0004 1007 1035 9021; SWIFT: PPABPLPK. Single issues, subsriptions orders and requests for sample copies should be send to e-mail: prenumerata@viamedica.pl. Electronic orders option available at: https://journals.viamedica.pl/cardiology_journal.

Editorial Address: VM Media sp. z o.o. VM Group sp.k., ul. Swietokrzyska 73, 80–180 Gdansk, tel: (+48 58) 320 94 94, fax: (+48 58) 320 94 60, www.cardiologyjournal.org, e-mail: cj@viamedica.pl

Journal has an international indexation in CrossRef, EBSCO, EMBASE, FMJ, Google Scholar, Science Citation Index Expanded, Index Copernicus (155.56 points), MEDLINE, Scopus, SJR, Ulrich's Periodicals Directory, Web of Science CC and WorldCat database, Ministry of Science and Higher Education score (40 points). Current Impact Factor of "Cardiology Journal" (2018) is 1.743.

Advertising: For details on media opportunities within this journal please contact the advertising sales department ul. Swietokrzyska 73, 80–180 Gdansk, tel: (+48 58) 320 94 94, e-mail: viamedica@viamedica.pl
The Editors take no responsibility for the published advertisements.

CARDIOLOGY JOURNAL

www.cardiologyjournal.org

May 2020, Vol. 27, No. 3

Table of Contents

VIA MEDICA

EDITORIAL COMMENTS

Cardiology Journal
2020, Vol. 27, No. 3, 225–229
DOI: 10.5603/CJ.2020.0080

ISSN 1897–5593

Combining anatomy and physiology: New angiography-based and computed tomography coronary angiography-derived fractional flow reserve indices

Mariusz Tomaniak[1], Patrick W. Serruys[2, 3]

[1]First Department of Cardiology, Medical University of Warsaw, Poland
[2]National Heart and Lung Institute, Imperial College London, United Kingdom
[3]Department of Cardiology, National University of Ireland, Galway, Ireland

The first reports on deriving pressure loss from anatomy by simulating coronary flow date back 40 years [1]. The pursuit of anatomy-based coronary physiology assessment and its clinical translation has since been accelerated by Paul Morris et al. (2013) and Shengxian Tu et al. (2014) who computed fractional flow reserve (FFR) by applying computational fluid dynamics (CFD) simulation to three-dimensional (3D) coronary artery geometries extracted from two angiographic projections [2–4], and by Michail Papafaklis et al. (2014) who developed the virtual functional assessment index (vFAI) to predict flow-limiting coronary stenosis [5].

Avoidance of a pressure wire or microcatheter insertion into the coronary tree, lowers cost, procedural time and patient discomfort — in cases where a hyperemic agent is used — well justify the development of new software for wire-free 3D quantitative coronary angiography (QCA)-based FFR estimation, and the efforts being made to bring such modalities into clinical practice. At present, three validated vendor specific technologies have the promise to substantially improve the clinical adoption of physiological coronary lesion assessment in the routine practice of catheterization laboratory: quantitative flow ratio (QFR, Angio XA 3D software, Medis Medical Imaging System bv, the Netherlands and AngioPlus, Pulse Medical Imaging Technology, Shanghai, China), vessel fractional flow reserve (vFFR, CAAS Workstation, Pie Medical Imaging, Maastricht, the Netherlands), and FFR_{angio} (FFR_{angio} system, CathWorks, Ltd, Kfar-Saba, Israel) [6–9]. Attempts of predicting pulsatile vascular physiology on the basis of steady flow assumptions in CFD analyses have resulted in the development of mathematical methods to accelerate computation of angiography-based FFR estimation [10]. Concurrently, computed tomography coronary angiography (CTCA)-based FFR (FFR_{CT}) has also shown high correlation with pressure wire-based FFR and a high accuracy in detecting ischemia causing lesions [11], avoiding both coronary instrumentation and invasive angiography (Fig. 1).

3D-QCA-derived FFR

QFR, vFFR and FFR_{angio} demonstrated a significantly higher diagnostic accuracy, compared with traditional two-dimensional- or 3D-QCA [7–9]. While the requirement of minimum two angio-

Address for correspondence: Prof. Patrick W. Serruys, MD, PhD, P.O. Box 2125, 3000 CC Rotterdam, the Netherlands, tel: +31-10-4635260, fax: +31-10-4369154, e-mail: patrick.w.j.c.serruys@gmail.com

Received: 20.12.2019 Accepted: 16.05.2020

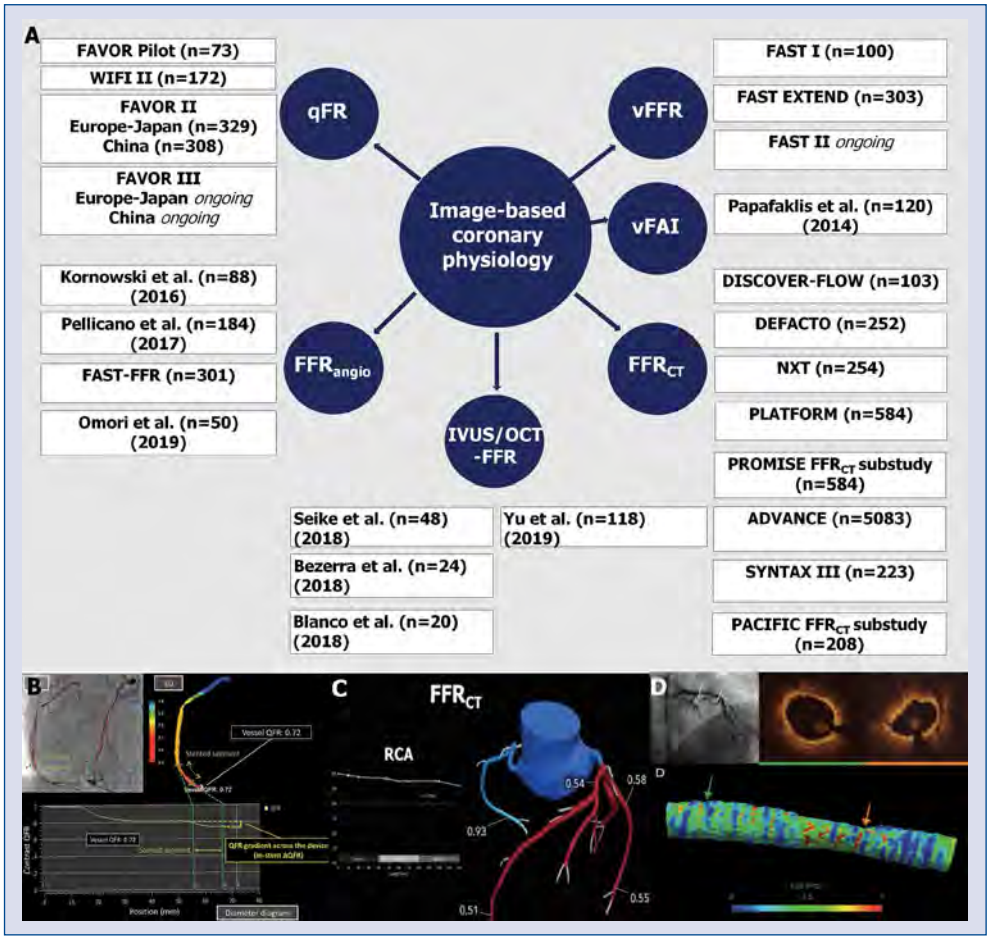

Figure 1. Imaging-based coronary physiology assessment; **A.** Graphic summary of imaging-based modalities for functional evaluation of coronary stenosis; **B, C.** Examples of quantitative coronary angiography- and computed coronary tomography angiography-based fractional flow reserve estimation; **D.** Computational fluid dynamics for wall shear stress computation; qFR — quantitative flow ratio; vFFR — vessel fractional flow reserve; FFR_{angio} — fractional flow reserve derived from angiography; vFAI — virtual functional assessment index; FFR — fractional flow reserve; IVUS — intravascular ultrasound; OCT — optical coherence tomography; RCA — right coronary artery. Adapted with permissions from: Asano T et al. EuroIntervention. 2018; 14: 570–579; Modolo R et al. Ann Cardiothorac Surg. 2018; 7: 470–482; Thondapu V et al. Eur Heart J. 2018; 7: 1602–1609.

graphic projections with views of at least 25° apart, brisk contrast injection and possibly minimized vessel overlap resulted in non-negligible exclusion rates in retrospectively analyzed cohorts to date [8, 12, 13], the feasibility of angiography-based FFR computation was relatively high in prospectively enrolled cohorts with optimized protocols for angiography acquisition [7, 8, 14]. Of note, none of the three technologies has demonstrated the safety or non-inferiority of angio-based FFR versus the pressure-wire based FFR/iFR with regard to impact on clinical endpoints to date. However, large prospective studies are ongoing with specific focus on clinical follow-up and prespecified angiography acquisition protocols: FAVOR III China (ClinicalTrial.gov: NCT03656848) and FAVOR III Europe-Japan (ClinicalTrials.gov: NCT03729739) will reveal whether QFR-guided revascularization may improve outcomes of patients undergoing percutaneous coronary intervention (PCI), as compared to subjects treated, respectively, based solely on angiography or angiography and pressure-wire based FFR (Fig. 1).

PCI optimization: IVUS-FFR, OCT-FFR and post-PCI 3D-QCA-FFR

Another promising multimodality approach to imaging of the coronary artery is derived from 3D artery models of angiography and grey-scale

intravascular ultrasound (IVUS) — a concept initially proposed in 2000 by Slager et al. [15], and more recently pursued by the groups of Seike and Bezerra, amongst others, who reported a correlation between IVUS-derived FFR and pressure-wire based FFR, with an area under the curve reaching 0.93. In addition, optical coherent tomography (OCT) can be utilized for FFR estimation (OCT-derived FFR [OFR]), with a high diagnostic accuracy, as compared with conventional FFR values [16, 17]. In a recent study by Huang et al. [17] in unselected patients with coronary syndrome, OFR was found superior to QFR in determining physiological significance of coronary stenosis and its diagnostic performance was not influenced by the presence of prior myocardial infarction or implanted stents. Both IVUS- and OCT-based FFR indices could serve as an additional means of final PCI result optimization, in particular when the procedure is already being guided with either of two imaging modalities. One of the major hurdles in reliable IVUS-FFR estimation related to stenosis length — subject to considerable inter-observer variability as reported in some prior studies — has been recently addressed by Kashiyama et al., who showed that stenosis length determined based on the area stenosis, rather than plaque burden, provides higher diagnostic accuracy of IVUS-FFR for physiologic ischemia detection (presented at the American Heart Association 2019 Conference, Philadelphia, US). However, clinical efficacy of intravascular imaging-based indices still remains to be confirmed in larger studies powered to evaluate clinical outcomes.

Interestingly, 3D-QCA-based functional indices computed using the angiograms acquired directly post PCI proved useful for stratification of risk after a successful procedure [18], including patients treated for de novo 3-vessel disease [19]; risk of vessel-oriented composite endpoint (vessel-related cardiac death, vessel-related myocardial infarction, and target vessel revascularization) was found to be 3-fold higher when post-PCI QFR was ≤ 0.89 [18] or ≤ 0.90 [19]. Consistent observations were also reported at the Transcatheter Cardiovascular Therapeutics 2019 (TCT 2019) for post PCI vFFR, with vessels presenting post-PCI vFFR values > 0.9 having lower risk of target vessel revascularization at 1 year, post procedure, as compared to vessels with post PCI vFFR ≤ 0.9 (1.8% vs. 4.2%, $p < 0.05$) (Masdjedi et al. presented at TCT 2019).

CTCA-based FFR (FFR_{CT})

Assessment of functional lesion severity based on CFD extends the CTCA capacities for lumen obstruction and plaque characteristics evaluation [11, 20, 21]. Recently, FFR_{CT} has demonstrated similar ability to predict invasive FFR values as classic single photon emission computed tomography, being, however, inferior to cardiac positron emission tomography (Fig. 1) [22]. It has also proved safe with deferring lesions with FFR_{CT} values above 0.8, and could efficiently guide revascularization strategy with coronary artery bypass grafting or PCI, as was shown in the prospective SYNTAX III Revolution trial [20, 23]. While the role of FFR_{CT} in patient screening, detailed assessment of coronary lesion complexity and procedural planning is increasingly recognized, relatively long computation times, costs and a need for telemedicine have to be considered. Although in the United Kingdom the HeartFlow FFR_{CT} analysis has been selected for reimbursement as part of the Innovation and Technology Payment (ITP) program, lack of reimbursement in majority of the countries nowadays represents non-negligible obstacle in rendering this technology more widely and clinically adoptable.

Future directions

In the recent ISCHEMIA (International Study of Comparative Health Effectiveness With Medical and Invasive Approaches) trial — presented by Judith S. Hochman at the American Heart Association Annual Scientific Sessions (AHA 2019) — routine invasive therapy failed to reduce major adverse ischemic events over a median of 3.3 years, compared with optimal medical therapy among chronic coronary syndrome patients with moderate to severe ischemia on noninvasive stress testing. There was also no benefit from invasive therapy regarding all-cause mortality or cardiovascular mortality/myocardial infarction. As such, additional diagnostic measures including more 'subtle' parameters such as frictional force exerted on the vessel wall by circulating blood, namely wall shear stress (WSS) — that currently can also be estimated *in vivo* based on either cine-angiography or CTCA scans — may prove efficient in improving risk stratification in the near future. It is conceivable that imaging modalities enriched with WSS information could facilitate appropriate identification of patients with signs of ischemia by traditional non-invasive

tests, in whom interventional treatment could prevent hard clinical endpoints beyond relieving the angina symptoms. Indeed, the CFD sub analysis of the FAME II (Fractional Flow Reserve Versus Angiography for Multivessel Evaluation II) trial showed, that among patients with chronic coronary syndromes and hemodynamically significant lesions, higher WSS in the proximal segments of atherosclerotic lesions was predictive of myocardial infarction and had incremental prognostic value over FFR [24]. Recent standardization of WSS metrics and computation protocols [25] paves the way for further enhancing the current state-of-the-art of functional lesion assessment, potentially optimizing treatment decisions and improving the results of physiology-based coronary revascularizations in the 'post ICHEMIA trial' era. Finally, it has to be noted that both angio- and CTCA-derived FFR indices are restricted to epicardial arteries and imply a maximal relaxation of the vascular tone. Therefore, in future, comprehensive multimodality diagnostics combining anatomic and physiologic approaches will also need to better account for the vasomotion and coronary microvasculature assessment.

Conflict of interest: Mariusz Tomaniak acknowledges funding received as the Laureatte of the European Society of Cardiology Research and Training Program in the form of the 2018 ESC Grant. Patrick W. Serruys reported personal fees from Abbott, Biosensors, Medtronic, Micell, Sinomed, Philips/ /Volcano, Xeltis and HeartFlow, outside the submitted work.

References

1. Brown BG, Bolson E, Frimer M, et al. Quantitative coronary arteriography: estimation of dimensions, hemodynamic resistance, and atheroma mass of coronary artery lesions using the arteriogram and digital computation. Circulation. 1977; 55(2): 329–337, doi: 10.1161/01.cir.55.2.329, indexed in Pubmed: 832350.
2. Serruys PW, Girasis C, Papadopoulou SL, et al. Non-invasive fractional flow reserve: scientific basis, methods and perspectives. EuroIntervention. 2012; 8(4): 511–519, doi: 10.4244/EIJV8I4A79, indexed in Pubmed: 22581414.
3. Tu S, Barbato E, Köszegi Z, et al. Fractional flow reserve calculation from 3-dimensional quantitative coronary angiography and TIMI frame count: a fast computer model to quantify the functional significance of moderately obstructed coronary arteries. JACC Cardiovasc Interv. 2014; 7(7): 768–777, doi: 10.1016/j.jcin.2014.03.004, indexed in Pubmed: 25060020.
4. Morris PD, Ryan D, Morton AC, et al. Virtual fractional flow reserve from coronary angiography: modeling the significance of coronary lesions: results from the VIRTU-1 (VIRTUal Fractional Flow Reserve From Coronary Angiography) study. JACC Cardiovasc Interv. 2013; 6(2): 149–157, doi: 10.1016/j.jcin.2012.08.024, indexed in Pubmed: 23428006.
5. Papafaklis MI, Muramatsu T, Ishibashi Y, et al. Fast virtual functional assessment of intermediate coronary lesions using routine angiographic data and blood flow simulation in humans: comparison with pressure wire - fractional flow reserve. EuroIntervention. 2014; 10(5): 574–583, doi: 10.4244/EIJY14M07_01, indexed in Pubmed: 24988003.
6. Collet C, Onuma Y, Sonck J, et al. Diagnostic performance of angiography-derived fractional flow reserve: a systematic review and Bayesian meta-analysis. Eur Heart J. 2018; 39(35): 3314–3321, doi: 10.1093/eurheartj/ehy445, indexed in Pubmed: 30137305.
7. Westra J, Andersen BK, Campo G, et al. Diagnostic performance of in-procedure angiography-derived quantitative flow reserve compared to pressure-derived fractional flow reserve: the FAVOR II Europe-Japan study. J Am Heart Assoc. 2018; 7(14), doi: 10.1161/JAHA.118.009603, indexed in Pubmed: 29980523.
8. Masdjedi K, van Zandvoort LJC, Balbi MM, et al. Validation of 3-Dimensional Quantitative Coronary Angiography based software to calculate Fractional Flow Reserve: Fast Assessment of STenosis severity (FAST)-study. EuroIntervention. 2019, doi: 10.4244/EIJ-D-19-00466, indexed in Pubmed: 31085504.
9. Fearon WF, Achenbach S, Engstrom T, et al. FAST-FFR Study Investigators. Accuracy of Fractional Flow Reserve Derived From Coronary Angiography. Circulation. 2019; 139(4): 477–484, doi: 10.1161/CIRCULATIONAHA.118.037350, indexed in Pubmed: 30586699.
10. Morris PD, Silva Soto DA, Feher JFA, et al. Fast Virtual Fractional Flow Reserve Based Upon Steady-State Computational Fluid Dynamics Analysis: Results From the VIRTU-Fast Study. JACC Basic Transl Sci. 2017; 2(4): 434–446, doi: 10.1016/j.jacbts.2017.04.003, indexed in Pubmed: 28920099.
11. Koo BK, Erglis A, Doh JH, et al. Diagnosis of ischemia-causing coronary stenoses by noninvasive fractional flow reserve computed from coronary computed tomographic angiograms. Results from the prospective multicenter DISCOVER-FLOW (Diagnosis of Ischemia-Causing Stenoses Obtained Via Noninvasive Fractional Flow Reserve) study. J Am Coll Cardiol. 2011; 58(19): 1989–1997, doi: 10.1016/j.jacc.2011.06.066, indexed in Pubmed: 22032711.
12. Buono A, Mühlenhaus A, Schäfer T, et al. QFR predicts the incidence of long-term adverse events in patients with suspected CAD: feasibility and reproducibility of the method. J Clin Med. 2020; 9(1), doi: 10.3390/jcm9010220, indexed in Pubmed: 31947542.
13. Kołtowski Ł, Zaleska M, Maksym J, et al. Quantitative flow ratio derived from diagnostic coronary angiography in assessment of patients with intermediate coronary stenosis: a wire-free fractional flow reserve study. Clin Res Cardiol. 2018; 107(9): 858–867, doi: 10.1007/s00392-018-1258-7, indexed in Pubmed: 30128817.
14. Xu Bo, Tu S, Qiao S, et al. Diagnostic accuracy of angiography-based quantitative flow ratio measurements for online assessment of coronary stenosis. J Am Coll Cardiol. 2017; 70(25): 3077–3087, doi: 10.1016/j.jacc.2017.10.035, indexed in Pubmed: 29101020.
15. Slager CJ, Wentzel JJ, Schuurbiers JC, et al. True 3-dimensional reconstruction of coronary arteries in patients by fusion of angiography and IVUS (ANGUS) and its quantitative validation. Circulation. 2000; 102(5): 511–516, doi: 10.1161/01.cir.102.5.511, indexed in Pubmed: 10920062.
16. Yu W, Huang J, Jia D, et al. Diagnostic accuracy of intracoronary optical coherence tomography-derived fractional flow reserve

for assessment of coronary stenosis severity. EuroIntervention. 2019; 15(2): 189–197, doi: 10.4244/EIJ-D-19-00182, indexed in Pubmed: 31147309.

17. Huang J, Emori H, Ding D, et al. Comparison of diagnostic performance of intracoronary optical coherence tomography-based and angiography-based fractional flow reserve for evaluation of coronary stenosis. EuroIntervention. 2020 [Epub ahead of print], doi: 10.4244/EIJ-D-19-01034, indexed in Pubmed: 31951207.
18. Biscaglia S, Tebaldi M, Brugaletta S, et al. Prognostic value of QFR measured immediately after successful stent implantation: the international multicenter prospective HAWKEYE study. JACC Cardiovasc Interv. 2019; 12(20): 2079–2088, doi: 10.1016/j.jcin.2019.06.003, indexed in Pubmed: 31563688.
19. Kogame N, Takahashi K, Tomaniak M, et al. Clinical implication of quantitative flow ratio after percutaneous coronary intervention for 3-vessel disease. JACC Cardiovasc Interv. 2019; 12(20): 2064–2075, doi: 10.1016/j.jcin.2019.08.009, indexed in Pubmed: 31563682.
20. Fairbairn TA, Nieman K, Akasaka T, et al. Real-world clinical utility and impact on clinical decision-making of coronary computed tomography angiography-derived fractional flow reserve: lessons from the ADVANCE Registry. Eur Heart J. 2018; 39(41): 3701–3711, doi: 10.1093/eurheartj/ehy530, indexed in Pubmed: 30165613.
21. Collet C, Miyazaki Y, Ryan N, et al. Fractional flow reserve derived from computed tomographic angiography in patients with multivessel CAD. J Am Coll Cardiol. 2018; 71(24): 2756––2769, doi: 10.1016/j.jacc.2018.02.053, indexed in Pubmed: 29802016.
22. Driessen RS, Danad I, Stuijfzand WJ, et al. Comparison of coronary computed tomography angiography, fractional flow reserve, and perfusion imaging for ischemia diagnosis. J Am Coll Cardiol. 2019; 73(2): 161–173, doi: 10.1016/j.jacc.2018.10.056, indexed in Pubmed: 30654888.
23. Andreini D, Modolo R, Katagiri Y, et al. SYNTAX III REVOLUTION Investigators. Coronary computed tomography angiography for heart team decision-making in multivessel coronary artery disease. Eur Heart J. 2018; 39(41): 3689–3698, doi: 10.1093/eurheartj/ehy581, indexed in Pubmed: 30312411.
24. Kumar A, Thompson EW, Lefieux A, et al. High coronary shear stress in patients with coronary artery disease predicts myocardial infarction. J Am Coll Cardiol. 2018; 72(16): 1926–1935, doi: 10.1016/j.jacc.2018.07.075, indexed in Pubmed: 30309470.
25. Gijsen F, Katagiri Y, Barlis P, et al. Expert recommendations on the assessment of wall shear stress in human coronary arteries: existing methodologies, technical considerations, and clinical applications. Eur Heart J. 2019; 40(41): 3421–3433, doi: 10.1093/eurheartj/ehz551, indexed in Pubmed: 31566246.

VIA MEDICA

ORIGINAL ARTICLE

Cardiology Journal
2020, Vol. 27, No. 3, 230–237
DOI: 10.5603/CJ.a2018.0105

ISSN 1897–5593

Reproducibility of quantitative flow ratio: An inter-core laboratory variability study

Yunxiao Chang[1]*, Liwei Chen[2]*, Jelmer Westra[3], Zhongwei Sun[4], Changdong Guan[4], Yimin Zhang[1], Daixin Ding[1], Bo Xu[4], Shengxian Tu[1]

[1]Biomedical Instrument Institute, School of Biomedical Engineering, Shanghai Jiao Tong University, Shanghai, China
[2]Department of Cardiology, Shin Kong Memorial Wu Ho-Su Hospital, Taipei, Taiwan
[3]Department of Cardiology, Aarhus University Hospital, Skejby, Denmark
[4]Fu Wai Hospital, National Center for Cardiovascular Diseases, Chinese Academy of Medical Sciences, Beijing, China

Abstract

Background: *Quantitative flow ratio (QFR) is a novel approach to derive fractional flow reserve (FFR) from coronary angiography. This study sought to evaluate the reproducibility of QFR when analyzed in independent core laboratories.*

Methods: *All interrogated vessels in the FAVOR II China Study were separately analyzed using the AngioPlus system (Pulse medical imaging technology, Shanghai) by two independent core laboratories, following the same standard operation procedures. The analysts were blinded to the FFR values and online QFR values. For each interrogated vessel, two identical angiographic image runs were used by two core laboratories for QFR computation. In both core laboratories QFR was successfully obtained in 330 of 332 vessels, in which FFR was available in 328 vessels. Thus, 328 vessels ended in the present statistical analysis.*

Results: *The mean difference in contrast-flow QFR between the two core laboratories was 0.004 ± ± 0.03 ($p = 0.040$), which was slightly smaller than that between the online analysis and the two core laboratories (0.01 ± 0.05, $p < 0.001$ and 0.01 ± 0.05, $p = 0.038$). The mean difference of QFR with respect to FFR were comparable between the two core laboratories (0.002 ± 0.06, $p = 0.609$, and 0.002 ± ± 0.06, $p = 0.531$). Receiver operating characteristic curve analysis showed that diagnostic accuracies of QFR analyzed by the two core laboratories were both excellent (area under the curve: 0.970 vs. 0.963, $p = 0.142$), when using FFR as the reference standard.*

Conclusions: *The present study showed good inter-core laboratory reproducibility of QFR in assessing functionally-significant stenosis. It suggests that QFR analyses can be carried out in different core laboratories if, and only if, highly standardized conditions are maintained.* (Cardiol J 2020; 27, 3: 230–237)

Key words: quantitative flow ratio, fractional flow reserve, reproducibility, core laboratories, coronary stenosis

Introduction

Revascularization strategies of stable coronary artery disease (CAD) have relied largely on non-invasive stress tests and coronary angiography in current practice [1]. For decades physiologic evaluation of myocardial perfusion has been proposed and experimented with as a potential tool to determine the ischemic severity of coronary artery stenosis. However, it was not until recent

Address for correspondence: Shengxian Tu, PhD, FACC, FESC, Med-X Research Institute, Shanghai Jiao Tong University, No. 1954, Huashan Road, Xuhui District, Shanghai, 200030, China, tel: +86-21-6293-2631, fax: +86-21-6293-2156, e-mail: sxtu@sjtu.edu.cn

Received: 15.08.2018 Accepted: 16.08.2018

**The first two authors equally contributed.*

years, after the invention of clinically feasible tools, that physiological assessment of coronary blood flow could be adopted to guide interventions. Coronary fractional flow reserve (FFR) acquired by a pressure-wire placed within target coronary vessels can assist in decision making for intermediate lesions during coronary intervention, with proven clinical and economic benefits [2–5]. A FFR value of ≤ 0.80 indicates a functionally significant stenosis [6]. The European Society of Cardiology has recommended this procedure as class I level A for the CAD revascularization approach [7]. Nevertheless, widespread utilization of FFR is limited by its invasive nature, relatively high cost and use of medication to achieve hyperemia states which may introduce complications or adverse events. A real-world survey reveals that FFR is used in less than 10% of intermediate coronary lesions (40–70% stenosis) [8].

Quantitative flow ratio (QFR) is a novel angiography-based computation to derive FFR using computer algorithms that omits the need for pressure guidewire and vasodilator administration [9, 10]. The entire analysis can be done in minutes without extra procedures during diagnostic coronary angiography, making it an appealing tool to be used in the catheterization laboratory. The recently published FAVOR II China Study demonstrated excellent accuracy of online QFR assessment in the catheterization laboratories when compared with the standard FFR measurement. Patient-level and vessel-level diagnostic accuracy of contrast-flow QFR were 92.4% (95% confidence interval [CI] 88.9–95.1%) and 92.7% (95% CI 89.3–95.3%), respectively [11].

In addition to the potential application in guiding coronary revascularization, QFR can be used to assess the efficacy of different stents by evaluating the physiological functionality of the coronary artery after stent implantation in a core laboratory setting [12]. The FAVOR II China Study also demonstrated that QFR showed excellent accuracy when analyzed in the core laboratory [11]. Nevertheless, the reproducibility of QFR when analyzed in other core laboratories has not been addressed. The aim of the present study was to evaluate the reproducibility of QFR when analyzed offline in two independent core laboratories.

Methods

Study materials

The FAVOR II China Study [11] is a prospective, multicenter study that enrolled patients who had at least one lesion with a diameter stenosis of 30% to 90% and a reference diameter ≥ 2 mm by visual estimation. Detailed inclusion and exclusion criteria of the study and the patient characteristics have been reported in the main study. All patients enrolled in the study were reanalyzed in a second core lab (CardHemo, Med-X Research Institute, Shanghai Jiao Tong University, Shanghai, China), hereafter noted as CoreLab2. The reference FFR values and the QFR values by the first core lab (CCRF, Beijing, China), hereafter noted as CoreLab1, were taken from the main study [11] to assess the inter-core laboratories variability and the difference in diagnostic accuracy by different core laboratories, when using FFR as the reference standard. The study procedure was approved by the institutional review board. All patients provided written informed consent.

QFR core-lab analysis

All QFR analyses in the CoreLab2 were performed by an experienced analyst (CY), following the same standard operation procedures (SOP) and by the AngioPlus system (Pulse medical imaging technology, Shanghai) as used by the CoreLab1. The analyst was blinded to the FFR values and the previously computed QFR values. For each interrogated vessel, the two identical angiographic image runs were used by the two core laboratories for QFR computation. The interrogated vessels were reconstructed based on two angiographic image runs with minimal overlap and foreshortening that were acquired with ≥ 25° difference in projection angles. Subsequently, the analyst performed modified frame count on one of the angiographic runs to obtain the mean contrast flow velocity, from which the computer modeled the hyperemic flow velocity and computed the contrast-flow QFR for the entire vessel. This methodology has been previously reported [9, 10]. In the same procedure, the computer used a fixed contrast flow velocity to derive the fixed-flow QFR (fQFR) [10]. Prior to QFR computation, the interrogated vessels and the segments where FFR was measured and reported to the analyst. However, the image frames used for three-dimensional (3D) angiographic reconstruction and the image runs used for modified frame count were selected by the analyst following SOP, being blinded to the online and the CoreLab1 selection results. Contour of the vessel lumen was first automatically delineated by the QFR measurement system and manual adjustment was allowed following SOP in case of suboptimal angiographic image quality.

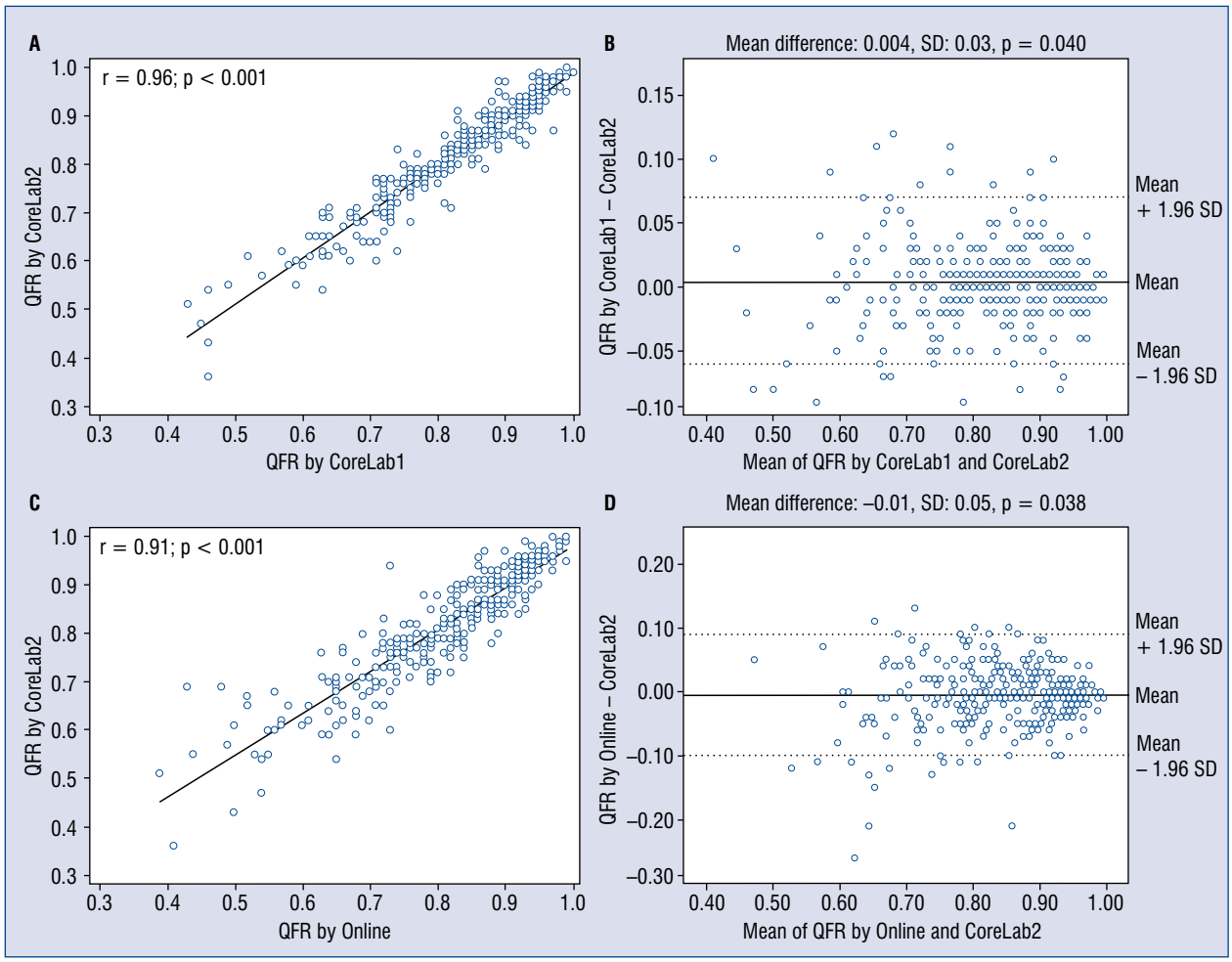

Figure 1. A–D. Correlation and agreement between quantitative flow ratio (QFR) analysis of CoreLab1 and CoreLab2, Online and CoreLab2; SD — standard deviation.

Statistical analysis

Continuous variables were depicted as mean ± standard deviation unless otherwise stated. The D'Agostino Pearson test was used to test normal distribution of the data. Pair-wise comparisons of different QFR analyses were assessed using Bland-Altman plots. The correlation between FFR and QFR was evaluated using the Pearson or Spearman correlation tests as appropriate. An FFR test ≤ 0.80 was considered for diagnosis of hemodynamically-significance. Sensitivity, specificity, positive predictive value (PPV), negative predictive value (NPV), positive likelihood ratio (+LR), negative likelihood ratio (–LR) of QFR with the FFR as the reference standard were calculated and the 95% CIs were added, as appropriate. The Student t test or Mann-Whitney U tests were performed for pair-wise comparisons. Receiver operator characteristic (ROC) curves were compared using the DeLong method. All statistical analyses were performed using MedCalc 14.12.0 (MedCalc Software, Mariakerke, Belgium). A two-sided p value of < 0.05 was considered statistically significant.

Results

In both core laboratories QFR and fQFR were successfully obtained in 330 of 332 interrogated vessels, in which FFR was available in 328 vessels from 304 patients. Thus, pairwise comparisons were performed in 328 vessels.

Correlation and agreement of QFR analysis

The computed QFR values by the two core laboratories demonstrated better correlations ($r = 0.96$ vs. 0.91, $p < 0.001$) and agreement ($0.004 \pm \pm 0.03$ vs. -0.01 ± 0.05, $p < 0.001$) than those by CoreLab2 and online analyses (Fig. 1). Similarly, computed fQFR by the two core laboratories had better correlations ($r = 0.93$ vs. 0.88, $p < 0.001$)

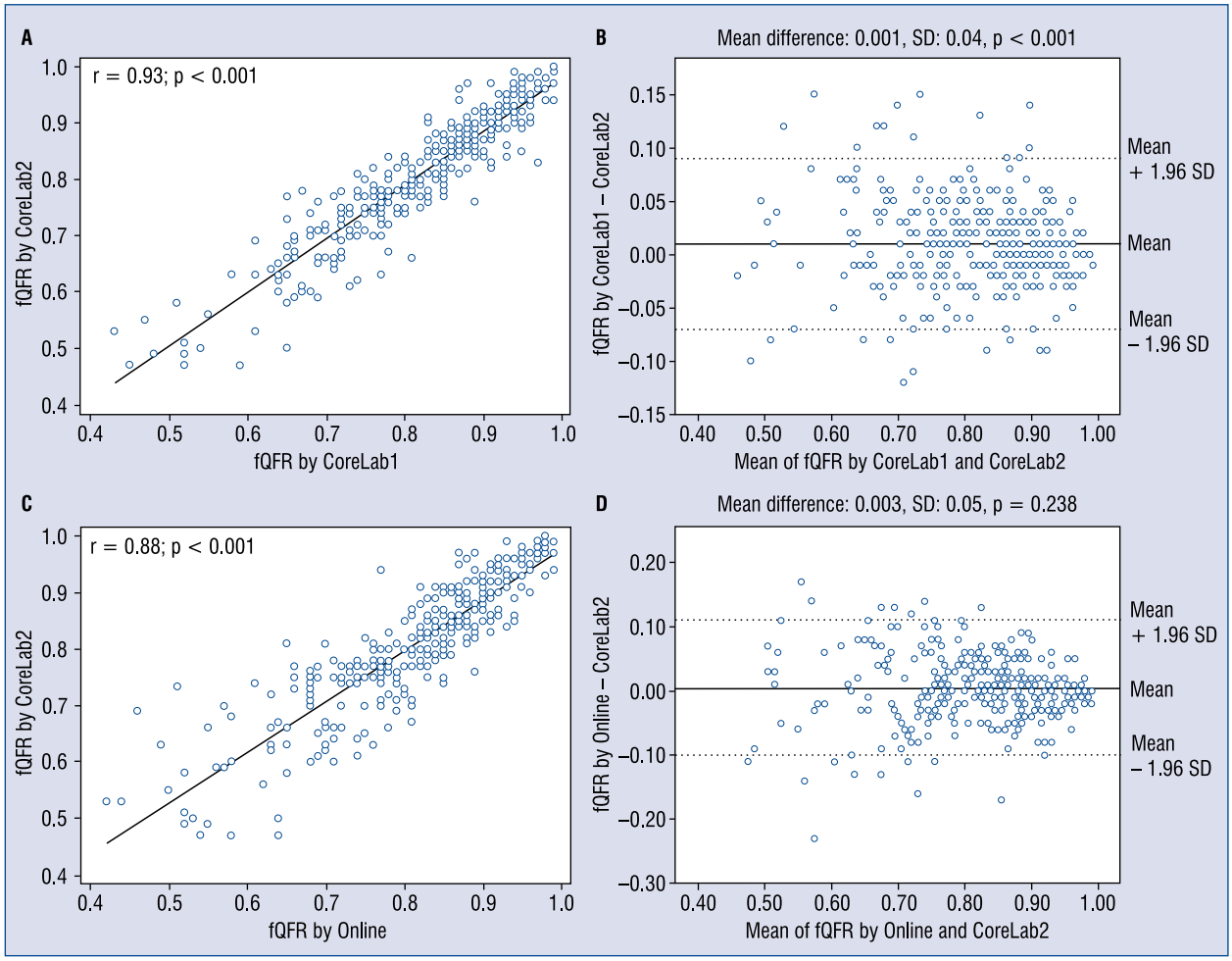

Figure 2. A–D. Correlation and agreement between fixed-flow quantitative flow ratio (fQFR) analysis of CoreLab1 and CoreLab2, Online and CoreLab2; SD — standard deviation.

and agreement (0.01 ± 0.04 vs. 0.003 ± 0.05, $p < 0.001$) than those by CoreLab2 and online analyses (Fig. 2). The computed QFR values by the two core laboratories demonstrated better correlations ($r = 0.96$ vs. 0.91, $p < 0.001$) and agreement (0.004 ± ± 0.03 vs. –0.01 ± 0.05, $p < 0.001$) than those by CoreLab1 and the online analyses reported in the FAVOR II China Study [11].

Correlation and agreement between FFR and QFR analysis

For CoreLab2 analyses, both QFR and fQFR had good correlations with FFR, with the Spearman correlation coefficients being significantly higher for QFR than fQFR measurements (0.86 vs. 0.79, $p < 0.001$). Both QFR and fQFR had good agreement with FFR, with a slightly smaller error for QFR than fQFR (0.002 ± 0.06, vs. 0.01 ± 0.08, $p < 0.001$) (Fig. 3). The mean difference of QFR with respect to FFR were comparable between the two core laboratories (0.0016 ± 0.06 vs. 0.0021 ± ± 0.06, $p = 0.915$).

Diagnostic performance of QFR and fQFR using FFR as the reference standard

ROC analyses show that QFR analyzed by the two core laboratories had comparable diagnostic performance, with areas under curve (AUC) being 0.970 and 0.963 ($p = 0.142$). The fQFR analyzed by the second core laboratory also had comparable but statistically significant AUC as the first core laboratory (0.950 vs. 0.935, $p = 0.047$) (Fig. 4).

Using FFR as the reference standard, the overall accuracy, sensitivity and specificity in diagnosis of hemodynamically-significant stenosis were all excellent for CoreLab2 (accuracy: 92.07% [95% CI 89.13–95.01%], sensitivity: 94.96% [95% CI 89.3–98.1%], specificity: 89.95% [95% CI 85.1–93.7%]), and those were comparable with CoreLab1 (accuracy: 93.3% [95% CI 90.0–95.7%], sensitivity:

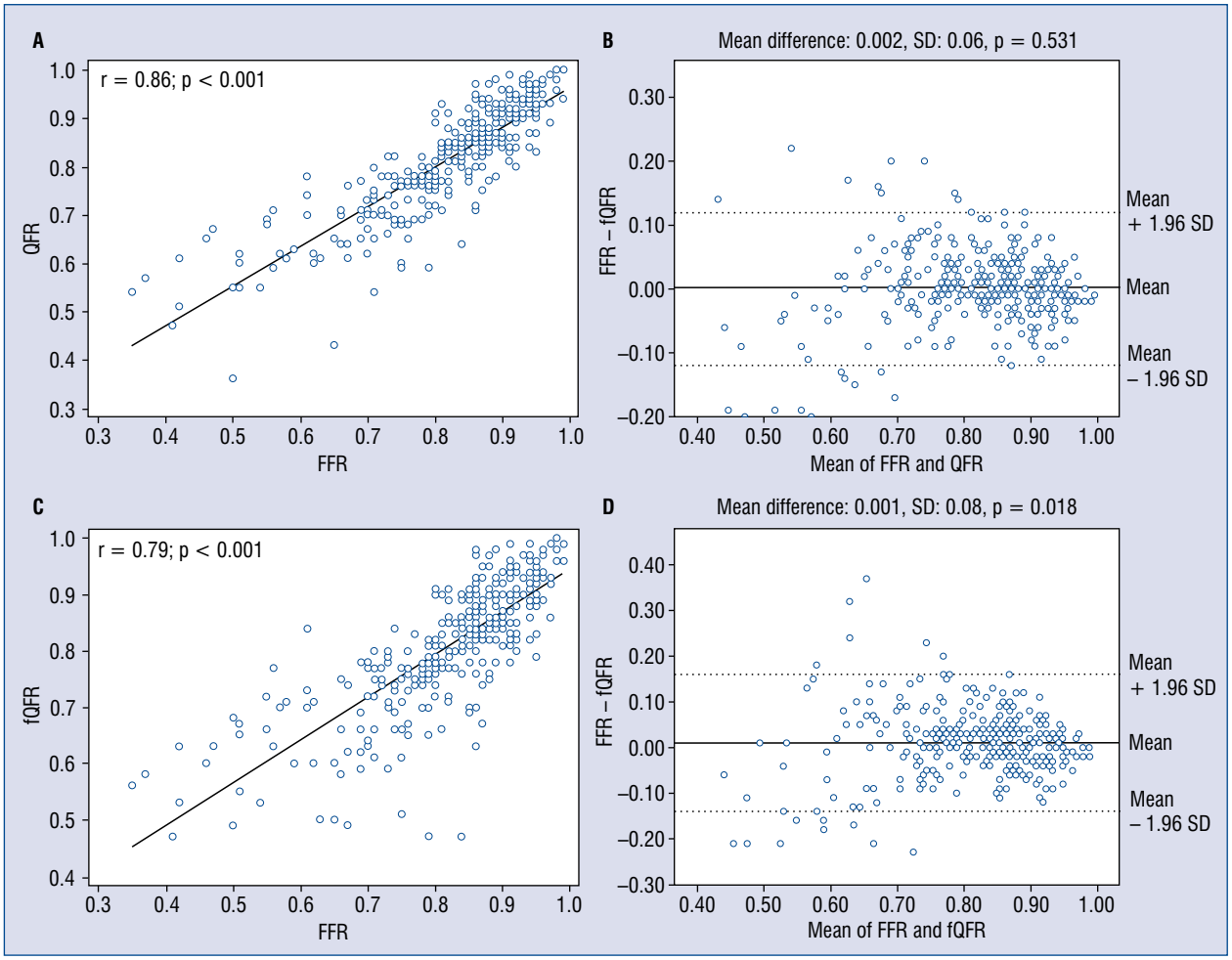

Figure 3. Correlation and agreement between fractional flow reserve (FFR) and quantitative flow ratio (QFR) analysis of CoreLab2 (**A**, **B**). Correlation and agreement between FFR and fixed-flow QFR analysis of CoreLab2 (**C**, **D**).

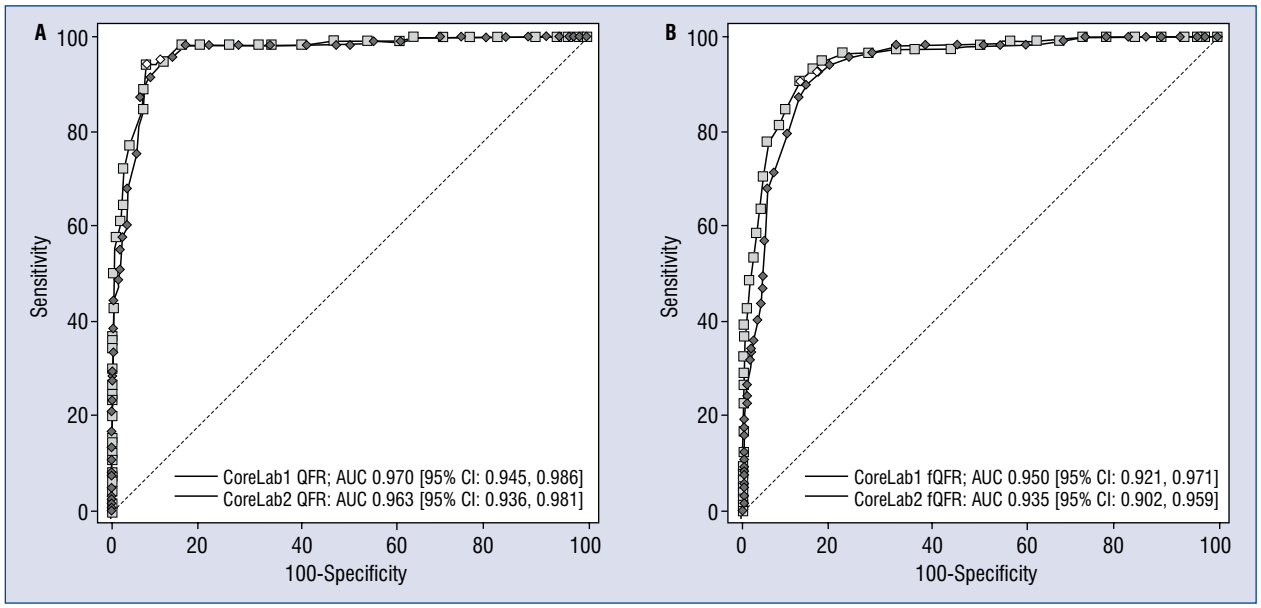

Figure 4. Comparison of receiver operating curves for the quantitative flow ratio (QFR) (**A**) and fixed-flow QFR (fQFR) (**B**) results of CoreLab1 and CoreLab2. QFR analyzed by the two core laboratories had comparable diagnostic performance. Fractional flow reserve was used as the reference standard; AUC — area under curve; CI — confidence interval.

94.1% [95% CI 88.3–97.6%], specificity: 92.8% [95% CI 88.4–95.9%]) as previously reported [11]. PPV, NPV, +LR and –LR for CoreLab2 was 84.3, 96.9, 9.45 and 0.056, respectively.

Discussion

This is the first study to report on the inter-corelab variation for QFR computation. The key finding was that QFR is reproducible and provides comparable diagnostic accuracy with FFR as a reference standard when analyzed by two independent core laboratories using the same dedicated SOP. It supports the use of QFR for evaluation of coronary physiology in a core laboratory setting.

The study focused on the technical and observer-dependent variation since user-interactions are needed to refine geometrical parameters of vessels and select an appropriate frame for contrast flow velocity assessment. It showed herein, that very similar QFR results could be acquired in different core laboratories when the analysts strictly followed SOP and that the extra frame-counting step needed to compute QFR compared to fQFR did not influence reproducibility.

Fractional flow reserve has emerged as the current gold standard to guide percutaneous coronary interventions by improving outcome compared to angiography-guided percutaneous coronary intervention in multiple clinical trials [6, 7, 13, 14]. Apart from the favorable clinical outcomes, FFR appears solid in terms of reproducibility. The absolute difference and standard deviation of repeated FFR measurements approaches 0.03 ± ± 0.02 as illustrated in the Fractional Flow Reserve to Determine the Appropriateness of Angioplasty in Moderate Coronary Stenosis A Randomized Trial (DEFER) where repeated FFR measurements were performed in 325 patients [15]. Application of the "smart minimum" algorithm to The Verification of Instantaneous Wave-Free Ratio and Fractional Flow Reserve for the Assessment of Coronary Artery Stenosis in Everyday Practice (VERIFY) study likewise found good repeatability of FFR (0.00 ± 0.02) [16]. The minor variability may be caused by several factors related to fluctuating hemodynamics, suboptimal vasodilation, drift and variation of wire-position. The presented inter-corelab variation for QFR of 0.00 ± 0.03 is in the same range as FFR and adds to the existing knowledge with multiple off-line and on-line studies proving high diagnostic accuracy of QFR when FFR is used as a reference standard [9–11, 17–23].

The present results confirm findings from a pilot study conducted by van Rosendael et al. [24] that presented an inter-observer variation of 0.02 ± ± 0.04 for QFR in a limited number of 20 lesions. Importantly, the present results are improved when compared to QFR intra-observer agreement of 0.00 ± 0.06 in 40 lesions, as recently reported by Westra et al. [19]. This is most likely due to a more refined SOP for image acquisition, better angiographic quality and a more elaborate protocol for QFR analysis. Further, results were marginally better than on-line QFR results in the FAVOR II China Study [11], which may be explained by multiple factors. In the on-line analyses, five centres participated in FAVOR II China Study [11] with their own technicians performing all measurements. Although highly skilled, inter-personnel differences may have contributed to slight variations. Further, time to QFR was recorded in the FAVOR II China Study [11]. Although this was not used for comparison, site staff facing time pressure to execute the measurements may have resulted in a minor bias.

Limitations of the study

This study has certain limitations. Firstly, intra-observer variation was not assessed. Secondly, despite the presented comparison of core-lab specific diagnostic accuracy estimates with FFR, it should be noted that this study does not report on true repeated QFR measurements since two independent core-labs used the same datasets to compute QFR at two different time-points. Hence, the biological variability of repeated QFR computation was not assessed. However, the majority of data on repeated FFR derives from repeated FFR measurements in the same patient within a small time-frame which likewise limits the evaluation of biological variability. Thirdly, optimal angiographic quality is crucial for optimal QFR computation. Since the repeated measurements were all performed on the same high-quality angiographic runs, the variation caused by potential suboptimal image quality was not included.

Conclusions

The present study showed good inter-core laboratory reproducibility for QFR in assessing the physiological significance of coronary stenosis. It suggests that QFR analyses can be carried out in different core laboratories if highly standardized operating procedures are maintained.

Funding

This study was supported by the National Key Research and Development Program of China (Grant No. 2016YFC0100500), the Natural Science Foundation of China (Grant No. 31500797), Shanghai ShenKang Hospital Development Center (16CR3035A), and Shanghai Jiao Tong University (YG2015ZD04).

Conflict of interest: None of the Authors have declared a conflict of interest in relation to this study, with the exception that S Tu received research support from Medis medical imaging and Pulse medical imaging. Other authors report no conflicts of interest regarding this manuscript.

References

1. Wijns W, Kolh P, Danchin N. Guidelines on myocardial revascularization. Eur Heart J. 2010; 31: 2501–2555.
2. Corcoran D, Hennigan B, Berry C. Fractional flow reserve: a clinical perspective. Int J Cardiovasc Imaging. 2017; 33(7): 961–974, doi: 10.1007/s10554-017-1159-2, indexed in Pubmed: 28577046.
3. Tu S, Echavarria-Pinto M, von Birgelen C, et al. Fractional flow reserve and coronary bifurcation anatomy: a novel quantitative model to assess and report the stenosis severity of bifurcation lesions. JACC Cardiovasc Interv. 2015; 8(4): 564–574, doi: 10.1016/j.jcin.2014.12.232, indexed in Pubmed: 25819180.
4. Johnson NP, Tóth GG, Lai D, et al. Prognostic value of fractional flow reserve: linking physiologic severity to clinical outcomes. J Am Coll Cardiol. 2014; 64(16): 1641–1654, doi: 10.1016/j.jacc.2014.07.973, indexed in Pubmed: 25323250.
5. Fearon WF. Percutaneous coronary intervention should be guided by fractional flow reserve measurement. Circulation. 2014; 129(18): 1860–1870, doi: 10.1161/CIRCULATIONAHA.113.004300, indexed in Pubmed: 24799502.
6. De Bruyne B, Pijls NHJ, Kalesan B, et al. FAME 2 Trial Investigators. Fractional flow reserve-guided PCI versus medical therapy in stable coronary disease. N Engl J Med. 2012; 367(11): 991–1001, doi: 10.1056/NEJMoa1205361, indexed in Pubmed: 22924638.
7. Kolh P, Windecker S, Alfonso F, et al. 2014 ESC/EACTS Guidelines on myocardial revascularization: the Task Force on Myocardial Revascularization of the European Society of Cardiology (ESC) and the European Association for Cardio-Thoracic Surgery (EACTS). Developed with the special contribution of the European Association of Percutaneous Cardiovascular Interventions (EAPCI). Eur J Cardiothorac Surg. 2014; 46(4): 517–592, doi: 10.1093/ejcts/ezu366, indexed in Pubmed: 25173601.
8. Götberg M, Cook CM, Sen S, et al. The Evolving Future of Instantaneous Wave-Free Ratio and Fractional Flow Reserve. J Am Coll Cardiol. 2017; 70(11): 1379–1402, doi: 10.1016/j.jacc.2017.07.770, indexed in Pubmed: 28882237.
9. Tu S, Barbato E, Köszegi Z, et al. Fractional flow reserve calculation from 3-dimensional quantitative coronary angiography and TIMI frame count: a fast computer model to quantify the functional significance of moderately obstructed coronary arteries. JACC Cardiovasc Interv. 2014; 7(7): 768–777, doi: 10.1016/j.jcin.2014.03.004, indexed in Pubmed: 25060020.
10. Tu S, Westra J, Yang J, et al. FAVOR Pilot Trial Study Group. Diagnostic Accuracy of Fast Computational Approaches to Derive Fractional Flow Reserve From Diagnostic Coronary Angiography: The International Multicenter FAVOR Pilot Study. JACC Cardiovasc Interv. 2016; 9(19): 2024–2035, doi: 10.1016/j.jcin.2016.07.013, indexed in Pubmed: 27712739.
11. Xu Bo, Tu S, Qiao S, et al. Diagnostic accuracy of angiography-based quantitative flow ratio measurements for online assessment of coronary stenosis. J Am Coll Cardiol. 2017; 70(25): 3077–3087, doi: 10.1016/j.jacc.2017.10.035, indexed in Pubmed: 29101020.
12. Asano T, Katagiri Y, Collet C, et al. Functional comparison between the BuMA Supreme biodegradable polymer sirolimus-eluting stent and a durable polymer zotarolimus-eluting coronary stent using quantitative flow ratio: PIONEER QFR substudy. EuroIntervention. 2018; 14(5): e570–e579, doi: 10.4244/EIJ-D-17-00461, indexed in Pubmed: 28994655.
13. Pijls NHJ, Fearon WF, Tonino PAL, et al. FAME Study Investigators. Fractional flow reserve versus angiography for guiding percutaneous coronary intervention. N Engl J Med. 2009; 360(3): 213–224, doi: 10.1056/NEJMoa0807611, indexed in Pubmed: 19144937.
14. Pijls NHJ, Fearon WF, Tonino PAL, et al. FAME Study Investigators. Fractional flow reserve versus angiography for guiding percutaneous coronary intervention in patients with multivessel coronary artery disease: 2-year follow-up of the FAME (Fractional Flow Reserve Versus Angiography for Multivessel Evaluation) study. J Am Coll Cardiol. 2010; 56(3): 177–184, doi: 10.1016/j.jacc.2010.04.012, indexed in Pubmed: 20537493.
15. Pijls NHJ, van Schaardenburgh P, Manoharan G, et al. Percutaneous coronary intervention of functionally nonsignificant stenosis: 5-year follow-up of the DEFER Study. J Am Coll Cardiol. 2007; 49(21): 2105–2111, doi: 10.1016/j.jacc.2007.01.087, indexed in Pubmed: 17531660.
16. Johnson NP, Johnson DT, Kirkeeide RL, et al. Repeatability of Fractional Flow Reserve Despite Variations in Systemic and Coronary Hemodynamics. JACC Cardiovasc Interv. 2015; 8(8): 1018–1027, doi: 10.1016/j.jcin.2015.01.039, indexed in Pubmed: 26205441.
17. Yazaki K, Otsuka M, Kataoka S, et al. Applicability of 3-dimensional quantitative coronary angiography-derived computed fractional flow reserve for intermediate coronary stenosis. Circ J. 2017; 81(7): 988–992, doi: 10.1253/circj.CJ-16-1261, indexed in Pubmed: 28331135.
18. Smit JM, Koning G, van Rosendael AR, et al. Relationship between coronary contrast-flow quantitative flow ratio and myocardial ischemia assessed by SPECT MPI. Eur J Nucl Med Mol Imaging. 2017; 44(11): 1888–1896, doi: 10.1007/s00259-017-3769-2, indexed in Pubmed: 28685228.
19. Westra J, Tu S, Winther S, et al. Evaluation of coronary artery stenosis by quantitative flow ratio during invasive coronary angiography: the WIFI II study (wire-free functional imaging II). Circ Cardiovasc Imaging. 2018; 11(3): e007107, doi: 10.1161/CIRCIMAGING.117.007107, indexed in Pubmed: 29555835.
20. Nam CW, Mangiacapra F, Entjes R, et al. FAME Study Investigators. Functional SYNTAX score for risk assessment in multivessel coronary artery disease. J Am Coll Cardiol. 2011; 58(12): 1211–1218, doi: 10.1016/j.jacc.2011.06.020, indexed in Pubmed: 21903052.
21. Spitaleri G, Tebaldi M, Biscaglia S, et al. Quantitative Flow Ratio Identifies Nonculprit Coronary Lesions Requiring Revascularization in Patients With ST-Segment-Elevation Myocardial Infarction and Multivessel Disease. Circ Cardiovasc

Interv. 2018; 11(2): e006023, doi: 10.1161/CIRCINTERVENTIONS.117.006023, indexed in Pubmed: 29449325.

22. Emori H, Kubo T, Kameyama T, et al. Diagnostic accuracy of quantitative flow ratio for assessing myocardial ischemia in prior myocardial infarction. Circ J. 2018; 82(3): 807–814, doi: 10.1253/circj.CJ-17-0949, indexed in Pubmed: 29343675.
23. Mejía-Rentería H, Lee JM, Lauri F, et al. Influence of microcirculatory dysfunction on angiography-based functional assessment of coronary stenoses. JACC Cardiovasc Interv. 2018; 11(8): 741–753, doi: 10.1016/j.jcin.2018.02.014, indexed in Pubmed: 29673505.
24. van Rosendael AR, Koning G, Dimitriu-Leen AC, et al. Accuracy and reproducibility of fast fractional flow reserve computation from invasive coronary angiography. Int J Cardiovasc Imaging. 2017; 33(9): 1305–1312, doi: 10.1007/s10554-017-1190-3, indexed in Pubmed: 28642995.

VIA MEDICA

ORIGINAL ARTICLE

Cardiology Journal
2020, Vol. 27, No. 3, 238–245
DOI: 10.5603/CJ.a2018.0111

ISSN 1897–5593

Coronary plaque redistribution after stent implantation is determined by lipid composition: A NIRS-IVUS analysis

Tomasz Roleder[1], Magdalena Dobrolinska[2], Elzbieta Pociask[3], Wojciech Wanha[2], Grzegorz Smolka[2], Wojciech Walkowicz[1], Radoslaw Parma[2], Mariusz Lebek[1], Tomasz Bochenek[4], Przemyslaw Pietraszewski[5], Elvin Kedhi[6], Andrzej Ochala[2], Zbigniew Gasior[1], Ziad A. Ali[7, 8], Wojciech Wojakowski[2]

[1]Department of Cardiology, School of Health Sciences, Medical University of Silesia in Katowice, Poland
[2]Division of Cardiology and Structural Heart Diseases, Medical University of Silesia in Katowice, Poland
[3]Department of Biocybernetics and Biomedical Engineering, AGH University of Science and Technology, Krakow, Poland
[4]First Division of Cardiology, Medical University of Silesia in Katowice, Poland
[5]Department of Sports Theory, Jerzy Kukuczka Academy of Physical Education in Katowice, Poland
[6]Isala Hartcentrum, Zwolle, Netherlands
[7]Center for Interventional Vascular Therapy, Division of Cardiology, Presbyterian Hospital and Columbia University, New York, United States
[8]Cardiovascular Research Foundation, New York, United States

Abstract

Background: *The composition of plaque impacts the results of stenting. The following study evaluated plaque redistribution related to stent implantation using combined near-infrared spectroscopy and intravascular ultrasound (NIRS-IVUS) imaging.*

Methods: *The present study included 49 patients (mean age 66 ± 11 years, 75% males) presenting with non-ST elevation myocardial infarction (8%), unstable angina (49%) and stable coronary artery disease (43%). The following parameters were analyzed: mean plaque volume (MPV, mm^3), plaque burden (PB, %), remodeling index (RI), and maximal lipid core burden index in a 4 mm segment ($maxLCBI_{4mm}$). High-lipid burden lesions (HLB) were defined as by $maxLCBI_{4mm} > 265$ with positive RI. Otherwise plaques were defined as low-lipid burden lesions (LLB). Measurements were done in the target lesion and in 4 mm edges of the stent before and after stent implantation.*

Results: *MPV and $maxLCBI_{4mm}$ decreased in both HLB (MPV 144.70 [80.47, 274.25] vs. 97.60 [56.82, 223.45]; $maxLCBI_{4mm}$: 564.11 ± 166.82 vs. 258.11 ± 234.24, $p = 0.004$) and LLB (MPV: 124.50 [68.00, 186.20] vs. 101.10 [67.87, 165.95]; $maxLCBI_{4mm}$: 339.07 ± 268.22 vs. 124.60 ± 160.96, $p < 0.001$), but MPV decrease was greater in HLB (28.00 [22.60, 57.10] vs. 13.50 [1.50, 28.84], $p = 0.019$). Only at the proximal stent edge of LLB, $maxLCBI_{4mm}$ decreased (34 [0, 207] vs. 0 [0, 45], $p = 0.049$) and plaque burden increased (45.48 [40.34, 51.55] vs. 51.75 [47.48, 55.76], $p = 0.030$).*

Conclusions: *NIRS-IVUS defined HLB characterized more significant decreases in plaque volume by stenting. Plaque redistribution to the proximal edge of the implanted stent occurred only in LLB.* (Cardiol J 2020; 27, 3: 238–245)

Key words: plaque redistribution, stenting, intravascular ultrasound, near-infrared spectroscopy, stent edges

Address for correspondence: Tomasz Roleder, MD, PhD, Department of Cardiology, School of Health Sciences, Medical University of Silesia in Katowice, ul. Ziołowa 45/47, 40–001 Katowice, Poland, tel: +48 884096034, fax: +48 323598884, e-mail: tomaszroleder@gmail.com

Received: 8.08.2018 Accepted: 11.09.2018

Introduction

Percutaneous coronary intervention (PCI) resolves ischemia by axial displacement of atherosclerotic plaque and increase of luminal area. However, the lipidic plaque is known to redistribute not only axially, but also longitudinally leading to tissue protrusion and stenosis at the stent edges. Both plaque protrusion [1, 2] and reference vessel disease have been identified as predictors of poor outcome after PCI [3]. Intravascular imaging modalities like intravascular ultrasound (IVUS), optical coherence tomography (OCT) and near-infrared spectroscopy (NIRS) provide insight into the morphology and composition of atherosclerotic plaque *in vivo*. OCT provides superior resolution, but its limited penetration depth, mainly through lipidic plaque, impairs the global assessment of the lesion, especially after stent implantation [4]. Due to superior penetration, IVUS overcomes this limitation of OCT, offering a global assessment of the lesion including the plaque structure behind the implanted stent [5]. Its combination with NIRS has augmented the capabilities of IVUS [6]. NIRS provides simplified algorithm of detection of lipid-rich lesions not only in atherosclerotic plaque but also in tissue located behind the implanted stent [6].

NIRS-IVUS studies demonstrated that lipid-rich plaques might be prone to distal embolization after stenting because of redistribution of lipidic plaque and release of its debris into circulation [7–9]. Indeed, stenting of lipid-rich lesions increases the risk of periprocedural myocardial infarction suggesting that plaque redistribution is related to composition and morphology [10, 11]. In the current study, the aim was to assess plaque redistribution after stent implantation by combined NIRS-IVUS imaging. It was hypothesized that the magnitude and geometry of plaque redistribution at the stent edges were related to its morphology and lipid content.

Methods

Study design

The present study was a prospective single-center study at the Medical University of Silesia in Katowice, Poland in which patients with stable coronary artery disease (SCAD) or non-ST-segment elevation-acute coronary syndrome (NSTE-ACS) were undergoing stent implantation with NIRS-IVUS. The investigators designed the trial and performed a retrospective analysis. Investigators assured data accuracy and collected source documents for adjudication. T.R. and M.D. performed intravascular imaging analysis, data management, and biostatistics. The institutional review board approved the study protocol. The study conformed to the Declaration of Helsinki and was approved by the Local Ethics Committee. All patients gave written informed consent.

Participants

Patients undergoing clinically indicated PCI for NSTE-ACS or SCAD using NIRS-IVUS guidance were screened. Patients with cardiogenic shock, New York Heart Association (NYHA) IV class heart failure, significant valvular heart disease, in-stent restenosis as the target lesion, reference vessel diameter less than 2.5 mm, excessive tortuosity, pregnancy, hemophilia, renal failure (creatinine > 1.5 mg/dL), and contrast allergy were excluded from the study.

Procedures

The current study employed combined NIRS-IVUS assessment of the target lesion pre- and post-stent implantation. All imaging was performed during the same procedure before predilatation or direct stenting, after stenting and final post-dilatation. The target lesion was selected at the operator's discretion after the diagnostic angiogram and fractional flow reserve assessement if needed. There were no complications related to NIRS-IVUS imaging, which was performed using heparin anticoagulation (activated clotting time > 300 s) and following intracoronary nitroglycerine (100–200 μm) administration. Combined NIRS and gray-scale IVUS image acquisition was performed using the commercially available TVC Imaging System™ and TVC Insight Catheter (InfraReDx, MA). The tip of the TVC catheter was positioned at least 10 mm distal to the imaging target lesion. Subsequently, the automated pullback was started at 0.5 mm/s (240 rotations/min) until the TVC catheter entered the guiding catheter.

NIRS images analysis

NIRS map analysis allows the calculation of a lipid core burden index (LCBI). LCBI is estimated by dividing the number of yellow pixels per all pixels (without black ones) within the analyzed pullback length and are expressed per mill (‰). The maximal LCBI was estimated in 4 mm pullback compartments for every analyzed segment pre- and post-stenting ($maxLCBI_{4\ mm}$).

Gray-scale IVUS image analysis

The region of interest (ROI) was defined as the length of the artery covered by the stent pre- and post-procedure. Quantitative gray-scale IVUS

measurements were performed every millimeter in scanned coronary segments pre and post-stenting. Cross-sectional images were quantified for lumen diameters and area, external elastic membrane (EEM) diameters and area, total plaque area, plaque burden, and lumen and EEM eccentricity. Additionally, after stenting, the stent area was estimated. The total plaque area was calculated as the difference between EEM area and lumen area (pre-stenting), or as a difference between EEM area and stent area (post-stenting). Plaque burden was calculated as total plaque area divided by EEM area × 100 (%). The IVUS reference lumen area was defined as the 4 mm located immediately proximal or distal to the ROI. The reference EEM area was calculated as an average of the proximal and distal EEM area. The remodeling index (RI) was calculated by dividing the EEM area at the minimal lumen area (MLA) by reference EEM area. Lesions with RI ≤ 0.95 were defined as negatively remodeled, while those with RI ≥ 1.05 were defined as positively remodeled. In every segment, a lumen vessel volume, EEM volume and stented volume (after stenting) was calculated based on the Simpson rule [mm^3]. These data were used to estimate plaque volume (pre-stenting: EEM volume – vessel volume, post-stenting: EEM volume – stented volume [mm^3]). All IVUS measurements were performed for the ROI and 1 mm and 4 mm long segments adjacent to the implanted stent (Fig. 1).

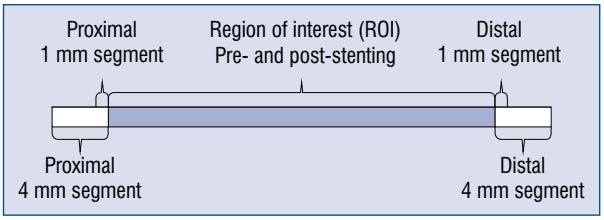

Figure 1. Intravascular ultrasound imaging measurements. The figure presents the analyzed segment by intravascular ultrasound imaging. The minimal lumen area and diameter external elastic lamina area and volume, lumen volume, plaque area volume, plaque burden and plaque eccentricity were measured for the region of interest, and for proximal and distal 1 mm and 4 mm long segments adjacent to the stent. All measurements were performed before and after stenting.

Co-registration of NIRS-IVUS pre- and post-stenting.

During NIRS-IVUS pullback, anatomical landmarks were imprinted on the chemogram and bookmarked on the IVUS images — i.e., fiducial points, side branches, stent edges. Those landmarks allowed matching of NIRS-IVUS images to corresponding sections pre- and post-stenting on angiography.

Lipid-rich lesions

NIRS-IVUS defined high lipid burden lesions (HLB) as lesions with $maxLCBI_{4\ mm} > 265$ with positive RI [12]. Non-HLB segments were considered as lowlipid burden lesions (LLB). NIRS-IVUS data were analyzed off-line using CAAS intravascular software (Pie Medical Imaging BV). Coronary segments with incomplete and/or poor quality NIRS, IVUS scans were excluded from analysis (1 coronary segment, 1 patient).

Statistical analysis

Normality of the distribution of values was assessed using the Kolmogorov-Smirnov statistic, and homogeneity of variances assessed using the Levene test. For normally distributed values, data are presented as mean with standard deviation (SD), for non-normally distributed values data are presented as median with interquartile range (IQR, 25 percentile, 75 percentile). Normally distributed data were compared using a paired t-test, and non-normally distributed data were compared using the Mann-Whitney-test. The categorical data were compared using the Fisher exact test or χ^2 test. A two-tailed p-value of 0.05 was considered as statistically significant. Data analysis was performed using Medcalc software version 17.1.

Results

Study group

Between September 2015 and August 2016 intravascular imaging was performed in 50 stents implanted in 49 patients with either SCAD (n = 33; 67%) or NSTE-ACS syndromes (n = 16; 33%). HLB lesions were identified in 9 patients, and LLB lesions were detected in 40 patients (50 ROIs). HLB patients were characterized by a higher level of total cholesterol and triglycerides, and trend towards a higher prevalence of diabetes. Baseline clinical characteristics are presented in Table 1.

Angiographic data analysis and procedure details

There were now differences in the location of HLB lesions and LLB lesions — left anterior descending artery: 5 (56%) vs. 19 (46%), circumflex artery: 3 (33%) vs. 10 (24%), ramus intermedius: 0 vs. 1 (2%), left main: 0 vs. 1 (2%), right coronary artery: 1 (11%) vs. 10 (24%), p = 0.846. Two HLB lesions (22%) and 14 (34%) LLB lesions were lo-

Table. 1. Patient characteristics.

	Patients with low lipid burden lesions (n = 40)	Patients with high lipid burden lesions (n = 9)	P
Age [years]	66.17 ± 11.32	65.5 ± 10.72	0.920
Male gender	32 (80%)	5 (55%)	0.113
Body mass index [kg/m^2]	26.7 (IQR 25.23, 27.93)	25.15 (IQR 20.70, 36.09)	0.771
NSTEMI/UA/SCAD	4 (10%)/20 (50%)/16 (30%)	0/5 (55%)/4 (45%)	0.433
Risk factors			
Hypertension	36 (90%)	8 (88%)	0.634
Hyperlipidemia	40 (100%)	9 (100%)	–
Diabetes mellitus	11 (27%)	6 (67%)	0.058
Current smoking	3 (7%)	1 (11%)	0.714
Pharmacological therapy			
Acetylsalicylic acid	38 (95%)	8 (88%)	0.765
Thienopyridine	27 (67%)	3 (33%)	0.153
Beta-adrenergic antagonist	32 (80%)	6 (67%)	0.519
Calcium channel antagonist	10 (25%)	5 (56%)	0.148
ARB/ACEI	27 (67%)	6 (67%)	0.732
Statin	36 (90%)	9 (100%)	0.623
Other lipid-lowering therapy	4 (10%)	2 (22%)	0.654
Oral antidiabetics	10 (25%)	5 (56%)	0.148
Insulin	1 (2%)	1 (11%)	0.792
Laboratory results			
Total cholesterol [mg/dL]	139 (IQR 127, 153)	171 (IQR 146.92, 244.64)	0.031
LDL cholesterol [mg/dL]	76 (IQR 69, 93)	99.00 (IQR 69.69, 132.03)	0.120
HDL cholesterol [mg/dL]	40.00 (IQR 36.76, 46.00)	44.50 (IQR 38.67, 50.16)	0.401
Triglyceride [mg/dL]	102.02 (IQR 91.58, 115.19)	154.50 (IQR 98.10, 355.03)	0.012
GRF [mL/min/1.73 m^2]	72.40 ± 15.93	67.62 ± 25.84	0.473

NSTEMI — non-ST-segment elevation myocardial infarction, UA — unstable angina, SCAD — stable coronary artery disease, ARB — angiotensin II receptor blocker, ACEI — angiotensin-converting-enzyme inhibitor; LDL — low density lipoprotein, HDL — high-density lipoprotein, GRF — glomerular filtration rate; IQR — interquartile range

cated in proximal segments of the coronary artery (p = 0.379).

There were also no differences in type of drug eluting stents implanted in HLB and LLB lesions — everolimus eluting: 7 (78%) vs. 21 (51%), sirolimus eluting 2 (22%) vs. 11 (27%), biolimus eluting 0 vs. 9 (22%); p = 0.106. There were no differences in the stent diameter [mm] — 3 (3, 3.5) vs. 3 (3, 3.5), p = 0.250 and stent length [mm] — 15 (12, 24) vs. 22 (18, 28), p = 0.306 implanted in HLB and LLB lesions.

Plaque modificationof the stented segment

Both HLB and LLB lesions were characterized by an increase of minimal lumen diameter (MLD), minimal lumen area (MLA), lumen volume and EEM volume and a decrease of maxLCBI$_{4\,mm}$, total plaque area, plaque burden and plaque volume after stenting. Although the plaque volume decreased in both HLB and LLB lesions, the change was significantly higher in HLB lesions (Table 2, Fig. 2). Stenting increased remodeling index only in LLB lesions, having no impact on the RI in HLB lesions.The observed differences in plaque volume correlated with maxLCBI$_{4\,mm}$ before stenting (r = 0.48; p < 0.01) in all 50 lesions (Fig. 2). NIRS-IVUS characteristics of stented lesions is presented in Table 2. Representative images of plaque modification are presented in Figure 3 and **Supplementary Figures 1 and 2.**

Assessment of the proximal segment adjacent to the stent after the procedure

In 4 mm proximal segment adjacent to stent, maxLCBI$_{4\,mm}$ decreased after stenting in LLB lesions — 34 (0, 207) vs. 0 (0, 45), p = 0.049. However, plaque

Table 2. Near-infrared spectroscopy and intravascular ultrasound results of the stented segment.

Parameters	Low lipid burden lesions (n = 41)			High lipid burden lesions (n = 9)		
	Pre-stenting	Post-stenting	P	Pre-stenting	Post-stenting	P
Stented segment						
ROI [mm]	21.98 ± 9.01	21.96 ± 8.98	0.804	25.71 ± 15.38	25.70 ± 15.39	0.346
MLD [mm]	1.64 ± 0.31	2.23 ± 0.37	< 0.001	1.53 ± 0.13	2.28 ± 0.34	< 0.001
MLA [mm^2]	2.65 ± 1.21	5.31 ± 1.68	< 0.001	2.94 ± 1.40	6.15 ± 1.39	< 0.001
Stenosis (MLA) on reference [%]	55.36 ± 13.01	17.90 ± 14.38	< 0.001	57.63 ± 10.19	19.00 ± 14.78	0.006
Lumen volume [mm^3]	98.80 (63.15, 131.45)	128.30 (86.97, 185.37)	< 0.001	96.70 (69.10, 112.62)	181.30 (76.22, 266.37)	0.004
EEM volume [mm^3]	226.70 (140.77, 315.82)	288.60 (169.42, 377.62)	< 0.001	244.40 (149.55, 379.10)	317.30 (144.47, 535.52)	0.012
ΔEEM volume [mm^3]	46.45 (21.50, 74.85)			67.40 (16.22, 116.62)		0.423
Plaque volume [mm^3]	124.50 (68.00, 186.20)	101.10 (67.87, 165.95)	< 0.001	144.70 (80.47, 274. 25)	97.60 (56.82, 223.45)	0.004
ΔMPV [mm^3]	13.50 (1.50, 28.84)			28.00 (22.60, 57.10)		0.019
maxLCBI4 [mm]	339.07 ± 268.22	124.60 ± 160.96	< 0.001	564.11 ± 166.82	258.11 ± 234.24	0.004
EEM area [mm^2]	10.00 (7.50, 11.60)	11.30 (9.27, 13.25)	< 0.001	12.70 (12.10, 13.47)	13.10 (11.72, 16.20)	0.820
EEM eccentricity	0.09 (0.07, 0.15)	0.09 (0.06, 0.13)	0.551	0.09 ± 0.01	0.11 ± 0.04	0.341
Lumen eccentricity	0.09 (0.06, 0.14)	0.13 (0.08, 0.18)	0.038	0.17 ± 1.12	0.20 ± 0.10	0.181
Total plaque area [mm^2]	7.4 (5.12, 8.62)	4.7 (3.67, 6.40)	< 0.001	11.51 ± 5.01	5.72 ± 1.80	0.009
Plaque burden [%]	72.19 ± 8.12	55.03 ± 6.87	< 0.001	79.26 ± 8.57	53.0 ± 9.9	< 0.001
Remodeling index	0.87 ± 0.23	1.09 ± 0.27	< 0.001	1.23 ± 0.11	1.20 ± 0.25	0.739

ROI — region of interest; MLD — minimal lumen diameter; MLA — minimal lumen area; EEM — external elastic lamina; maxLCBI4 mm — maximal lipid core burden index in four millimeters; ΔMPV — delta plaque volume

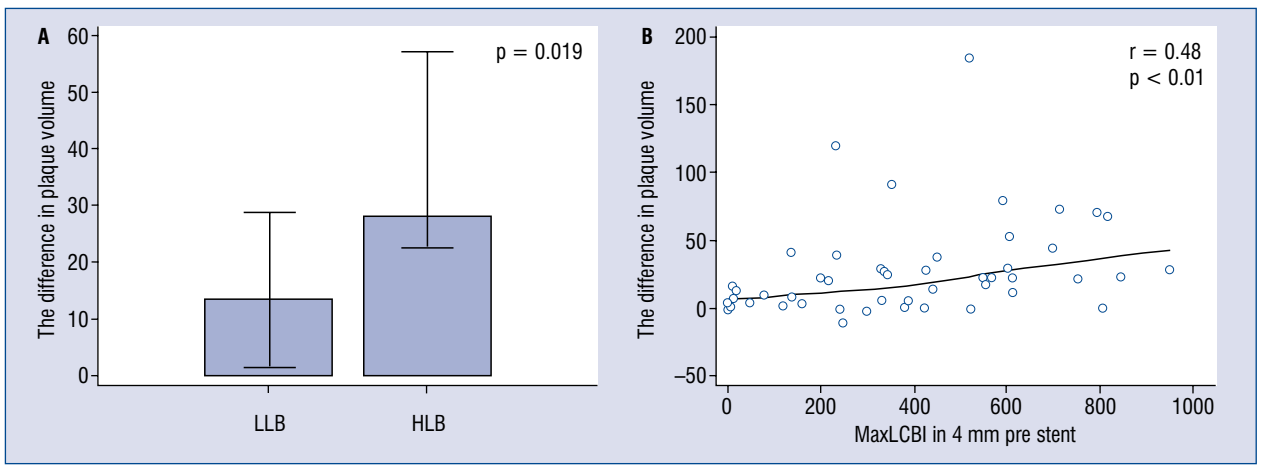

Figure 2. Plaque volume pre- and post-stenting and lipid core burden index (LCBI) values. **A.** The difference in plaque volume for near-infrared spectroscopy and intravascular ultrasound (NIRS-IVUS) high lipid burden lesions (HLB, $maxLCBI_{4\,mm}$ > 265 and positive vessel remodeling) and for NIRS-IVUS low lipid burden (LLB) lesions; **B.** The correlation between the difference in plaque volume pre- and post-stenting and $maxLCBI_{4\,mm}$ values in all lesions.

burden [%] — 45.48 (40.34, 51.55) vs. 51.75 (47.48, 55.76), p = 0.030 and total plaque area [mm^2] — 6.30 (5.17, 7.85) vs. 7.05 (6.08, 8.43), p = 0.005 increased in the first millimeter adjacent to the implanted stent in LLB lesions. Such plaque modification was not observed in HLB lesions. NIRS-IVUS characteristics of proximally segment adjacent to the implanted stent is presented in **Supplementary Table 1.**

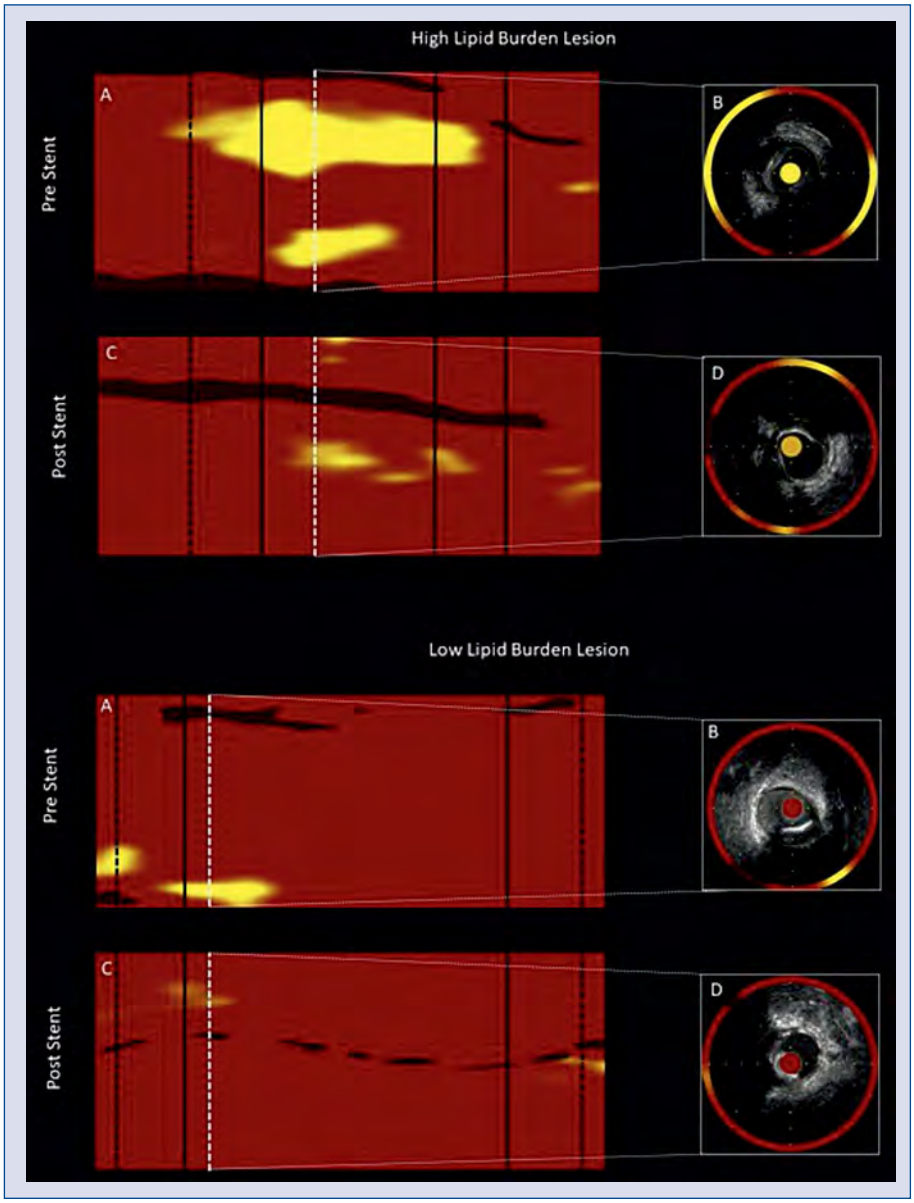

Figure 3. Representative image of near-infrared spectroscopy and intravascular ultrasound (NIRS-IVUS) imaging pre- and post-stenting of high lipid burden and low lipid burden lesions; **A, C.** NIRS maps pre- and post-stent implantation. Black lines indicate stent edges. Black dashed lines limit 4 mm proximal and distal segments adjacent to the stent. White dashed lines indicate the NIRS-IVUS cross-section image. **B, D.** NIRS-IVUS cross-sectional image of minimal lumen area (MLA), external elastic lamina (EEM) and stent contours. High lipid burden lesion: A. Pre-stenting $maxLCBI_{4\ mm}$ = 548; C. Post-stenting $maxLCBI_{4\ mm}$ = 202; B. Pre-stenting: MLA = 3.8 mm^2, plaque burden = 71%, plaque area = 9.2 mm^2, EEM area = 12.9 mm^2, remodeling index = 1.34; D. Post-stenting: MLA = 6.4 mm^2, plaque burden = 48.8%, plaque area = 6.1 mm^2, EEM area = 12.4 mm^2, stent area = 5.0 mm^2, remodeling index = 1.22; delta mean plaque volume = 22.9 mm^3. Low lipid burden lesion: A. Pre-stenting $maxLCBI_{4\ mm}$ = 137; C. Post-stenting $maxLCBI_{4\ mm}$ = 30; B. Pre-stenting: MLA = 3.5 mm^2, plaque burden = 61%, plaque area = 6.4 mm^2, EEM area = 10.6 mm^2, remodeling index = 0.72; D. Post-stenting: MLA = 5.8 mm^2, plaque burden = 53%, plaque area = 6.4 mm^2, EEM area = 12.0 mm^2, stent area = 6.6 mm^2, remodeling index = 1.29; delta mean plaque volume = 8.2 mm^3.

Assessment of the distal segment adjacent to the stent after the procedure

After the procedure, there were no differences in $maxLCBI_{4\ mm}$, plaque burden, plaque volume in distal 4 mm segment adjacent to the implanted stent in both HLB and LLB lesions. NIRS-IVUS characteristics of the segment located distally to the implanted stent is presented in **Supplementary Table 2.**

Discussion

This study expands previous observations from intravascular imaging on plaque redistribution and lipid burden following stenting, using NIRS-IVUS [13]. It is confirmed herein, that plaque redistribution caused by stenting is related to its composition. Lipid-rich lesions characterized a more significant decrease in plaque volume after stenting, especially in HLB. Interestingly, plaque redistribution to the proximal edges of the stent occurred only in LLB.

Initial IVUS studies conducted in patients with SCAD demonstrated that stent implantation redistributed plaque longitudinally across the vessel to the proximal and distal edges of the stent with the potential for release of plaque debris into coronary circulation [7–9]. NIRS imaging alone confirmed a lipidic component of these findings [14]. Combined NIRS-IVUS imaging has demonstrated that a decrease in LCBI with a reduction in plaque volume led to edge redistribution of lipidic plaque in ST-segment elevation myocardial infarction (STEMI) patients [13]. The current study of non-STEMI patients and SCAD patients confirms that stenting of HLB lesions is associated with a decrease in plaque volume.

Interestingly, plaque shift to the proximal stent edge was found only in LLB lesions. The smaller lumen volume after stenting LLB suggest that these plaques have a smaller potential to be compressed and are less likely to protrude through stent struts. Thus it may affect final stent expansion and prone redistribution of LLB plaques to the edges of implanted stent edges to make space for the stent. Moreover, as it was shown a correlation between HLB lesions and thin fibrous cap atheroma (TFCA) [12, 15], it is also possible that LLB lesions are less prone to embolization into the microcirculation from a thick cap. Indeed, OCT studies have shown that TFCA correlates with type IVa myocardial infarction after PCI [14], and OCT defined TFCA is a strong predictor of periprocedural infarction [10]. Taken together the present results suggest that both lipid-rich plaque and distinct plaque morphology may be necessary to trigger distal embolization [16]. Previous studies have shown that the use of aggressive lipid-lowering therapy can decrease lipid core and increase fibrous cap thickness [17, 18]. The routine use of high-dose statins before planned stent implantation to reduce no-reflow phenomenon requires further attention [19].

The Color Registry showed previously that lesions with $maxLCBI_{4\,mm} > 500$ had an increased risk of periprocedural myocardial infarction [11]. The findings prompted the CANARY trial, which tested the potential benefit of distal protection during PCI for lesions with $maxLCBI_{4\,mm} > 600$. The trial failed to show a benefit, perhaps due to the inherent morbidity of filter placement but was also stopped prematurely due to difficulties in identifying patients suitable for randomization [20]. The present data suggests that plaque morphology assessment should also be applied to assess the risk of distal embolization.

The current study showed that LLB lesions had a smaller decrease in plaque volume with an increase in plaque area and plaque burden at the proximal edge of the implanted stent, but not at the distal edge. It is possible that this is a result of the difference in size of the vessel proximally versus distally. The relatively large proximal vessel size may be able to accommodate plaque shift to a greater extent than the distal edge. Since NIRS cannot determine depth (axial dimension of the lipid), a decreased lipid length could result in decreased LCBI values but not an actual reduction in lipid burden, rather indicating an axial accumulation [21]. Nevertheless, the plaque shift to the proximal edge of the stent advocates use of the "red to red" (healthy to healthy segment) stenting strategy to reduce adverse clinical outcomes [22].

Limitations of the study

The study has several limitations. A small group of patients were included in the study, and both acute and stable coronary patients were assessed. The HLB lesion definition relied on previously presented NIRS-IVUS data against OCT [12]. The addition of OCT imaging to NIRS-IVUS imaging could have improved the accuracy of HLB detection in this study. Although there was no strict protocol for stent implantation, it does represent real-world practice.

Conclusions

NIRS-IVUS HLB lesions had a more significant decrease in plaque volume by stenting without plaque distribution to the edges of the stent. Plaque redistribution to the proximal edge of the implanted stent was observed only in LLB lesions.

Funding

The study was supported by the statutory funds of the Medical University of Silesia in Katowice, Poland.

Conflict of interest: None declared

References

1. Prati F, Romagnoli E, Gatto L, et al. Clinical Impact of Suboptimal Stenting and Residual Intrastent Plaque/Thrombus Protrusion in Patients With Acute Coronary Syndrome: The CLI-OPCI ACS Substudy (Centro per la Lotta Contro L'Infarto-Optimization of Percutaneous Coronary Intervention in Acute Coronary Syndrome). Circ Cardiovasc Interv. 2016; 9(12), doi: 10.1161/CIRCINTERVENTIONS.115.003726, indexed in Pubmed: 27965297.
2. Soeda T, Uemura S, Park SJ, et al. Incidence and clinical significance of poststent optical coherence tomography findings: one-year follow-up study from a multicenter registry. Circulation. 2015; 132(11): 1020–1029, doi: 10.1161/CIRCULATIONAHA.114.014704, indexed in Pubmed: 26162917.
3. Prati F, Romagnoli E, Burzotta F, et al. Clinical Impact of OCT Findings During PCI: The CLI-OPCI II Study. JACC Cardiovasc Imaging. 2015; 8(11): 1297–1305, doi: 10.1016/j.jcmg.2015.08.013, indexed in Pubmed: 26563859.
4. Jang IK, Bouma B, Kang DH, et al. Visualization of coronary atherosclerotic plaques in patients using optical coherence tomography: comparison with intravascular ultrasound. J Am Coll Cardiol. 2002; 39(4): 604–609, doi: 10.1016/s0735-1097(01)01799-5.
5. Yock PG, Linker DT. Intravascular ultrasound. Looking below the surface of vascular disease. Circulation. 1990; 81(5): 1715–1718, indexed in Pubmed: 2184950.
6. Ali ZA, Roleder T, Narula J, et al. Increased thin-cap neoatheroma and periprocedural myocardial infarction in drug-eluting stent restenosis: multimodality intravascular imaging of drug-eluting and bare-metal stents. Circ Cardiovasc Interv. 2013; 6(5): 507–517, doi: 10.1161/CIRCINTERVENTIONS.112.000248, indexed in Pubmed: 24065447.
7. Ahmed JM, Mintz GS, Weissman NJ, et al. Mechanism of lumen enlargement during intracoronary stent implantation: an intravascular ultrasound study. Circulation. 2000; 102(1): 7–10, indexed in Pubmed: 10880407.
8. Algowhary M, Matsumura A, Hashimoto Y, et al. Poststenting axial redistribution of atherosclerotic plaque into the reference segments and lumen reduction at the stent edge. Int Heart J. 2006; 47(2): 159–171, doi: 10.1536/ihj.47.159.
9. Maehara A, Takagi A, Okura H, et al. Longitudinal plaque redistribution during stent expansion. Am J Cardiol. 2000; 86(10): 1069–1072, indexed in Pubmed: 11074201.
10. Kini AS, Motoyama S, Vengrenyuk Y, et al. Multimodality Intravascular Imaging to Predict Periprocedural Myocardial Infarction During Percutaneous Coronary Intervention. JACC Cardiovasc Interv. 2015; 8(7): 937–945, doi: 10.1016/j.jcin.2015.03.016, indexed in Pubmed: 26088511.
11. Goldstein JA, Maini B, Dixon SR, et al. Detection of lipid-core plaques by intracoronary near-infrared spectroscopy identifies high risk of periprocedural myocardial infarction. Circ Cardiovasc Interv. 2011; 4(5): 429–437, doi: 10.1161/CIRCINTERVENTIONS.111.963264, indexed in Pubmed: 21972399.
12. Roleder T, Kovacic JC, Ali Z, et al. Combined NIRS and IVUS imaging detects vulnerable plaque using a single catheter system: a head-to-head comparison with OCT. EuroIntervention. 2014; 10(3): 303–311, doi: 10.4244/EIJV10I3A53, indexed in Pubmed: 24769522.
13. Noori M, Thayssen P, Veien KT, et al. Lipid-core burden response to stent implantation assessed with near-infrared spectroscopy and intravascular ultrasound evaluation in patients with myocardial infarction. Cardiovasc Revasc Med. 2017; 18(3): 182–189, doi: 10.1016/j.carrev.2016.12.018, indexed in Pubmed: 28109718.
14. Porto I, Di Vito L, Burzotta F, et al. Predictors of periprocedural (type IVa) myocardial infarction, as assessed by frequency-domain optical coherence tomography. Circ Cardiovasc Interv. 2012; 5(1): 89–96, S1, doi: 10.1161/CIRCINTERVENTIONS.111.965624, indexed in Pubmed: 22298799.
15. Biały D, Wawrzyńska M, Arkowski J, et al. Multimodality imaging of intermediate lesions: Data from fractional flow reserve, optical coherence tomography, near-infrared spectroscopy-intravascular ultrasound. Cardiol J. 2018; 25(2): 196–202, doi: 10.5603/CJ.a2017.0082, indexed in Pubmed: 28714527.
16. Wolny R, Dębski A, Kruk M, et al. Slow-flow phenomenon after elective percutaneous coronary intervention of computed tomography-detected vulnerable coronary lesion. Postepy Kardiol Interwencyjnej. 2014; 10(3): 181–184, doi: 10.5114/pwki.2014.45145, indexed in Pubmed: 25489304.
17. Nishio R, Shinke T, Otake H, et al. Stabilizing effect of combined eicosapentaenoic acid and statin therapy on coronary thin-cap fibroatheroma. Atherosclerosis. 2014; 234(1): 114–119, doi: 10.1016/j.atherosclerosis.2014.02.025, indexed in Pubmed: 24637411.
18. Chia S, Raffel OC, Takano M, et al. Association of statin therapy with reduced coronary plaque rupture: an optical coherence tomography study. Coron Artery Dis. 2008; 19(4): 237–242, doi: 10.1097/MCA.0b013e32830042a8, indexed in Pubmed: 18480667.
19. Zhao JL, Yang YJ, Pei WD, et al. The effect of statins on the no-reflow phenomenon. Am J Cardiovasc Drugs. 2012; 9(2): 81–89, doi: 10.1007/bf03256579.
20. Stone GW, Maehara A, Muller JE, et al. CANARY Investigators. Plaque Characterization to Inform the Prediction and Prevention of Periprocedural Myocardial Infarction During Percutaneous Coronary Intervention: The CANARY Trial (Coronary Assessment by Near-infrared of Atherosclerotic Rupture-prone Yellow). JACC Cardiovasc Interv. 2015; 8(7): 927–936, doi: 10.1016/j.jcin.2015.01.032, indexed in Pubmed: 26003018.
21. Gardner CM, Tan H, Hull EL, et al. Detection of lipid core coronary plaques in autopsy specimens with a novel catheter-based near-infrared spectroscopy system. JACC Cardiovasc Imaging. 2008; 1(5): 638–648, doi: 10.1016/j.jcmg.2008.06.001, indexed in Pubmed: 19356494.
22. Waxman S, Freilich MI, Suter MJ, et al. A case of lipid core plaque progression and rupture at the edge of a coronary stent: elucidating the mechanisms of drug-eluting stent failure. Circ Cardiovasc Interv. 2010; 3(2): 193–196, doi: 10.1161/CIRCINTERVENTIONS.109.917955, indexed in Pubmed: 20407116.

VIA MEDICA

ORIGINAL ARTICLE

Cardiology Journal
2020, Vol. 27, No. 3, 246–253
DOI: 10.5603/CJ.a2019.0068

ISSN 1897–5593

Echocardiographic assessment of left atrial morphology and function to predict maintenance of sinus rhythm after electrical cardioversion in patients with non-valvular persistent atrial fibrillation and normal function or mild dysfunction of left ventricle

Paweł Wałek[1], Janusz Sielski[1, 3], Katarzyna Starzyk[2], Iwona Gorczyca[2], Joanna Roskal-Wałek[3], Beata Wożakowska-Kapłon[2, 3]

[1]Intensive Cardiac Care Unit, Swietokrzyskie Cardiology Center, Kielce, Poland
[2]Department of Cardiology and Electrotherapy, Swietokrzyskie Cardiology Center, Kielce, Poland
[3]Faculty of Medicine and Health Sciences, The Jan Kochanowski University, Kielce, Poland

Abstract

Background: *The aim of this study was to assess whether echocardiographic measurements of left atrial (LA) morphology and function could predict sinus rhythm maintenance after electrical cardioversion among patients with atrial fibrillation (AF) and normal function or mild dysfunction of the left ventricle (LV).*

Methods: *One hundred seventeen patients with persistent AF who underwent successful electrical cardioversion were prospectively enrolled. Echocardiography was performed one day subsequent to successful cardioversion. Patients were followed up clinically and electrocardiographically at 1, 6, and 12 months. At 12 months, 61 (52%) patients had maintained sinus rhythm (SR).*

Results: *Compared to patients who maintained SR, those with AF recurrence had larger LAs, worse LA systolic function, and increased LV filling pressure. On multivariate stepwise logistic regression, E/A ratios (odds ratio [OR] 0.550, 95% confidence interval [CI] 0.341–0.886; p = 0.014) and E/e' ratios (OR 0.871, 95% CI 0.771–0.985; p = 0.027) were significant predictors of AF recurrence. On receiver operator characteristic curve analysis of AF recurrence at 12 months, the area under curve for both E/A and E/e' ratios were 0.726. With an E/A cutoff of 2.2, the sensitivity for predicting AF recurrence at 12 months was 72%, and specificity was 73%. With an E/e' cutoff of 9.17, the sensitivity for predicting AF recurrence at 12 months was 72%, and specificity was 74%.*

Conclusions: *Left ventricular filling pressure assessed with E/A and E/e' ratios predict AF recurrence after electrical cardioversions among patients with AF and normal function of LV.* (Cardiol J 2020; 27, 3: 246–253)

Key words: atrial fibrillation, direct current cardioversion, diastolic dysfunction

Introduction

Atrial fibrillation (AF) is the most common arrhythmia, and it is caused by structural, mechanical, and electrical remodeling of the atria, including atrial enlargement, fibrosis, and dysfunction of ion channels [1–3]. Management of AF is aimed at restoration and maintenance of sinus rhythm (SR) or control of the ventricular rate [4]. In the Euro Heart Survey, the effectiveness of cardioversion

Address for correspondence: Paweł Wałek, MD, Intensive Cardiac Care Unit, Świętokrzyskie Cardiology Center, ul. Grunwaldzka 45, 25–736 Kielce, Poland, tel: +48 41 3671493, fax: +48 41 3671510, e-mail: pawel.walek@o2.pl
Received: 22.04.2019 Accepted: 9.06.2019

was about 75–88%, depending on the cardioversion method and patient characteristics. In the same registry, about 70% of patients maintained SR for 12 months [5]. AF recurs in many patients after successful cardioversion, and this recurrence is associated with different clinical, electrocardiographic, echocardiographic, imaging, and laboratory factors [2, 6–9]. Risk factors for recurrence of AF can help select patients in whom cardioversion can restore SR in the long-term. Moreover, patients with a very high risk of AF recurrence could avoid the risk of cardioversion. Under investigation, in this study, was whether assessing left atrial (LA) morphology and function by echocardiography could help predict the recurrence of AF after electrical cardioversion.

Methods

The study protocol was approved by the local ethics committee. This prospective study enrolled 117 patients with persistent AF who underwent direct current cardioversion between August 2015 and April 2017 on a cardiology ward. The inclusion criteria were as follows: symptomatic persistent AF for ≥ 7 days, ejection fraction > 40%, and effective anticoagulation with warfarin, acenocumarol, or novel oral anticoagulants (dabigatran, rivaroxaban, apixaban) for ≥ 3 weeks prior to cardioversion. The exclusion criteria were as follows: age < 18 years, no consent to participate in the study, no consent for cardioversion, low quality of echocardiographic images, moderate or severe valve regurgitation or stenosis, valvular prosthesis, presence of thrombus in the left atrial appendage (LAA), acute decompensation of heart failure, acute myocardial infarction, previous pulmonary vein isolation, dysthyroidism, anemia (hemoglobin < 6.9 mmol/L), and cancer.

Patients were followed up at 1, 6, and 12 months to check for maintenance of SR (electrocardiogram on each visit and 24-h Holter monitoring at 1 and 12 months). Patients were asked to report to the cardiology department if they felt palpitations or thought that AF had recurred.

Clinical data were obtained on the day of cardioversion and included age, sex, body mass index (BMI), body surface area (BSA, calculated with the Gehan and George formula), glomerular filtration rate (GFR, calculated with the Cockroft--Gault formula), hypertension, diabetes mellitus, dyslipidemia, smoking status, history of coronary artery disease, European Heart Rhythm Association (EHRA) score, dysthyroidism, obstructive pulmonary disease, renal disease, and history of stroke or transient ischemic attack. Coronary artery disease was diagnosed when patients had a history of myocardial infarction, percutaneous coronary intervention, or coronary artery by-pass grafting. Data regarding AF duration and duration of the current AF episode is not taken into account because of the high percentage of patients who were unable to ascertain the onset of arrhythmias. CHA_2DS_2-VASc and HAS-BLED scores were recorded according to the current European guidelines on AF treatment [4].

All cardioversions were performed with anaesthesiologic assistance under general sedation. All cardioversions were performed with a biphasic defibrillator (150–300 J). If the first shock was ineffective, another attempt was performed with a higher energy (by 100 J). The success of cardioversion was defined as SR maintenance for ≥ 24 h. Patients with SR received anticoagulants, up-stream therapy, or antiarrhythmic drugs by clinical judgment. Antiarrhythmic drugs, like amiodarone and propafenone, were prescribed by a physician blinded to echocardiography results.

Echocardiography was performed on the day after successful cardioversion, during SR. One experienced investigator performed transthoracic echocardiography with the Vivid S6 device (General Electric Medical Systems, Horten, Norway) and the M4S RS transducer, according to current guidelines [10, 11]. Standard M-mode and Doppler images and 2-dimentional cine loops were obtained in the parasternal long and short axis views and apical 2-, 3-, and 4-chamber views. Echocardiographic data were stored and analysed offline with the EchoPAC PC software (GE Medical Systems). The maximal end-systolic volume of left atrium (LAV) and minimal end-diastolic volume (LAEDV) were measured by the Simpson method from apical 4- and 2-chamber views. Maximum volume of LA (LAV) was measured at the end of systole, on the frame just before mitral valve opening, by tracing the inner border of the atrium and avoiding the area under the valve annulus, appendage, and pulmonary veins. LAV was indexed to body surface area (BSA, LAVI). Minimum volume of LA was measured at the end of ventricular diastole on the frame of the mitral valve closure, and was indexed to BSA (LAEDVI). LA emptying fraction (LA EF) was calculated with the following formula: (LA maximum volume – LA minimum volume)/LA maximum volume × 100%. Left ventricular (LV) volume and ejection fraction (LVEF) were measured according to the Simpson formula. The area

of right atrium at systole (RAAs) was measured in an apical 4-chamber view at the end of the systole, and the right atrium area at the diastole (RAAd) was measured at the end of the diastole on the frame with the tricuspid valve closure. Blood flow velocities were measured by transmitral pulsed wave Doppler (PWD) from the apical 4-chamber view, with a 2-mm sample volume placed between the tips of the mitral leaflets. Mitral annulus motion was measured by tissue Doppler imaging (TDI) in an apical 4-chamber view with a 5-mm sample volume at the lateral and septal basal regions. Means of waves s', e', and a' were calculated as averages from the septal and lateral measurements.

Statistical analysis

Results are presented as means ± standard deviations (SD). Categorical variables are presented as counts and percentages. Normally distributed variables were compared with the Student t-test, and non-normally distributed variables were compared with the Mann-Whitney test or χ^2 test.

Predictors of SR maintenance were analyzed with univariate logistic regression. To identify independent predictors of AF recurrence, a multivariable model that included independent variables with p value of < 0.1 found in univariate analysis and adjusted by important cofactors that might have an influence on outcomes was performed. The stepwise inclusion was set at $p < 0.05$ and exclusion at $p > 0.1$. Receiver-operated characteristic (ROC) curves for predicting SR maintenance at 1, 6, and 12 months were calculated for selected echocardiographic variables. Optimal cutoffs were calculated based on the Youden statistic, and areas under the curve (AUC) were compared with the DeLong test with the AUC that indicated no diagnostic values (0.5). Significance was set at $p < 0.05$. Statistical analyses were performed with MedCalc Statistical Software version 18.6 (MedCalc Software bvba, Ostend, Belgium).

Results

One hundred seventeen patients who underwent successful electrical cardioversion were included in the study. Of these patients, 56 (47.8%) maintained SR at 12 months. Compared with patients with AF recurrence, patients who maintained SR at 12 months were younger ($p = 0.027$), were more often male ($p = 0.024$), had diabetes mellitus more often ($p = 0.047$), had higher GFR values ($p = 0.043$), used beta-blockers more often before and after cardioversion ($p \leq 0.030$), and used diuretics less often before and after cardioversion ($p \leq 0.010$). There were no other significant differences in baseline characteristics between patients who maintained SR over 12 months and the remaining patients (Table 1).

Nearly all patients had LA enlargement, with a mean LAVI of 49.7 ± 11.4 mL/m^2 and low or moderate LA enlargement in the antero-posterior dimension (44.5 ± 4.7 mm). Compared with patients with AF recurrence, patients who maintained SR at 12 months had significantly lower values of LAVI ($p = 0.001$) and LAEDVI ($p < 0.001$).

Compared with patients with AF recurrence, patients who maintained SR at 12 months had a significantly higher LA EF ($p < 0.001$), atrial filling wave A ($p = 0.033$), and late diastolic mitral annular velocity (wave a', $p = 0.041$).

Compared with patients with AF recurrence, patients who maintained SR at 12 months had significantly lower E/e' ratios ($p < 0.001$), E/A ratios ($p < 0.001$), and early filling velocities (wave E, $p < 0.001$), and they had significantly higher early diastolic mitral annular velocities (wave e, $p = 0.008$) and deceleration times of wave E (DT, $p = 0.003$).

Patients with AF recurrence and patients who maintained SR at 12 months did not differ significantly with respect to LV function. However, patients who maintained SR at 12 months tended to have higher values of mitral annular peak systolic velocity (wave s', $p = 0.051$). Table 2 presents values for all echocardiographic variables.

On univariate logistic regression, the following echocardiographic variables were significant predictors of SR maintenance at 12 months: LAVI, LAEDVI, LA EF, waves s', e', and E, E/e' and E/A ratios, and DT (Table 3). On multivariate stepwise, forward, and backward logistic regression, only E/e' and E/A ratios remained significant predictors of SR maintenance. In ROC curve analysis, both E/e' and E/A ratios had a similar value for predicting SR maintenance at 1, 6, and 12 months, with AUCs of about 0.7 and sensitivity, specificity, and predictive values of about 70–75% (Figs. 1 and 2, Table 4). In ROC curve analysis of E/e' and E/A for predicting SR maintenance at 12 months of observation AUC of E/e' was 0,726 (95% confidence interval [CI] 0.630–0.822) and E/A was 0.726 (95% CI 0.632–0.821).

Discussion

In this study, it was shown that LV filling pressure and atrial enlargement were significant predic-

Table 1. Baseline characteristics.

	Study population; n = 117	SR maintenance; n = 61 (52%)	No SR maintenance; n = 56 (47.8%)	P
Age [years]	65 ± 10.4	62.984 ± 11.5593	67.196 ± 8.6811	0.027
Age < 65 years	48 (41%)	29 (47.5%)	19 (33.9%)	0.137
Age 65–74 years	51 (43.6%)	24 (39.3%)	27 (48.2%)	0.336
Age ≥ 75 years	18 (15.4%)	9 (14.8%)	9 (16.1%)	0.844
Male	73 (62.4%)	44 (72.1%)	29 (51.8%)	0.024
Body mass index [kg/m^2]	30.9±7.7	31.6±9.4	30.1±5.3	0.324
Hypertension	98 (83.8%)	50 (82%)	48 (85.7%)	0.585
Diabetes mellitus	22 (18.8%)	13 (21.3%)	9 (16.1%)	0.047
Coronary artery disease	18 (15.5%)	10 (16.4%)	8 (14.5%)	0.785
EHRA III–IV	38 (32.5%)	21 (34.4%)	17 (30.4%)	0.640
Stroke/TIA	10 (8.5%)	5 (8.2%)	5 (8.9%)	0.888
Vascular disease	13 (11.1%)	8 (13.1%)	5 (8.9%)	0.474
CHA_2DS_2-VASC	2.7 ± 1.5	2.6 ± 1.5	2.8 ± 1.6	0.230
CHA_2DS_2-VASC = 0	7 (6%)	3 (4.9%)	4 (7.1%)	0.614
CHA_2DS_2-VASC =1	22 (18.8%)	14 (23%)	8 (14.3%)	0.233
CHA_2DS_2-VASC ≥ 2	88 (75.2%)	44 (72.1%)	44 (78.6%)	0.422
HAS-BLED	0.7 ± 0.6	0.8 ± 0.5	0.9 ± 0.4	0.566
Smokers	7 (6%)	4 (6.6%)	3 (5.4%)	0.785
GFR [mL/min]	85.6 ± 31.1	91 ± 30	79.6 ± 31.4	0.043
Beta-blockers pre	107 (92.2%)	59 (98.3%)	48 (85.7%)	0.012
Amiodarone pre	13 (11.1%)	6 (9.8%)	7 (12.5%)	0.648
ACEI/ARB pre	99 (84.6%)	51 (83.6%)	48 (85.7%)	0.753
Statins pre	74 (63.8%)	42 (70%)	32 (57.1%)	0.152
Diuretics pre	48 (42.1%)	18 (30.5%)	30 (54.5%)	0.009
Spironolactone/ /eplerenone pre	25 (22.1%)	16 (27.1%)	9 (16.7%)	0.183
Beta-blockers post	91 (79.1%)	53 (86.9%)	38 (70.4%)	0.030
Amiodarone post	37 (32.2%)	19 (31.1%)	18 (33.3%)	0.803
Propafenone post	37 (32.2%)	20 (32.8%)	17 (31.5%)	0.882
ACEI/ARB post	99 (84.6%)	52 (85.2%)	47 (83.9%)	0.844
Statins post	73 (63.5%)	40 (65.6%)	33 (61.1%)	0.621
Diuretics post	49 (43%)	19 (31.7%)	30 (55.6%)	0.010
Spironolactone/ /eplerenone post	28 (25%)	17 (28.3%)	11 (21.2%)	0.384

ACEI — angiotensin converting enzyme inhibitors; ARB — angiotensin II receptor blockers; EHRA — European Heart Rhythm Association; GFR — glomerular filtration rate; pre — before cardioversion; post — after cardioversion; SR — sinus rhythm; TIA — transient ischemic attack

tors of SR maintenance after electrical cardioversion in patients with AF. Moreover, parameters of LV filling pressure were independent predictors of AF recurrence.

Although electrical cardioversion is effective in most patients with AF, high rates of AF recurrence are observed regardless of anti-arrhythmic therapy used. The current study investigated the relationship between echocardiographic parameters and AF recurrence after electrical cardioversion among patients with normal function of LV. Also in the present study, about half of the patients maintained SR over 12 months after a successful electrical cardioversion, which is similar to the figure from the Euro Heart Survey registry (61%) [5]. A slightly higher rate in the Euro Heart Survey could be because this registry included patients with first detected, paroxysmal, and persistent AF.

Table 2. Echocardiographic variables.

	Study population, n = 117	SR maintenance, n = 61 (52%)	No SR maintenance, n = 56 (47.8%)	P
RV prox [mm]	31.2 ± 3.8	31.7 ± 4.1	30.6 ± 3.5	0.224
IVS [mm]	10.8 ± 1.8	10.6 ± 1.7	11.1 ± 1.8	0.229
LVEDD [mm]	51.4 ± 6.5	51.9 ± 6.6	50.8 ± 6.4	0.351
LVESD [mm]	36 ± 7.8	36.8 ± 8.2	35.2 ± 7.4	0.292
LVEDV [mL]	133.8 ± 39.4	138.2 ± 38.6	128.7 ± 40	0.192
LVESV [mL]	56.2 ± 25	58.6 ± 26.6	53.7 ± 23.1	0.435
LVSV [mL]	77.6 ± 23.2	80.2 ± 21.5	74.8 ± 24.8	0.213
EF [%]	59.3 ± 9.6	59.2 ± 9.9	59.4 ± 9.4	0.896
LA AP [mm]	44.5 ± 4.7	44 ± 4.1	44.9 ± 5.2	0.281
LAVI [mL/m^2]	49.7 ± 11.4	46.6 ± 10.4	53.1 ± 11.5	0.001
LAEDV index [mL/m^2]	32.5 ± 11.2	28.8 ± 9.3	36.5 ± 11.7	< 0.001
LA EF [%]	35.9 ± 10.6	39 ± 8.4	32.5 ± 11.7	< 0.001
RAA s [cm^2]	22.8 ± 5	22.5 ± 5.3	23.1 ± 4.6	0.517
RAA d [cm^2]	15.7 ± 3.9	15.9 ± 3.9	15.6 ± 3.9	0.799
s' mean [cm/s]	6.5 ± 1.8	6.8 ± 1.9	6.2 ± 1.6	0.051
e' mean [cm/s]	9.4 ± 2.3	10 ± 2.3	8.8 ± 2.1	0.008
a' mean [cm/s]	5.1 ± 2.2	5.4 ± 2.1	4.8 ± 2.2	0.041
E/e' mean	10.3 ± 4	9 ± 3.5	11.8 ± 4.1	< 0.001
E [m/s]	0.9 ± 0.2	0.9 ± 0.2	1 ± 0.2	< 0.001
A [m/s]	0.4 ± 0.2	0.5 ± 0.2	0.4 ± 0.2	0.033
E/A	2.4 ± 1.1	2 ± 0.8	2.9 ± 1.3	< 0.001
DT [ms]	183.4 ± 42.7	193.9 ± 42.9	171.7 ± 39.6	0.003

SR — sinus rhythm; RV prox — right ventricular proximal diameter; IVS — interventricular septum wall thickness; LVEDD — left ventricular end-diastolic diameter; LVESD — left ventricular end-systolic diameter; LVEDV — left ventricular end-diastolic volume; LVESV — left ventricular end-systolic volume; LVSV — left ventricular stroke volume; EF — ejection fraction; LAAP — left atrium anteroposterior diameter; LAVI — end-systolic volume of left atrium indexed to body surface area; LAEDV — minimal end-diastolic volume; LA EF — emptying fraction of left atrium; RAA — right atrium area; d — diastolic; s — systolic; DT — deceleration times of wave E

Table 3. Echocardiographic predictors of sinus rhythm maintenance at 12 months.

	Univariate analysis			Multivariable stepwise analysis		
	OR	95% CI	P	OR	95% CI	P
LAVI [mL/m^2]	0.946	0.912–0.982	0.003			
LAEDVI [mL/m^2]	0.928	0.891–0.968	< 0.001			
LA EF [%]	1.066	1.025–1.109	0.002			
s' mean [cm/s]	1.252	1.003–1.564	0.047			
e' mean [cm/s]	1.258	1.057–1.497	0.010			
E [m/s]	0.056	0.008–0.389	0.004			
A [m/s]	10.402	0.995–108.754	0.051			
E/e' mean	0.815	0.724–0.916	0.001	0.871	0.771–0.985	0.027
E/A	0.421	0.266–0.667	< 0.001	0.550	0.341–0.886	0.014
DT [ms]	1.014	1.004–1.024	0.007			

CI — confidence interval; OR — odds ratio; LAVI — end-systolic volume of left atrium indexed to body surface area; LAEDVI — minimal end--diastolic volume indexed to body surface area; LA EF — left atrium emptying fraction; DT — deceleration times of wave E

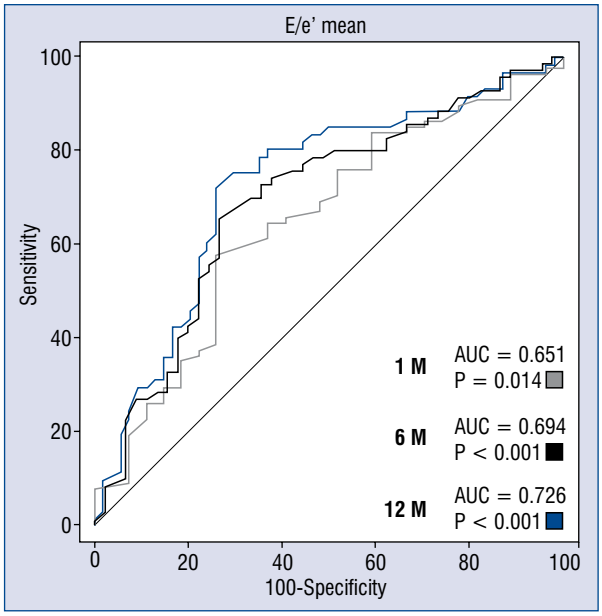

Figure 1. Prediction of sinus rhythm maintenance at 1, 6, and 12 months. Receiver operating characteristic curves for E/e' ratios. P values for AUC comparisons with no effect (AUC = 0.5, DeLong test); AUC — area under the curve; M — month.

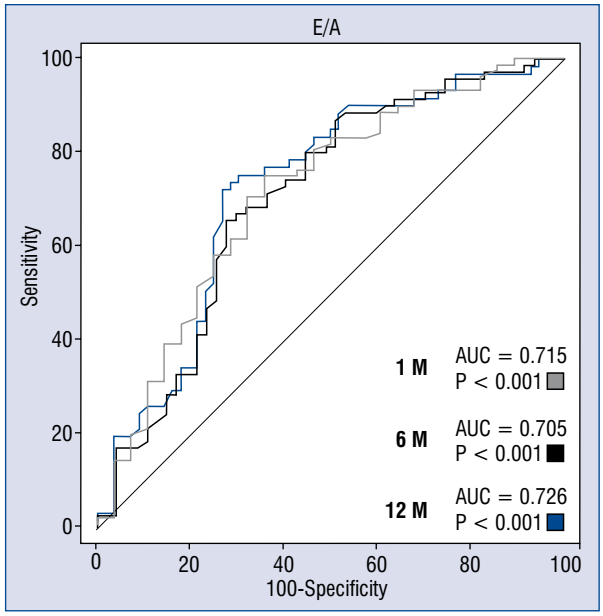

Figure 2. Prediction of sinus rhythm maintenance at 1, 6, and 12 months. Receiver operating characteristic curves for E/A ratios. P values for comparisons with no diagnostic vale (AUC = 0.5, DeLong test); AUC — area under the curve; M — month.

Table 4. Receiver operating curve analysis of E/A and E/e' ratios as predictors of sinus rhythm maintenance 12 months after electrical cardioversion.

Variable	AUC	Cutoff*	Sensitivity (%)	Specificity (%)	PPV (%)	NPV (%)
E/A	0.726	≤ 2.2	72.13	73.21	74.6	70.7
E/e'	0.726	≤ 9.17	72.1	74.1	75.9	70.2

*Cutoffs were calculated based on Youden's statistic; AUC — area under curve; NPV — negative predicting value; PPV — positive predicting value

In the current study, nearly all measures of LA size and systolic function and LV filling pressure were significant predictors of SR maintenance, this is in line with previous studies [2, 6–9, 12–19]. Importantly, it was found that echocardiographic measures of LV filling pressure were independent predictors of AF recurrence after electrical cardioversion. Similarly, several previous studies showed that E/e' ratios or E/A ratios were independent predictors of AF recurrences after cardioversion or pulmonary vain isolation [6, 14, 16, 17]. Although both E/e' and E/A ratios are measures of LV filling pressure, E/A values are more likely affected by loading status and thus depend on preload. In our study, E/A ratios predicted AF recurrence slightly better than E/e' (a higher odds ratio, but similar AUCs).

In the present study, patients regardless of LA size we included. Chung et al. [14] reported that E/e' ratios and LAVI were predictors of AF recurrence over 40 months in patients after pharmacological or electrical cardioversion, excluding patients with LA dimension > 50 mm [14]. Thus, LV filling pressure may be a predictor of AF even in patients with no visible structural remodeling. In the study by Chung et al. [14], an optimal E/e' cutoff for predicting AF recurrence (9.15) was very similar to that of the current study, with a similar sensitivity and specificity (75% and 73.1%, respectively). Those investigators did not analyse E/A ratios.

In another study, among 127 patients with LA enlargement and LAVI ≥ 34 mL/m^2, AF recurred

in 29% patients over 3 months [6]. In that study, septal E/e' ratios calculated during SR were the best predictor of AF recurrence after electrical cardioversion, with a cutoff ≥ 11 better than ≥ 8. In those patients with LA enlargement, LAVI was not a significant predictor of AF recurrence. Similarly, in another study, non-indexed LA volume and LA anteroposterior dimension did not differ between patients with maintenance of SR and AF recurrence [15].

Similar to our findings, Kosiuk et al. [17] showed that E/A ratios were an independent risk factor for AF recurrence within 1 week after pulmonary vein isolation, but not 3–12 months after the procedure. Supposedly, E/A ratios can predict AF recurrence only shortly after pulmonary vein isolation because atrial haemodynamic function may be reduced transiently after this procedure.

Most studies on the predictors of SR maintenance after cardioversion have concentrated on LV and LA. However, Luong et al. [13] showed that the emptying fraction of RA predicted SR after electrical cardioversion better than did the emptying fraction of LA. Moreover, in another study, these investigators showed that RAVI was a better predictor of sinus rhythm maintenance after electrical cardioversion than LAVI [18]. In contrast, RA area was not a significant predictor of SR maintenance in our study.

Our study was carried out in one centre and involved a small sample. However, our study is one of the largest studies to date on echocardiographic predictors of SR maintenance after electrical cardioversion of AF. When interpreting our results, one should remember that echocardiography is operator-dependent and requires experience and skill. Therefore, in our study, all echocardiographic measurements were taken by one experienced investigator. We carried out echocardiography after successful cardioversion during SR. Our current work is concentrated on finding echocardiographic predictors of SR maintenance that could be measured before cardioversion, i.e., during AF. In our study, we did not measure RA EF, which could be a predictor of SR maintenance after electrical cardioversion of AF. In this study, we did not analyse AF duration because we were not able to ascertain it reliably. AF is often asymptomatic or its symptoms can develop slowly [20, 21]. Many of our patients were unable tell when AF started. Lastly, heart rhythm monitoring was limited to a 24-h Holter, at months 1 and 12, and a 12-lead electrocardiogram at the remaining follow-up visits.

Conclusions

Increased LV filling pressure assessed with E/A and E/e' ratios may be an important risk factor for AF recurrence after successful electrical cardioversion. These findings are in line with previous research showing that increased filling pressure (septal E/e' ratios) is an independent predictor of mortality [19]. Our findings may help predict SR maintenance after electrical cardioversion, but further studies should investigate whether reducing E/A or E/e' ratios could improve the outcomes of electrical cardioversions or ablation among patients with AF.

Conflict of interest: None declared

References

1. Magnani JW, Rienstra M, Lin H, et al. Atrial fibrillation: current knowledge and future directions in epidemiology and genomics. Circulation. 2011; 124(18): 1982–1993, doi: 10.1161/CIRCULATIONAHA.111.039677, indexed in Pubmed: 22042927.
2. Vizzardi E, Curnis A, Latini MG, et al. Risk factors for atrial fibrillation recurrence: a literature review. J Cardiovasc Med. 2014; 15(3): 235–253, doi: 10.2459/JCM.0b013e328358554b, indexed in Pubmed: 23114271.
3. Goette A, Kalman J, Aguinaga L, et al. EHRA/HRS/APHRS/SOLAECE expert consensus on atrial cardiomyopathies: definition, characterization, and clinical implication. Europace. 2016; 18(10): 1455–1490, doi: 10.1093/europace/euw161.
4. Kirchhof P, Benussi S, Kotecha D, et al. 2016 ESC Guidelines for the management of atrial fibrillation developed in collaboration with EACTS. Europace. 2016; 18(11): 1609–1678, doi: 10.1093/europace/euw295.
5. Pisters R, Nieuwlaat R, Prins MH, et al. Clinical correlates of immediate success and outcome at 1-year follow-up of real-world cardioversion of atrial fibrillation: the Euro Heart Survey. Europace. 2012; 14(5): 666–674, doi: 10.1093/europace/eur406.
6. Fornengo C, Antolini M, Frea S, et al. Prediction of atrial fibrillation recurrence after cardioversion in patients with left-atrial dilation. Eur Heart J Cardiovasc Imaging. 2015; 16(3): 335–341, doi: 10.1093/ehjci/jeu193, indexed in Pubmed: 25274966.
7. Wożakowska-Kapłon B, Bartkowiak R. Biomarkers for prognosis in atrial fibrillation: unfulfilled hopes. Pol Arch Med Wewn. 2015; 125(6): 400–401, indexed in Pubmed: 26134392.
8. Bartkowiak R, Wożakowska-Kapłon B, Janiszewska G. Plasma NT-proANP in patients with persistent atrial fibrillation who underwent successful cardioversion. Kardiol Pol. 2010; 68(1): 48–54, indexed in Pubmed: 20131188.
9. Wożakowska-Kaplon B, Bartkowiak R, Janiszewska G. A decrease in serum aldosterone level is associated with maintenance of sinus rhythm after successful cardioversion of atrial fibrillation. Pacing Clin Electrophysiol. 2010; 33(5): 561–565, doi: 10.1111/j.1540-8159.2009.02673.x, indexed in Pubmed: 20059712.

10. Lang R, Badano L, Mor-Avi V, et al. Recommendations for Cardiac Chamber Quantification by Echocardiography in Adults: An Update from the American Society of Echocardiography and the European Association of Cardiovascular Imaging. Eur Heart J Cardiovasc Imaging. 2015; 16(3): 233–271, doi: 10.1093/ehjci/jev014.
11. Nagueh SF, Smiseth OA, et al. Appleton CP Recommendations for the Evaluation of Left Ventricular Diastolic Function by Echocardiography: An Update from the American Society of Echocardiography and the European Association of Cardiovascular Imaging. Eur Heart J Cardiovasc Imaging. 2016; 17(12): 1321–1360.
12. Toufan M, Kazemi B, Molazadeh N. The significance of the left atrial volume index in prediction of atrial fibrillation recurrence after electrical cardioversion. J Cardiovasc Thorac Res. 2017; 9(1): 54–59, doi: 10.15171/jcvtr.2017.08, indexed in Pubmed: 28451089.
13. Luong CL, Thompson DJS, Gin KG, et al. Usefulness of the atrial emptying fraction to predict maintenance of sinus rhythm after direct current cardioversion for atrial fibrillation. Am J Cardiol. 2016; 118(9): 1345–1349, doi: 10.1016/j.amjcard.2016.07.066, indexed in Pubmed: 27658922.
14. Chung H, Lee BK, Min PKi, et al. Left ventricular filling pressure as assessed by the e/e' ratio is a determinant of atrial fibrillation recurrence after cardioversion. Yonsei Med J. 2016; 57(1): 64–71, doi: 10.3349/ymj.2016.57.1.64, indexed in Pubmed: 26632384.
15. Wożakowska-Kapłon B, Opolski G. The dubious value of echocardiographic and plasma ANP measurements in predicting outcome of cardioversion in patients with persistent atrial fibrillation. Int J Cardiol. 2005; 103(3): 280–285, doi: 10.1016/j.ijcard.2004.08.062, indexed in Pubmed: 16098390.
16. Caputo M, Urselli R, Capati E, et al. Usefulness of left ventricular diastolic dysfunction assessed by pulsed tissue Doppler imaging as a predictor of atrial fibrillation recurrence after successful electrical cardioversion. Am J Cardiol. 2011; 108(5): 698–704, doi: 10.1016/j.amjcard.2011.04.018, indexed in Pubmed: 21723530.
17. Kosiuk J, Breithardt OA, Bode K, et al. The predictive value of echocardiographic parameters associated with left ventricular diastolic dysfunction on short- and long-term outcomes of catheter ablation of atrial fibrillation. Europace. 2014; 16(8): 1168–1174, doi: 10.1093/europace/eut415, indexed in Pubmed: 24569573.
18. Luong C, Thompson DJS, Bennett M, et al. Right atrial volume is superior to left atrial volume for prediction of atrial fibrillation recurrence after direct current cardioversion. Can J Cardiol. 2015; 31(1): 29–35, doi: 10.1016/j.cjca.2014.10.009, indexed in Pubmed: 25547547.
19. Okura H, Takada Y, Kubo T, et al. Tissue Doppler-derived index of left ventricular filling pressure, E/E', predicts survival of patients with non-valvular atrial fibrillation. Heart. 2006; 92(9): 1248–1252, doi: 10.1136/hrt.2005.082594, indexed in Pubmed: 16449507.
20. Strickberger SA, Ip J, Saksena S, et al. Relationship between atrial tachyarrhythmias and symptoms. Heart Rhythm. 2005; 2(2): 125–131, doi: 10.1016/j.hrthm.2004.10.042, indexed in Pubmed: 15851283.
21. Ziegler PD, Koehler JL, Mehra R. Comparison of continuous versus intermittent monitoring of atrial arrhythmias. Heart Rhythm. 2006; 3(12): 1445–1452, doi: 10.1016/j.hrthm.2006.07.030, indexed in Pubmed: 17161787.

VIA MEDICA

ORIGINAL ARTICLE

Cardiology Journal
2020, Vol. 27, No. 3, 254–261
DOI: 10.5603/CJ.a2018.0137

ISSN 1897–5593

Significance of congestive heart failure as a cause of pleural effusion: Pilot data from a large multidisciplinary teaching hospital

Piotr Korczyński[1], Katarzyna Górska[1], Damian Konopka[2], Dżamila Al-Haj[2], Krzysztof J. Filipiak[3], Rafał Krenke[1]

[1]Department of Internal Medicine, Pulmonary Diseases and Allergy, Medical University of Warsaw, Poland
[2]Students' Research Group "Alveolus", Medical University of Warsaw, Poland
[3]Department of Cardiology, Medical University of Warsaw, Poland

Abstract

Background: *Epidemiological data on the causes of pleural effusion (PE) are scarce. Data on the local prevalence of various causes of PE may play a crucial role in the management strategy of patients with PE. The aim of the study was to investigate the causes of PE and to assess 30-day mortality rate in unselected adult patients treated in a large, multidisciplinary hospital.*

Methods: *Retrospective analysis of medical records, including chest radiographs, of 2835 consecutive patients admitted to the hospital was performed. Radiograhic signs of PE were found in 195 of 1936 patients in whom chest radigraphs were available. These patients formed the study group.*

Results: *The leading causes of PE were as follows: congestive heart failure (CHF; 37.4%), pneumonia (19.5%), malignancy (15.4%), liver cirrhosis (4.2%) and pulmonary embolism. The cause of PE in 6.7% patients was not established. There was a significant predominance of small volume PE as compared to a moderate or large volume PEs (153, 28 and 14 patients, respectively). Almost 80% of patients with CHF presented with small volume PE, while almost 50% of patients with malignant PE demonstrated moderate or large volume PE. Thirty-day mortality rate ranged from 0% for tuberculous pleurisy to 40% for malignant PE (MPE).*

Conclusions: *Pleural effusion was found in 10.1% of patients treated in a large multidisciplinary hospital. CHF was the leading cause of PE. Although 30-day mortality in patients with CHF was relatively high, it was lower than that in parapneumonic PE and MPE.* (Cardiol J 2020; 27, 3: 254–261)

Key words: epidemiology, pleural effusion, congestive heart failure, pleuritic, pneumonia, tuberculosis, cancer

Introduction

Pleural effusion (PE) affects approximately 1.5 million patients per year in the United States [1]. This condition may be associated with a wide range of underlying diseases, including pneumonia, tuberculous pleurisy, malignancies, chronic heart failure, liver cirrhosis and many other diseases. Therefore, causative diagnosis in patients with PE is challenging and often requires not only a thorough clinical assessment but also the use of different imaging techniques, diagnostic thoracentesis with pleural fluid analysis, pleural biopsy and/or thoracoscopy. As some of the above procedures are relatively invasive, it is critically important to properly select patients who require comprehensive diagnostics. In this context, epidemiological data on the local prevalence of different causes of

Address for correspondence: Dr. Katarzyna Górska, Department of Internal Medicine, Pulmonary Diseases and Allergy, Medical University of Warsaw, ul. Banacha 1A, 02–097 Warszawa, Poland, tel: +48 22 599 25 62, fax: +48 22 599 15 60, e-mail: drkpgorska@gmail.com

Received: 29.08.2018 Accepted: 28.10.2018

PE may play a crucial role in the management strategy of patients with this condition. For instance, a predominance of benign and self-limited underlying diseases questions the necessity of more advanced diagnostic procedures in a significant proportion of patients with PE.

According to data from the United States, the most common cause of PE was congestive heart failure (CHF) — 36.3%, while the relative incidence of malignant (MPE) and tuberculous pleural effusion (TPE) among all patients with PE was 14.5% and 0.2%, respectively [1]. In contrast, a retrospective analysis of all patients with PE who underwent diagnostic thoracentesis over a 19-year period at a university hospital in Spain showed that malignancies and tuberculosis (TB) were responsible for approximately 2-fold, and 45-fold higher percentage than those reported in the United States (27.3% and 9%, respectively). In one fifth of 3077 patients with PE (20.8%), CHF was diagnosed as an underlying disease [2]. It was most prevalent in elderly patients (45% of all causes were in patients older than 80 years of age), while TB was the most common etiology in patients < 34 years of age (52% of all causes of PE in this age group) [2].

Comparison of the above studies demonstrates that the epidemiological data should be interpreted with caution, as they may show significant local variability. This is because they are affected by a number of factors, such as ethnicity, local burden of different diseases, age structure of the population and the availability and quality of a healthcare system. Tuberculous PE may serve as a good example. There are not only huge regional differences in the incidence rate of TB, but also significant differences in TB manifestations. In regions with low and intermediate TB incidence, only 2–5% of all TB patients present with TPE [3, 4]. On the other hand, in low income and high TB incidence countries the percentage of patients with TPE in TB patients can be as high as 22.8% and 68.8% [5, 6].

The undeniable progress in healthcare quality over the years has undoubtedly affected epidemiological data. The age adjusted death rate for the leading cause of mortality, i.e. cardiovascular diseases (CVDs), has decreased since 1993. The annual death rate for the second leading cause of mortality, i.e. lung cancer decreased from 91.1 in 1990 to 49.8 in 2015 [7]. Deaths from these two conditions accounted for as many as 45.3% of all deaths in the United States in 2015 [8].

Cardiovascular diseases have also been a leading cause of death in Poland. For a number of years, nearly half of all deaths have been caused by CVDs. Nonetheless, in the last few decades, a gradual decline in relative death rate from CVDs has been observed. At the same time a change in the relative contribution of deaths associated with coronary artery disease and CHF was noted, with a significant decline for the first and an increase for the latter [9]. Significant changes in the epidemiology of two other common causes of PE, i.e. TB and malignancies were also reported. In Poland, the relative incidence of TB pleurisy decreased from 2.7% to 1.9% between 2002 and 2006 and to 0.9% in 2015 [10]. Mortality due to breast cancer increased from 28.2 to 86.3 per 100,000 between 1980 and 2013. At the same time, lung cancer mortality increased from 29.6 to 56.0 over the same period [11].

According to available research, there are no current data on the etiology of PE effusion in Central and Eastern Europe. Therefore, a pilot study herein was undertaken on the causes of PE in all patients admitted to a large multidisciplinary teaching hospital.

The specific study objectives were as follows: (i) to determine the causes of PE in a non-selected group of patients admitted to a multidisciplinary teaching hospital located in a large urban area; (ii) to assess 30-day mortality in hospitalized patients with PE.

Methods

This retrospective cross-sectional study was performed at the Central Teaching Hospital of the Medical University of Warsaw, Poland. This is a multidisciplinary hospital with more than 1000 beds which provide medical services on different levels.

The study included all patients admitted to the hospital between January 1st and February 1st, 2017. Data were extracted from the Hospital Information System and Picture Archiving and Communication System (PACS). Chest radiographs of all patients were initially analyzed by two medical faculty students to identify all radiographs with radiological signs of PE. The findings were further confirmed by two pulmonologists, who also reviewed other imaging studies (e.g. computed tomography scans and thoracic ultrasound) of these patients. Only patients with pleural effusion confirmed by both pulmonologists were included in further analysis.

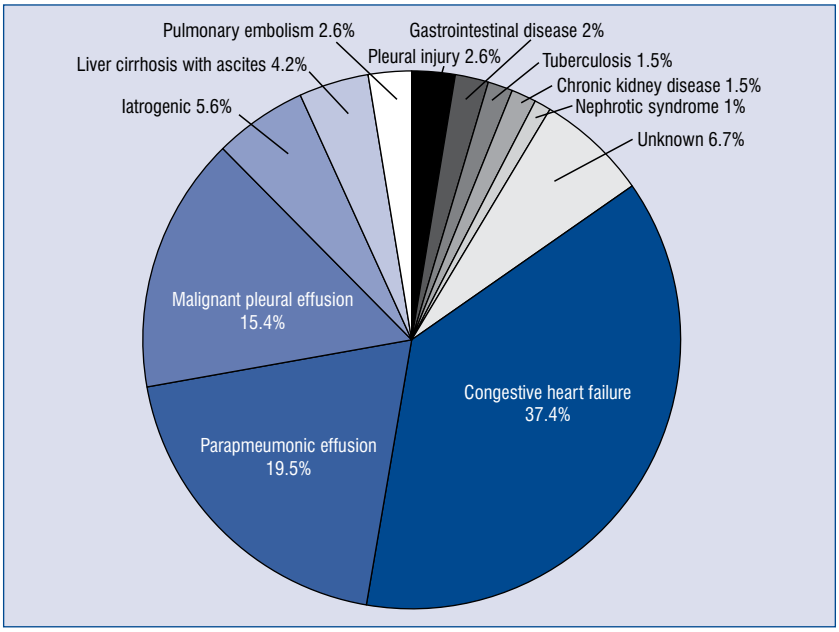

Figure 1. Percentage of patients with various causes of pleural effusion in the investigated group.

Cause of PE was determined by the analysis of medical data and reports, radiology and laboratory findings. Definitions and criteria used for the diagnosis of underlying diseases were consistent with those presented in the previous studies [12, 13]. Patients in whom the available data were insufficient to make a diagnosis, were allocated to the "undiagnosed pleural effusion" group. At the next stage, 30-day mortality was assessed with the date of the first chest radiograph with PE construed as day "zero".

Laterality and semiquantitative assessment of pleural fluid volume were based on chest radiographs performed in the erect position (standing or sitting). Pleural effusions were classified as small when occupied ≤ 1/3 of the ipsilateral hemithorax on plain chest radiograph, moderate when occupied between 1/3 and 2/3 of the hemithorax, and large when occupied more than 2/3 of the hemithorax.

Statistical analysis

Data are presented as median and interquartile ranges (IQR). The D'Agostino-Pearson test was used to assess normality of data distribution. Differences between continuous variables were tested using the Kruskal-Wallis or Mann-Whitney U test. Categorical variables were expressed as numbers and percentages and were compared using the Fisher exact test. All p values were 2-tailed and $p < 0.05$ was considered statistically significant. Statistical analysis was performed with MedCalc statistical software version 18.5 (MedCalc Software bvba, Ostend, Belgium).

Results

Four thousand one hundred and sixty-eight patients were admitted to the hospital between January 1st and February 1st, 2017. Almost 70% of these patients (2835) were admitted to non-surgical departments, while the remaining patients (1333) were admitted to surgical departments or intensive care unit. Chest radiographs were performed in 1936 patients and in 220 of these, radiographic signs of PE were initially identified. The initial findings were further verified by pulmonary specialists and 195 patients with chest radiographs demonstrating PE were eventually selected.

The most common cause of pleural effusion was heart failure, which accounted for 37.4% of cases. The second most common cause was parapneumonic effusion (19.5%) and the third was malignant pleural involvement (15.4%). Detailed data on PE etiology are presented in Figure 1.

The median age of patients with PE caused by CHF was 80 (IQR 70–87) years and was significantly higher than that of patients with parapneumonic pleural effusion (PPE) and MPE, $p = 0.01$. Thirty-day mortality in CHF was 19.2%, and this percentage was 9.7% lower than in PPE

Table 1. Comparative analysis of patients with various causes of pleural exudate.

	PPE (n = 38)	TPE (n = 3)	MPE (n = 30)	Others (n = 9)	P
Sex: male/female	17 (44.7%)/ /21 (55.3%)	3 (100%)/ /0 (0%)	14 (46.7%)/ /16 (53.3%)	3 (33.3%)/ /6 (66.7%)	0.2
Age [years]*	76.5 (67–89.3)	44 (29.7–50)	70.3 (62.25–79.5)	69.9 (56–81)	0.014**
30-day mortality	11 (28.9%)	0 (0%)	12 (40.0%)	1 (11.1%)	0.27
Affected side: L/R/B	10 (26.3%)/17 (44.7%)/11 (28.9%)	1 (33.3%)/2 (66.6%)/0 (0%)	8 (26.7%)/15 (50%)/7(23.3%)	1 (11.1%)/7 (77.8%)/1 (11.1%)	0.6377

*Results presented as median (interquartile range); **Significant difference between PPE vs. TPE (p = 0.024); B — bilateral; L — left; MPE — malignant pleural effusion; PPE — parapneumonic pleural effusion; R — right; TPE — tuberculous pleural effusion

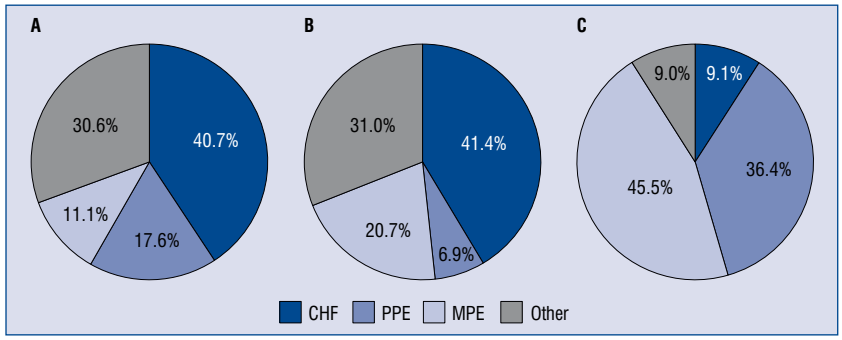

Figure 2. Distribution of underlying causes of pleural fluid formation in patients with small (n = 158; **A**), moderate (n = 28; **B**) and large (n = 14; **C**) volume of pleural effusion; CHF — congestive heart failure; MPE — malignant pleural effusion; PPE — parapneumonic pleural effusion.

(p = 0.24) and 21.8% lower than in MPE (p = 0.027). Comparative analysis of patients with the most common causes of pleural exudate did not reveal significant differences in terms of gender distribution and 30-day mortality. Patients with TPE were significantly younger than patients with PPE, p = 0.024. There was also a relevant (although statistically insignificant) difference between the age of TPE and PPE patients (Table 1).

The vast majority of patients (n = 153) presented with small volume of pleural fluid. The most common causes of PE in patients with small amount of fluid were CHF 40.7%, PPE (17.6%), and MPE (11.1%), p < 0.0001 (Fig. 2). Similarly, in patients with moderate volume pleural effusion CHF (41.4%) was also the most common underlying disease, followed by MPE (20.7%), and PPE (6.9%), p = 0.02. There were only 14 patients with large volume pleural effusion and the differences between the number of patients with other underlying diseases did not reach statistical significance.

There was a significantly uneven distribution of PE volume in patients with CHF and PPE, with a marked predominance (77.2%) of small volume of pleural fluid. Even though over half of the patients with MPE were found to have a small amount of PE, 47.8% of these patients had a moderate to large volume of pleural fluid (Fig. 3).

The prevalence of CHF, MPE and PPE in relation to pleural fluid volume and its localization (unilateral or bilateral) is shown in Table 2.

Discussion

The present analysis of chest radiographs and medical records of almost 2000 patients treated in one of the largest multidisciplinary hospitals in Poland showed that PE was present in 10.1% of patients. The most common cause of PE was heart failure (37.4%), followed by parapneumonic (19.5%) and malignant (15.4%) effusion. Importantly, CHF alone was responsible for a number of cases comparable to the summed number of cases caused by the three other of the most common entities associated with PE, i.e. parapneumonic pleural effusion, pleural malignancies and hepatic hydrothorax (73 vs. 76 patients, respectively). Thus, these results emphasize the role of CHF as

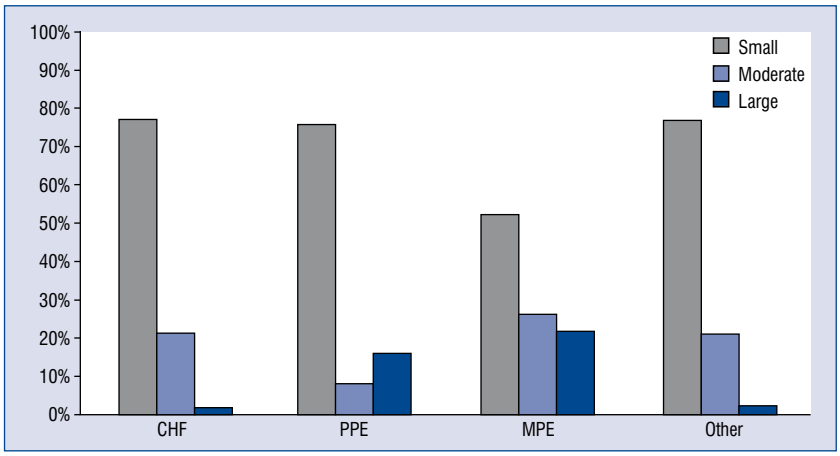

Figure 3. Differences between distribution of pleural fluid volume in patients with various causes of pleural effusion; CHF — congestive heart failure; MPE — malignant pleural effusion; PPE — parapneumonic pleural effusion.

Table 2. The percentage of patients with unilateral and bilateral pleural effusion and various effusion causes (congestive heart failure, parapneumonic effusion and malignant pleural effusion) in relation to pleural fluid volume (small, moderate and large). Percentages form 100% in each pleural fluid volume category (small, moderate and large).

	Pleural fluid volume								
	Small			Moderate			Large		
	UL	B	p	UL	B	p	UL	B	p
CHF	28%	31%	**0.05**	30%	30%	0.79	10%	0%	0.85
PPE	17%`	8%		5%	5%		30%	10%	
MPE	13%	3%		20%	10%		40%	10%	

B — bilateral; CHF — congestive heart failure; MPE — malignant pleural effusion; PPE — parapneumonic pleural effusion; UL — unilateral

the most common underlying disease in patients with PE and indicate that CHF should be a major differential diagnosis in these patients. It was also observed that almost 80% of patients with CHF presented with only a small volume PE.

According to available research, this is the most recent and one of the very few studies from Central or Eastern Europe presenting epidemiological data on the causes of PE. In fact, the previous study which evaluated the incidence of PE in a well-defined region of Central Bohemia was published 25 years ago. Although there were numerous differences between the current study and a study by Marel et al. [14], both studies showed that CHF was, and still is, the most common cause of PE in Central Europe.

Several important studies on the causes of PE have been performed in other countries and world regions. In 2014, Porcel et al. [2] published the results of a Spanish study which included data on 3007 patients who underwent diagnostic thoracentesis during the previous 19 years. The authors found that the most common cause of pleural fluid were pleural malignancies (27.3%), while heart failure was the second leading cause responsible for 20.8% of cases [2]. Chronic heart failure is believed to be the most common cause of PE in the United States. The estimated annual incidence of various causes of PE in this country showed that CHF was responsible for 36.3% of cases [1]. Pleural effusion associated with CHF was 1.7 and 2.5-fold more common than PPE and MPE, respectively [1]. The differences between the results of various studies are multifactorial and were related not only to local epidemiological situations and study group characteristics, but also to the definitions and methods used in the particular studies. For instance, only patients who underwent diagnostic thoracentesis were included in the study by Porcel et al. [2]. This obviously may result in selection

Table 3. Comparison of data on causes of pleural effusion presented by various authors.

Disease	Light et al. [1] (2011) N = 1,377,500	Porcel et al. [2] (2014) N = 3077	Korczynski et al. (current study) N = 195
Congestive heart failure	36.3%	20.8%	37.4%
Parapneumonic effusion	21.8%	18.9%	19.5%
Malignant pleural effusion	14.5%	27.3%	15.4%
Pulmonary embolism	10.9%	1.6%	2.6%
Liver cirrhosis with ascites	3.6%	3.2%	4.2%
Gastrointestinal disease	1.8%	3.6%	2.0%
Tuberculosis	0.2%	8.9%	1.5%
Post-CABG surgery	3.6%	1.0%	NA
Pleural injury	NA	2.5%	2.6%
Other	7.3%	9.1%	8.1%
Unknown	NA	3.1%	6.7%

CABG — coronary artery bypass grafting; NA — not applicable

bias, as according to common guidelines, not all patients with PE due to heart failure require diagnostic thoracentesis [15]. On the other hand, a high level of agreement between different studies in terms of the three most common causes of PE should be noted. The numerical data found in the present study is fully consistent with United States data published by Light [1]. To show this agreement, data from three different publications are presented in Table 3.

A significant proportion of patients with PE due to CHF may have various practical implications. Although a diagnostic thoracentesis to differentiate between transudate and exudate is necessary only in a small proportion of these patients, the high overall number of patients with PE due to CHF may result in a significant number of patients undergoing the procedure. In this context, it should be remembered that Light's criteria were commonly applied to differentiate between transudate and exudate and were only moderately specific for exudate. Hence, even more than 20% of transudates (mainly due to CHF) can be incorrectly classified as exudates [16]. Therefore, additional criteria distinguishing between pleural transudate and exudate have been proposed for patients with suspicion of CHF-related PE which was classified as exudate by Light's criteria. These include pleural fluid-serum albumin gradient and pleural fluid or serum N-terminal pro-B-type natriuretic peptide levels [17–19]. It should also be noted that, in spite of a high diagnostic sensitivity of Light's criteria for PE, some MPEs can be diagnosed as transudates. In a study by Ferreiro et al. [20] 26/281 (9.3%) of pleural transudates were caused by malignancies.

Due to the anatomical and functional relationships, PE in patients with CHF is mainly related to left ventricular failure. Also, the number of patients with left ventricular dysfunction or dysfunction of both ventricles is significantly higher than the number of patients with right ventricular failure [21]. Therefore, in daily clinical practice, the vast majority of PEs in patients with CHF is related to left ventricular dysfunction. Nonetheless, PE may also be associated with right ventricular failure. Tang et al. [22] found PE in 19 of 147 patients (13%) with isolated right heart failure due to idiopathic or familial pulmonary hypertension.

The prevalence of PE depends on the sensitivity of methods used to detect pleural fluid. As the majority of patients with CHF-related PE have small volume effusions, the sensitivity of imaging methods may significantly affect the results of studies on PE in CHF. It has been shown that plain chest radiograph (CXR) revealed PE only in 25% of patients in a series of 447 patients with heart failure [23]. On the other hand, the use of more sensitive tools, such as computed tomography, ultrasound or autopsy resulted in a much higher reported PE prevalence (even more than 80%) [24–26].

As mentioned above, the volume of CHF-related PE is usually small. This was also the case in the present study. More than 77% of patients with PE due to CHF presented with only small volume of pleural fluid. These results are consistent with data published by Porcel and Vives [27].

In the current study 51% of patients with PE due to CHF presented with bilateral pleural fluid. This number is lower than that reported in previous studies. Woodring et al. [28] found bilateral pleural involvement in 72.5% of patients with pleural effusion due to CHF. Also, the study by Porcel and Vives [27] published in 2006 showed virtually the same percentage of patients with bilateral pleural effusion (70%). On the other hand, later studies by Porcel [29] and de Araujo et al. [30] reported that the percentages of patients with bilateral PE were only slightly higher than demonstrated in the present study (61% and 51%, respectively). Again, the differences between the results of these studies can probably be largely attributed to methods of pleural fluid detection.

In the present study, 30-day mortality rate in patients with various causes of PE ranged from 0% to 40%. Thirty-day mortality rate for CHF was 19.2%. This number seems to be high when compared to data published by Maggioni et al. [31] or Tyminska et al. [32]. These authors reported 1-year mortality rate in all patients admitted to hospital for acute HF 17.4% and 13–21%, respectively. However, there were many differences between the studies that may have been responsible for the fact that the 30-day mortality rate in the current study was not comparable to 1-year mortality rate in studies by Maggioni et al. [31] and Tyminska et al. [32]. These include a primarily lower age with a median of 71 (IQR 61–79) years and selection of all patients with acute HF. What is worth emphasizing, pulmonary congestion was an independent predictor of all-cause 1-year mortality with a hazard ratio (95% confidence interval): 2.73 (1.71–4.35) [31]. It is suspected that the present results remain in agreement with previously cited studies and the presence of PE in heart failure patients is a negative prognostic factor.

Limitations of the study

There are some limitations in the present study. First, data for analysis were collected from only 1 month during winter. Hence, although the total number of patients in whom CXR was performed was almost 2000, the number of patients with PE was relatively low in the context of an epidemiological study [31]. Furthermore, there might have been a bias in the true annual proportion of patients with different causes of PE related to seasonal infections [33]. Second, CXR was the only tool to select patients with PE. It may be supposed that the use of more sensitive tools could have resulted in an even higher percentage of patients with a diagnosis of small volume PE. Third, this study included only hospitalized patients. This probably refers also to patients with CHF, as many of these patients did not require diagnostic thoracentesis and could have been be treated as outpatients [34]. Finally, the present results could have been affected by the profile of hospital departments and predominating spectrum of their patients.

Conclusions

Pleural effusion was found in 10.1% of patients treated in a large multidisciplinary hospital. CHF was responsible for 37.4% of all cases. Almost 80% of patients with CHF-related PE presented with only a small volume of pleural fluid. Although 30-day mortality in patients with CHF with PE was relatively high, it was lower than that in PPE and MPE.

Conflict of interest: None declared

References

1. Light RW. Pleural effusions. Med Clin North Am. 2011; 95(6): 1055–1070, doi: 10.1016/j.mcna.2011.08.005, indexed in Pubmed: 22032427.
2. Porcel JM, Esquerda A, Vives M, et al. Etiology of pleural effusions: analysis of more than 3,000 consecutive thoracenteses. Arch Bronconeumol. 2014; 50(5): 161–165, doi: 10.1016/j.arbres.2013.11.007, indexed in Pubmed: 24360987.
3. Baumann MH, Nolan R, Petrini M, et al. Pleural tuberculosis in the United States: incidence and drug resistance. Chest. 2007; 131(4): 1125–1132, doi: 10.1378/chest.06-2352, indexed in Pubmed: 17426219.
4. Porcel JM. Advances in the diagnosis of tuberculous pleuritis. Ann Transl Med. 2016; 4(15): 282, doi: 10.21037/atm.2016.07.23, indexed in Pubmed: 27570776.
5. Mortazavi-Moghaddam SG, Sharifzadeh GR, Rezvani MR. Status of Exudative Pleural Effusion in Adults of South Khorasan Province, Northeast Iran: Pleural Tuberculosis Tending toward Elderly. Iran J Med Sci. 2016; 41(4): 322–327, indexed in Pubmed: 27365554.
6. Rafiee S, Besharat S, Jabbari A, et al. Epidemiology of tuberculosis in Northeast of Iran: a population-based study. Iran J Med Sci. 2015; 34(3): 193–197.
7. U.S. Cancer Statistics Working Group. U.S. Cancer Statistics Data Visualizations Tool, based on November 2017 submission data (1999-2015): U.S. Department of Health and Human Services, Centers for Disease Control and Prevention and National Cancer Institute;. www.cdc.gov/cancer/dataviz(Accessed June 2018).
8. Murphy SL, Xu J, Kochanek KD, et al. Deaths: Final Data for 2015. Natl Vital Stat Rep. 2017; 66(6): 1–75.
9. Cierniak-Piotrowska M, Marciniak G, Stanczuk J. Statystyka Zgonow i Umieralnosci Z Powodu Chorob Układu Krazenia. In: Strzelecki Z, Szymborski J, editors. Zachorowalnosc i umieral-

nosc na choroby ukladu krazenia a sytuacja demograficzna Polski: Rzadowa Rada Ludnosci. 2015.
10. Korzeniowska-Kosela M. Gruzlica w Polsce w 2016 roku. Biuletyn IGiChP. 2016.
11. Didkowska J, Wojciechowska U. Zachorowania i zgony na nowotwory zlosliwe w Polsce. Krajowy Rejestr Nowotworow, Centrum Onkologii - Instytut im. Marii Sklodowskiej-Curie. http://onkologia.org.pl/k/epidemiologia (Accesed June 2018).
12. Krenke R, Nasilowski J, Korczynski P, et al. Incidence and aetiology of eosinophilic pleural effusion. Eur Respir J. 2009; 34(5): 1111–1117, doi: 10.1183/09031936.00197708, indexed in Pubmed: 19386682.
13. Klimiuk J, Krenke R, Safianowska A, et al. Diagnostic performance of different pleural fluid biomarkers in tuberculous pleurisy. Adv Exp Med Biol. 2015; 852: 21–30.
14. Marel M, Zrůstová M, Stasný B, et al. The incidence of pleural effusion in a well-defined region. Epidemiologic study in central Bohemia. Chest. 1993; 104(5): 1486–1489, indexed in Pubmed: 8222812.
15. Hooper C, Lee YC, Maskell N. Investigation of a unilateral pleural effusion in adults: British Thoracic Society Pleural Disease Guideline 2010. Thorax. 2010; 65 Suppl 2: ii4–i17, doi: 10.1136/thx.2010.136978, indexed in Pubmed: 20696692.
16. Porcel JM. Pearls and myths in pleural fluid analysis. Respirology. 2011; 16(1): 44–52, doi: 10.1111/j.1440-1843.2010.01794.x, indexed in Pubmed: 20573057.
17. Bielsa S, Porcel JM, Castellote J, et al. Solving the Light's criteria misclassification rate of cardiac and hepatic transudates. Respirology. 2012; 17(4): 721–726, doi: 10.1111/j.1440-1843.2012.02155.x, indexed in Pubmed: 22372660.
18. Han ZJ, Wu XD, Cheng JJ, et al. Diagnostic Accuracy of Natriuretic Peptides for Heart Failure in Patients with Pleural Effusion: A Systematic Review and Updated Meta-Analysis. PLoS One. 2015; 10(8): e0134376, doi: 10.1371/journal.pone.0134376, indexed in Pubmed: 26244664.
19. Porcel J. Identifying transudates misclassified by Light's criteria. Current Opinion in Pulmonary Medicine. 2013; 19(4): 362–367, doi: 10.1097/mcp.0b013e32836022dc.
20. Ferreiro L, Gude F, Toubes ME, et al. Predictive models of malignant transudative pleural effusions. J Thorac Dis. 2017; 9(1): 106–116, doi: 10.21037/jtd.2017.01.12, indexed in Pubmed: 28203412.
21. Ponikowski P, Voors A, Anker S, et al. 2016 ESC Guidelines for the diagnosis and treatment of acute and chronic heart failure: The Task Force for the diagnosis and treatment of acute and chronic heart failure of the European Society of Cardiology (ESC). Developed with the special contribution of the Heart Failure Association (HFA) of the ESC. Eur J Heart Fail. 2016; 18(8): 891–975, doi: 10.1002/ejhf.592.
22. Tang KJ, Robbins IM, Light RW. Incidence of pleural effusions in idiopathic and familial pulmonary arterial hypertension patients. Chest. 2009; 136(3): 688–693, doi: 10.1378/chest.08-0659, indexed in Pubmed: 19395582.
23. Knudsen CW, Omland T, Clopton P, et al. Diagnostic value of B-Type natriuretic peptide and chest radiographic findings in patients with acute dyspnea. Am J Med. 2004; 116(6): 363–368, doi: 10.1016/j.amjmed.2003.10.028, indexed in Pubmed: 15006584.
24. Kataoka H. Pericardial and pleural effusions in decompensated chronic heart failure. Am Heart J. 2000; 139(5): 918–923, indexed in Pubmed: 10783228.
25. Kataoka H, Takada S. The role of thoracic ultrasonography for evaluation of patients with decompensated chronic heart failure. J Am Coll Cardiol. 2000; 35(6): 1638–1646, indexed in Pubmed: 10807471.
26. Edwards JE, Race GA, Scheifley CH. Hydrothorax in congestive heart failure. Am J Med. 1957; 22(1): 83–89, indexed in Pubmed: 13381740.
27. Porcel JM, Vives M. Distribution of pleural effusion in congestive heart failure. South Med J. 2006; 99(1): 98–99, doi: 10.1097/01.smj.0000199278.81401.2f, indexed in Pubmed: 16466136.
28. Woodring LA, Cancelli AA, Ponterotto JG, et al. A qualitative investigation of adolescents' experiences with parental HIV/AIDS. Am J Orthopsychiatry. 2005; 75(4): 658–675, doi: 10.1037/0002-9432.75.4.658, indexed in Pubmed: 16262522.
29. Porcel J. Pleural effusions from congestive heart failure. Semin Respir Crit Care Med. 2011; 31(06): 689–697, doi: 10.1055/s-0030-1269828.
30. de Araujo BS, Reichert R, Eifer DA, et al. Trepopnea may explain right-sided pleural effusion in patients with decompensated heart failure. Am J Emerg Med. 2012; 30(6): 925–931.e2, doi: 10.1016/j.ajem.2011.04.013, indexed in Pubmed: 21665407.
31. Maggioni AP, Dahlström U, Filippatos G, et al. EURObservational Research Programme: regional differences and 1-year follow-up results of the Heart Failure Pilot Survey (ESC-HF Pilot). Eur J Heart Fail. 2013; 15(7): 808–817, doi: 10.1093/eurjhf/hft050, indexed in Pubmed: 23537547.
32. Tymińska A, Kapłon-Cieślicka A, Ozierański K, et al. Anemia at Hospital Admission and Its Relation to Outcomes in Patients With Heart Failure (from the Polish Cohort of 2 European Society of Cardiology Heart Failure Registries). Am J Cardiol. 2017; 119(12): 2021–2029, doi: 10.1016/j.amjcard.2017.03.035, indexed in Pubmed: 28434647.
33. Kim ES, Park KU, Lee SH, et al. Comparison of viral infection in healthcare-associated pneumonia (HCAP) and community-acquired pneumonia (CAP). PLoS One. 2018; 13(2): e0192893, doi: 10.1371/journal.pone.0192893, indexed in Pubmed: 29447204.
34. Mirra M, Vitulano G, Virtuoso N, et al. Heart Failure in a Dedicated Outpatient Clinic: Results after 58 Month Follow-Up. Can it be Enough? Transl Med UniSa. 2015; 11: 59–62, indexed in Pubmed: 25674552.

VIA MEDICA

ORIGINAL ARTICLE

Cardiology Journal
2020, Vol. 27, No. 3, 262–271
DOI: 10.5603/CJ.a2018.0097

ISSN 1897–5593

Association between mild thyroid dysfunction and clinical outcome in acute coronary syndrome undergoing percutaneous coronary intervention

Qian Cao, Yundi Jiao, Tongtong Yu, Zhaoqing Sun

Department of Cardiology, Shengjing Hospital of China Medical University, Shenyang, Liaoning, P.R. China

Abstract

Background: *Thyroid hormones profoundly influence the cardiovascular system, but the effects of mild thyroid dysfunction on the clinical outcome of acute coronary syndrome (ACS) patients undergoing percutaneous coronary intervention (PCI) are not well defined. This study aimed to determine the effect of mild thyroid dysfunction on 12-month prognosis in ACS patients undergoing PCI.*

Methods: *In this prospective cohort study with a 12-month follow-up, 1560 individuals were divided into four groups based on thyroid hormone levels upon admission: euthyroidism (used as a reference group), subclinical hypothyroidism, subclinical hyperthyroidism, and low triiodothyronine syndrome (low T3 syndrome). The outcomes measured were all-cause mortality, cardiac mortality, nonfatal reinfarction, and unplanned repeat revascularization.*

Results: *In this study, the prevalence of mild thyroid dysfunction was 10.8%. Multivariate analysis showed that low T3 syndrome, but not subclinical hypothyroidism or subclinical hyperthyroidism, was associated with a higher rate of all-cause (HR 2.553, 95% CI 1.093–5.964, p = 0.030) and cardiac mortality (HR 2.594, 95% CI 1.026–6.559, p = 0.034), compared with the euthyroidism group.*

Conclusions: *Mild thyroid dysfunction was frequent in patients with ACS undergoing PCI. Low T3 syndrome was the predominant feature and was associated with 12-month adverse outcomes in these patients.* (Cardiol J 2020; 27, 3: 262–271)

Key words: mild thyroid dysfunction, clinical outcome, acute coronary syndrome, percutaneous coronary intervention

Introduction

Patients with acute coronary syndrome (ACS) frequently have a poor prognosis, and ACS is a major health and economic burden [1–4]. Although the use of percutaneous coronary intervention (PCI) and new antiplatelet drugs have greatly improved the prognosis [5], patients with ACS still suffer high rates of mortality (up to 5%) and heart failure (up to 20%) [6]. Thyroid hormones act on multiple systems within the body, and the cardiovascular system is the foremost target [7]. The cardiovascular system may be adversely affected even if thyroid hormone levels only change slightly [7]. In patients with ACS, a decrease in serum triiodothyronine (T3), as well as the impaired conversion of thyroxine (T4) into T3, have been reported [8, 9]. Thyroid hormone related indicators are also predictors for thrombus burden [10], severity of coronary artery lesions [11, 12], cardiac function [13, 14] and myocardial injury size [8, 9, 15] in ACS patients. However, the screening and treatment of mild thyroid dysfunction is still controversial [16–20] and not recommended for ACS patients [1–4]. However, mild thyroid dysfunction, including subclinical hypothyroidism, subclinical hyperthyroidism, and euthyroid sick syndrome, is frequently present in patients with ACS [21–23]. Additionally, mild thyroid dysfunction can also be

Address for correspondence: Dr. Zhaoqing Sun, Department of Cardiology, Shengjing Hospital of China Medical University, Shenyang, Liaoning, P.R. China, tel: 86-24-9661522211, fax: 86-24-9661522211, e-mail: sunzhaoqing@vip.163.com

Received: 12.02.2018 Accepted: 2.08.2018

predicative of an increased risk of mortality in heterogeneous patients with various cardiac diseases [21]. However, few studies have focused on the association between mild thyroid dysfunction and adverse prognoses in patients with coronary heart disease [22, 23]. In this study, the aim was to assess the prevalence of mild thyroid dysfunction and the association of mild thyroid dysfunction with 12-month prognosis in ACS patients undergoing PCI.

Methods

Study design and setting

This study was based on a prospective cohort, the P-PUSH study, which has been previously described [24]. In brief, from January 1, 2015 to July 31, 2016, 1768 patients with ACS were hospitalized and underwent PCI at a large hospital in Northeast China (Shengjing Hospital of China Medical University, Shenyang, China). Clinical and procedural data were obtained by the investigators using electronic medical records, interventional imaging data (Picture Archiving and Communications Systems [PACS] technology), and operation records. GRACE scores were determined as defined previously [1–4]. Prospective clinical follow-up after discharge was performed regularly in all cases by direct hospital visits and telephone interviews with the patient's general practitioner/cardiologist, the patient, or the patient's family. All events were adjudicated and classified by two cardiologists. The exclusion criteria of this study were as follows: 1) primary hypothyroidism or hyperthyroidism (36 cases); 2) concomitant treatment with synthetic thyroid hormones, antithyroid drugs, corticosteroids, dopamine, dobutamine, or amiodarone (19 cases); 3) loss of follow-up (68 cases); 4) no thyroid data (20 cases); and 5) atypical thyroid status (65 cases), including high T4 syndrome (12 cases), low T3-low T4 syndrome (20 cases), and other abnormalities (33 cases). 1560 patients were ultimately included in this study (Fig. 1). This study complies with the Declaration of Helsinki, and the Shengjing Hospital of China Medical University Research Ethics Committee which approved the research protocol. Written informed consent was formally obtained from all participants.

Participants and procedures

Acute coronary syndrome was classified according to current guidelines [1–4]. Briefly, unstable angina is defined as chest discomfort or anginal equivalent, ST-segment depression, transitory ST-segment elevation or prominent T-wave inversion, and negative cardiac biomarkers (CK-MB, T/I troponin). Non-ST-segment elevation myocardial infarction (MI) is defined as chest discomfort or anginal equivalent, ST-segment depression, transitory ST-segment elevation or prominent T-wave inversion, and positive cardiac biomarkers (CK-MB, T/I troponin). ST-segment elevation MI (STEMI) is defined as chest pain and significant ST-segment elevation (≥ 0.1 mV in at least two standard leads or ≥ 0.2 mV in at least two contiguous precordial leads) or new left bundle branch block. PCI was performed in accordance with current guidelines, with aspiration thrombectomy and glycoprotein IIb/IIIa inhibitor administration performed at the discretion of the operators [1–4]. The operators also prescribed periprocedural and postprocedural anti-platelet regimens and other cardiovascular medications according to the guidelines [1–4].

Thyroid hormone sampling

In all cases, venous blood samples were drawn upon admission in standard tubes at room temperature, rapidly centrifuged and measured for thyroid-stimulating hormone (TSH), free T3 (fT3) and free T4 (fT4) by a completely automated immunoassay analyzer (i2000, Abbott, USA) in the core laboratory of Shengjing Hospital. The reference intervals for the laboratory were as follows: TSH: 0.3–4.8 uIu/mL; fT3: 2.63–5.71 pmol/L; fT4: 9.01–19.05 pmol/L. Based on thyroid hormone values, patients were categorized into four groups: (1) euthyroidism, with all circulating levels of TSH, fT3, and fT4 in the reference range; (2) subclinical hypothyroidism (SHypo), with TSH levels between 4.8 and 10 uIu/mL and fT3 and fT4 in the reference range; (3) subclinical hyperthyroidism (SHyper), with TSH levels less than 0.3 mIU/L and fT3 and fT4 in the reference range; and (4) low T3 syndrome, with fT3 levels less than 2.63 mIU/L and TSH and fT4 levels in the reference range [7].

Clinical endpoints

The clinical endpoints of this study were all-cause mortality, cardiac mortality, nonfatal reinfarction, and unplanned repeat revascularization, including any unplanned repeat PCI or surgical bypass of target or non-target vessels. All endpoints are defined by the standardized definitions [25].

Data availability

All data generated or analyzed during this study are included in this published article and its supplementary information files (**Suppl. Appendix**).

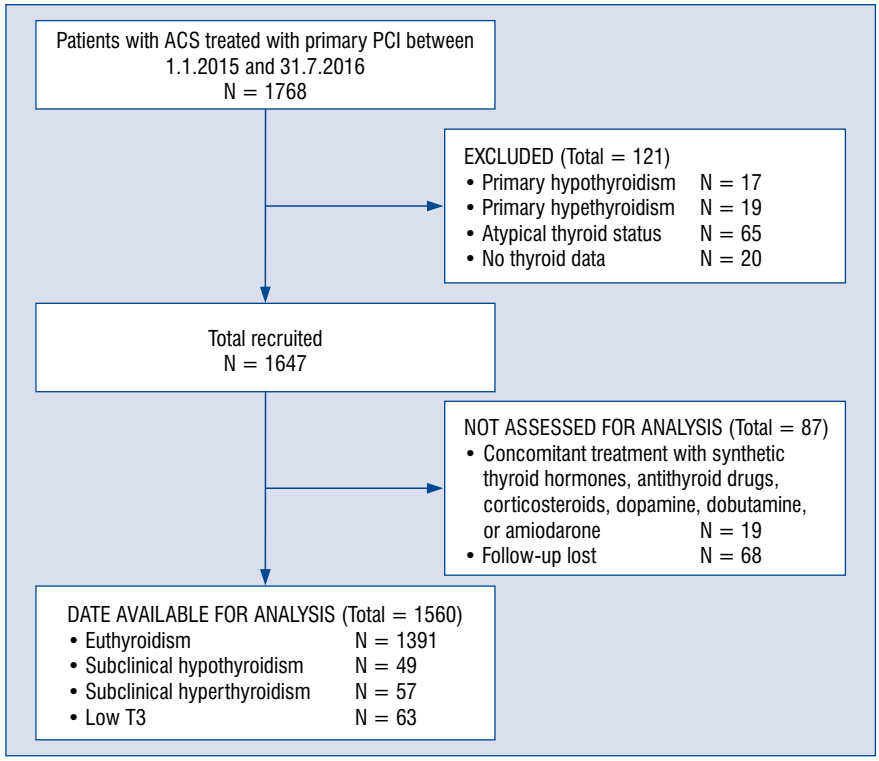

Figure 1. Flow diagram of participant selection; ACS — acute coronary syndrome; PCI — percutaneous coronary intervention.

Statistical analysis

Quantitative variables with normal distribution are represented as mean ± standard deviation (SD) and compared by variance analysis. Quantitative variables without normal distribution are represented as median (interquartile range [IQR]) and compared with a Kruskal-Wallis H test. Categorical variables are presented as counts and proportions (%) and were compared with the χ^2 test. Cox proportional hazards regression modeling by forward stepwise procedure was used to analyze the effect of variables on event-free survival. The euthyroidism group was considered the reference group. Variables included in the model were chosen by separate univariate analyses (**Suppl. Appendix S1 and S2**); those with p value of < 0.05 were included in the final model (see Table 3). Age, gender, current smoking, prior heart failure (HF), heart rate on admission, left ventricular ejection fraction (LVEF), MI on admission, creatinine, left main coronary artery disease, number of stents, drug-eluting stent, and angiotensin converting enzyme inhibitor/angiotensin receptor blockers (ACEI/ARBs) were included in the Cox regression multivariable analysis of all-cause mortality (**Suppl. Appendix S1**). Age, gender, prior HF, heart rate on admission, LVEF, MI on admission, creatinine, left main coronary artery disease, drug-eluting stent and ACEI/ARBs were included in the Cox regression multivariable analysis of cardiac mortality (**Suppl. Appendix S2**). Results were reported as hazard ratios (HRs) with associated 95% confidence intervals (CIs). The cumulative event rate was estimated from Kaplan-Meier curves and compared using the log-rank test. All tests were two-sided, and statistical significance was defined as $p < 0.05$. All statistical analyses were performed with SPSS version 19 (SPSS Inc., Chicago, Illinois, USA).

Results

Participants and baseline characteristics

Figure 1 represents the flowchart for patient selection. The final study cohort included 1560 ACS patients undergoing PCI, including 169 patients with mild thyroid dysfunction (10.8%), and were divided into four groups: 1) euthyroidism group, 1391 (89.2%) patients; 2) SHypo group, 49 (3.1%) patients; 3) SHyper group, 57 (3.7%) patients; and 4) low T3 syndrome group, 63 (4.0%) patients. Clinical characteristics are shown in Table 1. The SHypo and low T3 syndrome groups had significantly higher percentages of females (51.0% and 49.2%, respectively) compared to the euthyroidism (27.7%) and SHyper (21.1%) groups. The low T3 syndrome group had a tendency towards older age and higher troponin-I levels on admission and lower

Table 1. Baseline patient characteristics.

Variable	All (n = 1560)	Euthyroidism (n = 1391)	Subclinical hypothyroidism (n = 49)	Subclinical hyperthyroidism (n = 57)	Low T3 (n = 63)	P
Clinical characteristics						
Age	61.8 ± 11.1	61.5 ± 11.1	63.9 ± 9.5	62.3 ± 13.3	65.6 ± 9.7*	0.018
Female	453 (29.0%)	385 (27.7%)	25 (51.0%)	12 (21.1%)	31 (49.2%)*	< 0.001
Diabetes mellitus	486 (31.2%)	417 (30.0%)	19 (38.8%)	23 (40.4%)	27 (31.2%)	0.057
Hypertension	905 (58.0%)	801 (57.6%)	31 (63.3%)	30 (52.6%)	43 (68.3%)	0.256
Dyslipidemia	1121 (71.9%)	1016 (73.0%)	30 (61.2%)	34 (59.6%)	41 (65.1%)*	0.025
Current smoking	711 (45.6%)	640 (46.0%)	16 (32.7%)	29 (50.9%)	26 (41.3%)	0.210
History of MI	169 (10.8%)	146 (10.5%)	6 (12.2%)	9 (15.8%)	8 (12.7%)	0.585
Prior PCI	149 (9.6%)	131 (9.4%)	6 (12.2%)	7 (12.3%)	5 (7.9%)	0.772
Prior HF	74 (4.7%)	59 (4.2%)	4 (8.2%)	4 (7.0%)	7 (11.1%)*	0.039
MI on admission	1055 (67.7%)	918 (66.0%)	29 (59.2%)	51 (89.5%)	57 (90.5%)*	< 0.001
Cardiogenic shock	18 (1.2%)	10 (0.7%)	1 (2.0%)	2 (3.5%)	5 (7.9%)	< 0.001
SBP on admission [mmHg]	136.1 ± 22.7	136.7 ± 22.6	138.3 ± 22.3	127.7 ± 23.5	129.3 ± 23.4*	0.001
HR on admission [bpm]	75.4 ± 14.3	75.2 ± 14.1	74.3 ± 10.6	77.4 ± 14.7	77.9 ± 18.6	0.510
LVEF [%]	58.3 ± 8.7	58.5 ± 8.6	60.5 ± 8.0	55.9 ± 10.2	55.7 ± 8.5	0.002
Laboratory characteristics						
Creatinine [μmol/L], median (Q1, Q3)	71 (61, 85)	71 (61, 84)	70 (62, 94)	66 (58, 88)	75 (58, 113)	0.358
Troponin-I on admission [ng/mL], median (Q1, Q3)	0.67 (0.01, 21.00)	0.65 (0.01, 18.18)	0.27 (0.01, 12.02)	16.00 (0.67, 82.00)	25.20 (2.10, 66.60)*	< 0.001
TSH [μIU/mL], median (Q1, Q3)	1.41 (0.83, 2.26)	1.41 (0.88, 2.16)	6.00 (5.23, 6.82)	0.22 (0.13, 0.27)	1.40 (0.61, 2.37)	< 0.001
fT_3 [pmol/L], median (Q1, Q3)	3.93 (3.47, 4.34)	3.95 (3.55, 4.36)	4.04 (3.41, 4.41)	3.97 (3.37, 4.34)	2.36 (2.05, 2.52)	< 0.001
fT_4 [pmol/L], median (Q1, Q3)	12.92 (11.77, 14.29)	12.98 (11.82, 14.32)	12.14 (10.79, 13.08)	13.49 (12.33, 15.14)	12.32 (10.54, 13.74)	< 0.001
PCI characteristics						
Left main disease	145 (9.3%)	119 (8.6%)	8 (16.3%)	7 (12.3%)	11 (17.5%)*	0.025
Three-vessel disease	369 (23.7%)	331 (23.8%)	9 (18.4%)	14 (24.6%)	15 (23.8%)	0.849
Number of stents, median (Q1, Q3)	2 (1, 2)	2 (1, 2)	2 (1, 2)	1 (1, 2)	2 (1, 2)	0.910
Drug-eluting stent	1504 (96.4%)	1342 (96.5%)	47 (95.9%)	53 (93.0%)	62 (98.4%)	0.437
Medications at discharge						
ASA	1550 (99.4%)	1383 (99.4%)	49 (100.0%)	57 (100.0%)	61 (96.8%)	0.068
Clopidogrel	1417 (90.8%)	1266 (91.0%)	44 (89.8%)	52 (91.2%)	55 (87.3%)	0.784
Ticagrelor	119 (7.6%)	103 (7.4%)	5 (10.2%)	4 (7.0%)	7 (11.1%)	0.643
Statin	1534 (98.3%)	1373 (98.7%)	49 (100.0%)	54 (94.7%)	58 (92.1%)	< 0.001
ACEI/ARBs	808 (51.8%)	734 (52.8%)	19 (38.8%)	29 (50.9%)	26 (41.3%)	0.083
Beta-blockers	782 (50.1%)	705 (50.7%)	17 (34.7%)	32 (56.1%)	28 (44.4%)	0.091

ASA — acetylsalicylic acid; ACEI/ARBs — angiotensin-converting enzyme inhibitors/angiotensin receptor blockers; HF — heart failure; HR — heart rate; LVEF — left ventricular ejection fraction; MI — myocardial infarction; PCI — percutaneous coronary intervention; SBP — systolic blood pressure

Table 2. Frequency of clinical outcomes by thyroid status.

	All (n = 1560)	Euthyroidism (n = 1391)	Subclinical hypothyroidism (n = 49)	Subclinical hyperthyroidism (n = 57)	Low T3 (n = 63)	P
All-cause mortality	59 (3.8%)	47 (3.4%)	1 (2.0%)	4 (7.0%)	7 (11.1%)	0.007
Cardiac mortality	48 (3.1%)	37 (2.7%)	1 (2.0%)	4 (7.0%)	6 (9.5%)	0.005
Nonfatal reinfarction	22 (1.4%)	18 (1.3%)	1 (2.0%)	1 (1.8%)	2 (3.2%)	0.629
Unplanned repeat revascularization	60 (3.8%)	50 (3.6%)	4 (8.2%)	5 (8.8%)	1 (1.6%)	0.062

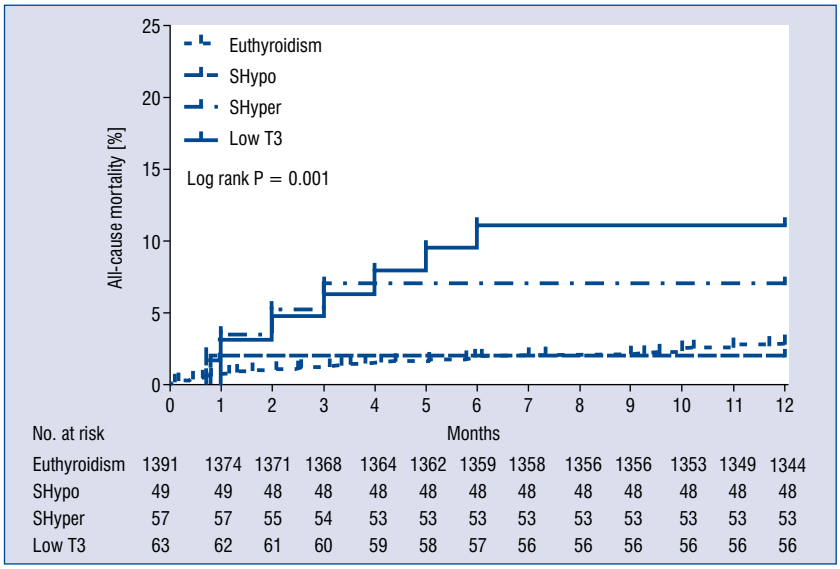

Figure 2. Kaplan-Meier cumulative event curves for all-cause mortality by thyroid status; SHypo — subclinical hypothyroidism; SHyper — subclinical hyperthyroidism.

LVEF and rate of statin use at discharge. The percentage of prior HF, MI on admission, cardiogenic shock and left main coronary artery disease were also significantly higher in the low T3 syndrome group. Individuals in the SHyper group were more likely to have dyslipidemia. There was a significant trend of lower systolic blood pressure upon admission in SHyper group (Table 1).

Clinical endpoints by thyroid status

The clinical endpoints are shown in Table 2. During the 12-month follow-up period, there was a significant trend of higher all-cause mortality and cardiac mortality in the low T3 syndrome group.

The cumulative event curves for all-cause mortality can be seen in Figure 2. Log-rank tests indicated significant differences among the four groups ($p = 0.001$). Furthermore, as shown in Table 3, a significantly increased risk of all-cause mortality was found in the low T3 syndrome group, but not in the SHypo or SHyper groups, compared with the euthyroidism group (HR 3.496, 95% CI 1.579–7.729, $p = 0.002$). After adjusting for covariates, the low T3 syndrome group still displayed a significantly higher all-cause mortality, compared with the euthyroidism group (HR 2.553, 95% CI 1.093–5.964, $p = 0.030$) (Table 3).

Using Kaplan-Meier analysis (Fig. 3), it was found that there were significant differences in cardiac mortality among the four groups ($p < 0.001$). Univariate analysis also revealed that the low T3 syndrome group, but not the SHypo or SHyper groups, had a higher rate of cardiac mortality, compared with the euthyroidism group (HR 3.781, 95% CI 1.596–8.959, $p = 0.003$) (Table 3). This was confirmed again by Cox regression multivariable analysis (HR 2.594, 95% CI 1.026–6.559, $p = = 0.034$) (Table 3). There were no significant differences in nonfatal reinfarction or unplanned repeat revascularization among the four groups (Table 3).

Table 3. Hazard ratios for all-cause and cardiac mortality by thyroid status.

	Univariate analysis		Multivariate analysis[a]	
	Hazard ratio (95% CI)	P	Hazard ratio (95% CI)	P
All-cause mortality				
Euthyroidism	**1 [Reference]**		**1 [Reference][a]**	
Subclinical hypothyroidism	0.603 (0.083–4.367)	0.616	0.557 (0.077–4.043)	0.563
Subclinical hyperthyroidism	2.165 (0.780–6.009)	0.138	1.970 (0.706–5.494)	0.195
Low T3	3.493 (1.579–7.729)	0.002	2.553 (1.093–5.964)	0.030
Cardiac mortality				
Euthyroidism	**1 [Reference]**		**1 [Reference][b]**	
Subclinical hypothyroidism	0.767 (0.105–5.589)	0.793	0.696 (0.095–5.087)	0.721
Subclinical hyperthyroidism	2.749 (0.980–7.714)	0.055	2.431 (0.860–6.874)	0.094
Low T3	3.781 (1.596–8.959)	0.003	2.594 (1.026–6.559)	0.034
Nonfatal reinfarction				
Euthyroidism	**1 [Reference]**			
Subclinical hypothyroidism	1.589 (0.212–11.900)	0.652		
Subclinical hyperthyroidism	1.368 (0.183–10.244)	0.761		
Low T3	2.478 (0.575–10.681)	0.223		
Unplanned repeat revascularization				
Euthyroidism	**1 [Reference]**			
Subclinical hypothyroidism	2.342 (0.846–6.485)	0.101		
Subclinical hyperthyroidism	2.047 (0.739–5.668)	0.168		
Low T3	0.435 (0.060–3.147)	0.409		

[a]Adjusted for age, gender, current smoking, prior HF, HR on admission, LVEF, myocardial infarction on admission, cardiogenic shock, creatinine, left main disease, number of stents, drug-eluting stent, and ACEI/ARBs
[b]Adjusted for age, gender, prior HF, HR on admission, LVEF, myocardial infarction on admission, cardiogenic shock, creatinine, left main disease, drug-eluting stent, and ACEI/ARBs
Abbreviations — see Table 1

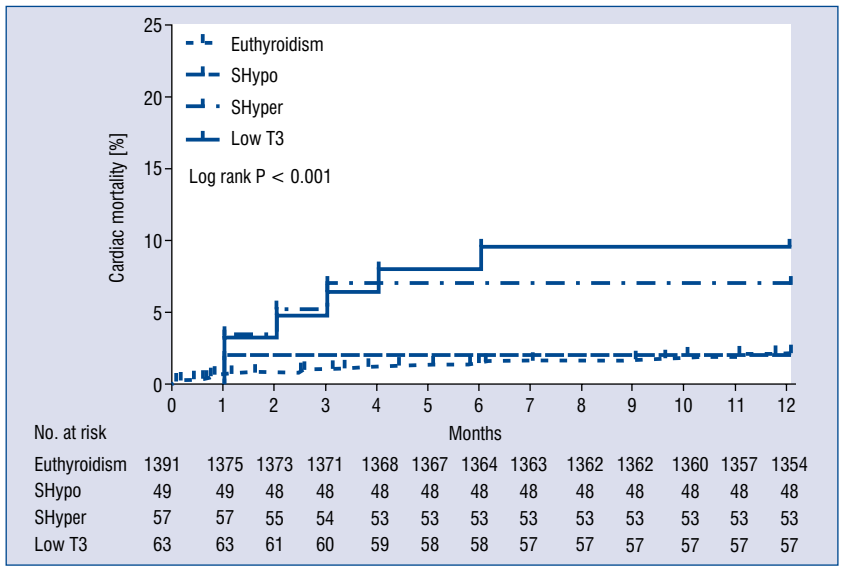

Figure 3. Kaplan-Meier cumulative event curves for cardiac mortality by thyroid status; SHypo — subclinical hypothyroidism; SHyper — subclinical hyperthyroidism.

Discussion

The present study examined the association between mild thyroid dysfunction and 12-month prognosis in ACS patients undergoing PCI, and demonstrated that: 1) the prevalence of mild thyroid dysfunction was as high as 10.8% in patients with ACS undergoing PCI; 2) low T3 syndrome, but not subclinical hypothyroidism or subclinical hyperthyroidism, was associated with a higher rate of all-cause and cardiac mortality; and 3) there was no association between mild thyroid dysfunction and nonfatal reinfarction or unplanned repeat revascularization in ACS patients undergoing PCI.

Mild thyroid dysfunction is frequently present in patients with various cardiac diseases [21]. Further, plasma thyroid hormone levels may also change in ACS patients [8, 9]. Iervasi et al. [21] found that the prevalence of thyroid dysfunction was up to 40% in cardiac patients undergoing coronary angiography. Another study showed a 15% prevalence of mild thyroid dysfunction in patients with STEMI who underwent PCI [23]. In this study, there was a 10.8% prevalence of mild thyroid dysfunction in patients with ACS undergoing PCI. However, the current guidelines do not recommend the routine assessment of thyroid function in ACS patients [1–4]. The prevalence of mild thyroid dysfunction in the present study was far lower than that reported by Iervasi et al. [21]. This is mainly due to differing definitions of thyroid dysfunction. Iervasi et al. [21] used a broader scope of definition: euthyroid patients with normal values of TSH, fT3, and fT4; low T3 syndrome patients with fT3 < 2.0 pg/mL; hypothyroid patients with TSH > 3.8 uIU/mL; and hyperthyroid patients with TSH < 0.3 uIU/mL.

Thyroid hormones extensively affect the physiological and pathological processes of the cardiovascular system [7] and are associated with coronary atherosclerosis [11, 12], thrombus burden [10], cardiomyocyte injury [8, 9, 15], and cardiac function recovery [13, 14]. For the first time, in a total of 573 consecutive heterogeneous cardiac patients undergoing thyroid function evaluation, Iervasi et al. [21] reported that subclinical hypothyroidism and subclinical hyperthyroidism were associated with an increased risk of cardiac mortality. In contrast, patients with STEMI undergoing PCI, had no significant differences in adverse prognoses between subclinical hypothyroidism or subclinical hyperthyroidism and euthyroidism [23]. In addition, the present study found that neither subclinical hypothyroidism or subclinical hyperthyroidism were associated with a higher rate of all-cause or cardiac mortality, nor were they associated with a higher rate of nonfatal reinfarction or unplanned repeat revascularization in ACS patients undergoing PCI. The reason for different conclusions may be that the latter two studies only included ischemic heart disease patients undergoing PCI, but not heterogeneous patients with various cardiac diseases. Also, PCI could greatly improve the prognosis of ischemic heart disease [1–4].

Low T3 syndrome was found to be a strong prognostic predictor of death in patients with cardiac disease [21, 26–28]. It then was verified by other research that low T3 syndrome was associated with adverse outcomes in patients after experiencing ACS [29]. However, only 27.7% patients in that study received PCI, which can greatly improve the prognosis of ischemic heart disease and is now widely available for ACS patients [1–4]. For the first time, we studied the association between low T3 syndrome and the prognosis of ACS patients undergoing PCI. The present study found that low T3 syndrome was associated with a higher rate of all-cause and cardiac mortality in ACS patients undergoing PCI. Mechanistic correlates of these findings have been demonstrated. T3, which is the most important bioactive thyroid hormone for cardiomyocytes, is mostly produced by a process of deiodination of T4 [7]. It can affect cardiomyocytes via genomic and nongenomic actions [7]. T3 regulates transcription by binding hormone receptors (TRs) in the nucleus, which then bind to thyroid hormone response elements (TREs) present in regulatory regions of target genes. Nongenomic actions of T3 include thyroid hormone signaling, changes in thyroid hormone levels, and changes in thyroid hormone receptors. Previous studies have confirmed that the thyroid hormone receptor TRα1 can limit myocardial injury and post-ischemic cardiac remodeling through T3 binding, and it regulates genes related to contractile proteins, pacemaker activity and conduction, cell growth, differentiation and metabolism [30–32]. Also, thyroid hormones could affect cardiac apoptosis through the suppression of ischemia reperfusion-induced activation of the pro-apoptotic p38 mitogen-activated protein kinase (MAPK) and upregulation of cardio-protective molecules such as heat shock protein 27 (HSP27) and heat shock protein 70 (HSP70), which are also involved in ischemic preconditioning [30–32]. T3 may also regulate plasma membrane ion currents, activate survival pathways, and decrease oxidative stress in mitochondria [7]. Therefore, heart rate, cardiac contractility, vascular smooth muscle, and

endothelial function will be modulated [7]. When T3 is low, negative effects on the cardiovascular system, such as delayed diastolic filling, decreased cardiac contractility, and increased vascular resistance will occur [7]. Thyroid hormones also indirectly effect myocytes by activating the inflammatory immune response through genomic and nongenomic mechanisms [33]. Clinical studies also confirmed that low T3 was associated with larger thrombus burden [10], higher severity of coronary artery lesions [11, 12], worse cardiac function [13, 14] and larger myocardial injury size [8, 9, 15] in ACS patients.

Taken together, in ACS patients, decreased levels of T3 have a severe pathological effect, rather than acting as an adaptive response to minimize catabolism [34]. Considering the results of this study and the others mentioned, it is worthwhile to monitor thyroid hormone levels in patients with ACS. Doing so will help to identify patients at high risk of adverse events and mortality. Also, of interest is the potential of thyroid hormones as a therapeutic target for improving the prognosis of ACS since patients still suffer adverse outcomes [6]. In fact, experimental evidence from animal models has shown that T3 therapy could limit infarct extension, protect against reperfusion injury, improve cardiac structure and function, decrease the incidence of tachyarrhythmias, and reduce adverse left ventricular remodeling [7]. Furthermore, a previous study found that thyroid replacement therapy was beneficial in preventing coronary disease progression and other cardiovascular events in patients with hypothyroidism undergoing PCI [35]. However, the efficacy and safety of T3 therapy has not yet been confirmed in randomized, controlled clinical trials in patients with ACS and low T3 syndrome undergoing PCI. Moreover, there are still several problems related to thyroid hormone replacement, such as the type of thyroid hormone used (T3 or T4), medication route (parenteral or oral), the timing related to onset of ACS, the duration of medication use, and complications associated with overtreatment, including atrial fibrillation and bone fracture. Adequately powered randomized studies need to be performed to obtain meaningful conclusions before thyroid hormone replacement can become a routine clinical treatment for ACS patients, such as the ThyrAMI trial (Trial registration: ISRCTN; trial number: ISRCTN52505169) and the TRUST trial (Specific Program Cooperation — Theme Health, Proposal No: 278148-2, NCT01660126) [36, 37].

Limitations of the study

This study had several limitations. First, this study was prospective and observational, so potential confounders and selection bias could not be completely eliminated. Second, when patients suffer from ACS, the secretion of thyroid hormone will fluctuate in the early phase of the disease [7]. Particularly, the level of T3 will drop in the first 2–3 days after the ischemic event. However, in this study, thyroid function tests were only performed at admission and not repeated later, as recommended by the guidelines [16–19]. Thus, transient forms of thyroid dysfunction could be excluded and low T3 syndrome was likely underestimated. Third, studies have indicated that iodinated contrast media may influence thyroid function [22, 38, 39]. In this study, the thyroid function of some patients was tested after the use of iodinated contrast media because they needed emergency PCI. Finally, the raw number of events in this study was quite small during the follow-up period, which may be a limitation in the overall interpretation of the study results.

Conclusions

Mild thyroid dysfunction was frequent in patients with ACS undergoing PCI, and low T3 syndrome was the predominant feature. Low T3 syndrome, but not subclinical hypothyroidism or subclinical hyperthyroidism, was associated with a higher rate of all-cause and cardiac mortality.

Acknowledgements

This research project was supported by grants from the Social Development Research Program of Liaoning Province (2011225020).

Conflict of interest: None declared

References

1. Amsterdam EA, Wenger NK, Brindis RG, et al. 2014 AHA/ACC Guideline for the Management of Patients with Non-ST-Elevation Acute Coronary Syndromes: a report of the American College of Cardiology/American Heart Association Task Force on Practice Guidelines. J Am Coll Cardiol. 2014; 64(24): e139–e228, doi: 10.1016/j.jacc.2014.09.017, indexed in Pubmed: 25260718.
2. O'Gara P, Kushner F, Ascheim D, et al. 2013 ACCF/AHA Guideline for the Management of ST-Elevation Myocardial Infarction. J Am Coll Cardiol. 2013; 61(4): e78–e140, doi: 10.1016/j.jacc.2012.11.019.
3. Roffi M, Patrono C, Collet JP, et al. 2015 ESC Guidelines for the management of acute coronary syndromes in patients present-

ing without persistent ST-segment elevation: Task Force for the Management of Acute Coronary Syndromes in Patients Presenting without Persistent ST-Segment Elevation of the European Society of Cardiology (ESC). Eur Heart J. 2016; 37(3): 267–315, doi: 10.1093/eurheartj/ehv320, indexed in Pubmed: 26320110.
4. Steg PhG, James SK, Atar D, et al. Task Force on the management of ST-segment elevation acute myocardial infarction of the European Society of Cardiology (ESC). ESC Guidelines for the management of acute myocardial infarction in patients presenting with ST-segment elevation. Eur Heart J. 2012; 33(20): 2569–2619, doi: 10.1093/eurheartj/ehs215, indexed in Pubmed: 22922416.
5. Ibáñez B, Heusch G, Ovize M, et al. Evolving therapies for myocardial ischemia/reperfusion injury. J Am Coll Cardiol. 2015; 65(14): 1454–1471, doi: 10.1016/j.jacc.2015.02.032, indexed in Pubmed: 25857912.
6. Eapen ZJ, Tang WH, Felker GM, et al. Defining heart failure end points in ST-segment elevation myocardial infarction trials: integrating past experiences to chart a path forward. Circ Cardiovasc Qual Outcomes. 2012; 5(4): 594–600, doi: 10.1161/CIRCOUTCOMES.112.966150, indexed in Pubmed: 22811505.
7. Jabbar A, Pingitore A, Pearce SHS, et al. Thyroid hormones and cardiovascular disease. Nat Rev Cardiol. 2017; 14(1): 39–55, doi: 10.1038/nrcardio.2016.174, indexed in Pubmed: 27811932.
8. Friberg L, Werner S, Eggertsen G, et al. Rapid down-regulation of thyroid hormones in acute myocardial infarction: is it cardioprotective in patients with angina? Arch Intern Med. 2002; 162(12): 1388–1394, indexed in Pubmed: 12076238.
9. Smith SJ, Bos G, Gerbrandy J, et al. Lowering of serum 3,3',5-triiodothyronine thyroxine ratio in patients with myocardial infarction; relationship with extent of tissue injury. Eur J Clin Invest. 1978; 8(2): 99–102, indexed in Pubmed: 417942.
10. Viswanathan G, Balasubramaniam K, Hardy R, et al. Blood thrombogenicity is independently associated with serum TSH levels in post-non-ST elevation acute coronary syndrome. J Clin Endocrinol Metab. 2014; 99(6): E1050–E1054, doi: 10.1210/jc.2013-3062, indexed in Pubmed: 24628547.
11. Coceani M, Iervasi G, Pingitore A, et al. Thyroid hormone and coronary artery disease: from clinical correlations to prognostic implications. Clin Cardiol. 2009; 32(7): 380–385, doi: 10.1002/clc.20574, indexed in Pubmed: 19609889.
12. Bai Mf, Gao Cy, Yang Ck, et al. Effects of thyroid dysfunction on the severity of coronary artery lesions and its prognosis. J Cardiol. 2014; 64(6): 496–500, doi: 10.1016/j.jjcc.2014.03.009, indexed in Pubmed: 24951271.
13. Lymvaios I, Mourouzis I, Cokkinos DV, et al. Thyroid hormone and recovery of cardiac function in patients with acute myocardial infarction: a strong association? Eur J Endocrinol. 2011; 165(1): 107–114, doi: 10.1530/EJE-11-0062, indexed in Pubmed: 21490121.
14. Jankauskienė E, Orda P, Barauskienė G, et al. Relationship between left ventricular mechanics and low free triiodothyronine levels after myocardial infarction: a prospective study. Intern Emerg Med. 2016; 11(3): 391–398, doi: 10.1007/s11739-015-1370-x, indexed in Pubmed: 26692085.
15. Kim DH, Choi DH, Kim HW, et al. Prediction of infarct severity from triiodothyronine levels in patients with ST-elevation myocardial infarction. Korean J Intern Med. 2014; 29(4): 454–465, doi: 10.3904/kjim.2014.29.4.454, indexed in Pubmed: 25045293.
16. Jonklaas J, Bianco AC, Bauer AJ, et al. American Thyroid Association Task Force on Thyroid Hormone Replacement. Guidelines for the treatment of hypothyroidism: prepared by the american thyroid association task force on thyroid hormone replacement. Thyroid. 2014; 24(12): 1670–1751, doi: 10.1089/thy.2014.0028, indexed in Pubmed: 25266247.
17. Ross DS, Burch HB, Cooper DS, et al. 2016 American Thyroid Association Guidelines for Diagnosis and Management of Hyperthyroidism and Other Causes of Thyrotoxicosis. Thyroid. 2016; 26(10): 1343–1421, doi: 10.1089/thy.2016.0229, indexed in Pubmed: 27521067.
18. Biondi B, Bartalena L, Cooper DS, et al. The 2015 European Thyroid Association Guidelines on Diagnosis and Treatment of Endogenous Subclinical Hyperthyroidism. Eur Thyroid J. 2015; 4(3): 149–163, doi: 10.1159/000438750, indexed in Pubmed: 26558232.
19. LeFevre ML. U.S. Preventive Services Task Force. Screening for thyroid dysfunction: U.S. Preventive Services Task Force recommendation statement. Ann Intern Med. 2015; 162(9): 641–650, doi: 10.7326/M15-0483, indexed in Pubmed: 25798805.
20. Chopra IJ. Clinical review 86: Euthyroid sick syndrome: is it a misnomer? J Clin Endocrinol Metab. 1997; 82(2): 329–334, doi: 10.1210/jcem.82.2.3745, indexed in Pubmed: 9024211.
21. Iervasi G, Molinaro S, Landi P, et al. Association between increased mortality and mild thyroid dysfunction in cardiac patients. Arch Intern Med. 2007; 167(14): 1526–1532, doi: 10.1001/archinte.167.14.1526, indexed in Pubmed: 17646607.
22. Marraccini P, Bianchi M, Bottoni A, et al. Prevalence of thyroid dysfunction and effect of contrast medium on thyroid metabolism in cardiac patients undergoing coronary angiography. Acta Radiol. 2013; 54(1): 42–47, doi: 10.1258/ar.2012.120326, indexed in Pubmed: 23125395.
23. Özcan KS, Osmonov D, Toprak E, et al. Sick euthyroid syndrome is associated with poor prognosis in patients with ST segment elevation myocardial infarction undergoing primary percutaneous intervention. Cardiol J. 2014; 21(3): 238–244, doi: 10.5603/CJ.a2013.0108, indexed in Pubmed: 23990180.
24. Yu T, Tian C, Song J, et al. Derivation and Validation of Shock Index as a parameter for Predicting Long-term Prognosis in Patients with Acute Coronary Syndrome. Sci Rep. 2017; 7(1): 11929, doi: 10.1038/s41598-017-12180-2, indexed in Pubmed: 28931945.
25. Cutlip DE, Windecker S, Mehran R, et al. Academic Research Consortium. Clinical end points in coronary stent trials: a case for standardized definitions. Circulation. 2007; 115(17): 2344–2351, doi: 10.1161/CIRCULATIONAHA.106.685313, indexed in Pubmed: 17470709.
26. Iervasi G, Pingitore A, Landi P, et al. Low-T3 syndrome: a strong prognostic predictor of death in patients with heart disease. Circulation. 2003; 107(5): 708–713, indexed in Pubmed: 12578873.
27. Wang B, Liu S, Li L, et al. Non-thyroidal illness syndrome in patients with cardiovascular diseases: A systematic review and meta-analysis. Int J Cardiol. 2017; 226: 1–10, doi: 10.1016/j.ijcard.2016.10.039, indexed in Pubmed: 27776249.
28. Pfister R, Strack N, Wielckens K, et al. The relationship and prognostic impact of low-T3 syndrome and NT-pro-BNP in cardiovascular patients. Int J Cardiol. 2010; 144(2): 187–190, doi: 10.1016/j.ijcard.2009.03.137, indexed in Pubmed: 19423177.
29. Brozaitiene J, Mickuviene N, Podlipskyte A, et al. Relationship and prognostic importance of thyroid hormone and N-terminal pro-B-Type natriuretic peptide for patients after acute coronary syndromes: a longitudinal observational study. BMC Cardiovasc

Disord. 2016; 16: 45, doi: 10.1186/s12872-016-0226-2, indexed in Pubmed: 26892923.

30. Pantos C, Mourouzis I, Cokkinos DV. New insights into the role of thyroid hormone in cardiac remodeling: time to reconsider? Heart Fail Rev. 2011; 16(1): 79–96, doi: 10.1007/s10741-010-9185-3, indexed in Pubmed: 20668933.
31. Pantos C, Mourouzis I, Cokkinos DV. Thyroid hormone and cardiac repair/regeneration: from Prometheus myth to reality? Can J Physiol Pharmacol. 2012; 90(8): 977–987, doi: 10.1139/y2012-031, indexed in Pubmed: 22762197.
32. Pantos C, Mourouzis I. Translating thyroid hormone effects into clinical practice: the relevance of thyroid hormone receptor 1 in cardiac repair. Heart Fail Rev. 2015; 20(3): 273–282, doi: 10.1007/s10741-014-9465-4, indexed in Pubmed: 25501869.
33. De Vito P, Incerpi S, Pedersen JZ, et al. Thyroid hormones as modulators of immune activities at the cellular level. Thyroid. 2011; 21(8): 879–890, doi: 10.1089/thy.2010.0429, indexed in Pubmed: 21745103.
34. De Groot LJ. Dangerous dogmas in medicine: the nonthyroidal illness syndrome. J Clin Endocrinol Metab. 1999; 84(1): 151–164, doi: 10.1210/jcem.84.1.5364, indexed in Pubmed: 9920076.
35. Zhang M, Sara JDS, Matsuzawa Y, et al. Clinical outcomes of patients with hypothyroidism undergoing percutaneous coronary intervention. Eur Heart J. 2016; 37(26): 2055–2065, doi: 10.1093/eurheartj/ehv737, indexed in Pubmed: 26757789.
36. Jabbar A, Ingoe L, Pearce S, et al. Thyroxine in acute myocardial infarction (ThyrAMI) - levothyroxine in subclinical hypothyroidism post-acute myocardial infarction: study protocol for a randomised controlled trial. Trials. 2015; 16: 115, doi: 10.1186/s13063-015-0621-5, indexed in Pubmed: 25872532.
37. Stott DJ, Gussekloo J, Kearney PM, et al. Study protocol; Thyroid hormone Replacement for Untreated older adults with Subclinical hypothyroidism - a randomised placebo controlled Trial (TRUST). BMC Endocr Disord. 2017; 17(1): 6, doi: 10.1186/s12902-017-0156-8, indexed in Pubmed: 28158982.
38. Gartner W, Weissel M. Do iodine-containing contrast media induce clinically relevant changes in thyroid function parameters of euthyroid patients within the first week? Thyroid. 2004; 14(7): 521–524, doi: 10.1089/1050725041517075, indexed in Pubmed: 15307941.
39. van der Molen AJ, Thomsen HS, Morcos SK, et al. Contrast Media Safety Committee, European Society of Urogenital Radiology (ESUR). Effect of iodinated contrast media on thyroid function in adults. Eur Radiol. 2004; 14(5): 902–907, doi: 10.1007/s00330-004-2238-z, indexed in Pubmed: 14997334.

VIA MEDICA

ORIGINAL ARTICLE

Cardiology Journal
2020, Vol. 27, No. 3, 272–277
DOI: 10.5603/CJ.a2018.0104

ISSN 1897–5593

Cardiac sarcoidosis and ventricular arrhythmias. A rare association of a rare disease. A retrospective cohort study from the National Inpatient Sample and current evidence for management

Amr Salama[1], Abdullah Abdullah[1], Abdul Wahab[1], George Eigbire[1], Ryan Hoefen[1, 2, 4], Richard Alweis[1,2, 3]

[1]Department of Medicine, Unity Hospital, Rochester, New York, United States
[2]Department of Medicine, University of Rochester School of Medicine and Dentistry, Rochester, New York, United States
[3]School of Health Sciences, Rochester Institute of Technology, New York, United States
[4]Department of Cardiology, Rochester Regional Health, New York, United States

Abstract

Background: *Sarcoidosis is an increasingly recognized multi-systemic condition. Cardiac sarcoidosis is associated with ventricular arrhythmias and higher mortality rates. Little epidemiological data is available regarding the disease and associated ventricular arrhythmias.*

Methods: *Data from the National Inpatient Sample (NIS) database 2012–2014, were reviewed. Discharges associated with sarcoidosis were identified as the target population using relevant ICD-9-CM codes. Primary outcome was a diagnosis of ventricular tachycardia (VT) in the sarcoidosis population. Secondary outcomes include rate of ventricular fibrillation (VF) and cardiac arrest. Subgroup analyses were performed to examine the association of VT with multiple potential confounding clinical variables.*

Results: *Of 18,013,878 health encounters, 46,289 (0.26%) subjects had a diagnosis of sarcoidosis. VT and VF were more prevalent among patients with sarcoidosis compared to those without a diagnosis of sarcoidosis (2.29% vs. 1.22%; $p < 0.001$ and 0.25% vs. 0.21%; $p < 0.001$, respectively). Sarcoidosis was also associated with a higher prevalence of cardiac arrest (0.72% vs. 0.6%; $p < 0.001$). In unadjusted analyses, all examined comorbidities were significantly more common in those with sarcoidosis, including diabetes mellitus (31.6% vs. 21.25%; $p < 0.001$), hypertension (65.2% vs. 51.74%; $p < 0.001$), chronic kidney disease (21.09% vs. 14.02%; $p < 0.001$), heart failure (24.87% vs. 15%; $p < 0.001$) and acute coronary syndrome (4.32% vs. 3.35%; $p < 0.001$).*

Conclusions: *The present study showed that sarcoidosis was associated with increased rates of ventricular tachyarrhythmia, which can affect the overall disease morbidity and mortality.* (Cardiol J 2020; 27, 3: 272–277)

Key words: cardiac sarcoidosis, ventricular tachycardia, ventricular fibrillation, cardiac death

Address for correspondence: Amr Salama, MD, Department of Medicine, Unity Hospital, 1555 Long Pond Road, Rochester, New York, USA, 14626, tel: +1 5852982834, e-mail: Amr.salama@rochesterregional.org

Received: 17.07.2018 Accepted: 3.08.2018

Introduction

Sarcoidosis is a multi-system granulomatous disease of unclear etiology with variable presentation. The prevalence ranges from 10.9 per 100,000 for whites to 35.5 per 100,000 for blacks [1]. The pathological hallmark of the disease is non-caseating granulomas. Cardiac sarcoidosis (CS) is increasingly recognized and associated with higher morbidity and mortality rates. Studies show a wide range (3.7–54.9%) of cardiac involvement in patients with systemic sarcoidosis [2].

Conduction abnormalities and arrhythmias are the most common clinical manifestations of CS, followed by congestive heart failure (HF) and sudden death [3]. The prevalence of specific arrhythmias is as follows: 26–62% atrioventricular block, 0–15% supraventricular tachycardia, 2–42% ventricular tachycardia (VT), and 12–65% sudden cardiac death [4]. Given the very rare nature of CS, electrophysiologists rely on small observational studies. It is hypothesized herein, that CS could be a significant independent predictor for development of VT. The National Inpatient Sample (NIS) was analyzed to test this possibility.

Methods

Study design and data source

Data from the NIS database, part of the Healthcare Cost and Utilization Project (HCUP), an Agency for Healthcare Research and Quality (AHRQ) was used. This is the largest inpatient healthcare database available to the public in the United States of America. The study utilized data for the years from 2012 to 2014. The NIS includes a 20-percent stratified sample of all discharges from United States hospitals participating in the HCUP, 7–8 million discharges per year, excluding rehabilitation and long-term acute care hospitals. It contains variables extracted from hospital discharge records, including demographic characteristics, principal diagnosis, secondary diagnoses or comorbidities, insurance, cost and the procedures performed. The database allows for calculating national estimates by providing a "weight" variable [5]. When the data expands to estimate nation-wide discharges, it provides estimates corresponding to about 38 million annual hospitalizations or 97% of discharges nationwide [6]. Estimates from the NIS have been validated against the Centers for Medicare and Medicaid Services registry [5, 7]. Each discharge record was treated as an individual database entry. The databases used International Classification of Diseases-9th Edition (ICD-9) codes to identify diagnoses and procedures.

Subjects and variables

The study population was derived from 18,013,878 hospital discharges available in the NIS. Patients with VT and sarcoidosis were identified using ICD-9 codes, 427.1 and 135, respectively. Primary outcome was a diagnosis of VT in the sarcoidosis population. Secondary outcomes include rate of ventricular fibrillation (VF) and cardiac arrest. Analyses of clinical variables were performed to examine the association of VT with multiple confounding factors.

Confounding variables were identified using the ICD-9 diagnosis codes including both patient and hospital level variables, in addition to data year. Patient characteristics included age, gender, diabetes mellitus, HF, hypertension, acute coronary syndrome (ACS) (during the same hospitalization) and chronic kidney disease.

Statistical analysis

Normally distributed continuous variables were expressed as means ± standard deviation and compared using the Student t-test. Continuous variables that were not normally distributed were expressed as medians with interquartile ranges and compared using Mann-Whitney test. Categorical variables were compared using the χ^2 test. In order to adjust for potential confounders, multivariable logistic regression was performed.

A median Charlson-Deyo Index (CDI) was calculated for both sarcoidosis and non-sarcoidosis groups. CDI is a validated measure of comorbidities for administrative data [8]. All analyses were performed using STATA 2015 TX: Stata Corp LP. Two-tailed p-value < 0.05 was considered statistically significant.

Results

18,013,878 health encounters were identified from the NIS that represent hospitalizations from 2012 to 2014. Of these, 46,289 (0.26%) subjects had a diagnosis of sarcoidosis, and the remaining 17,967,589 (99.7%) do not have sarcoidosis among their discharge diagnoses. Baseline characteristics of patients with and without sarcoidosis diagnosis are shown in Table 1.

In unadjusted analyses, patients with sarcoidosis were middle-aged (mean 58.2 ± 13.6 years) and predominantly female (64.2%). All examined comorbidities were significantly more common in

Table 1. Baseline variables between target group (sarcoidosis patients) and control group.

Variables	Sarcoidosis (n = 46,289)	No sarcoidosis (n = 17,967,589)	P
Age [years]	58.2 ± 13.6	57.3 ± 20.6	< 0.001
Male	35.8% (16,556)	40.9% (7,352,675)	< 0.001
Diabetes mellitus	31.60% (14,626)	21.25% (3,818,578)	< 0.001
Hypertension	65.20% (30,179)	51.74% (9,297,154)	< 0.001
Chronic kidney disease	21.09% (9,763)	14.02% (2,519,784)	< 0.001
Acute coronary syndrome	3.35% (1,551)	4.32% (777,054)	< 0.001
Heart failure	24.87% (11,510)	15.01% (2,696,906)	< 0.001
Charlson-Deyo Index	2.3 ± 2.07	1.7 ± 2.15	< 0.001
Ventricular tachycardia	2.29% (1,059)	1.22% (218,330)	< 0.001
Ventricular fibrillation	0.25% (118)	0.21% (38,012)	< 0.001
Cardiac arrest	0.72% (331)	0.60% (108,312)	< 0.001

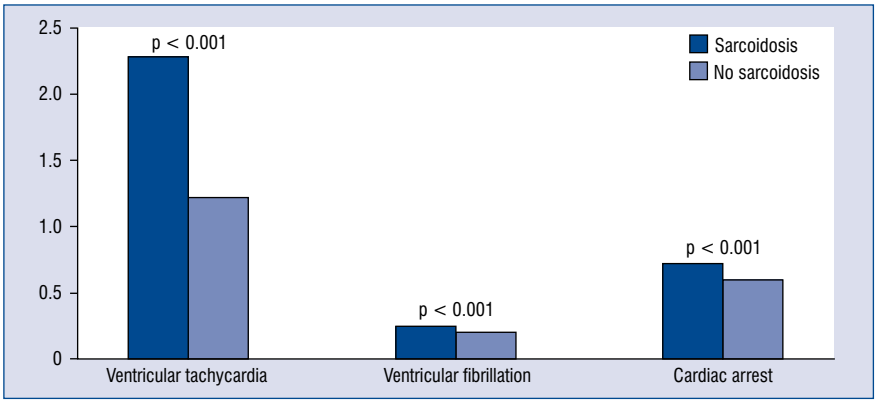

Figure 1. Summaries of outcomes in patients with and without sarcoidosis.

those with sarcoidosis, including diabetes mellitus (31.6% vs. 21.25%; p < 0.001), hypertension (65.2% vs. 51.74%; p < 0.001), chronic kidney disease (21.09% vs. 14.02%; p < 0.001), HF (24.87% vs. 15%; p < 0.001) and ACS (4.32% vs. 3.35%; p < 0.001).

The CDI was 2.3 in the sarcoidosis group vs. 1.7 in the control group. 2.29% (1,059) of patients in the sarcoidosis group had a diagnosis of VT vs. 1.22% (218,330) of the control group, p < 0.001 (Fig. 1).

The adjusted odds ratio (OR) of VT in the sarcoidosis group was 1.83 (95% confidence interval [CI] 1.72–1.95; p < 0.001). Table 2 shows independent predictors of VT among CS patients in a multivariable analysis. HF (OR 5.24; 95% CI 5.19–5.29; p < 0.001) and ACS (OR 2.84; 95% CI 2.81–2.87; p < 0.001) were associated with higher OR for VT.

Ventricular fibrillation was also more common in the sarcoidosis group (0.25% vs. 0.21%; p < 0.001). The OR of VF in the sarcoidosis group after multivariable logistic regression analysis was 1.24 (95% CI 1.03–1.49; p < 0.019; Table 3). Rates of VF was higher with ACS (OR 10.45; 95% CI 10.22–10.68; p < 0.001) and HF (OR 3.58; 95% CI 3.50–3.67; p < 0.001).

Finally, sarcoidosis carries a higher prevalence of cardiac arrest (0.72% vs. 0.6%; p < 0.001). Cardiac arrest remained more prevalent in sarcoidosis patients (OR 1.21; 95% CI 1.08–1.35; p < 0.001) as well as ACS 4.91 (95% CI 4.84–4.98; p < 0.001) and HF (OR 2.14; 95% CI 2.11–2.17; p < 0.001) in multivariable logistic regression analysis as shown in Table 4.

Discussion

Cardiac involvement in sarcoidosis is associated with increased morbidity and mortality. Isolated CS is much more common than suspected;

Table 2. Independent predictors of ventricular tachycardia.

Variables	Odds ratio	95% CI	P
Age	1.01	1.013–1.014	< 0.001
Female	0.44	0.43–0.44	< 0.001
Sarcoidosis	1.83	1.72–1.95	< 0.001
ACS	2.84	2.81–2.87	< 0.001
Heart failure	5.24	5.19–5.29	< 0.001

ACS — acute coronary syndrome; CI — confidence interval

Table 3. Independent predictors of ventricular fibrillation.

Variables	Odds ratio	95% CI	P
Age	0.998	0.997–0.999	< 0.001
Female	0.44	0.43–0.45	< 0.001
Sarcoidosis	1.24	1.03–1.49	0.019
ACS	10.45	10.22–10.68	< 0.001
Heart failure	3.58	3.50–3.67	< 0.001

ACS — acute coronary syndrome; CI — confidence interval

Table 4. Independent predictors of cardiac arrest.

Variables	Odds ratio	95% CI	P
Age	1.01	1.013–1.014	< 0.001
Female	0.65	0.65–0.67	< 0.001
Sarcoidosis	1.21	1.08–1.35	< 0.001
ACS	4.91	4.84–4.98	< 0.001
Heart failure	2.14	2.11–2.17	< 0.001

ACS — acute coronary syndrome; CI — confidence interval

in a retrospective study, 66% of patients with CS had disease isolated to the heart [9]. To date, CS has been extremely difficult to diagnose due to non-specific clinical manifestations, and the limited sensitivity and specificity of various diagnostic modalities [10]. There is also a lack of consensus regarding the diagnostic criteria for CS. Ventricular arrhythmias (VT, multifocal or frequent PVCs) are one of the minor criteria of the Japanese Ministry of Health and Welfare Criteria for diagnosis of CS, while the Heart Rhythm Society consensus statement did not include ventricular arrhythmias as a criteria for diagnosing CS [11].

The present study analyzed a large database and revealed an increased rate of VT in patients with sarcoidosis (2.29%) compared to patients without sarcoidosis (1.22%); $p < 0.001$. HF, hypertension, chronic kidney disease and diabetes mellitus were more common in the sarcoidosis group. Even after adjustment for possible biological confounders, the odds for having VT was still higher (1.82; 95% CI 1.72–1.95; $p < 0.001$) in sarcoidosis patients, which suggest that CS may be an independent risk factor for VT.

Other reports suggested VT is the most frequent arrhythmia noted in CS with a reported incidence of 23% [12]. ACS and HF are traditional risk factors for development of VT, a fact that was confirmed after multivariable logistic regression analyses that showed higher odds of VT in ACS and HF population (2.84; 95% CI 2.81–5.87; $p < 0.001$ and 5.24; 95% CI 5.19–5.29; $p < 0.001$, respectively.

Secondary outcomes of VF and cardiac arrest were both higher in the sarcoidosis group (0.25% vs. 0.21%; $p < 0.001$ and 0.72% vs. 0.6%; $p < 0.001$, respectively. Moreover, ACS and HF were associated with higher cardiac arrest rates (Table 4). This is consistent with a high mortality rate in CS seen by Roberts et al. [13], where sudden death was the most common manifestation of CS. The

present analysis shows increased rates for VF in sarcoidosis patients (OR 1.24; 95% CI 1.03–1.49; $p < 0.019$; Table 3).

The causality between VT and sarcoidosis cannot be assessed in a retrospective database study such as this one. Postulated mechanisms include active inflammation [11], enhanced automaticity [12], and ventricular activation and recovery process, which explains the reentry mechanism that leads to VT, the most frequent arrhythmia noted in CS [14]. A multicenter registry of patents with CS who underwent an electrophysiology study showed that the mechanism of VT was reentry in virtually all patients [15].

Management of arrhythmias in CS is difficult, and effective control of VT is often not achievable with a single method therapy. Steroids remain central in the management of CS as it can ameliorate cardiac dysfunction [16]. However, recurrent VT may increase with steroid therapy as active granulomas are replaced by fibrosis, a substrate for reentrant arrhythmias [17]. Corticosteroids have been associated with ventricular aneurysm formation [13], so immunosuppressive therapies are recommended in cases of resistant arrhythmias or as a steroid-sparing strategy [18].

Amiodarone and sotalol are widely used to treat VT in patients with CS, although adverse reactions may limit their practicality [15]. Amiodarone use may be limited by the incidence of pulmonary complications which are often difficult to distinguish from pulmonary sarcoidosis. beta-blockers have been shown to increase the incidence of heart block in patients with CS, thus limiting the utility of sotalol [14].

Prophylactic implantable cardioverter-defibrillator (ICD) placement is recommended for patients with sarcoidosis who develop sustained VT or left ventricular systolic dysfunction with left ventricular ejection fraction ≤ 35% despite optimal medical therapy and immunosuppression. It may also be a reasonable treatment for patients with CS, regardless of their left ventricular function, after syncope, near syncope, or inducible VT [11]. ICD placement will prevent VT progression but will not prevent recurrence. Therefore, concurrent treatment with anti-arrhythmic therapy is necessary in refractory VT [19]. Some experts recommend ICD placement in patients with sarcoidosis and non-sustained VT given the high rate of recurrent VT despite antiarrhythmic and corticosteroid treatment [10].

Radiofrequency ablation is very effective in decreasing or eliminating VT in patients with CS according to data from a multicenter registry that showed a 98% reduction in VT burden in the first 3 months after ablation [15]. Resistant ventricular tachyarrhythmia and severe intractable HF, especially in younger patients, are indications for cardiac transplantation in patient with CS [14].

Study power

According to available research, this is the largest epidemiological study to assess the role of sarcoidosis in VT. Primary analysis confirms an increased rate of VT in sarcoidosis, even after adjustment for possible biological confounders. The strength of these findings lies in the fact that HCUP is a well-validated database that has been previously utilized in similar research studies.

Limitation of the study

ICD-9 codes were used to identify patient comorbidities. However, prior studies have demonstrated that ICD-9 codes exhibit high (> 90%) sensitivity, specificity and positive predictive value for cardiovascular disorders such as HF, myocardial infarction and arrhythmias, when compared to full medical chart review [7]. Also, due to the nature of the NIS database analysis, functional outcomes and long-term data were not available. Moreover, specific information regarding medications, electrophysiological studies, or echocardiographic parameters were not available. Lastly, due to the observational nature of the study, and unmeasured confounding factors may have affected interpretation and causality cannot be demonstrated.

Conclusions

Sarcoidosis carries a risk of various cardiac complications. The present analysis shows that hospitalized patients with sarcoidosis have elevated risk of VT, VF, and cardiac arrest.

Conflict of interest: None declared

References

1. Rybicki BA, Major M, Popovich J, et al. Racial differences in sarcoidosis incidence: a 5-year study in a health maintenance organization. Am J Epidemiol. 1997; 145(3): 234–241, doi: 10.1093/oxfordjournals.aje.a009096.
2. Nery PB, Leung E, Birnie DH. Arrhythmias in cardiac sarcoidosis: diagnosis and treatment. Curr Opin Cardiol. 2012; 27(2): 181–189, doi: 10.1097/HCO.0b013e32834e4c7c, indexed in Pubmed: 22186166.
3. Hulten E, Aslam S, Osborne M, et al. Cardiac sarcoidosis-state of the art review. Cardiovasc Diagn Ther. 2016; 6(1):

50–63, doi: 10.3978/j.issn.2223-3652.2015.12.13, indexed in Pubmed: 26885492.
4. Ipek E, Demirelli S, Ermis E, et al. Sarcoidosis and the heart: A review of the literature. Intractable Rare Dis Res. 2015; 4(4): 170–180, doi: 10.5582/irdr.2015.01023, indexed in Pubmed: 26668777.
5. Healthcare Cost and Utilization Project (HCUP). Introduction to the HCUP National Inpatient Sample (NIS) 2014. 2016; 4287: 1–52.
6. Agency for Healthcare Research and Quality. National Inpatient Sample (NIS) Redesign Final Report. HCUP Methods Ser. 2014; 04: 1–32.
7. Tamariz L, Harkins T, Nair V. A systematic review of validated methods for identifying ventricular arrhythmias using administrative and claims data. Pharmacoepidemiol Drug Saf. 2012; 21 Suppl 1: 148–153, doi: 10.1002/pds.2340, indexed in Pubmed: 22262601.
8. Charlson ME, Pompei P, Ales KL, et al. A new method of classifying prognostic comorbidity in longitudinal studies: development and validation. J Chronic Dis. 1987; 40(5): 373–383, indexed in Pubmed: 3558716.
9. Lynch, J. P. Cardiac involvement in sarcoidosis: Evolving concepts in diagnosis and treatment. Semin. Respir. Crit. Care Med. 2014; 35: 372–390.
10. Doughan AR, Williams BR. Cardiac sarcoidosis. Heart. 2006; 92(2): 282–288, doi: 10.1136/hrt.2005.080481.
11. Birnie DH, et al. HRS expert consensus statement on the diagnosis and management of arrhythmias associated with cardiac sarcoidosis. Heart Rhythm. 2014; 11: 1305–1324.
12. Mehta D, Lubitz SA, Frankel Z, et al. Cardiac involvement in patients with sarcoidosis: diagnostic and prognostic value of outpatient testing. Chest. 2008; 133(6): 1426–1435, doi: 10.1378//chest.07-2784, indexed in Pubmed: 18339784.
13. Roberts WC, McAllister HA, Ferrans VJ. Sarcoidosis of the heart. A clinicopathologic study of 35 necropsy patients (group I) and review of 78 previously described necropsy patients (group II). Am J Med. 1977; 63(1): A81, doi: 10.1016/0002-9343(77)90145-0.
14. Sekhri V, Sanal S, Delorenzo LJ, et al. Cardiac sarcoidosis: a comprehensive review. Arch Med Sci. 2011; 7(4): 546–554, doi: 10.5114/aoms.2011.24118, indexed in Pubmed: 22291785.
15. Jefic D, Joel B, Good E, et al. Role of radiofrequency catheter ablation of ventricular tachycardia in cardiac sarcoidosis: report from a multicenter registry. Heart Rhythm. 2009; 6(2): 189–195, doi: 10.1016/j.hrthm.2008.10.039, indexed in Pubmed: 19187909.
16. Kopriva P, Griva M, Tüdös Z. Management of cardiac sarcoidosis: A practical guide. Cor et Vasa. 2018; 60(2): e155–e164, doi: 10.1016/j.crvasa.2017.05.012.
17. Koplan BA, Soejima K, Baughman K, et al. Refractory ventricular tachycardia secondary to cardiac sarcoid: electrophysiologic characteristics, mapping, and ablation. Heart Rhythm. 2006; 3(8): 924–929, doi: 10.1016/j.hrthm.2006.03.031, indexed in Pubmed: 16876741.
18. Winters S, Cohen M, Greenberg S, et al. Sustained ventricular tachycardia associated with sarcoidosis: Assessment of the underlying cardiac anatomy and the prospective utility of programmed ventricular stimulation, drug therapy and an implantable antitachycardia device. J Am Coll Cardiol. 1991; 18(4): 937–943, doi: 10.1016/0735-1097(91)90750-4.
19. Epstein A, DiMarco J, Ellenbogen K, et al. ACC/AHA/HRS 2008 Guidelines for Device-Based Therapy of Cardiac Rhythm Abnormalities. Heart Rhythm. 2008; 5(6): e1–e62, doi: 10.1016/j.hrthm.2008.04.014.

VIA MEDICA

ORIGINAL ARTICLE

Cardiology Journal
2020, Vol. 27, No. 3, 278–284
DOI: 10.5603/CJ.a2018.0076

ISSN 1897–5593

Psoriasis is an independent predictor of increased risk of allergic reaction during percutaneous coronary interventions. Big data analysis from the Polish National PCI Registry (ORPKI)

Zbigniew Siudak[1], Kalina Wysocka-Dubielecka[2], Krzysztof Malinowski[3], Artur Dziewierz[4], Tomasz Tokarek[4], Krzysztof Plens[5], Dariusz Dudek[4]

[1]Faculty of Medicine and Health Science, Jan Kochanowski University, Kielce, Poland
[2]Department of Dermatology, Szpital Miedzyleski, Warsaw, Poland
[3]Institute of Public Health, Faculty of Health Sciences, Jagiellonian University Medical College, Krakow, Poland
[4]2nd Department of Cardiology, Jagiellonian University Medical College, Krakow, Poland
[5]KCRI Ltd., Poland

Abstract

Background: *The presence of psoriasis is currently considered by the European Society of Cardiology cardiovascular prevention guidelines of 2016 as one possible cardiovascular risk factor. Patients with psoriasis and concomitant coronary artery disease treated by means of percutaneous coronary intervention (PCI) are a fairly large subgroup of patients that have been usually omitted in mainstream research. The aim herein, was to identify the incidence of psoriasis, baseline characteristics and periprocedural outcome with a special focus on procedural complications in patients undergoing percutaneous coronary procedures.*

Methods: *All consecutive patients who had either coronary angiography or coronary angiography with immediate PCI in Poland in 2014 and 2015 were included. Patients were assigned to two groups based on previous diagnosis: with psoriasis and without psoriasis. Clinical outcome was defined as any periprocedural death.*

Results: *There were 405,078 patients included in this analysis. Psoriasis (moderate or severe) was diagnosed in 1507 (0.4%) of them. Psoriasis was an independent predictor of allergic reaction occurrence (odds ratio [OR] 6.02; 95% confidence interval [CI] 1.44–25.22; $p = 0.014$). After propensity score adjustment, psoriasis remained a significant predictor of allergic reaction (OR 5, 95% CI 1.2–20.7; $p = 0.0245$). There were no differences in rates of periprocedural deaths in patients with or without psoriasis (death: 0.95% vs. 0.62%, $p > 0.05$).*

Conclusions: *Severe or moderate psoriasis is an independent risk factor for the occurrence of allergic reaction during percutaneous coronary procedures. There were no differences in periprocedural mortality and complications in patients with versus those without psoriasis.* (Cardiol J 2020; 27, 3: 278–284)

Key words: infarction, coronary, psoriasis, anaphylaxis

Address for correspondence: Assoc. Prof. Zbigniew Siudak MD, PhD, Faculty of Medicine and Health Science, Jan Kochanowski University, IX Wiekow Kielc 19, 25–317 Kielce, Poland, tel: +48 41 349 69 09, fax: +48 41 349 69 16, e-mail: zbigniew.siudak@gmail.com

Received: 22.03.2018 Accepted: 7.07.2018

Introduction

Psoriasis is a chronic autoimmune inflammatory disease, the prevalence of which ranges from 1.5% to 4.7% in the general population making it a significant healthcare issue [1–3]. The immune-mediated inflammatory pathogenesis of psoriasis is linked to another inflammatory disease which is atherosclerosis [4, 5]. The presence of psoriasis is currently considered by the European Society of Cardiology (ESC) cardiovascular prevention guidelines of 2016 as one possible cardiovascular risk factors within a wide group of autoimmune and inflammatory diseases [6]. Currently the American Heart Association (AHA) recommendations include risk factor screening in patients with psoriasis from as early as age 20 and by the age 40 a full list of these including various cardio-metabolic parameters need to be identified [7, 8]. Retrospective data concerning the effect of psoriasis on cardiovascular morbidity and mortality seem to confirm its adverse outcome on the occurrence of myocardial infarction or development of coronary artery disease, however, meta-analysis and literature reviews provide inconclusive data, probably because of confounding factors and the moderate quality of cardiovascular risk factor reporting (psoriasis) in large datasets [9–13]. In the Rotterdam study, authors did not find a correlation between mild psoriasis and risk for the development of cardiovascular events or atherosclerosis which seems to support the general consensus that if any, psoriasis may have its deleterious effect only if at least moderate or severe presentation is expressed [14]. A combined clinical endpoint of death, myocardial infarction and stroke was more frequent in patients with severe psoriasis than in those without, which is the only prospective observation available thus far [15, 16].

Patients with psoriasis and concomitant coronary artery disease treated by means of percutaneous coronary intervention (PCI) are a fairly large (in definite numbers) subgroup of patients that have usually been omitted in mainstream research.

The main aim of this analysis was to identify the incidence of psoriasis, baseline characteristics and periprocedural outcome with a special focus on procedural complications in this subgroup of patients.

Methods

The Polish National PCI database (ORPKI) is a registry (with eCRF) for all percutaneous coronary procedures that have been performed in Poland since 2004 and is currently operated by the Jagiellonian University Medical College in Krakow. Annual reports are published each year and the registry rationale has been described before [17, 18]. In this manuscript, data for the calendar year 2014 (January–December) and 2015 (January–December) were analyzed. All consecutive patients who had either coronary angiography or coronary angiography with immediate PCI in 155 interventional cardiology centers in Poland were included in this analysis. Patients with incomplete records concerning baseline characteristics were excluded. The reason for analyzing data from 2014 onwards was due to the fact that psoriasis was implemented for the first time into eCRF of the ORPKI database on January 1st, 2014.

Periprocedural mortality was defined as death from any cause during angiography/PCI. Psoriasis was defined as severe or moderate presentation as confirmed by prior diagnosis by a dermatologist (PASI index > 10). Only moderate and severe presentations were taken into account since they have been proven to have an impact on cardiovascular disease [6, 11, 13]. Allergic reaction was defined as any hypersensitive response of the immune system presenting as: bronchospasm, asthma exacerbation, conjunctivitis, urticaria, eczema, angioedema, anaphylactic shock. All these symptoms had to be revealed during a patient stay at a catheterization laboratory and had not been present prior to admission.

Other complications or adverse events were diagnosed at the operator's discretion according to current ESC definitions. Clinical outcome was defined as any periprocedural death. No further evaluation or follow-up of patients was performed. All patients provided informed consent. The study complied with ethical principles for clinical research based on the Declaration of Helsinki with later amendments. No external funding was used to support this registry.

Statistical analysis

Categorical variables were presented as numbers and percentages. The distributions of continuous variables were expressed as mean ± standard deviation (SD), standard error (SE), median with interquartile range (IQR). Additionally, the number of available cases and minimum and maximum values were also presented. Normality was assessed by the Lilliefor test. Equality of variances were assessed using the Levene test. Differences between groups were compared using the Stu-

dent or Welch t-test depending on the equality of variances for normally distributed variables. The Mann-Whitney U test was used for non-normally distributed continuous variables. Categorical variables were compared with the Fisher exact test for the 2 × 2 tables or by the Pearson χ^2 test for the other tables. P-values less than 0.05 were assumed to indicate statistical significance.

Simple logistic regression was used for each of potential factor as a predictor for occurrence of allergic reaction. Then if p-value for a specific factor was less than 0.2 such factor was introduced into multiple logistic regression. The recommendation for using a significance level as high as 0.20 or 0.25 as screening criterion for initial variable selection is based on work by Bendel and Afifi (1977) [19] on linear regression and on work by Mickey and Greenland (1989) [20] on logistic regression. Only significant predictors and potential confounders (for adjustment) remained in the final model. The same procedure was repeated considering correction for rare events [21]. Both models were diagnosed using receiver operating characteristic curve and area under curve parameter.

The propensity score for psoriasis was calculated based on diabetes, hypertension, smoking, clinical diagnosis, kidney disease, presence of multivessel disease glycoprotein inhibitor use, access site, contrast volume, radiation, age, weight and gender. Then the odds for allergic reaction were calculated using logistic regression with presence of psoriasis as a covariate and was conditioned on propensity score.

Analysis was performed in JMP® 9.0.0. (SAS Institute Inc., Cary, NC, 1989–2007) and R 3.3.0. (A language and environment for statistical computing. R Foundation for Statistical Computing, Vienna, Austria).

Results

There were 405,078 patients with full records in the ORPKI database for the period of January 1st 2014 till December 31st 2015 were included in this analysis. Psoriasis (moderate or severe) was diagnosed in 1507 (0.4%) of them. Patient baseline and clinical characteristics are presented in Table 1. Procedural outcome as well as frequency of complications in patients with and without psoriasis are presented in Table 2. The occurrence of periprocedural death, stroke and sudden cardiac arrest did not differ between the groups even though baseline and clinical characteristics in patients with psoriasis were high risk (significantly higher prevalence of diabetes, prior myocardial infarction, smoking and hypertension). Allergic reaction was more frequent during PCI in patients with psoriasis than in those without psoriasis (0.08% vs. 0.41%, p = 0.0226). There was no differences in the occurrence of periprocedural complications and death between the studied groups. Independent predictors of allergic reaction occurrence are presented in Table 3. Psoriasis was an independent predictor of allergic reaction occurrence (odds ratio [OR] 6.02; 95% confidence interval [CI] 1.44–25.22; p = 0.014). After propensity score adjustment psoriasis remained a significant predictor of allergic reaction (OR 5; 95% CI 1.2–20.7, p = 0.0245). Model adjustment for logistic regression is presented in Figure 1.

Discussion

Since psoriasis usually presents for the first time in adolescents and young adults, it is a lifelong burden and has a possible impact for development of other comorbidities. Psoriatic arthritis may appear in up to 30% of patients leading to decreased mobility and thus permanent disability which is an adverse condition for primary prevention of cardiovascular disease, metabolic syndrome and insulin resistance in diabetes mellitus [12]. The present study has confirmed more aggravating past medical history, comorbidities and higher risk demographics for patients with diagnosed psoriasis who were scheduled for coronary angiography and or PCI, either elective or urgent one. Mild psoriasis accounts for approx. 60% of all cases. The overall frequency of psoriasis (0.4%) was lower than in previous studies, however, the present focus was only on severe and moderate forms of psoriasis which have been documented to impact cardiovascular morbidity [11, 16, 22].

Recent coronary computed tomography studies revealed that patients with psoriasis had greater plaque burden and high risk plaque prevalence which was reduced at 1 year of observation following effective anti-inflammatory treatment which was revealing for the first time that such a correlation was observed [23]. Severe forms of psoriasis have also been named as a strong and independent predictor of ischemic stroke [24]. As previously observed, it seems that if any, psoriasis may have its deleterious effect only if it was at least expressed as moderate or severe presentation and this is the group which was under investigation herein. Even though patients with psoriasis in the registry were higher risk in-

Table 1. Baseline demographic, clinical characteristic and procedure.

Variable	No psoriasis N = 403,571	Psoriasis N = 1507	P
Male gender	250,127 (62%)	1041 (69.1%)	< 0.0001
Age	66.3 ± 10.9	63.3 ± 10.6	< 0.0001
Diabetes	90,043 (22.3%)	492 (32.7%)	< 0.0001
Prior MI	91,235 (22.6%)	383 (25.4%)	0.01
Prior PCI	102,131 (25.3%)	389 (25.8%)	0.656
Prior CABG	23,406 (5.8%)	81 (5.4%)	0.508
Smoking — active	68,486 (17%)	427 (28.3%)	< 0.0001
Hypertension	284,271 (70.4%)	1129 (74.9%)	0.0001
Indication:			0.0002
STEMI	48317 (11.9%)	219 (14.5%)	
NSTEMI	52864 (13.1%)	240 (15.9%)	
Unstable angina	124,322 (30.8%)	440 (29.2%)	
Stable angina	158,635 (39.3%)	542 (35.9%)	
Angiography only	221,327 (54.8%)	767 (50.9%)	0.0022
Multivessel disease with or without LMCA involvement	151,538 (37.7%)	643 (42.8%)	< 0.0001
P2Y12 during the procedure	88,757 (21.9%)	397 (26.3%)	0.0002
UFH during PCI	153,985 (84.5%)	644 (87%)	0.0595
LMWH during PCI	5980 (3.3%)	25 (3.4%)	0.8361
GP IIb/IIIa during PCI	12,056 (6.6%)	68 (9.2%)	0.0075
Thrombolysis during PCI	376 (0.2%)	1 (0.1%)	1.000
Contrast volume [mL]	128 ± 79	135 ± 83	< 0.0001
Radiation dose [Gy]	0.796 ± 0.952	0.957 ± 1.227	< 0.0001

CABG — coronary artery bypass grafting surgery; GP — glycoprotein; Gy — Grey; LMCA — left main coronary artery; LMWH — low molecular weight heparin; MI — myocardial infarction; NSTEMI — non-ST-segment elevation myocardial infarction; PCI — percutaneous coronary intervention; STEMI — ST-segment elevation myocardial infarction; UFH — unfractionated heparin

Table 2. Clinical outcome and procedural complications.

Variable	No psoriasis N = 182,244 (PCI) N = 221,327 (Angiography)	Psoriasis N = 740 (PCI) N = 767 (Angiography)	P
Death during angiography	172 (0.08%)	0 (0%)	1.000
Death during PCI	983 (0.54%)	7 (0.95%)	0.128
SCA during angiography	905 (0.22%)	7 (0.46%)	0.0901
SCA during PCI	884 (0.49%)	6 (0.81%)	0.1818
Allergic reaction during angiography	160 (0.07%)	0 (0%)	1.000
Allergic reaction during PCI	145 (0.08%)	3 (0.41%)	0.0226
Stroke during angiography or PCI	55 (0.01%)	0 (0%)	1.000
Coronary artery perforation during PCI	295 (0.16%)	0 (0%)	0.6373
MI during PCI	173 (0.09%)	0 (0%)	1.000
No-reflow during PCI	1062 (0.58%)	8 (1.08%)	0.0850

MI — myocardial infarction; PCI — percutaneous coronary intervention; SCA — sudden cardiac arrest

Table 3. Independent predictors of allergic reaction during angiography and/or percutaneous coronary intervention.

Variable	OR	95% CI	P
Psoriasis	6.02	1.44–25.22	0.014
Diabetes mellitus	0.47	0.24–0.92	0.026
Hypertension	0.57	0.36–0.89	0.014
STEMI/NSTEMI vs. other	0.58	0.35–0.97	0.036
GP IIb/IIIa inhibitors use	4.56	2.74–7.59	< 0.001
$\log_e$ per 1 Gy (radiation dose)	1.67	1.22–2.28	0.001
Male gender	0.54	0.33–0.87	0.012

CI — confidence interval; GP — glycoprotein; Gy — Grey; STEMI — ST-segment elevation myocardial infarction; NSTEMI — non-ST-segment elevation myocardial infarction; OR — odds ratio

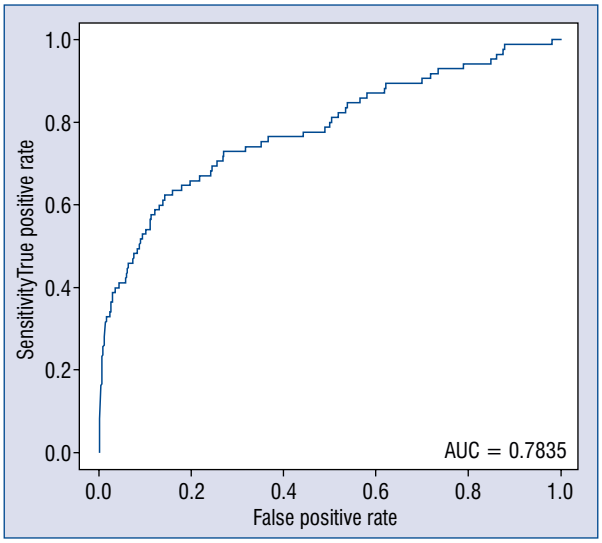

Figure 1. Model adjustment for logistic regression; AUC — area under curve.

dividuals with more frequent diabetes, hypertension and acute myocardial infarction (ST-segment elevation myocardial infarction, non-ST-segment elevation myocardial infarction) presentation as well as multivessel and more pronounced atherosclerosis, their immediate periprocedural individual outcomes like death, stroke or sudden cardiac arrest were similar to those without psoriasis (< 1%). Presently it is believed that this may stem from the fact that a majority of complications related to psoriasis, if any, occur at a later stage and may be recorded only if a longer follow up period is available and only in severe forms of psoriasis [15, 16]. Adjusting for confounders, the presence of psoriasis does not seem to at least effect the periprocedural outcome of this group of patients.

The ORPKI database is one of the biggest datasets of consecutive patients with coronary artery disease treated invasively in European Union countries which continuously collects data on severe/moderate psoriasis occurrence since 2014. No previous studies with as large numbers of individuals as in the present registry (> 400,000 for a period of 2 consecutive calendar years) have been performed so far in investigating psoriasis as a comorbidity in the setting of PCIs. Big data analysis in this case helped identify interesting associations such as more frequently observed allergic reaction occurrence in patients with psoriasis than in those without, which has remained an independent predictor even after statistical adjustments. It is known that several factors may contribute to anaphylaxis or hypersensitivity reactions during percutaneous coronary procedures, namely acetylsalicylic acid, P2Y12, heparin, glycoprotein IIb/IIIa inhibitors and contrast use itself [25–28]. Stent platforms and polymers used in drug eluting stents may potentially induce such reactions as well [29, 30]. In the present study a majority of all these variables were taken into consideration while performing multivariate analysis for independent predictors, however, not all were available in the database. The results indicate that glycoprotein IIb/IIIa inhibitor plays a significant role in allergic reaction occurrence as well as radiation doses which are a derivative of time of the procedure. It is worth noting that psoriasis conferred as the highest adjusted risk for allergic reaction even after propensity score adjustment. These findings need further investigation and suggest that caution should be used for patients presenting with severe or moderate forms of psoriasis when referred for invasive diagnostic and treatment. The results of the study may become hypotheses generating for

future clinical studies. According to available research, this is the first report of such a relationship and requires further study.

Limitations of the study

The main limitation of this study is the non-randomized design. Only periprocedural outcome could be provided which limits the observation and incidence of complications that appeared in periods after the procedure. Statistical measures were undertaken to compensate for possible biases like propensity score matching and multivariate analysis in order to identify independent predictors but since this is an observational study not all possible confounders may have been identified. An underreporting of psoriasis may be possible but only moderate or severe forms (which are less frequent in general population) were gathered in ORPKI Registry. Finally, the diagnosis of psoriasis (moderate or severe) was based on prior recognition by a physician and no additional data concerning its treatment or systemic complications were gathered in this registry.

Conclusions

Severe or moderate psoriasis is a rare comorbidity in patients undergoing percutaneous coronary procedures (< 1%). However, it is an independent risk factor for allergic reaction occurrence during percutaneous coronary procedures. The adjusted periprocedural mortality and complications rates were similar in those with psoriasis versus those without.

Conflict of interest: None declared

References

1. Gelfand JM, Mehta NN, Langan SM. Psoriasis and cardiovascular risk: strength in numbers, part II. J Invest Dermatol. 2011; 131(5): 1007–1010, doi: 10.1038/jid.2011.32, indexed in Pubmed: 21494241.
2. Gulliver W. Long-term prognosis in patients with psoriasis. Br J Dermatol. 2008; 159 Suppl 2: 2–9, doi: 10.1111/j.1365-2133.2008.08779.x, indexed in Pubmed: 18700909.
3. Schäfer T. Epidemiology of psoriasis. Review and the German perspective. Dermatology. 2006; 212(4): 327–337, doi: 10.1159/000092283, indexed in Pubmed: 16707882.
4. Hansson GK, Libby P. The immune response in atherosclerosis: a double-edged sword. Nat Rev Immunol. 2006; 6(7): 508–519, doi: 10.1038/nri1882, indexed in Pubmed: 16778830.
5. Kremers HM, McEvoy MT, Dann FJ, et al. Heart disease in psoriasis. J Am Acad Dermatol. 2007; 57(2): 347–354, doi: 10.1016/j.jaad.2007.02.007, indexed in Pubmed: 17433490.
6. Piepoli M, Hoes A, Agewall S, et al. 2016 European Guidelines on cardiovascular disease prevention in clinical practice. The Sixth Joint Task Force of the European Society of Cardiology and Other Societies on Cardiovascular Disease Prevention in Clinical Practice (constituted by representatives of 10 societies and by invited experts) Developed with the special contribution of the European Association for Cardiovascular Prevention & Rehabilitation (EACPR). Atherosclerosis. 2016; 252: 207–274, doi: 10.1016/j.atherosclerosis.2016.05.037.
7. Kimball AB, Gladman D, Gelfand JM, et al. National Psoriasis Foundation. National Psoriasis Foundation clinical consensus on psoriasis comorbidities and recommendations for screening. J Am Acad Dermatol. 2008; 58(6): 1031–1042, doi: 10.1016/j.jaad.2008.01.006, indexed in Pubmed: 18313171.
8. Jneid H, Anderson JL, Wright RS, et al. 2012 ACCF/AHA focused update of the guideline for the management of patients with unstable angina/non-ST-elevation myocardial infarction (updating the 2007 guideline and replacing the 2011 focused update): a report of the American College of Cardiology Foundation/ /American Heart Association Task Force on Practice Guidelines. J Am Coll Cardiol. 2012; 60: 645–681.
9. El-Mongy S, Fathy H, Abdelaziz A, et al. Subclinical atherosclerosis in patients with chronic psoriasis: a potential association. J Eur Acad Dermatol Venereol. 2010; 24(6): 661–666, doi: 10.1111/j.1468-3083.2009.03481.x, indexed in Pubmed: 19888942.
10. Ludwig RJ, Herzog C, Rostock A, et al. Psoriasis: a possible risk factor for development of coronary artery calcification. Br J Dermatol. 2007; 156(2): 271–276, doi: 10.1111/j.1365-2133.2006.07562.x, indexed in Pubmed: 17223866.
11. Ogdie A, Yu Y, Haynes K, et al. Risk of major cardiovascular events in patients with psoriatic arthritis, psoriasis and rheumatoid arthritis: a population-based cohort study. Ann Rheum Dis. 2015; 74(2): 326–332, doi: 10.1136/annrheumdis-2014-205675, indexed in Pubmed: 25351522.
12. Horreau C, Pouplard C, Brenaut E, et al. Cardiovascular morbidity and mortality in psoriasis and psoriatic arthritis: a systematic literature review. J Eur Acad Dermatol Venereol. 2013; 27 Suppl 3: 12–29, doi: 10.1111/jdv.12163, indexed in Pubmed: 23845149.
13. Armstrong EJ, Harskamp CT, Armstrong AW. Psoriasis and major adverse cardiovascular events: a systematic review and meta-analysis of observational studies. J Am Heart Assoc. 2013; 2(2): e000062, doi: 10.1161/JAHA.113.000062, indexed in Pubmed: 23557749.
14. Dowlatshahi EA, Kavousi M, Nijsten T, et al. Psoriasis is not associated with atherosclerosis and incident cardiovascular events: the Rotterdam Study. J Invest Dermatol. 2013; 133(10): 2347–2354, doi: 10.1038/jid.2013.131, indexed in Pubmed: 23492918.
15. Ahlehoff O, Lindhardsen J, Gislason GH, et al. Prognosis after percutaneous coronary intervention in patients with psoriasis: a cohort study using Danish nationwide registries. BMC Cardiovasc Disord. 2012; 12: 79, doi: 10.1186/1471-2261-12-79, indexed in Pubmed: 23006590.
16. Egeberg A, Thyssen JP, Jensen P, et al. Risk of myocardial infarction in patients with psoriasis and psoriatic arthritis: a nationwide cohort study. Acta Derm Venereol. 2017; 97(7): 819–824, doi: 10.2340/00015555-2657, indexed in Pubmed: 28350413.
17. Ochała A, Siudak Z, Legutko J, et al. Percutaneous interventions in cardiology in Poland in the year 2014. Summary report of the Association of Cardiovascular Interventions of the Polish Cardiac Society AISN PTK. Postepy Kardiol Interwencyjnej. 2015; 11(3): 177–181, doi: 10.5114/pwki.2015.54009, indexed in Pubmed: 26677356.

18. Siudak Z, Tokarek T, Dziewierz A, et al. Reduced periprocedural mortality and bleeding rates of radial approach in ST-segment elevation myocardial infarction. Propensity score analysis of data from the ORPKI Polish National Registry. EuroIntervention. 2017; 13(7): 843–850, doi: 10.4244/EIJ-D-17-00078, indexed in Pubmed: 28606891.
19. Bendel R, Afifi AA. Comparison of stopping rules in forward "stepwise" regression. J Am Stat Ass. 1977; 72(357): 46–53, doi: 10.1080/01621459.1977.10479905.
20. Mickey RM, Greenland S. The impact of confounder selection criteria on effect estimation. Am J Epidemiol. 1989; 129(1): 125–137, doi: 10.1093/oxfordjournals.aje.a115101, indexed in Pubmed: 2910056.
21. Tomz M, King G, Zeng L. ReLogit: rare Events Logistic Regression. J Statistical Software. 2003; 8: 1–27.
22. Armstrong AW, Harskamp CT, Armstrong EJ. Psoriasis and metabolic syndrome: a systematic review and meta-analysis of observational studies. J Am Acad Dermatol. 2013; 68(4): 654–662, doi: 10.1016/j.jaad.2012.08.015, indexed in Pubmed: 23360868.
23. Lerman JB, Joshi AA, Chaturvedi A, et al. Coronary Plaque Characterization in Psoriasis Reveals High-Risk Features That Improve After Treatment in a Prospective Observational Study. Circulation. 2017; 136(3): 263–276, doi: 10.1161/CIRCULATIONAHA.116.026859, indexed in Pubmed: 28483812.
24. Gelfand JM, Dommasch ED, Shin DB, et al. The risk of stroke in patients with psoriasis. J Invest Dermatol. 2009; 129(10): 2411––2418, doi: 10.1038/jid.2009.112, indexed in Pubmed: 19458634.
25. Schiano P, Steg PG, Barbou F, et al. A strategy for addressing aspirin hypersensitivity in patients requiring urgent PCI. Eur Heart J Acute Cardiovasc Care. 2012; 1(1): 75–78, doi: 10.1177/2048872612441580, indexed in Pubmed: 24062892.
26. Gollapudi RR, Teirstein PS, Stevenson DD, et al. Aspirin sensitivity: implications for patients with coronary artery disease. JAMA. 2004; 292(24): 3017–3023, doi: 10.1001/jama.292.24.3017, indexed in Pubmed: 15613671.
27. Juergens CP, Khaing AMi, McIntyre GJ, et al. Adverse reactions of low osmolar non-ionic and ionic contrast media when used together or separately during percutaneous coronary intervention. Heart Lung Circ. 2005; 14(3): 172–177, doi: 10.1016/j.hlc.2005.06.013, indexed in Pubmed: 16352273.
28. Hofmeier KS. Hypersensitivity reactions to modern antiplatelet and anticoagulant drugs. Allergo J Int. 2015; 24(2): 58–66, doi: 10.1007/s40629-015-0048-2, indexed in Pubmed: 26120548.
29. Montone RA, Sabato V, Sgueglia GA, et al. Inflammatory mechanisms of adverse reactions to drug-eluting stents. Curr Vasc Pharmacol. 2013; 11(4): 392–398, indexed in Pubmed: 23905634.
30. Kogias JS, Papadakis EX, Tsatiris CG, et al. Kounis syndrome: a manifestation of drug-eluting stent thrombosis associated with allergic reaction to contrast material. Int J Cardiol. 2010; 139(2): 206–209, doi: 10.1016/j.ijcard.2008.08.026, indexed in Pubmed: 18805597.

VIA MEDICA

ORIGINAL ARTICLE

Cardiology Journal
2020, Vol. 27, No. 3, 285–294
DOI: 10.5603/CJ.a2019.0036

ISSN 1897–5593

MiR-1/133 attenuates cardiomyocyte apoptosis and electrical remodeling in mice with viral myocarditis

Wei Li[1]*, Mengmeng Liu[2]*, Cuifen Zhao[2], Cai Chen[1], Qingyu Kong[2], Zhifeng Cai[2], Dong Li[3]

[1]Biomedical Engineering Institute, School of Control Science and Engineering, Shandong University, Jinan, China
[2]Department of Pediatrics, Qilu Hospital of Shandong University, Jinan, China
[3]Research Room of Hypothermia Medicine, Qilu Hospital of Shandong University, Jinan, China

Abstract

Background: *The role of miR-1 and miR-133 in regulating the expression of potassium and calcium ion channels, and mediating cardiomyocyte apoptosis in mice with viral myocarditis (VMC) is investigated herein.*

Methods: *Male Balb/c mice were randomly divided into groups: control group, VMC group, VMC + + miR-1/133 mimics group, or VMC + miR-1/133 negative control (NC) group. VMC was induced with coxsackievirus B3 (CVB3). MiR-1/133 mimics ameliorated cardiac dysfunction in VMC mice and was compared to the VMC+NC group.*

Results: *Hematoxylin and eosin staining showed a well-arranged myocardium without inflammatory cell infiltration in the myocardial matrix of the control group. However, in the VMC and VMC+NC groups, the myocardium was disorganized and swollen with necrosis, and the myocardial matrix was infiltrated with inflammatory cells. These changes were alleviated by miR-1/133 mimics. TUNEL staining revealed decreased cardiomyocyte apoptosis in the VMC + miR-1/133 mimics group compared with the VMC group. In addition, miR-1/133 mimics up-regulated the expression of miR-1 and miR-133, the potassium channel genes Kcnd2 and Kcnj2, as well as Bcl-2, and down-regulated the expression of the potassium channel suppressor gene Irx5, L-type calcium channel subunit gene α1c (Cacna1c), Bax, and caspase-9 in the myocardium of VMC mice. MiR-1/133 also up-regulated the protein levels of Kv4.2 and Kir2.1, and down-regulated the expression of CaV1.2 in the myocardium of VMC mice.*

Conclusions: *MiR-1 and miR-133 decreased cardiomyocyte apoptosis by mediating the expression of apoptosis-related genes in the hearts of VMC mice.* (Cardiol J 2020; 27, 3: 285–294)

Key words: miR-1, miR-133, viral myocarditis, ion channels, cell apoptosis

Introduction

MicroRNA (miR)-1 and miR-133 are members of a miRNA cluster expressed exclusively in skeletal and cardiac muscle cells [1], and are essential for heart development [2]. MiR-1 and miR-133 have been shown to regulate the expression of gap junctions [3], pacemaker channels [4] and potassium (K^+) channels, including inward-rectifying Kir2.1, which stabilizes resting potential [5] and Kv4.2, which dominates the outward-transient current (I_{to}) [6]. In addition, miR-133 has been shown to target CaV1.2, the primary α-subunit for L-type calcium (Ca^{2+}) channels underlying cardiac excitability [7].

Address for correspondence: Dr. Cuifen Zhao, Department of Pediatrics, Qilu Hospital of Shandong University, No. 107 Wenhuaxi Road, Jinan 250012, PR. China, tel: 086-531-82169941, fax: 086-531-86927544, e-mail: zhaocuifen@sdu.edu.cn

Dr. Wei Li, Biomedical Engineering Institute, School of Control Science and Engineering, Shandong University, Jinan 250061, China, tel: 086-531-88392824, fax: 086-531-88392824, e-mail: cindy@sdu.edu.cn

Received: 24.05.2018 Accepted: 28.09.2018

*These authors contributed equally to this work.

Previous studies have shown that approximately 20% of infant deaths due to fatal arrhythmia and severe heart failure were caused by acute severe viral myocarditis (VMC), mainly caused by coxsackievirus B3 (CVB3) [8]. However, there is currently a lack of effective etiological treatment for severe VMC. Introducing miR-1/133 can reduce virus escape and mutation, and as such, one of the major treatments involves the use of RNA interference (RNAi) combined with miR mimics [9, 10]. A previous study showed that approximately 20% of miR-1/133 mimics, labeled with Dy547 and packaged in RNA-LANCEr II neutral ionic lipids, arrived in cardiomyocytes and exhibited intracellular Dy547 particle signals when administered by tail vein injection [10]. In addition, miR-133 has been shown to target caspase-9, a pro-apoptotic factor, and promotes cardiac cell apoptosis by interfering with the expression of mRNA [11].

With rapid advances in molecular biology, miRs have been widely studied in different fields. However, reports regarding the effects of miRs on VMC have been limited. Under investigation in the present study, was the impact of miR-1/133 mimics and the appropriate miR-1/133 negative control on a mouse model of acute VMC, and the hypothesis that miR-1 and miR-133 could etiologically help to treat severe VMC was examined.

Methods

This study was in accordance with the National Research Council Guide for the care and use of laboratory animals. The animal experiments in this study were performed with approval by the Animal Care Committee of the Medical School of Shandong University.

Mouse model of acute VMC and interference

CVB3 was passaged in HeLa cells by transfection as described previously [12]. Virus titer was determined using a tissue culture infective dose 50 (TCID50) assay at the beginning of the experiments. HeLa cells were cultured in Dulbecco's Modified Eagle medium (DMEM, Life Technologies, USA) supplemented with fetal bovine serum (10%; Gibco, Australia) and penicillin-streptomycin (100 IU/mL; Invitrogen, USA).

Forty healthy male Balb/c mice (6–8 weeks old) were randomly divided into four groups: control group (n = 10), in which mice were injected intraperitoneally with Eagle's medium (0.1 mL); VMC group (n = 10), in which VMC was induced by intraperitoneal injection of 10^4 TCID50 CVB3 (0.1 mL); VMC + miR-1/133 mimics group (n = 10), in which VMC mice were injected intraperitoneally with miR-1/133 mimics (1 μg/g, GenePharma, Shanghai, China) on the day following VMC induction; VMC + NC group (n = 10), in which VMC mice were injected intraperitoneally with miR-1/133 NC (1 μg/g, GenePharma, Shanghai, China) via the tail vein on the day following VMC induction.

MiR-1/133 mimics, which were composed of mmu-miR-1 mimics and mmu-miR-133 mimics, were packaged in Lipofectamine 2000 Reagent (Invitrogen, US), and then directly mixed in the ultrasonic field to improve targeting ability. Feeding conditions of mice in each group were the same. Following virus injection, the diet, activity level, and coat appearance of the mice were observed on a daily basis.

Cardiac functional analysis

On the 7th day following establishment of the VMC model, i.e. the 6th day after miR-1/133 intervention, mice were anesthetized with an intraperitoneal injection of chloral hydrate (10%, 4 mg/g). After the mice were fixed in a supine position, the chest was shaved, and an M-echocardiograph was performed to measure the left ventricular ejection fraction (LVEF) and left ventricular fractional shortening (LVFS) of the mice in each group.

Specimen collection and disposition

On the 7th day after modeling, after all mice in the groups were anesthetized, their hearts were removed under sterile conditions, washed with normal saline, and then weighed. Half of each heart of the mice were frozen with liquid nitrogen and stored at –80°C for use in molecular biological experiments (half of each heart was used for quantitative reverse transcription followed by polymerase chain reaction (qRT-PCR) and Western blot, which were carried out by two people), the other half of the heart were fixed in 10% neutral formaldehyde, embedded in paraffin, and sectioned at 4.5 μm intervals for histological study (H&E staining and TUNEL staining).

Hematoxylin and eosin staining

Tissue sections were stained by hematoxylin and eosin (H&E; Beyotime, Shanghai, China), and cardiomyocyte morphology changes were observed under a light microscope.

TUNEL staining

Cardiomyocyte apoptosis was detected by terminal deoxynucleotidyl transferase dUTP nick end labeling (TUNEL) staining according to the manufacturer protocol (Roche, USA). Ten randomly selected fields from each slide were scored at a high magnification. The ratio of the number of brown cells, i.e. apoptotic cells, to a total of 30 cardiomyocytes counted per field was defined as the myocardial cell apoptotic ratio.

Quantitative real time RT-PCR

Total RNA was extracted from a part of each of frozen mouse heart using a TRIzol reagent (Ambion, USA). According to the manufacturer protocol (Thermo Scientific, USA), qRT-PCR was performed to detect the expression of miR-1 and miR-133, inward rectifier potassium current (I_{k1}) channel gene *Kcnd2*, its transcription repressor *Irx5*, transient outward potassium current (I_{to}) channel gene *Kcnj2,* the L-type calcium channel subunit α1c (*Cacna1c*), and apoptosis-related genes *Bax*, *Bcl-2* and caspase-9 (*Casp9*) using an ABI 7500 real-time PCR system. β-actin was used as a reference for gene expression and U6 was used as a reference for expression of miR-1 and miR-133. The relative expression of genes was calculated using the $2^{-\Delta\Delta Ct}$ method. The primers were synthesized by Guangzhou Saibo Corp, China. The sequences of gene primers used in the present study are shown in Table 1.

Western blot

To examine protein levels of Kv4.2, Kir2.1, and CaV1.2, total protein lysates were purified from the rest of frozen heart samples using RIPA buffer (Beyotime, Shanghai, China). A bicinchoninic acid (BCA) protein assay kit (Beyotime, Shanghai, China) was used to determine protein concentration. Protein (30–50 μg) was separated on an 8–15% gel with sodium dodecyl sulfate polyacrylamide gel electrophoresis (SDS-PAGE) and transferred to a polyvinylidene fluoride (PVDF) membrane. The membrane was then blocked in 5% milk, followed by incubation at 4°C overnight with the primary antibodies of interest (rabbit polyclonal anti-Kv4.2 and anti-Kir2.1, Bioss, Beijing, China, diluted 1:300; mouse monoclonal anti-CACNA1C, Abcam, USA; and mouse anti-GAPDH, ZSGB-BIO Beijing, China, diluted 1:1000). Membranes were then washed (3 times) with tris-buffered saline with Tween (TBST), and incubated with the appropriate secondary antibodies (ZSGB-BIO Beijing, China, diluted 1:10000). Immunoreactive bands were detected by enhanced chemiluminescence (ECL; Millipore, USA) and quantified using C-digit (Model: 3600, Image Studio Digits Ver 4.0, Licor, Lincoln, NE, USA). Glyceraldehyde 3-phosphate dehydrogenase (GAPDH) was used as a reference loading control. Data were collected from at least three independent experiments.

Data analysis

The experimental data are presented as mean ± standard error (SE). Statistical comparisons in multiple groups were performed using one-way analysis of variance (ANOVA), and the comparison between two groups was performed with the Fisher least significant difference *t* test. A probability value of $p < 0.05$ was considered statistically significant.

Results

MiR-1/133 mimics improved general status of VMC mice

Compared with mice in the control group, on the third day following CVB3 injection, mice in the VMC group and in the VMC + NC group had disordered fur, were irritated easily or insensitive to irritation, ate little food and lost weight (data not shown). These conditions were improved in mice receiving the miR-1/133 mimics (data not shown). Figure 1A shows the specific myocardial staining, shown using antibodies against α-actinin (green) and miR-1/133 (red).

The hearts from mice in the VMC group and NC group were bigger than those in the control and VMC + miR-1/133 mimics groups (Fig. 1B) and heart weight/body weight ratio was increased as well (Fig. 1C). There were also spot-like necrotic areas on the surface of the hearts of mice in the VMC group and the VMC + NC group (Fig. 1B).

MiR-1/133 mimics improved cardiac function of VMC mice

Compared with those in the control group, EF and FS of mice in the VMC and VMC + NC groups were significantly decreased ($p < 0.01$), suggesting impaired cardiac function of VMC mice. However, treatment with miR-1/133 mimics improved EF and FS of VMC mice ($p < 0.05$, $p < 0.01$; Fig. 2).

MiR-1/133 mimics attenuated pathological changes of VMC hearts

Compared with control group hearts, H&E staining showed that myocardia in VMC and VMC + NC groups were swollen and disordered, they

Table 1. Prime sequences for quantitative reverse transcription followed by polymerase chain reaction (qRT-PCR).

Gene	Primer Sequences (5′-3′)
β-actin	
sense	CCAGCCTTCCTTCTTGGGTAT
antisense	TTGGCATAGAGGTCTTTACGG
Kcnd2	
sense	TGACAACACTGGGGTATGGC
antisense	CCGACTGAAGTTCGACACGA
Kcnj2	
sense	TCTCACTTGCTTCGGCTCAT
antisense	ACTTGTCCTGTTGCTGGTACA
Irx5	
sense	GCCTTCTCTTACGTGGGCTC
antisense	AGTGGCATTCTTCCGGTACG
α1c (*Cacna1c*)	
sense	TCCCGAGCACATCCCTACTC
antisense	ACTGACGGTAGAGATGGTTGC
Bax	
sense	AAACTGGTGCTCAAGGCCC
antisense	CTTGGATCCAGACAAGCAGC
Bcl-2	
sense	GCTACCGTCGTGACTTCGC
antisense	CCCACCGAACTCAAAGAAGG
Casp9	
sense	TCAGGGGACATGCAGATATGG
antisense	TTGGCAGTCAGGTCGTTCTTC
U6	ATGACGTCTGCCTTGGAGAAC
sense	TCAGTGTGCTACGGAGTTCAG
antisense	
Mmu-miR-1a-3p	
reverse transcription prime	
CTCGTATCCAGTGCAGGGTCCGAGGTATTCGCACTGGATACGAGATACAT	
sense	GCCGCTGGAATGTAAAGAAGT
antisense	GTCCGAGGTATTCGCACTGGATA
Mmu-miR-133a-3p	
reverse transcription prime	
GTCGTATCCAGTGCAGGGTCCGAGGTATTCGCACTGGATACGACCAGCTG	
sense	GCTTTGGTCCCCTTCAAC
antisense	GTCCGAGGTATTCGCACTGGATA

were also infiltrated by inflammatory cells in the myocardial matrix. MiR-1/133 mimics reduced the edema of cardiomyocytes, improved arrangements, and diminished inflammatory cell infiltrate in the myocardial matrix (Fig. 3A).

MiR-1/133 mimics reduced cardiomyocyte apoptosis

TUNEL staining showed increased numbers of brown nuclei in the VMC and VMC + NC groups compared with those in the control group

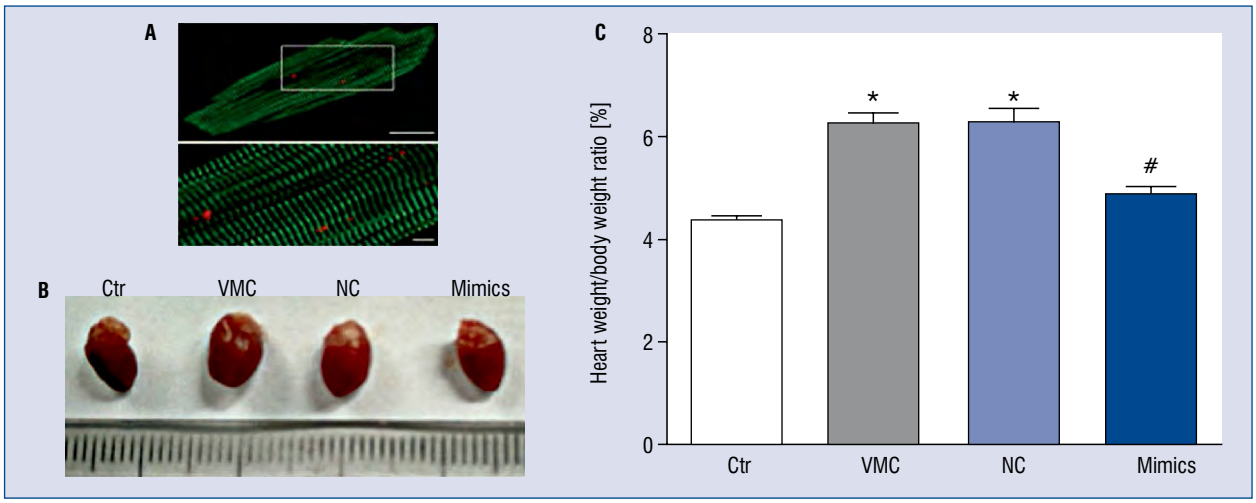

Figure 1. Macroscopic view of hearts from different groups. **A.** Fluorescence showing specific staining of green (α-actinin) and red (Dy547) for miR-1/133; **B.** Global view of representative heart from each group; **C.** The statistical analysis of the heart weight/body weight ratio of mice in each group; Ctr — control group; VMC — viral myocarditis (VMC) group; NC — VMC + miR-1/133 negative control (NC) group; Mimics — VMC + miR-1/133 mimics (Mimics) group. Data are expressed as mean ± standard error (SE). N = 10, *p < 0.01 vs. control group, #p < 0.05 vs. VMC and VMC + NC group; for other abbreviations — see text.

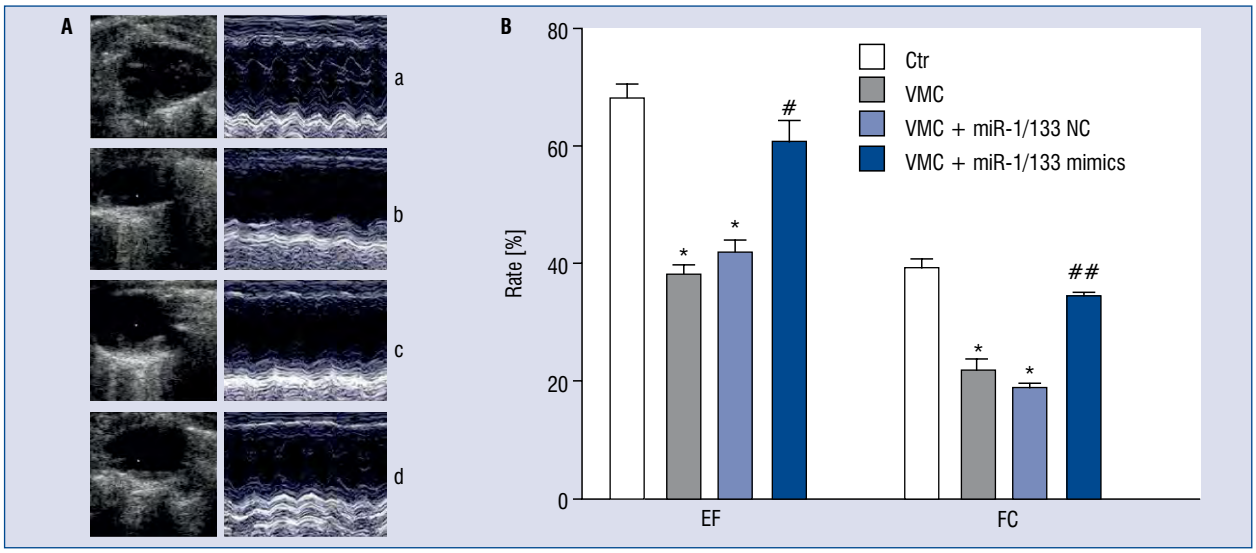

Figure 2. MiR-1/133 mimics improved cardiac function of viral myocarditis (VMC) mice. **A.** Echocardiography showed ejection fraction (EF) and fractional shortening (FS) of mice in each group; **a.** Control group (Ctr), **b.** VMC group, **c.** VMC + NC group, **d.** VMC + miR-1/133 mimics group. **B.** Statistical analysis of EF and FS of different groups. Data are expressed as mean ± standard error (SE). N = 10, *p < 0.01 vs. control group, #p < 0.05, ##p < 0.01 vs. VMC and VMC + NC group; for other abbreviations — see text.

($p < 0.01$), revealing increased cell death. MiR-1/133 mimics significantly reduced the number of brown nuclei ($p < 0.01$), indicating decreased cell death. The VMC + NC group had the highest rate of apoptosis while the control group had the lowest (Fig. 3B, C).

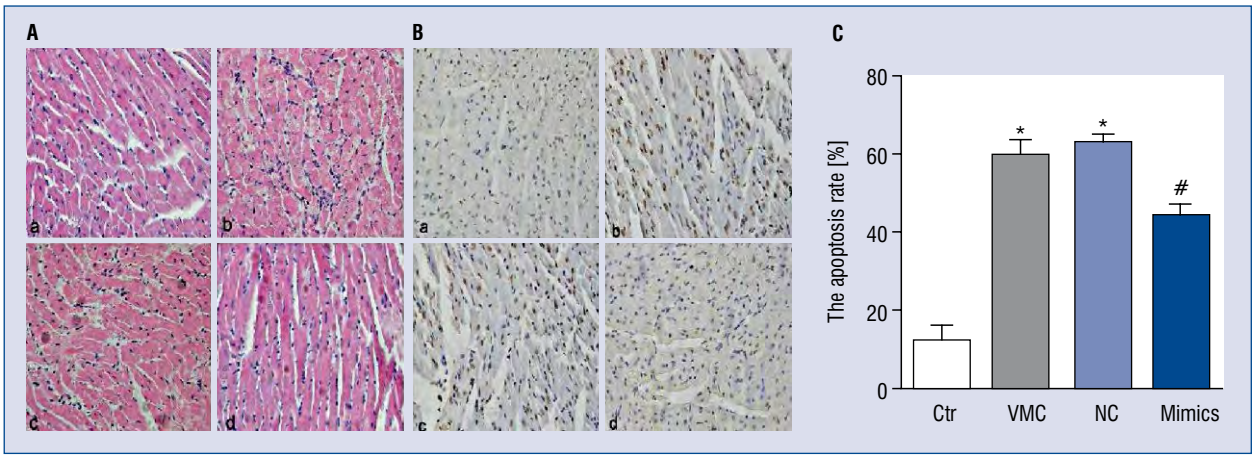

Figure 3. MiR-1/133 mimics improved pathological changes and reduced cardiomyocyte apoptosis in viral myocarditis (VMC) mouse hearts. **A.** H&E staining of myocardium in different group mice (magnification: 10 × 40); **a.** Control group (Ctr), **b.** VMC group, **c.** VMC + negative control (NC) group, **d.** VMC + miR-1/133 mimics group; **B.** TUNEL staining showed cardiomyocytes apoptosis of different group mice (10 × 40). Cells with brown nuclei were TUNEL positive, and cells with blue nuclei represented normal cells; **a.** Control group, **b.** VMC group, **c.** VMC+miR-1/133 NC group, **d.** VMC + miR-1/133 mimics group; **C.** Quantified cell apoptosis data. Data are expressed as mean ± standard error (SE). N = 10, *p < 0.01 vs. control, #p < 0.01 vs. VMC and VMC + NC group; for other abbreviations — see text.

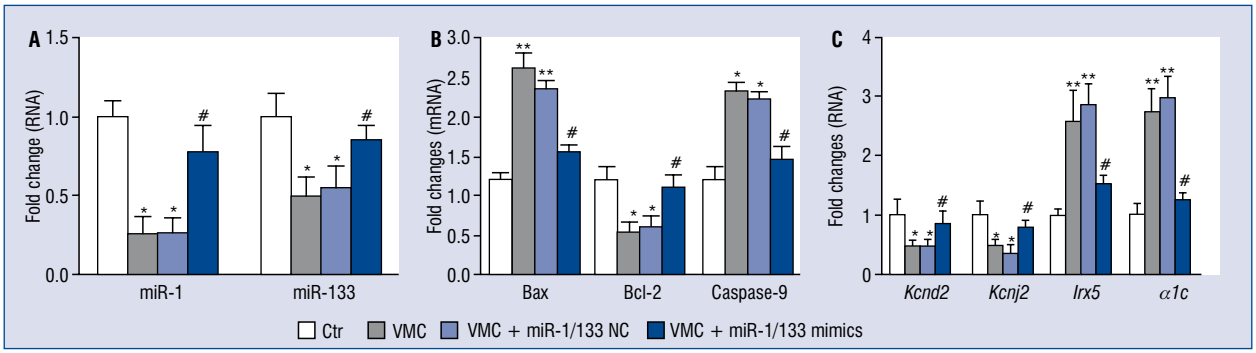

Figure 4. MiR-1/133 mimics regulated the expressions of miR-1 and miR-133, apoptosis-related genes, potassium channel genes and a calcium channel gene. **A.** The fold changes of miR-1 and miR-133 expression. U6 was used as an internal reference and data was normalized to the control group (Ctr). N = 10, *p < 0.05 vs. control group, #p < < 0.05 vs. viral myocarditis (VMC) and VMC + NC groups; **B, C.** The fold changes of apoptosis-related genes *Bax*, *Bcl-2*, and *Casp9*, and potassium channel genes *Kcnd2*, *Irx5*, *Kcnj2*, and L-type calcium channel subunit α1c, *Cacna1c*. Values were normalized against β-actin as an endogenous control. Data are expressed as mean ± standard error (SE). The fold changes of qRT-PCR were determined using the $2^{-\Delta\Delta Ct}$ method. N = 10, *p < 0.05, **p < 0.01 vs. control group, #p < 0.05 vs. VMC and VMC + NC groups; for other abbreviations — see text.

MiR-1/133 mimics improved expression of miR-1 and miR-133 in VMC hearts

qRT-PCR data showed that the relative expression of miR-1 and miR-133 in mouse hearts of the VMC and VMC + NC groups was significantly decreased compared to the control group ($p < 0.05$), but miR-1/133 mimics increased the expression of miR-1 and miR-133 ($p < 0.05$; Fig. 4A).

MiR-1/133 regulated the mRNA expression of apoptosis-related genes *Bax*, *Bcl-2* and *caspase-9* in VMC hearts

The relative expression of pro-apoptosis-related genes *Bax* ($p < 0.01$), and *Casp9* ($p < 0.05$) mRNA in the VMC and VMC + NC groups were significantly up-regulated compared with those in the control group. However, miR-1/133 mimics

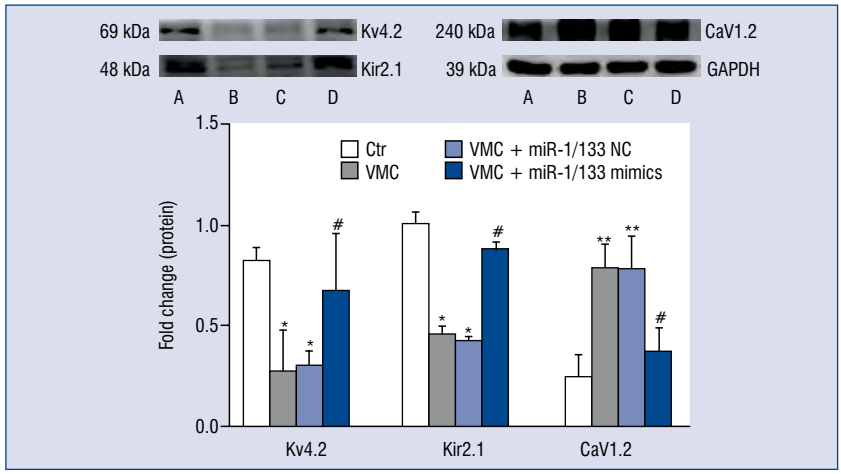

Figure 5. MiR-1/133 mimics complex regulated the protein levels of Kv4.2, Kir2.1 and CaV1.2. Upper panel: Western blot. **A.** Control group (Ctr); **B.** Viral myocarditis (VMC) group; **C.** VMC + NC group; **D.** VMC + miR-1/133 mimics complex group. Lower panel: Statistical analysis of the upper panel. Data are expressed as mean ± standard error (SE). GAPDH was used as an internal reference, and data were normalized to the control group. N = 10, *$p < 0.05$, **$p < 0.01$ vs. control group, #$p < 0.05$ vs. VMC and VMC + NC groups; for other abbreviations — see text.

greatly decreased their expression ($p < 0.05$). While the expression of the anti-apoptosis-related gene *Bcl-2* mRNA was down-regulated in the VMC and VMC+NC groups, miR-1/133 mimics increased its expression ($p < 0.05$; Fig. 4B).

MiR-1/133 regulated the relative expressions of ion channel genes *Kcnd2*, *Kcnj2*, *Irx5* and *α1c* in VMC hearts

Compared with those in the control group, the relative expression of *Kcnd2* and *Kcnj2* in the VMC and VMC + NC groups were significantly down-regulated as revealed by qRT-PCR data ($p < 0.05$), which was attenuated by miR-1/133 mimics interference ($p < 0.05$). Also, the relative expression of *Irx5* and α1c (*Cacna1c*) was increased in VMC and VMC + NC groups compared with the control group ($p < 0.01$), and this increase was suppressed by miR-1/133 mimics interference ($p < 0.05$; Fig. 4C).

MiR-1/133 regulated the protein levels of Kv4.2, Kir2.1 and L-type calcium channel subunit CaV1.2 in VMC hearts

Compared with control mice, the protein levels of I_{to} target protein Kv4.2 and I_{k1} target protein Kir2.1 in the VMC and VMC + NC groups were significantly decreased ($p < 0.05$), but this decrease was suppressed by miR-1/133 mimics. Also, the expression of the L-type calcium channel subunit protein CaV1.2 was significantly increased in the VMC and VMC + NC groups compared with the control group ($p < 0.01$), but again, this increase was attenuated by miR-1/133 mimics interference ($p < 0.05$; Fig. 5).

Discussion

MiRs have been shown to be implicated in a variety of human diseases, and may serve as potential bio-markers in certain diseases once released into the circulatory system [13]. Currently, more than 100 miRs have been identified in myocardial cells, and some, if not all, were dysregulated in heart diseases [14, 15]. MiR-1 and miR-133, which translate together in a bicistronic way [16], are specific to muscle and are abundant in the heart [17, 18]. MiR-1 and miR-133 play an important role in normal cardio genesis [19] and in the pathogenesis of several cardiovascular diseases including myocardial ischemia-reperfusion injury [11], cardiac hypertrophy [20, 21], arrhythmia [22], and myocardial infarction [23]. However, their involvement in VMC-linked cardiac phenotypes has not been explored. The major findings from the present investigation include: 1) miR-1/133 was downregulated in the hearts of VMC mice, 2) miR-1/133 mimics attenuated cardiac dysfunction and apoptosis in VMC mouse hearts, 3) miR-1/133 mimics mediated the expression of apoptosis-related genes in VMC mouse hearts, and 4) miR-1/133 mimics mediated the expression of potassium and calcium channels in VMC mouse hearts.

Viral invasion of myocardial cells causes persistent chronic inflammation, subsequently resulting in myocardial cell hypertrophy, myocardial cell apoptosis, and myocardial fibrosis [24–26]. Therefore, the progression of VMC will eventually lead to heart failure and fatal arrhythmias, which is linked to sudden death. In agreement with the above findings, in the present study, the VMC mice induced by CVB3 exhibited impaired cardiac function as evidenced by reduced EF and FS compared with control mice. Under further testing the effects of miR1/133 on cardiac function and pathology in VMC mice, and found that miR-1/133 mimics ameliorated cardiac function and pathological changes of VMC mice. This miR-1/133-induced improvement of cardiac function and pathology might be attributed to decreased cardiomyocyte apoptosis in VMC mouse hearts. To further understand the molecular basis underlying reduced apoptosis by miR-1/133 mimics, qRT-PCR was used to examine the relative expression of apoptosis-related genes *Bax*, *Bcl-2* and *Casp9* in VMC hearts of the different groups. The pro-apoptosis-related genes *Bax* and *Casp9*, as well as the anti-apoptosis-related gene *Bcl-2* are the main genes involved in the progression of cell apoptosis. The present findings suggest that viral infection increased the expression of *Bax* and *Casp9* but decreased the expression of *Bcl-2*, and that miR-1/133 mimics attenuated the changes in the expression of these three genes. Therefore, it is possible that these miR1/133-induced changes contributed to the improved cardiac function and pathology of VMC mice by miR1/133 mimics. In addition, the current findings demonstrate that miR-133 expression was inversely proportional with the expression of Casp9 and was in line with a previous study identifying caspase-9 as a target of miR-133 [27].

Viral myocarditis patients display different arrhythmias, and severe arrhythmia can cause sudden cardiac death. Electrical remodeling and myocardium structural remodeling are the main mechanisms leading to arrhythmia [28], which is associated with changes in the activity of ion channels present on the myocardial cell membrane [29], including potassium and calcium ion channels. Although many miRs are expressed abnormally in many heart diseases, there are few reports regarding the relationship between miR-1 and miR-133 and the activity of potassium ion channels and calcium ion channels in VMC. For example, miR-1 and miR-133 were shown to be involved in the regulation of Kv4.2 and Kir2.1 expression [30], the latter of which is the main component of I_{k1} and is linked to arrhythmia [31]. Also, the aberrant expression of miR-1 influenced the activity of I_{k1} and its expression [32, 33]. Kir2.1, which is the main potassium channel subunit,plays important roles in initiating and maintaining resting membrane potential of cardiomyocytes [34], is encoded by *Kcnj2*, and *Kcnj2* was targeted by miR-1 [3]. Therefore, the aberrant expression of miR-1 could cause abnormality in the structure and function of potassium channels, influencing membrane potential stability, and result in arrhythmia. In addition, the potassium channel subunit Kv4.2, the main component of $I_{to,}$ is rich in cardiomyocytes, and is encoded by the *Kcnd2* gene. Irx5, a transcriptional repressor of *Kcnd2*, and regulated potassium ion current and repolarization of action potentials. MiR-1 was found to target Irx5 and thus influenced the expression of *Kcnd2* [35]. In the present study, it was observed that the aberrant expression of *Kcnd2* and *Kcnj2* in VMC cardiomyocytes, which can result in a change of potassium ion concentration and influence membrane potential, and therefore may contribute to arrhythmia. In line with the above reports, it was also shown herein that there was a negative correlation between miR-1 and Irx5. Therefore, it was believed that miR-1 improved arrhythmia at least in part through mediating the expression of *Kcnd2* and *Kcnj2* and thus, regulating potassium concentrations. In addition, the L-type calcium channel subunit α1c is the main calcium ion channel in myocardium and plays an important role in stabilizing calcium concentration in the cell and maintaining action potential repolarization. α1c was identified as a potential target of miR-133 [7], which was consistent with the present findings that demonstrated a negative correlation between miR-133 and α1c. Taken together, it was speculated that miR-1 and miR-133 reduced arrhythmia by mediating the expression and activity of ion channels, and could serve as potential anti-arrhythmic targets.

Conclusions

In summary, this study reports that miR-1/133 mimics ameliorate cardiac function in VMC mice. Mechanistically, miR-1/133 mimics reduce cardiomyocyte apoptosis by regulating the expressions of apoptosis-related genes, improves arrhythmia through regulating the expressions of calcium and potassium ion channel genes of cardiomyocytes, and diminishes cardiac fibrosis in VMC mouse hearts. Therefore, miR-1/133 may serve as a potential therapeutic target for treatment of VMC in clinics.

Acknowledgements

This study was supported in part by grants from the National Natural Science Foundation (#21728701), The ministry of education postdoctoral fund (#2015M572044), Shandong Province Science and Technology Development Project (#GG201709260070).

Conflict of ineterest: None declared

References

1. Lagos-Quintana M, Rauhut R, Yalcin A, et al. Identification of tissue-specific microRNAs from mouse. Curr Biol. 2002; 12(9): 735–739, indexed in Pubmed: 12007417.
2. Zhao Y, Samal E, Srivastava D. Serum response factor regulates a muscle-specific microRNA that targets Hand2 during cardiogenesis. Nature. 2005; 436(7048): 214–220, doi: 10.1038/nature03817, indexed in Pubmed: 15951802.
3. Yang B, Lin H, Xiao J, et al. The muscle-specific microRNA miR-1 regulates cardiac arrhythmogenic potential by targeting GJA1 and KCNJ2. Nat Med. 2007; 13(4): 486–491, doi: 10.1038/nm1569, indexed in Pubmed: 17401374.
4. Li YD, Hong YF, Yusufuaji Y, et al. Altered expression of hyperpolarization-activated cyclic nucleotide-gated channels and microRNA-1 and -133 in patients with age-associated atrial fibrillation. Mol Med Rep. 2015; 12(3): 3243–3248, doi: 10.3892/mmr.2015.3831, indexed in Pubmed: 26005035.
5. Girmatsion Z, Biliczki P, Bonauer A, et al. Changes in microRNA-1 expression and IK1 up-regulation in human atrial fibrillation. Heart Rhythm. 2009; 6(12): 1802–1809, doi: 10.1016/j.hrthm.2009.08.035, indexed in Pubmed: 19959133.
6. da Costa Martins PA, Bourajjaj M, Gladka M, et al. Conditional dicer gene deletion in the postnatal myocardium provokes spontaneous cardiac remodeling. Circulation. 2008; 118(15): 1567–1576, doi: 10.1161/CIRCULATIONAHA.108.769984, indexed in Pubmed: 18809798.
7. Lu Y, Xiao J, Lin H, et al. A single anti-microRNA antisense oligodeoxyribonucleotide (AMO) targeting multiple microRNAs offers an improved approach for microRNA interference. Nucleic Acids Res. 2009; 37(3): e24, doi: 10.1093/nar/gkn1053, indexed in Pubmed: 19136465.
8. Feldman A, McNamara D. Myocarditis. N Engl J Med. 2000; 343(19): 1388–1398, doi: 10.1056/nejm200011093431908.
9. Xu F, Liu G, Liu Q, et al. RNA interference of influenza A virus replication by microRNA-adapted lentiviral loop short hairpin RNA. J Gen Virol. 2015; 96(10): 2971–2981, doi: 10.1099/jgv.0.000247, indexed in Pubmed: 26296570.
10. Myers R, Timofeyev V, Li N, et al. Feedback mechanisms for cardiac-specific microRNAs and cAMP signaling in electrical remodeling. Circ Arrhythm Electrophysiol. 2015; 8(4): 942–950, doi: 10.1161/CIRCEP.114.002162, indexed in Pubmed: 25995211.
11. Kinali M, Arechavala-Gomeza V, Cirak S, et al. Muscle histology vs MRI in Duchenne muscular dystrophy. Neurology. 2011; 76(4): 346–353, doi: 10.1212/WNL.0b013e318208811f, indexed in Pubmed: 21263136.
12. Liu Z, Carthy CM, Cheung P, et al. Structural and functional analysis of the 5' untranslated region of coxsackievirus B3 RNA: In vivo translational and infectivity studies of full-length mutants. Virology. 1999; 265(2): 206–217, doi: 10.1006/viro.1999.0048, indexed in Pubmed: 10600593.
13. Li LM, Cai WB, Ye Q, et al. Comparison of plasma microRNA-1 and cardiac troponin T in early diagnosis of patients with acute myocardial infarction. World J Emerg Med. 2014; 5(3): 182–186, doi: 10.5847/wjem.j.1920-8642.2014.03.004, indexed in Pubmed: 25225581.
14. Cheng Y, Ji R, Yue J, et al. MicroRNAs are aberrantly expressed in hypertrophic heart: do they play a role in cardiac hypertrophy? Am J Pathol. 2007; 170(6): 1831–1840, doi: 10.2353/ajpath.2007.061170, indexed in Pubmed: 17525252.
15. Busk PK, Cirera S. MicroRNA profiling in early hypertrophic growth of the left ventricle in rats. Biochem Biophys Res Commun. 2010; 396(4): 989–993, doi: 10.1016/j.bbrc.2010.05.039, indexed in Pubmed: 20470752.
16. Carè A, Catalucci D, Felicetti F, et al. MicroRNA-133 controls cardiac hypertrophy. Nat Med. 2007; 13(5): 613–618, doi: 10.1038/nm1582, indexed in Pubmed: 17468766.
17. Liang Yu, Ridzon D, Wong L, et al. Characterization of microRNA expression profiles in normal human tissues. BMC Genomics. 2007; 8: 166, doi: 10.1186/1471-2164-8-166, indexed in Pubmed: 17565689.
18. Luo X, Zhang H, Xiao J, et al. Regulation of human cardiac ion channel genes by microRNAs: theoretical perspective and pathophysiological implications. Cell Physiol Biochem. 2010; 25(6): 571–586, doi: 10.1159/000315076, indexed in Pubmed: 20511702.
19. Lin CC, Chang YM, Pan CT, et al. Functional evolution of cardiac microRNAs in heart development and functions. Mol Biol Evol. 2014; 31(10): 2722–2734, doi: 10.1093/molbev/msu217, indexed in Pubmed: 25063441.
20. Sayed D, Hong C, Chen IY, et al. MicroRNAs play an essential role in the development of cardiac hypertrophy. Circ Res. 2007; 100(3): 416–424, doi: 10.1161/01.RES.0000257913.42552.23, indexed in Pubmed: 17234972.
21. Diniz GP, Lino CA, Guedes EC, et al. Cardiac microRNA-133 is down-regulated in thyroid hormone-mediated cardiac hypertrophy partially via type 1 angiotensin II receptor. Basic Res Cardiol. 2015; 110(5): 49, doi: 10.1007/s00395-015-0504-7, indexed in Pubmed: 26202011.
22. Hedley PL, Carlsen AL, Christiansen KM, et al. MicroRNAs in cardiac arrhythmia: DNA sequence variation of MiR-1 and MiR-133A in long QT syndrome. Scand J Clin Lab Invest. 2014; 74(6): 485–491, doi: 10.3109/00365513.2014.905696, indexed in Pubmed: 24809446.
23. Wang GK, Zhu JQ, Zhang JT, et al. Circulating microRNA: a novel potential biomarker for early diagnosis of acute myocardial infarction in humans. Eur Heart J. 2010; 31(6): 659–666, doi: 10.1093/eurheartj/ehq013, indexed in Pubmed: 20159880.
24. Woodruff JF. Viral myocarditis. A review. Am J Pathol. 1980; 101(2): 425–484, indexed in Pubmed: 6254364.
25. Reyes MP, Lerner AM. Coxsackievirus myocarditis — with special reference to acute and chronic effects. Prog Cardiovasc Dis. 1985; 27(6): 373–394, indexed in Pubmed: 2988014.
26. Kishimoto C, Misaki T, Crumpacker CS, et al. Serial immunologic identification of lymphocyte subsets in murine coxsackievirus B3 myocarditis: different kinetics and significance of lymphocyte subsets in the heart and in peripheral blood. Circulation. 1988; 77(3): 645–653, indexed in Pubmed: 2830046.
27. Xu C, Lu Y, Pan Z, et al. The muscle-specific microRNAs miR-1 and miR-133 produce opposing effects on apoptosis by targeting HSP60, HSP70 and caspase-9 in cardiomyocytes. J Cell Sci. 2007; 120(Pt 17): 3045–3052, doi: 10.1242/jcs.010728, indexed in Pubmed: 17715156.

28. Zhang L, Dong Y, Zhu N, et al. microRNA-139-5p exerts tumor suppressor function by targeting NOTCH1 in colorectal cancer. Mol Cancer. 2014; 13: 124, doi: 10.1186/1476-4598-13-124, indexed in Pubmed: 24885920.
29. Besser J, Malan D, Wystub K, et al. MiRNA-1/133a clusters regulate adrenergic control of cardiac repolarization. PLoS One. 2014; 9(11): e113449, doi: 10.1371/journal.pone.0113449, indexed in Pubmed: 25415383.
30. Costantini DL, Arruda EP, Agarwal P, et al. The homeodomain transcription factor Irx5 establishes the mouse cardiac ventricular repolarization gradient. Cell. 2005; 123(2): 347–358, doi: 10.1016/j.cell.2005.08.004, indexed in Pubmed: 16239150.
31. Gómez R, Caballero R, Barana A, et al. Structural basis of drugs that increase cardiac inward rectifier Kir2.1 currents. Cardiovasc Res. 2014; 104(2): 337–346, doi: 10.1093/cvr/cvu203, indexed in Pubmed: 25205296.
32. Wang Lu, Yuan Ye, Li J, et al. MicroRNA-1 aggravates cardiac oxidative stress by post-transcriptional modification of the antioxidant network. Cell Stress Chaperones. 2015; 20(3): 411–420, doi: 10.1007/s12192-014-0565-9, indexed in Pubmed: 25583113.
33. Lu Y, Zhang Y, Shan H, et al. MicroRNA-1 downregulation by propranolol in a rat model of myocardial infarction: a new mechanism for ischaemic cardioprotection. Cardiovasc Res. 2009; 84(3): 434–441, doi: 10.1093/cvr/cvp232, indexed in Pubmed: 19581315.
34. Diaz RJ, Zobel C, Cho HC, et al. Selective inhibition of inward rectifier K+ channels (Kir2.1 or Kir2.2) abolishes protection by ischemic preconditioning in rabbit ventricular cardiomyocytes. Circ Res. 2004; 95(3): 325–332, doi: 10.1161/01.RES.0000137727.34938.35, indexed in Pubmed: 15231687.
35. Zhao Y, Ransom JF, Li A, et al. Dysregulation of cardiogenesis, cardiac conduction, and cell cycle in mice lacking miRNA-1-2. Cell. 2007; 129(2): 303–317, doi: 10.1016/j.cell.2007.03.030, indexed in Pubmed: 17397913.

VIA MEDICA

ORIGINAL ARTICLE

Cardiology Journal
2020, Vol. 27, No. 3, 295–302
DOI: 10.5603/CJ.a2018.0110

ISSN 1897–5593

Characteristics of circulating endothelial cells obtained from non-ST-segment elevation myocardial infarction patients with additional diastolic dysfunction of left ventricle observed in echocardiography

Pawel Burchardt[1, 2, 3], Maura Farinacci[4], Magdalena Mayer[5], Klaus Luecke[6], Thomas Krahn[7], Jaroslaw Manczak[2], Marek Slomczynski[2], Jaroslaw Hiczkiewicz[3], Janusz Rzezniczak[2]

[1]Biology of Lipid Disorders Department, Chair of Biology and Environmental Sciences, Poznan University of Medical Sciences, Poznan, Poland
[2]Department of Cardiology, J. Strus Hospital, Poznan, Poland
[3]Department of Cardiology, Hospital of Nowa Sol, Poland
[4]Institute for Medical Immunology, Berlin-Brandenburg Center für Regenerative Therapies, Core Unit Biomarker, Charité University Medicine Berlin, Germany
[5]Zablab sp. z o.o, Poznan, Poland
[6]HaimaChek Inc., Santa Monica, CA, United States
[7]Bayer AG, Biomarker Research, Berlin, Germany

Abstract

Background: *Circulating endothelial cells (CEC) may be used to find new strategies for the early diagnosis of cardiovascular diseases. The major objective of the project is to broaden knowledge of CEC biology by determining their phenotypic characteristics. The additional aim is to clarify whether on the basis of these information it is possible to identify the origin of CEC release (from various cardiovascular compartments).*

Methods: *Circulating endothelial cells were collected from arterial blood prior to angiography, as well as from arterial and venous blood obtained after angiography/coronary angioplasty, from 18 patients with non-ST-segment elevation myocardial infarction (NSTEMI). CECs were quantified by flow cytometry and defined as Syto16 (dye)$^+$, CD45dim/neg, CD31$^+$ and CD146$^+$. The additional CD36$^+$ was establish as a marker of endothelial cells released from small vessels of the microcirculation.*

Results: *The total number of CECs increased significantly after the percutaneous transluminal coronary angioplasty (PTCA) in the arterial system. Number of CECs isolated at similar time points (after invasive procedure) did not differ significantly between arteries and veins, but the number of CD36$^+$ CECs after coronary angioplasty was significantly higher in the venous system, than in the arterial system.*

Conclusions: *The number of CD36$^+$ in artery samples obtained after coronary angioplasty (PTCA) had tendency to be decreased (in comparison to the sample obtained before angiography). It was major difference between those who had PTCA performed vs. those who had not.* (Cardiol J 2020; 27, 3: 295–302)

Key words: circulating endothelial cells, NSTEMI, diastolic dysfunction

Address for correspondence: Pawel Burchardt, PhD, MD, MSc, FESC, Biology of Lipid Disorders Department, Chair of Biology and Environmental Sciences, Poznan University of Medical Sciences; Department of Cardiology, J. Strus Hospital, ul. Szwajcarska 3, 61–285 Poznań, Poland, tel: +48 618739333, fax: +48 618739333, e-mail: pab2@tlen.pl

Received: 19.01.2018 Accepted: 4.09.2018

Introduction

The Holy Grail in cardiology is to 'predict the unpredictable'. This means, that 50% of all new cases of ischemic heart disease (IHD) occur as myocardial infarction or sudden cardiac death [1–7]. It is strange, but there are no clinical tools to predict and avoid these episodes. Neither can new cardio-vascular episodes be predicted among those who suffer from the established IHD [1].

Circulating endothelial cells (CEC) may be used to find early and new strategies for the diagnosis of cardiovascular diseases [8–13]. They are released into the blood due to reduced adhesion to the vessels basement membrane (VBM) as a result of mechanical injury, necrosis or apoptosis [8, 13, 14]. Very little is known about the CEC phenotype, which may depend on their state of activation, way of release, vascular beds they originate from or the caliber of the vessel from which they are derived. The isolation and determination of CEC phenotype may allow, in combination with troponin assessment, for more sophisticated diagnosis of patients with acute coronary syndrome (ACS), as well as to distinguish from this group subjects with impaired coronary microcirculation. Additionally, it could be possible that based on the assessment of CEC phenotype, patients who are at risk for a new or another cardiovascular event would be identified.

Owing to the above, it was decided to focus on a cohort with a new onset of coronary artery disease in shape of ACS (with no history of cardiovascular events). The CECs level can be increased in all ACS patients, but the most pleasant objects for CEC studies are subjects with non-ST-segment elevation myocardial infarction (NSTEMI). The first reason is the wide variety of CEC sources (large epicardial CEC, microvascular CEC's) and the mechanisms leading to their release, i.e. mechanical injury and microvascular disturbances.

Secondly, the fact that according to European Society of Cardiology (ESC) guidelines more time is possible for clinical evaluation of NSTEMI patients before the decision to perform the diagnostic angiography to be done.

The purpose of the study is to:

- find differences in number of CECs between subjects who underwent percutaneous transluminal coronary angioplasty (PTCA) and those who did not;
- find quantitative differences between CECs depending on vascular beds that they are derived from (venous system vs. arterial system);
- establish the origin of isolated CECs depending on the compartment of arterial system of origin (artery vs. microcirculation);
- find differences in the amount of CECs isolated from the arterial system, depending on the way of their release before and after mechanical injury, (i.e. before and after PTCA).

Methods

Patients and study design

The study was carried out at the Department of Cardiology of J. Strus Hospital, Poznan, Poland between 2014 and 2016. Protocol was conducted according to guidelines stated in the Declaration of Helsinki and was approved by the local bioethics commission. All subjects were informed about the aim of the study and gave their written consent.

The study group consisted of patients suffering from ACS/NSTEMI/their first cardiovascular episode ever. The additional inclusion criteria was an impaired left ventricular (LV) diastolic function in echocardiography. Left diastolic dysfunction was defined when all echocardiographic features at admission were observed: $E/A < 1$, $e'/a' < 1$ from lateral wall, isovolumetric relaxation time > 0.1 s, deceleration time of wave E was > 0.15 s.

Patients were qualified for an acute coronary angiography (due to the ACS guidelines). Research material was arterial blood obtained before angiography (when the arterial sheet was fixed) and after coronary angiography/angioplasty (blood was collected from the arterial sheet before it was released after the invasive procedure). The last, venous blood collection was done from the ulnar vein. It was performed strictly 30 min after removing the arterial sheet after the angiography/angioplasty.

The exclusion criteria was lack of diastolic dysfunction in ACS/NSTEMI subjects, observed in screening echocardiography before diagnostic coronary angiography.

Coronary angiography was performed no later than 24 h after admission, in accordance with the ESC guidelines for management in NSTEMI.

The study was organized in three phases:

- selection of 18 patients with appropriate clinical characteristics;
- identification and quantification of CECs and microvascular CEC (mvCECs) using flow cytometry;
- statistical analysis of collected data.

CEC quantification and characterization by flow cytometry

Circulating endothelial cells were detected by flow cytometry using a panel of monoclonal antibodies and nuclear staining Syto16. CECs were defined as DNA^+, $CD45^{dim}$, $CD31^+$ and $CD146^+$. mvCECs were identified as $CD36^+$ CEC. In the staining procedure, whole blood samples (500 μL) were incubated with FcR blocking Reagent (Miltenyi) for 15 min at 4°C, and then with the respective antibody mixtures for 40 min at 4°C. After red cell lysis with High-Yield Lyse (Life technologies) for 15 min at room temperature, samples were centrifuged and resuspended in FACS buffer (PBS + 0.5% BSA + 0.5 mM EDTA + 0.05% NaN_3). Due to high variability associated with the detection of cell populations with low frequency, samples were stained and measured in triplicate. Acquisition was done using a LSR II Flow Cytometer (BD Biosciences), equipped with 488-, 633-, and 405-nm lasers. Flow cytometer setup and calibration were performed using CS&T beads (BD Biosciences). For sample acquisition, mononuclear cells (PMNCs) were set as the stopping gate with a threshold of 5×10^5 PMNCs. Data was acquired using FACSDiva 6.0 Software (BD Biosciences) and data analysis was performed using Flowjo 10. Fluorescence compensation was performed by using BD™ CompBeads Set Anti-Mouse Ig. CECs and EPCs levels were first calculated as a percentage of PMNC. Absolute counts (cells/mL) were then determined by multiplying the CEC or EPC percentage of the PMNC by the absolute PMNC count obtained in separate tubes by using Flow-Count™ Fluorospheres (Beckmann Coulter).

Laboratory tests

Laboratory tests were performed using commercially available diagnostic kits. The serum creatinine concentration was determined by Jaffe's reaction using Roche Cobas C (Hitachi, Germany). Creatinine clearance and glomerular filtration rate were estimated using formulas from Cockroft-Gault. Potassium and sodium concentrations were determined by potentiometry using the Cobas System 6000 (Roche Diagnostics, Germany). Assessments of peripheral blood counts were performed using Sysmex XT2000i, the US system. Concentration of urea, uric acid, total cholesterol, triglycerides and high-density lipoproteins were quantified using enzymatic colorimetric method (Cobas C Roche/Hitachi, Germany) with specific reagents. The concentration of low-density lipoproteins was calculated using the Friedewald formula.

Statistical analysis

After applying the Shapiro-Wilks test to determine a normal distribution of data, noncategorical data distributed normally was expressed as mean (SD) and data distributed non-normally was expressed as median (interquartile range [IQR]). The Student t-test was used for variables with normal distribution (for two independent and dependent variables). The Mann-Whitney U test (for two independent variables) and the Sign test as well as the Wilcoxon matched pairs test (for two dependent variables) were used for variables without normal distribution. Statistical significance was set at $p < 0.05$. The correlation between variables showing a normal distribution was evaluated with the Pearson coefficient, whereas the Spearman rang correlation coefficient was applied for variables with a non-normal distribution. All analyses were performed with STATISTICA 7.0 (Statsoft, USA) and SPSS-20 (IBM, USA).

Results

Demographic data

The study group consisted of 18 patients (14 males, 4 females) with a median age of 66.6 (60–73) years with NSTEMI, and with additional echocardiographic features of LV diastolic dysfunction; moreover, this was their first episode of cardiovascular disease. The median body mass index of the study group was 24.7 (22.6-28.7) kg/m^2. Each patient received pharmacotherapy before index hospitalization. The clinical, biochemical and demographic characteristics are provided in Table 1.

Coronary artery angiography was performed in all patients and additional coronary angioplasty was performed in 14 (77.8%) cases. Among the patients who underwent angioplasty, 5 (27.8%) had stents placed in the left descending artery, 3 (16.7%) in left circumflex artery and 1 (5.5%) in left intermedia artery. One patient received stents to both the left circumflex and left intermedia artery. The right coronary artery had been stented in 4 (22.2%) subjects.

During hospitalization patients received angiotensin converting enzyme inhibitors (75% of the subjects), angiotensin receptor blockers (10% of the subjects), beta-blockers in (85% of the subjects), statins (100% of the subjects), diuretics (20% of the subjects), and mineralocorticoid receptor antagonists (10% of the subjects).

Echocardiographic characteristics

The echocardiographic parameters at hospital admission are provided in Table 2. LV diastolic

Table 1. Biochemical, clinical and demographic characteristics of patients at hospital admission.

	Median	Percent	Interquartile range
Laboratory parameter			
RBC [$10^6/\mu L$]	4.4		4.2–4.7
HGB [g/dl]	13.8		12.6–14.7
HCT [%]	39.8		38.2–42.5
WBC [$10^3/\mu L$]	7.1		6.2–8.5
K^+ [mmol/L]	4.2		3.8–4.47
TSH [uIU/mL]	1.1		0.7–2.1
TC [mmol/L]	4.9		4.5–5.8
LDL [mmol/l]	3.1		2.2–4.1
HDL [mmol/L]	1.3		1.1–1.4
TG [mmol/L]	1.6		1.1–1.8
CRP [mg/L]	1.7		1.1–5.5
BNP [pg/mL]	89.6		49.3–221.5
Creatinine [μmol/L]	94		79–105
ALAT [U/L]	19		15–29
Tn max [ng/L]	2645		1910–4244
Radiology parameter			
Mean time of coronary angiography + PTCA [min]	27.7		17–34
The balloon inflation time during angioplasty [s]	25		12.5–30
Number of patients with performed PTCA = 14			
Average number of implanted stent per patient = 1.14			
Demographic data			
Dysglicemia (IFG, IGT, diabetes)		65%	
Dyslipidemia		55%	
Hypertension		55%	
Chronic kidney disease		20%	
Heart failure		15%	

RBC — red blood count; HGB — hemoglobin; HCT — hematocrit; WBC — white blood count; K^+ — potassium; TSH — thyroid stimulating hormone; TC — total cholesterol; LDL — low density lipoprotein; HDL — high density lipoprotein; TG — triglycerides; CRP — C-reactive protein; BNP — B-type natriuretic protein; ALAT — alanine aminotransferase; Tn — troponin; PTCA — percutaneous transluminal coronary angioplasty; IFG — impaired fasting glucose; IGT — impaired glucose tolerance

dysfunction (inclusion criteria) at various levels of severity were present in all patients.

There was no significant improvement observed in diastolic function in echocardiography the following day, subsequent to angiography (or coronary artery angioplasty following ACS) (data not provided).

Characterization of CECs present before angiography in radial artery, and after coronary angiography/angioplasty in radial artery and brachial vein

Characteristics and levels of CECs obtained in the studied groups are shown in Table 3. The number of CECs after the angiography/angioplasty increased in the arterial system in the whole group. In the venous system, although observed CEC cell numbers were highest, differences were not statistically significant. The number of $CD36^+$ (microvascular) cells after coronary angiography/ /angioplasty did not change significantly in the arterial system, but was significantly higher in vein, although the blood was collected during a similar period following an invasive cardiac procedure (30 min after the invasive procedure).

A comparison between subjects who had coronary angioplasty performed vs. those who did not (in artery before and after angiography and artery vs. vein after angioplasty) is provided in Table 4. The number of CEC, CEC per 10^6 PMNC, the percentage of mvCEC on total CECs, measured before and after angiography in artery (as well as before

Table 2. Echocardiographic characteristics (before coronary-angiography).

Echocardiographic parameter	Median	Interquartile range
Ejection fraction [%]	58.5	55–63
Right ventricular diastolic diameter [mm]	27	23–31
Interventricular septum diastolic diameter [mm]	12.5	12–15
Posterior wall diastolic diameter [mm]	11.5	10–12
Left ventricular end-diastolic diameter [mm]	45.5	44–48
Left atrium diameter [mm]	34.5	34–38
Diameter of aorta (valve ring) [mm]	19.5	19–23
Mitral flow rate, wave E [m/s]	0.4	0.38–0.56
Mitral flow rate, wave A [m/s]	0.6	0.52–0.67
E/a'	9.5	7–11
Deceleration time of E wave mitral flow [ms]	196.5	156–247
Isovolumetric relaxation time [ms]	118.5	104–133
Lateral wall, flow rate, wave e' (tissue Doppler) [m/s]	0.05	0.04–0.07
Lateral wall, flow rate, wave a' (tissue Doppler) [m/s]	0.07	0.05–0.08
Acceleration time of right ventricular outflow [ms]	121	104–133

Table 3. Characterization and quantification of circulating endothelial cells (CEC) in the radial artery before angiography, and after coronary angiography/angioplasty from the radial artery and brachial vein.

Parameter	Before angiography (artery A1)	After angiography (artery A2)	After angiography (vein)
CEC/mL	63.9 (35.8–91.2)	99.1 (49.8–189.9)*	123.0 (28.4–299.2)
CEC per 10^6 PMNC	23.4 (13.0–32.4)	42.1 (22.8–61.9)**	58.5 (9.8–95.3)#
mvCEC/mL	28.9 (13.3–47.8)	26.2 (9.8–43.0)	51.2 (16.4–107.8)
mvCEC% of total CEC	53.5 (34.0–78.3)	23.2 (11.2–44.8)***	41.4 (14.5–77.6)$

Data are shown as median (interquartile range). Arterial 1 vs. arterial 2: *$p < 0.005$, **$p < 0.05$, ***$p < 0.05$; Arterial 1 vs. vein: #$p < 0.05$; Arterial 2 vs. vein: $$p < 0.05$

Table 4. The comparison between subjects who had percutaneous transluminal coronary angioplasty (PTCA) performed vs those who did not have the operation performed.

Parameter	Patients without PTCA before angiography	Patients with PTCA performed before angiography
	Artery A1	**Artery A1**
CEC/mL	255.5 (85.5–425.5)	63.4 (35.7–87.4)
CEC per 10^6 PMNC	48.6 (28.8–68.5)	21.1 (12.4–27.9)
mvCEC/mL	90.5 (46.1–135)	36.5 (16.5–49.5)
mvCEC% to CEC [%]	53.8 (31.1–76.4)	55.9 (43.3–80)
	Artery A2	**Artery A2**
CEC/mL	401.8 (53.9–749.7)	88.7 (33.6–188.6)
CEC per 10^6 PMNC	73.5 (20.6–126.4)	42 (19.9–61)
mvCEC/mL	92.5 (44.4–140.6)	25 (8.8–42.2)
mvCEC% to CEC [%]	50.6 (19.3–81.2)	30.2 (14.6–45)
	Vein	**Vein**
CEC/mL	403 (72.1–734)	135.3 (34.8–230.8)
CEC per 10^6 PMNC	62 (33.4–90.6)	61.1 (9.6–100)
mvCEC/mL	160.6 (55.4–265.8)	53 (24.8–73.5)
mvCEC% to CEC [%]	56.4 (35.4–77.3)	46.1 (24.1–77.8)

Data are shown as median (interquartile range). P = not significant. CEC/ml — CEC per mL of peripheral blood; PMNC — CEC per 10^6 peripheral mononuclear blood cells, mvCEC/mL — $CD36^+$ per mL of peripheral blood, %mvCEC to CEC — the $CD36^+$ to all CEC per ml of peripheral blood

angiography in artery and after angiography in vein) did not change significantly between patients who underwent PTCA and those who didn't. Proper analysis of dependent samples in the mentioned groups were unable to perform due to small number of subjects (only group comparisons were done).

Coronary angiography characteristics and its potential influence on CEC counts

In 1 patient a myocardial bridge, which significantly narrowed the left descending artery, was found. He did not have PTCA performed. One patient was diagnosed with severe coronary atherosclerosis and was qualified for acute surgical coronary artery by-pass grafting procedure, so no PTCA performed. Another subject showed no significant coronary stenosis. In this case PTCA was also not performed, but from the clinical data it was possible to diagnose takotsubo cardiomyopathy. Angioplasty with implantation of 2 drug-eluting stents was performed in 2 patients. Long-lasting (58, 50, 40 min) and very complicated PTCA took place in 3 patients. High values of myocardial necrosis-troponin released markers were observed in 6 patients (25000, 6580, 5904, 4244, 3280, 2645 ng/mL). In 1 patient, no reflow phenomenon was observed after angioplasty. In another patient, additional severe aortic stenosis was observed but PTCA had not been performed.

Circulating endothelial cells and clinical data

Total CECs and $CD36^+$ mvCEC were associated with individual clinical parameters. The ratio of $CD36^+$ to all CEC per ml in arterial blood before angiography correlated with hemoglobin level ($r = = 0.61$) and reversely correlate with mean platelet volume (MPV; $r = –0.78$). MPV was positively correlated with CEC count ($r = 0.57$). $CD36^+$ in arterial blood before angiography correlated with high density lipoprotein ($r = 0.6$), and reversely with triglycerides ($r = 0.6$).

In arterial blood after coronary angiography/ /angioplasty: CEC count was correlated with sodium and creatinine concentration ($r = 0.49$, $r = 0.52$, respectively), $CD36^+$ with creatinine and white blood count ($r = 0.49$, $r = –0.55$, respectively. In vein blood CEC count was reversely correlated with total cholesterol and low density lipoprotein ($r = –0.63$, $r = –0.063$, respectively). Venous $CD36^+$ were positively correlated with platelets ($r = 0.49$) and reversely correlated with MPV ($r = –0.56$), Total CECs and $CD36^+$ mvCEC were also associated with various echocardiographic markers of LV relaxation dysfunction. However, due to weak correlation and lack of repeatability, these results were not provided.

Discussion

Circulating endothelial cells were identified and described for the first time in the 1970s. However, available literature is ambiguous in several key issues [8, 14]. In the beginning, there was no clear definition of the term "circulating endothelial cells" [15]. Discrepancies in the definition of CECs were caused by a lack of the consensus on the nature of specific surface antigens, as well as what the size and shape of isolated particles/cells needed to be [8]. For these reasons, results obtained from individual authors significantly differed one from another [14].

After finding consensus on phenotypic characteristics specific to the CECs ($CD146^+$, $CD31^+$, $CD36^+$), another source of variability between different studies was caused by the different technologies used for identification and quantification of these cells [8, 15–17]. Immunomagnetic methods allowed for isolation of cells on the basis of one specified surface antigen, therefore with less of specificity than compared to flow cytometry, which can use several different fluorescent-active antibodies. Moreover, most of the studies aimed only to quantify circulating cells rather than qualitatively analyze them [16–20].

The presence of CECs in the bloodstream is a physiological phenomenon resulting from impaired adhesive interactions between the basement membrane and endothelium [8, 14, 15]. The observed increase in the number of CECs is caused by a temporary impairment of the adhesive homeostasis by mechanical injury, apoptosis or necrosis [8, 14, 15]. Moreover, released CECs have different phenotypes depending on the activation properties, mode of their release (necrosis, apoptosis, mechanical damage) or their vascular origin. The most important factors which contribute to pathogenesis of CECs production are myocardial ischemia, inflammation, diabetes as well as thyroid or renal disturbances [21]. In the present study no significant CEC association with dysglicemia was observed, dyslipidemia with reduced LV ejection fraction or hypertension was also not observed. There were also no quantitative and phenotypic differences in CEC isolated from arterial and venous blood samples among patients with dysglicemia, dyslipidemia and reduced ejection fraction. Nevertheless, proper statistical analysis was not possible due to the small group and large heterogeneity of the cohort.

Literature data shows that the number of CECs detected in the arterial system or venous system are similar, while there is no data concerning CEC phenotype differences between these compartments [8, 14, 15]. The goal herein, was to compare the number and type of cells present in the arterial system after angiography/angioplasty, and 30 min after an invasive procedure from the venous system. It was found that the total number of CEC cells isolated at similar time points did not differ significantly between arterial and venous compartments. Little variation in CEC count was probably due to different time points of cell isolation (30 min delay between arterial and venous blood collection), rather than differences between these vascular compartments. A significantly higher number of cells with $CD36^+$ phenotype was observed in the venous system when it was compared to artery samples (before or after angiography/angioplasty). This was the only difference between arterial and venous systems in the context of isolated endothelial cells, that hadn't been described previously in the literature.

In the studied cohort, the total number of CECs detected in the blood before angiography was lower than the number of CECs obtained after angiography/angioplasty from both arterial and venous system. It may be speculated that this confirms results of other authors and possible cause of the phenomenon is increased CEC release after mechanical injury during angioplasty [8, 14, 15]. There was no such observation in those who had not been treated with PTCA. The number of CECs was high at baseline and in the following time it was increasing, but not significantly. It may be speculated, that it could be explained rather by chronic myocardial ischemia which leads to low or moderate CECs increase, than other causes. However, absolute variability of the CECs number between patients who had vs. those who had not been treated with PTCA was not relevant.

This pilot study also aimed to find various sources of CEC. In subjects with clinically relevant ischemia (according to ESC ACS guidelines) accompanied by clinical probability of microcirculatory disturbances represented by diastolic dysfunction which were hoped to collect CEC originated from different vascular beds. It was found and distinguished that $CD36^+$ from $CD36^-$. There were no significant differences in the number of $CD36^+$ in various blood collection time points. Interestingly, the number of $CD36^+$ in artery samples obtained after coronary angioplasty (PTCA) had tended to be decreased (in comparison to samples obtained before angiography). The $CD36^+$ in following blood samples tended to be increased in patients who had no angioplasty performed. There was major difference between those who had PTCA performed vs. those who had not. This phenomenon could not be properly explained. It is possible that it may have been a chance result. Secondly, it may only be speculated that angioplasty preserves blood supply to the myocardium and also improves homeostasis of microcirculation, which reduces the unpleasant effect of ischemia and diminishes CEC release. Patients without PTCA had their ischemia not reversed (complex epicardial and microcirculatory ischemia), and could explain the $CD36^+$ increase.

The clinical application of this study is that isolation and determination of CEC phenotype is possible and that angioplasty of the epicardial coronary artery may influence the profile of released endothelial cells. Further studies on quantitative CEC properties are required, the purpose is to allow better distinction in angina subjects and those with impaired coronary microcirculation.

Limitations of the study

Due to a very small size of the group studied and the fact that statistical analysis cannot be performed for some parameters, results of the project should be interpreted as descriptive statistics. Another limitation was that the CEC results were not compared to other clinical groups of patients (i.e. healthy volunteers), which however was not a primary endpoint of the project's plan. The purpose of the study was confirmation of the notion that CEC count's variability depends on their vascular origin. It is worth noting that although the study group was small due to the highly selective inclusion criteria, its undoubted advantage is its homogeneity (according to various sources of CEC). The blood was obtained from patients with suspected coronary microvascular disturbances and hemodynamic decompensation due to concomitant changes in the epicardial artery during the course of NSTEMI. Such groups with various sources of CEC in average patients have, as of yet, not been described in the literature.

Finally, there are no known markers that can be used to distinguish CECs derived from coronary microcirculation from other microcirculation locations. That is why, they were excluded from patients studied having suspected peripheral artery disease of any kind. The phenotypic features that differentiate CEC from various micro-circulating beds are a separate subject of interest.

Conclusions

The number of CECs after PTCA increased significantly in the arterial system. In the venous system, although the observed CEC cell numbers were the highest, differences were not statistically significant.

The number of cells with $CD36^+$ phenotype after coronary angioplasty did not change significantly in the arterial system, but was significantly higher in vein, although the blood was collected during a similar period following an invasive cardiac procedure.

Conflict of interest: None declared

References

1. Montalescot G, Sechtem U, Achenbach S, et al. 2013 ESC guidelines on the management of stable coronary artery disease: the Task Force on the management of stable coronary artery disease of the European Society of Cardiology. Eur Heart J. 2013; 34(38): 2949–3003, doi:10.1093/eurheartj/eht296, indexed in Pubmed: 23996286.
2. Burchardt P, Goździcka-Józefiak A, Siminiak T. [IGF-1--a new risk factor for coronary atherosclerosis]. Kardiol Pol. 2006; 64(11): 1297–1302, indexed in Pubmed: 17165168.
3. Kassab GS, Rider CA, Tang NJ, et al. Morphometry of pig coronary arterial trees. Am J Physiol. 1993; 265(1 Pt 2): H350–H365, doi: 10.1152/ajpheart.1993.265.1.H350, indexed in Pubmed: 8342652.
4. Bugiardini R, Pozzati A, Ottani F, et al. Vasotonic angina: a spectrum of ischemic syndromes involving functional abnormalities of the epicardial and microvascular coronary circulation. J Am Coll Cardiol. 1993; 22(2): 417–425, indexed in Pubmed: 8166784.
5. Crea F. Angina pectoris and normal coronary arteries: cardiac syndrome X. Heart. 2004; 90(4): 457–463, doi: 10.1136/hrt.2003.020594.
6. Maseri A, Crea F, Kaski J, et al. Mechanisms of angina pectoris in syndrome X. J Am Coll Cardiol. 1991; 17(2): 499–506, doi: 10.1016/s0735-1097(10)80122-6.
7. Bugiardini R, Bairey Merz CN. Angina with "normal" coronary arteries: a changing philosophy. JAMA. 2005; 293(4): 477–484, doi: 10.1001/jama.293.4.477, indexed in Pubmed: 15671433.
8. Erdbruegger U, Haubitz M, Woywodt A. Circulating endothelial cells: a novel marker of endothelial damage. Clin Chim Acta. 2006; 373(1-2): 17–26, doi: 10.1016/j.cca.2006.05.016, indexed in Pubmed: 16836991.
9. Bouvier CA, Gaynor E, Cintron JR, et al. Circulating endothelium as an indication of vascular injury. Thromb Diath Haemorrh. 1970; 40: 163.
10. Woywodt A, Blann AD, Kirsch T, et al. Isolation and enumeration of circulating endothelial cells by immunomagnetic isolation: proposal of a definition and a consensus protocol. J Thromb Haemost. 2006; 4(3): 671–677, doi: 10.1111/j.1538-7836.2006.01794.x, indexed in Pubmed: 16460450.
11. Hladovec J, Prerovský I, Staněk V, et al. Circulating endothelial cells in acute myocardial infarction and angina pectoris. Klin Wochenschr. 1978; 56(20): 1033–1036, indexed in Pubmed: 723184.
12. Goon PKY, Lip GYH, Boos CJ, et al. Circulating endothelial cells, endothelial progenitor cells, and endothelial microparticles in cancer. Neoplasia. 2006; 8(2): 79–88, doi: 10.1593/neo.05592, indexed in Pubmed: 16611400.
13. Mutin M, Canavy I, Blann A, et al. Direct evidence of endothelial injury in acute myocardial infarction and unstable angina by demonstration of circulating endothelial cells. Blood. 1999; 93(9): 2951–2958, indexed in Pubmed: 10216090.
14. Schmidt DE, Manca M, Hoefer IE. Circulating endothelial cells in coronary artery disease and acute coronary syndrome. Trends Cardiovasc Med. 2015; 25(7): 578–587, doi: 10.1016/j.tcm.2015.01.013, indexed in Pubmed: 25753180.
15. Burger D, Touyz RM. Cellular biomarkers of endothelial health: microparticles, endothelial progenitor cells, and circu-lating endothelial cells. J Am Soc Hypertens. 2012; 6(2): 85–99, doi: 10.1016/j.jash.2011.11.003, indexed in Pubmed: 22321962.
16. Lanuti P, Santilli F, Marchisio M, et al. A novel flow cytometric approach to distinguish circulating endothelial cells from endothelial microparticles: relevance for the evaluation of endo-thelial dysfunction. J Immunol Methods. 2012; 380(1-2): 16–22, doi: 10.1016/j.jim.2012.03.007, indexed in Pubmed: 22484509.
17. Sinning JM, Losch J, Walenta K, et al. Circulating CD31+/Annexin V+ microparticles correlate with cardiovascular outcomes. Eur Heart J. 2011; 32(16): 2034–2041, doi: 10.1093/eurheartj/ehq478, indexed in Pubmed: 21186238.
18. Blann AD, Woywodt A, Bertolini F, et al. Circulating endothelial cells. Biomarker of vascular disease. Thromb Haemost. 2005; 93(2): 228–235, doi: 10.1160/TH04-09-0578, indexed in Pubmed: 15711737.
19. Sabatier F, Camoin-Jau L, Anfosso F, et al. Circulating endothelial cells, microparticles and progenitors: key players towards the definition of vascular competence. J Cell Mol Med. 2009; 13(3): 454–471, doi: 10.1111/j.1582-4934.2008.00639.x, indexed in Pubmed: 19379144.
20. Bertolini F, Shaked Y, Mancuso P, et al. The multifaceted circulating endothelial cell in cancer: towards marker and target identification. Nat Rev Cancer. 2006; 6(11): 835–845, doi: 10.1038/nrc1971, indexed in Pubmed: 17036040.
21. Solovey A, Lin Y, Browne P, et al. Circulating activated endothelial cells in sickle cell anemia. N Engl J Med. 1997; 337(22): 1584–1590, doi: 10.1056/NEJM199711273372203, indexed in Pubmed: 9371854.

VIA MEDICA

BRIEF COMMUNICATION

Cardiology Journal
2020, Vol. 27, No. 3, 303–306
DOI: 10.5603/CJ.a2020.0075

ISSN 1897–5593

Colocalization of plaque macrophages and calcification in coronary plaques as detected by optical coherence tomography predicts cardiovascular outcome

Mathias Burgmaier[1]*, Andrea Milzi[1]*, Rosalia Dettori[1]*, Kathrin Burgmaier[2], Martin Hellmich[3], Mohammad Almalla[1], Nikolaus Marx[1], Sebastian Reith[1]

[1]Department of Cardiology, University Hospital of the RWTH Aachen, Germany
[2]Department of Pediatrics, University Hospital of Cologne, Germany
[3]Institute of Medical Statistics and Computational Biology (IMSB), University of Cologne, Faculty of Medicine and University Hospital Cologne, Germany

Both plaque macrophage infiltration [1] and calcification [2] are recently suggested characteristics of plaque vulnerability in coronary lesions. Each of these two morphologic characteristics may foster the other [3, 4]. Thus, the aim herein, is to evaluate this interdependence using optical coherence tomography (OCT), which, due to its supreme resolution, has the ability to detect both features. A recent study defined colocalization of macrophages and calcification (ColocCaMa) as a distance < 100 μm between plaque macrophages and calcification. In this work an association was described between ColocCaMa and the more heavily calcified, but also less advanced and more vulnerable coronary lesions [5]. An example of ColocCaMa is shown in Figure 1A. In the present follow-up study, the aim was to investigate whether this more vulnerable plaque phenotype in the presence of ColoCaMa translates into more cardiovascular events.

One hundred and fifty five patients were prospectively enrolled, who underwent percutaneous coronary intervention (PCI) of the target lesion due to stable angina (116, 74.8%) or acute coronary syndrome (ACS; 39, 25.2%) between 2012 and 2014 at the University Hospital of the RWTH Aachen, Germany. Patients were enrolled consecutively on days in which the study team was available. Further inclusion criteria were the suitability of the coronary target lesion for OCT analysis, as well as the presence of calcification within the target segment. A standardized follow-up was then performed with a median follow-up of 5.4 years (IQR 4.4–5.8). 25 patients were lost to follow-up, thus resulting in 130 patients with complete information. Death from any cause, new onset of myocardial infarction (MI), as well as emergent coronary revascularization and the composite endpoint of the three were noted. Written informed consent was obtained from all patients. The study was approved by the local ethics committee and conforms to the declaration of Helsinki. All statistical analyses were performed with SPSS (IBM Corp., Armonk, NY, USA).

Baseline age was 69.6 ± 8.4 years; 26 (20%) patients suffered an ACS at inclusion. Prevalence of cardiovascular risk factors was high: 63.1% presented with diabetes, 85.4% hypertension and 62.3% hyperlipidemia. A thin-capped fibroatheroma was present in 34 (26.1%) patients, macrophage infiltration in 48 (36.9%) patients and ColocCaMa in 23 (17.6%) patients. Frequency of thin-capped fibroatheroma was similar in patients with and without ColocCaMa (28 [26.2%] vs. 6 [26.1%], p = 0.393). Inter- and intraobserver variability for the assessment of the presence of macrophages were 0.916 and 0.925, respectively.

Address for correspondence: PD Dr. Sebastian Reith, MD, Department of Cardiology / Medical Clinic I, University Hospital of the RWTH Aachen, Pauwelsstr. 30, D-52074 Aachen, Germany, tel: ++49-241-80-36265, fax: ++49-241-80-33-36304, e-mail: sreith@ukaachen.de

Received: 14.01.2020 Accepted: 23.04.2020

Mathias Burgmaier, Andrea Milzi und Rosalia Dettori contributed equally.

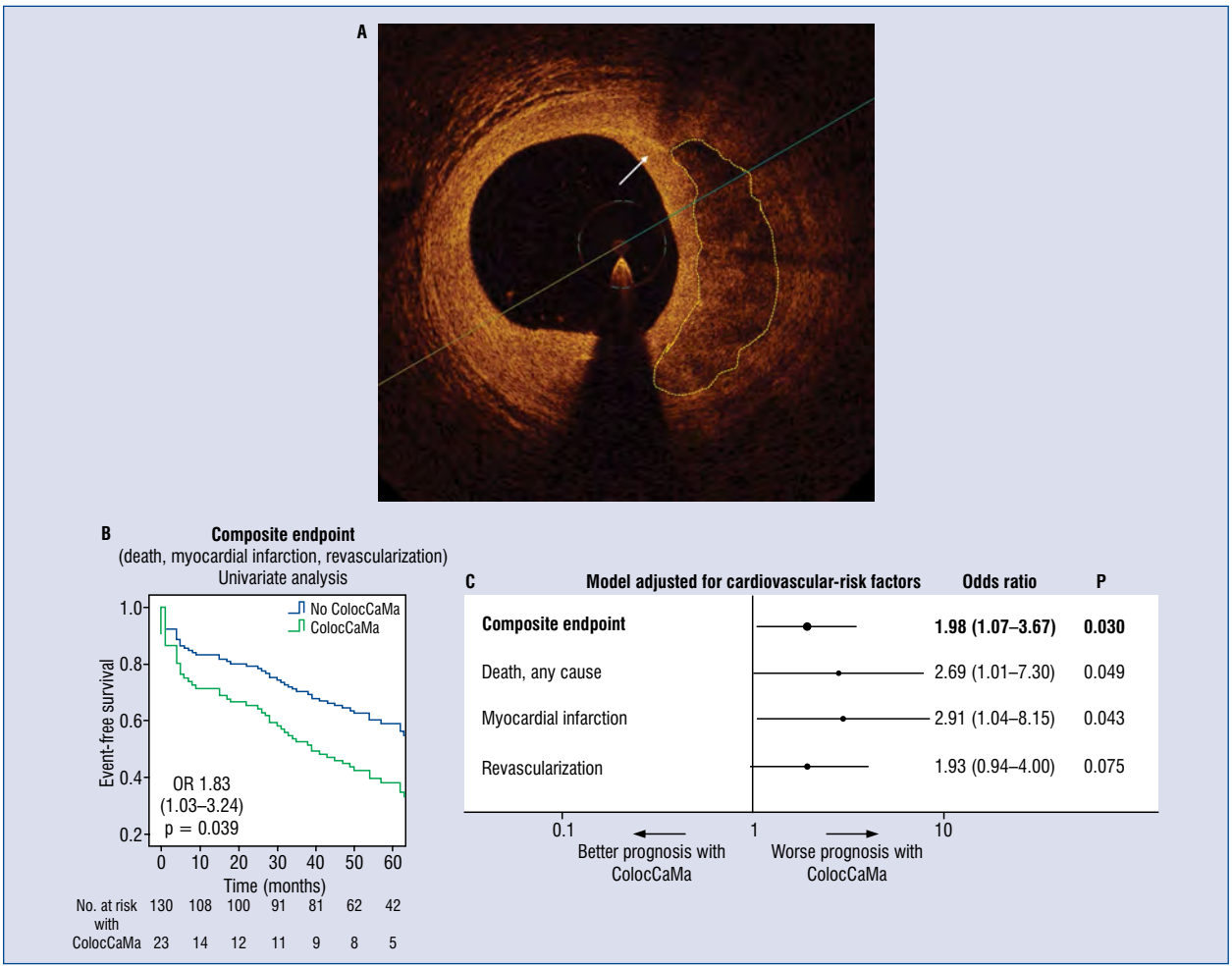

Figure 1. ColocCaMa in the coronary target/culprit lesion is associated with adverse cardiovascular outcome; **A.** A representative optical coherence tomography image of a ColocCaMa is shown; macrophage accumulation is marked with a white arrow, and calcification with a yellow border; **B.** The event-free curves derived from the Cox--regression show that in the presence of ColocCaMa (green line) in the target/culprit lesion, patients show a higher incidence of the composite endpoint of death from any cause, myocardial infarction and coronary revascularization; **C.** The forest-plot for single and composite endpoints is shown after adjustment for clinical presentation (acute coronary syndrome vs. stable angina), age, sex, glomerular filtration rate and relevant cardiovascular risk factors (body mass index, active nicotine use, presence of diabetes mellitus, hypertension, hyperlipidemia).

At follow-up, 29 (22.3%) deaths, 26 (20%) new MI and 43 (33.1%) emergent coronary revascularizations were registered. The composite endpoint was met by 65 (50%) patients. This high incidence of adverse cardiovascular events may be explained by the high cardiovascular risk profile of the enrolled population. No difference in the frequency of thin-capped fibroatheroma (20 [35.1%] vs. 14 [28.6%], p = 0.617) was detected among patients with or without adverse outcome at follow-up, whereas patients with adverse outcome showed more frequent plaque macrophage infiltration (32 [53.3%] vs. 20 [32.3%], p = 0.019). In contrast to a previous study [6], in-stent minimal lumen area < 4.5 mm^2, narrowing of proximal or distal stent edges or distal dissection did not predict adverse outcome, probably due to the routine use of OCT-guided PCI-optimization. Using Cox-regression analysis, patients with ColocCaMa showed a significantly higher incidence of the composite endpoint of death from any cause, MI and coronary revascularization (HR 1.83, 95% CI 1.03–3.24, p = 0.039). In patients with ColocCaMa this increased risk for the composite endpoint is sustained over time and curves derived from Cox regression analysis are depicted in Figure 1B. Following adjustment for clinical presentation (ACS vs. stable angina), age, sex, glomerular filtra-

tion rate and relevant cardiovascular risk factors (body mass index, active nicotine use, presence of diabetes mellitus, hypertension, hyperlipidemia) ColocCaMa still represented a significant risk factor for the composite endpoint (HR 1.98, 95% CI 1.07–3.67, p = 0.030, Fig. 1C). Furthermore, ColocCaMa was associated with death from any cause (HR 2.69, 95% CI 1.01–7.30, p = 0.049) and MI (HR 2.91, 95% CI 1.04–8.15, p = 0.043), whereas emergent coronary revascularization (HR 1.93, 95% CI 0.94–4.00, p = 0.075) did not reach significance in the adjusted model. Furthermore, in order to avoid any possible bias due to patients lost at follow-up, a multiple imputation analysis was performed, which confirmed the higher risk of the composite endpoint in patients with ColocCaMa (OR 1.78–1.82, p = 0.039–0.046).

The present group previously demonstrated that ColocCaMa is associated with a more vulnerable plaque phenotype [5]. In this study it was demonstrated that this translates into higher incidence of the composite endpoint of death from any cause, MI and coronary revascularization at follow-up.

Postinterventional OCT was performed in all patients, and relevant stent edge dissections or stent malappositions were treated immediately. Thus, it seems unlikely that the higher event rate in patients with ColocCaMa is caused by mechanical effects following coronary intervention. Furthermore, it has to be noticed that the survival curves progressively diverge over time suggesting an atherosclerosis-mediated effect. This is in line with the role of macrophages and microcalcifications as active players in atherogenesis and plaque destabilization. Even though stent implantation was performed in all the current patients, the data may be interpreted in light of the current concept of "vulnerable patient", i.e. patients with a tendency towards multifocal vulnerable lesions [7]. Specifically, previous OCT studies demonstrated more vulnerable lesions in non-culprit vessels of patients with ACS compared to stable coronary artery disease [1, 8]. In this scenario, ColocCaMa may be a marker of patient vulnerability, thus unmasking the higher risk of certain sub-populations. On the other hand, ColocCaMa could also be associated with an accelerated local neo-atherosclerosis following stent implantation, which may therefore lead to re-stenosis and eventually to adverse outcomes. However, as standardized follow-up coronary angiographies were not performed in this study due to ethical reasons, it is still unclear if the composite endpoint is driven by a non-culprit lesion or culprit lesion stent failure due to ColocCaMa — this needs to be investigated in future studies.

Given that both plaque macrophages and microcalcifications increase plaque destabilization, it is tempting to speculate about a causal role of ColocCaMa in the genesis of plaque vulnerability and future cardiovascular events. However, due to the study design it remains unclear whether ColocCaMa is causally involved in plaque destabilization or merely reflects a localized or systemic vulnerable coronary artery disease. In the present study, there was not sufficient information on target lesion revascularization during follow-up. Moreover, although the inter- and intraobserver variability in detecting macrophage infiltration is acceptable and a recent study using directional atherectomy showed good accuracy of accepted OCT-criteria [9] in detecting macrophages [10], the presence of ColocCaMa was not directly validated using histopathology in this study due to the study design. A promising tool for macrophage detection may be offered by computer-based reconstructions, however, they were not used in this project. Furthermore, the small number of patients did not allow drawing definite conclusions about a possible correlation of other features of plaque vulnerability with adverse outcome.

In summary, the present data suggests and may allow others to identify a subgroup of patients with high cardiovascular risk and indicates ColocCaMa to be a novel vulnerable plaque feature.

Conflict of interest: None declared

References

1. Kato K, Yonetsu T, Kim SJ, et al. Nonculprit plaques in patients with acute coronary syndromes have more vulnerable features compared with those with non-acute coronary syndromes: a 3-vessel optical coherence tomography study. Circ Cardiovasc Imaging. 2012; 5(4): 433–440, doi: 10.1161/CIRCIMAGING.112.973701, indexed in Pubmed: 22679059.
2. Reith S, Milzi A, Dettori R, et al. Predictors for target lesion microcalcifications in patients with stable coronary artery disease: an optical coherence tomography study. Clin Res Cardiol. 2018; 107(9): 763–771, doi: 10.1007/s00392-018-1243-1, indexed in Pubmed: 29654434.
3. Aikawa E, Nahrendorf M, Figueiredo JL, et al. Osteogenesis associates with inflammation in early-stage atherosclerosis evaluated by molecular imaging in vivo. Circulation. 2007; 116(24): 2841–2850, doi: 10.1161/CIRCULATIONAHA.107.732867, indexed in Pubmed: 18040026.
4. Nadra I, Mason JC, Philippidis P, et al. Proinflammatory activation of macrophages by basic calcium phosphate crystals via protein kinase C and MAP kinase pathways: a vicious cycle of inflammation and arterial calcification? Circ Res. 2005; 96(12):

1248–1256, doi: 10.1161/01.RES.0000171451.88616.c2, indexed in Pubmed: 15905460.
5. Burgmaier M, Milzi A, Dettori R, et al. Co-localization of plaque macrophages with calcification is associated with a more vulnerable plaque phenotype and a greater calcification burden in coronary target segments as determined by OCT. PLoS One. 2018; 13(10): e0205984, doi: 10.1371/journal.pone.0205984, indexed in Pubmed: 30356326.
6. Prati F, Romagnoli E, La Manna A, et al. Long-term consequences of optical coherence tomography findings during percutaneous coronary intervention: the Centro Per La Lotta Contro L'infarto — Optimization Of Percutaneous Coronary Intervention (CLI-OPCI) LATE study. EuroIntervention. 2018; 14(4): e443–e451, doi: 10.4244/EIJ-D-17-01111, indexed in Pubmed: 29633940.
7. Naghavi M, Libby P, Falk E, et al. From vulnerable plaque to vulnerable patient. A call for new definitions and risk assessment strategies: Part I. Circulation. 2003; 108(14): 1664–1672, doi: 10.1161/01.cir.0000087480.94275.97.
8. Vergallo R, Ren X, Yonetsu T, et al. Pancoronary plaque vulnerability in patients with acute coronary syndrome and ruptured culprit plaque: a 3-vessel optical coherence tomography study. Am Heart J. 2014; 167(1): 59–67, doi: 10.1016/j.ahj.2013.10.011, indexed in Pubmed: 24332143.
9. Tearney GJ, Regar E, Akasaka T, et al. Consensus standards for acquisition, measurement, and reporting of intravascular optical coherence tomography studies: a report from the International Working Group for Intravascular Optical Coherence Tomography Standardization and Validation. J Am Coll Cardiol. 2012; 59(12): 1058–1072, doi: 10.1016/j.jacc.2011.09.079, indexed in Pubmed: 22421299.
10. Habara M, Otsuka F, Tsuchikane E, et al. In vivo tissue characterization of human atherosclerotic plaques by optical coherence tomography: A directional coronary atherectomy study with histopathologic confirmation. Int J Cardiol. 2018; 268: 1–10, doi: 10.1016/j.ijcard.2018.05.022, indexed in Pubmed: 29804698.

VIA MEDICA

BRIEF COMMUNICATION

Cardiology Journal
2020, Vol. 27, No. 3, 307–308
DOI: 10.5603/CJ.a2020.0042

ISSN 1897–5593

Repeat physical stress echocardiography in asymptomatic severe aortic stenosis

Elena Ferrer-Sistach, Josep Lupón, Silvia Serrano-García, Albert Teis-Soley, Francisco Gual-Capllonch, Gladys Juncà-Puig, Nuria Vallejo-Camazón, Jorge López-Ayerbe, Antoni Bayés-Genís

Heart Institute, Hospital Universitari Germans Trias i Pujol, Badalona, Spain; Department of Medicine, Autonomous University of Barcelona, Barcelona, Spain; and CIBERCV, Instituto Carlos III, Madrid, Spain

In severe aortic stenosis (SAS), the presence of symptoms is associated with ominous prognosis with 5-year mortality of 15–50% [1], and is a well-established indication for valve replacement [2]. On the other hand, in asymptomatic SAS, case management requires clinical skills, and the timing of valve replacement is unclear. Holistic assessment of the clinical situation (including co-morbidities and frailty), risk stratification, and complementary tests are critical for managing asymptomatic SAS and determining optimal valve replacement timing.

In clinical practice, at the time of SAS diagnosis, approximately 50% of patients report being asymptomatic in their day-to-day life [1]. However, this may be due to an unconscious adaptive process causing them to limit the intensity of their physical activity. Thus, it can be difficult to determine whether a patient truly lacks symptoms, especially in elderly patients. Stress testing is useful for exposing symptoms, and is a safe technique for use in stable patients [3]; clinical practice guidelines recommend the use of stress testing when assessing asymptomatic SAS patients [2]. Valve replacement is indicated in patients who exhibit clinical signs during stress testing, or lower blood pressure during physical activity. However, it remains unclear whether it is of value to repeat a stress test to uncover symptoms in asymptomatic SAS.

The incidence of a positive stress test in SAS ranges from 15% to 65% [3]. Despite this variability, stress testing exhibits good negative predictive value for cardiovascular events [4]. Performing echocardiographic assessment before and after the stress test (physical stress echocardiography [PE]) provides additional physiological parameters that can help establish the cause of symptoms [5].

From June 2014 to August 2019, the value of PE and repeat PE during follow-up in 85 asymptomatic SAS patients who were prospectively enrolled in a specialized valve clinic (Table 1) was investigated. Baseline PE was the key indicator for aortic valve replacement in 23 (27%) patients: 8 (9.4%) had dyspnea, 2 (2.4%) angina, and 16 (18.8%) abnormal blood pressure response. Furthermore, 17 (20%) exhibited electric changes suggestive of ischemia, PE revealed a median gradient increase of > 20 mmHg during stress in 31 (36.9%) patients, ventricular dysfunction in 2 (2.4%) patients, and segmental disorders in 8 (9.5%) patients. Of the alterations observed during PE, those which were the reason to indicate valve replacement were only symptoms and abnormal blood pressure response. The rest of the information obtained helped to make the decision but it was not the main reason.

A second PE was performed in 27 patients (median time 16 months after the first PE), and a third PE was completed in 5 patients (median time 16 months after the second PE). The second PE was the key indication for aortic valve replacement in 9 (33.3%) patients; it was clinically positive by symptoms in 6 (22.2%) patients: 3 (12%) patients had dyspnea, and 4 (14.8%) angina and abnormal blood pressure response was found in 4 (14.8%) patients. Electric changes occurred in 9 (33.3%) patients, and a median gradient increase of > 20 mmHg

Address for correspondence: Antoni Bayes-Genis, MD, PhD, FESC, Head, Heart Institute. Hospital Universitari Germans Trias i Pujol, Carretera de Canyet s/n 08916, Badalona (Barcelona), Spain, e-mail: abayesgenis@gmail.com

Received: 28.01.2020 Accepted: 19.02.2020

Table 1. Data of asymptomatic severe aortic stenosis patients undergoing physical stress echocardiography.

Demographic data	
Women	32 (37.6)
Age [years]	74.1 ± 9.4
Smokers	9 (10.6)
High blood pressure	70 (82.3)
Diabetes mellitus	30 (35.3)
Dyslipidemia	65 (76.4)
Echocardiographic data	
Bicuspid aortic valve	22 (25.9)
Peak aortic velocity [m/s]	4.3 ± 0.3
Maximum aortic gradient [mmHg]	74.5 ± 11.1
Mean aortic gradient [mmHg]	47 ± 8
Aortic valve area [cm^2]	0.77 ± 0.12
LVEF [%]	67.9 ± 0.12
Blood count	
NT-proBNP [ng/L]	294.0 (148–661)

Data presented as number (%), mean ± standard deviation, or median and percentiles of 25–75 (Q1–Q3). LVEF — left ventricular ejection fraction; NT-proBNP — N-terminal pro-B-type natriuretic peptide

in 15 (55.5%) patients. Finally the third PE was the key indicator for aortic valve replacement in 2 (40%) patients, because it was clinically positive by symptoms.

Present findings indicated that repeating PE during follow-up was useful for asymptomatic SAS management. Indeed, the key indication for valve replacement increased from 27% of cases at baseline PE to 33% in the second PE, and 40% in the third PE. This pilot study in patients with asymptomatic SAS demonstrated that PE at both the first visit and during follow-up was useful in indicating valve replacement. Further studies in larger cohorts are needed to confirm these findings, and to establish the optimal time-frames for serial PE in such patients.

Funding

Elena Ferrer-Sistach was supported by grants from Societat Catalana de Cardiologia.

Conflict of interest: None declared

References

1. Pellikka PA, Sarano ME, Nishimura RA, et al. Outcome of 622 adults with asymptomatic, hemodynamically significant aortic stenosis during prolonged follow-up. Circulation. 2005; 111(24): 3290–3295, doi: 10.1161/CIRCULATIONAHA.104.495903, indexed in Pubmed: 15956131.
2. Baumgartner H, Falk V, Bax JJ, et al. 2017 ESC/EACTS Guidelines for the management of valvular heart disease. Eur Heart J. 2017; 38(36): 2739–2791, doi: 10.1093/eurheartj/ehx391, indexed in Pubmed: 28886619.
3. Redfors B, Pibarot P, Gillam LD, et al. Stress testing in asymptomatic aortic stenosis. Circulation. 2017; 135(20): 1956–1976, doi: 10.1161/CIRCULATIONAHA.116.025457, indexed in Pubmed: 28507251.
4. Rafique AM, Biner S, Ray I, et al. Meta-analysis of prognostic value of stress testing in patients with asymptomatic severe aortic stenosis. Am J Cardiol. 2009; 104(7): 972–977, doi: 10.1016/j.amjcard.2009.05.044, indexed in Pubmed: 19766766.
5. Ennezat PV, Maréchaux S, Iung B, et al. Exercise testing and exercise stress echocardiography in asymptomatic aortic valve stenosis. Heart. 2009; 95(11): 877–884, doi: 10.1136/hrt.2008.150011, indexed in Pubmed: 18812409.

VIA MEDICA

TECHNOLOGY NOTE

Cardiology Journal
2020, Vol. 27, No. 3, 309–311
DOI: 10.5603/CJ.a2020.0077

ISSN 1897–5593

Atrial flow regulator as a novel therapy for patients with chronic heart failure

Łukasz Lewicki[1, 2*], Robert Sabiniewicz[3*], Janusz Siebert[1, 4], Marek Szołkiewicz[2]

[1]University Center for Cardiology, Gdansk, Poland
[2]Department of Cardiology and Angiology, Kashubian Center for Heart and Vascular Diseases, Pomeranian Hospitals, Wejherowo, Poland
[3]Department of Pediatric Cardiology and Congenital Heart Disease, Medical University of Gdansk, Poland
[4]Department of Family Medicine, Medical University of Gdansk, Poland

Mortality and morbidity among patients with heart failure (HF) remain high, despite advances in therapy.

Heart failure with preserved ejection fraction (HFpEF) is driven by diminished left ventricle relaxation and elevated filling pressures, all of which lead to pulmonary congestion [1, 2]. In these patients, therapeutic options impacting prognosis are limited.

Recently, a novel therapy has been proposed. It is based on creating a communication between both atria using a trans-septal puncture and balloon septostomy. The concept is based on the well-known Lutembacher syndrome, which is defined as a combination of mitral stenosis and atrial septal defect (ASD). The left to right interatrial shunt enables decompression of the left atrium and thus, may improve patient symptoms.

Moreover, observations made in elderly subjects with masked left ventricle restriction, who underwent ASD closure, showed that temporary ASD occlusion with a balloon resulted in significant elevated left atrial pressure [3]. A fenestrated ASD septal occlude has been designed to enable bidirectional flow both in systolic and diastolic impairment [4]. Implantable pressure systems have provided data that left atrial pressure is highly variable over the course of a day and sustained elevations precede clinical events, averaging > 25 mmHg for several days before admission or death [5].

Therefore, a therapy focused on decreasing left atrial filling pressures seems to be promising.

Several small studies proved initial safety and efficacy of three different interatrial shunting devices in therapy for patients either with heart failure with reduced ejection fraction (HFrEF) or HFpEF [6, 7]. There are three different devices available for patients with either HFrEF or HFpEF: interatrial shunt device (IASD, Corvia Medical Inc., Tewksbury, MA, USA), V-Wave shunt (V-Wave Ltd., Caesarea, Israel) and Atrial Flow Regulator (AFR, Occlutech, Heslingborg, Sweden).

Atrial Flow Regulator is a self-expandable a double-disc nitinol wire mesh construction allowing communication across the interatrial septum (Fig. 1). In contrast to V-wave and IASD, it is available in different sizes. The offered fenestration diameter ranges from 4 to 10 mm, but for HF patients only 8 mm and 10 mm have the European Conformité Européenne (CE) mark. Additionally, there are two available heights of the device: 5 and 10 mm, chosen according to interatrial septal thickness. The device is repositionable and retrievable.

First AFR implantation in Poland was done in a 28-year-old patient with severe pulmonary arterial hypertension (PAH) [8]. More recently, AFR has been successfully used as a bridge to lung transplantation in a young patient with drug-resistant idiopathic PAH [9].

Recently four AFR devices in patients with severe HFrEF were successfully implanted. These procedures were done as a part of ongoing PROLONGER trial (Pomeranian atRial flOw

Address for correspondence: Łukasz Lewicki, MD, PhD, University Center for Cardiology, ul. Dębinki 2, 80–211 Gdańsk, Poland, tel: +48 501 702 885, e-mail: luklewicki@gmail.com

Received: 8.03.2020 Accepted: 16.05.2020

**The first two authors contributed equally to this work.*

Figure 1. Atrial Flow Regulator (AFR, Occlutech, Heslingborg, Sweden).

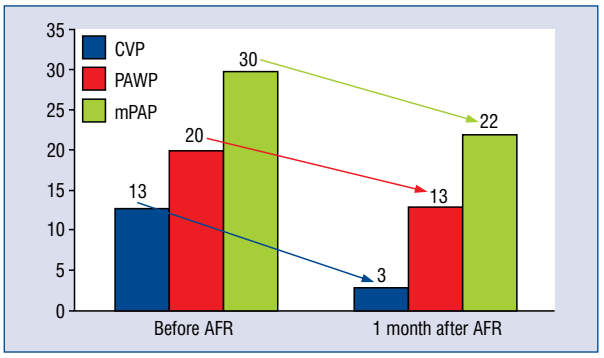

Figure 2. Hemodynamic parameters taken from diagnostic right heart catheterization before, and 1 month after implantation of Atrial Flow Regulator (AFR); CVP — central venous pressure; PAWP — pulmonary artery wedge pressure; mPAP — mean pulmonary artery pressure.

reguLatOr iN conGestive hEart failuRe; No. NCT04334694 at clinicaltrials.gov).

Herein presented, are the results of a 66-year-old male with HFrEF (LVEF 25%), history of three myocardial infarctions, arterial hypertension and paroxysmal atrial fibrillation. Despite an optimal therapy, the patient remained symptomatic with New York Heart Association (NYHA) III. His 6-minute walk test distance (6MWT) was 200 m. The patient underwent diagnostic right heart catheterization with the Swan-Ganz catheter, which revealed decreased cardiac output accompanied with significantly increased pulmonary artery wedge pressure (PAWP).

According to PROLONGER protocol, hemodynamic indications for AFR are: PAWP above 15 mmHg or 25 mmHg at rest and exertion respectively. A right atrial pressure above 20 mmHg or exceeding PAWP is the contraindication for an atrial shunting procedure.

The AFR procedure was performed under general anesthesia. A three-dimensional transesophageal echocardiography (TEE) guided trans-septal puncture was performed followed by a 12 mm balloon septostomy. An AFR (8 mm fenestration, 5 mm height) was successfully implanted using a 12 F dedicated delivery system. The left to right mean gradient obtained from TEE was 2.7 mmHg. The patient was discharged home on the third day. As the patient had a history of atrial fibrillation, he was given non-vitamin K antagonist oral anticoagulants. There was no other specific indication for anticoagulation in this patient, because flow through the device was left to right.

The first follow-up visit after 1 month was complete, significant clinical improvement was noticed. The patient moved from NYHA III to NYHA II and 6MWT distance increased from 200 m to 397 m. Diagnostic right heart catheterization revealed significant reduction in PAWP, mean pulmonary artery and right atrial pressures (Fig. 2). The mean left to right gradient in TEE was 10 mmHg compared to 2.7 mmHg directly after AFR implantation. This difference could be explained by the fact that left atrial pressure had changed dynamically according to fluid overload, exertion and other conditions. Similar variability in all 4 patients thus far were observed.

The second follow-up visit was scheduled at 2 months.

This experience with AFR device is a promising option for patients with severe HF and further results will be published soon.

Conflict of interest: None declared

References

1. Lam CSP, Voors AA, de Boer RA, et al. Heart failure with preserved ejection fraction: from mechanisms to therapies. Eur Heart J. 2018; 39(30): 2780–2792, doi: 10.1093/eurheartj/ehy301, indexed in Pubmed: 29905796.

2. Borlaug BA, Paulus WJ. Heart failure with preserved ejection fraction: pathophysiology, diagnosis, and treatment. Eur Heart J. 2011; 32(6): 670–679, doi: 10.1093/eurheartj/ehq426, indexed in Pubmed: 21138935.
3. Ewert P, Berger F, Nagdyman N, et al. Masked left ventricular restriction in elderly patients with atrial septal defects: a contraindication for closure? Catheter Cardiovasc Interv. 2001; 52(2): 177–180, doi: 10.1002/1522-726x(200102)52:2<177::aid-ccd1043>3.0.co;2-g, indexed in Pubmed: 11170324.
4. Bruch L, Winkelmann A, Sonntag S, et al. Fenestrated occluders for treatment of ASD in elderly patients with pulmonary hypertension and/or right heart failure. J Interv Cardiol. 2008; 21(1): 44–49, doi: 10.1111/j.1540-8183.2007.00324.x, indexed in Pubmed: 18086135.
5. Ritzema J, Troughton R, Melton I, et al. Physician-directed patient self-management of left atrial pressure in advanced chronic heart failure. Circulation. 2010; 121(9): 1086–1095, doi: 10.1161/CIRCULATIONAHA.108.800490, indexed in Pubmed: 20176990.
6. Shah SJ, Feldman T, Ricciardi MJ, et al. One-Year safety and clinical outcomes of a transcatheter interatrial shunt device for the treatment of heart failure with preserved ejection fraction in the reduce elevated left atrial pressure in patients with heart failure (REDUCE LAP-HF I) trial: a randomized clinical trial. JAMA Cardiol. 2018; 3(10): 968–977, doi: 10.1001/jamacardio.2018.2936, indexed in Pubmed: 30167646.
7. Paitazoglou C, Özdemir R, Pfister R, et al. The AFR-PRELIEVE trial: a prospective, non-randomised, pilot study to assess the Atrial Flow Regulator (AFR) in heart failure patients with either preserved or reduced ejection fraction. EuroIntervention. 2019; 15(5): 403–410, doi: 10.4244/EIJ-D-19-00342, indexed in Pubmed: 31130524.
8. Dąbrowska-Kugacka A, Ciećwierz D, Żuk G, et al. Atrial flow regulator for severe drug resistant pulmonary arterial hypertension after congenital heart defect correction. Cardiol J. 2019; 26(1): 102–104, doi: 10.5603/CJ.2019.0016, indexed in Pubmed: 30882193.
9. Janus M, Sławek-Szmyt S, Araszkiewicz A, et al. Atrial flow regulator as a bridge to lung transplantation in a young patient with drug-resistant idiopathic pulmonary arterial hypertension. Kardiol Pol. 2020; 78(5): 461–462, doi: 10.33963/KP.15178, indexed in Pubmed: 32024808.

VIA MEDICA

TECHNOLOGY NOTE

Cardiology Journal
2020, Vol. 27, No. 3, 312–315
DOI: 10.5603/CJ.a2019.0064

ISSN 1897–5593

Telescopic coronary sinus cannulation for mapping and ethanol ablation of arrhythmia originating from left ventricular summit

Artur Baszko, Piotr Kałmucki, Tomasz Siminiak, Andrzej Szyszka

Poznan University of Medical Sciences, Poznan, Poland

Introduction

The radiofrequency ablation (RFA) of arrhythmia from left ventricular (LV) summit encounters several difficulties [1]. There are several ablative techniques used to treat LV summit arrhythmia: high energy irrigated ablation [2], ablation through the great cardiac vein [3], epicardial ablation [4] or bipolar ablation [5, 6]. The technique which has recently gained interest is transvenous ethanol ablation [7]. As there is no generally accepted method for alcohol ablation, herein the telescopic coronary sinus (CS) cannulation technique from femoral vein was introduced.

Description of the method

The telescopic system consists of an 8 F SL0 catheter, a 5 F guide catheter and microcatheter. All procedures were performed using the FD10 Allura Xper angiography (Philips, Netherlands) and electroanatomic system Carto 3 (Biosense Webster, Inc, Diamond Bar, CA, USA) or Ensite Velocity (St. Jude Medical Inc., St. Paul, MN, USA).

Coronary sinus angiography

After preparation, the left femoral vein is punctured and two electrodes are positioned in His region (5 F 4-pole) and CS (steerable 4 F 10 poles, Abbott). The 4F electrode records the activation from the distal part of CS to confirm epicardial character of the arrhythmia [3]. The 8 F SL0 sheath (Abbott) is inserted through right femoral vein and positioned at the level of CS ostium. Access to CS is obtained with an ablation electrode (Fig. 1A). After CS intubation, a venography is performed (Fig. 1B, 2C). For wide CS, Attain Clarity™ 6225l (Medtronic, B.V, Netherlands) venography balloon catheter is optimal. It is 90 cm long, and the balloon diameter is 13 mm. For smaller CS, CORODYN P1 F6 80 cm (Braun, Melsungen AG, Germany) can be used with different balloon diameters (5 F: 8 mm, 6 F: 10 mm, 7 F: 12 mm). The venography is routinely performed in several projections.

Intubation and mapping of small venous branches

After angiography is completed, the 5 F guide catheter (JR4 or IMA) is introduced through SL0 sheath. The guide catheter is a better than diagnostic tool as it has shorter, soft and non-tapered distal tip. The 0.014'' BMW wire (Abbot Vascular, Diegam, Belgium) is advanced to the distal part of catheter. At this stage the microcatheter is introduced over the wire (Finecross, Terumo, Tokyo, Japan). The microcatheter has 1.8 F (0.6 mm) radiopaque distal tip. After the vein of interest is wired, the microcatheter is advanced to cover most of the wire leaving the distal 0.5 cm part for recording the unipolar signal (Fig. 1C, 2C). The recording of intracardiac signals and pacing is possible after connecting the percutaneous coronary intervention (PCI) wire in unipolar mode with electrophysiological system. At this stage the wire is removed and a small amount of contrast is given to confirm that the correct vein has been selected, to assess the diameter of the vein and the presence of collaterals, which can be responsible for irregular distribution of ethanol and its wash up (Fig. 2E). Thereafter the guidewire is inserted again and microcatheter is replaced for over-the-wire (OTW) balloon. As the Finecross microcatheter is shorter

Address for correspondence: Artur Baszko, MD, PhD, 2nd Department of Cardiology, Poznan University of Medical Sciences, ul. 28 Czerwca 1956 r. No. 194, 61–485 Poznań, Poland, tel: +48 61 2274164, e-mail: abaszko@wp.pl

Received: 21.11.2018 Accepted: 3.05.2019

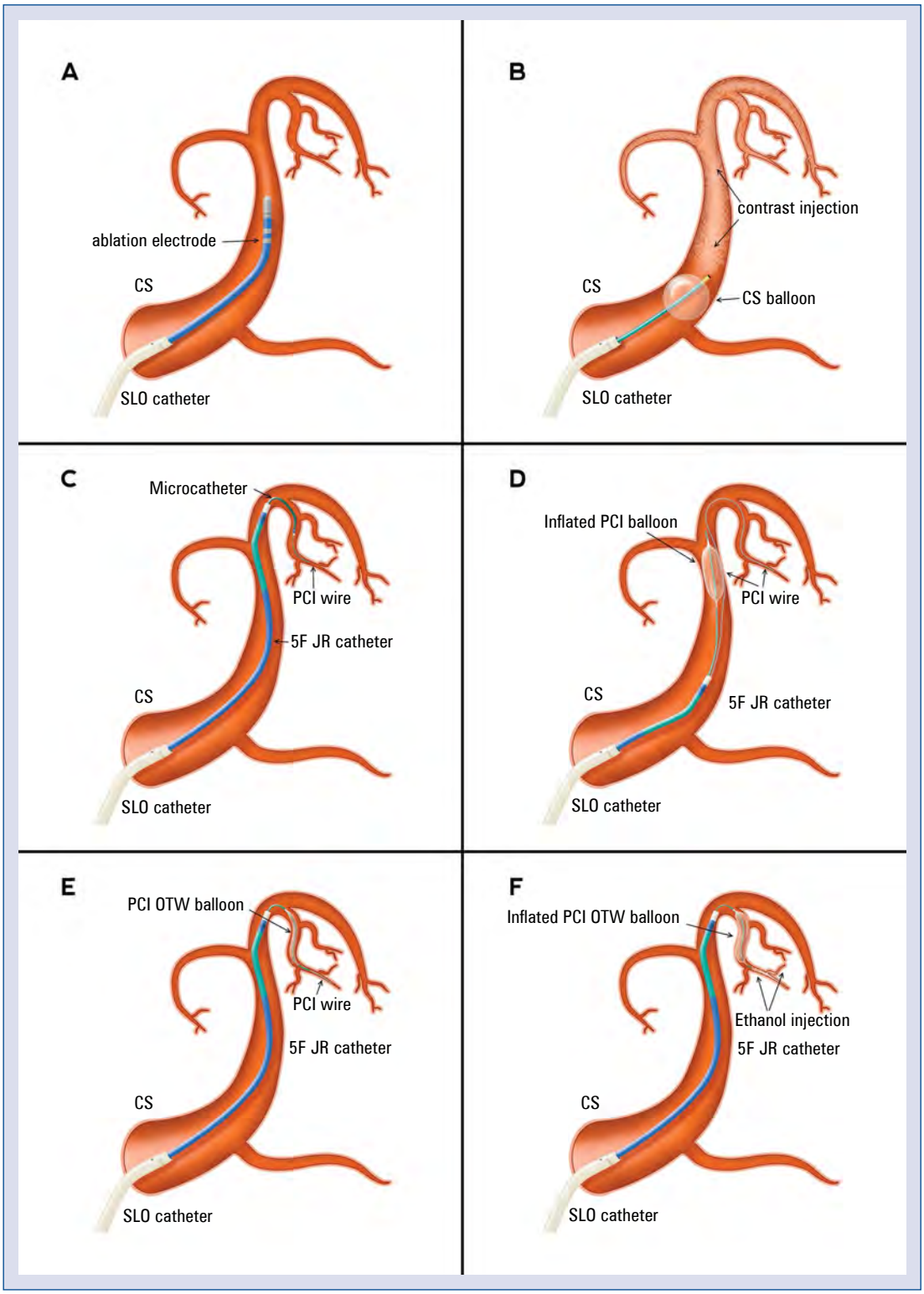

Figure 1. The crucial steps in performing transvenous ethanol ablation of arrhythmia with telescopic system; **A.** The intubation of the coronary sinus (CS) with ablation electrode and 8.5 F SL0 sheath; **B.** Coronary sinus venography through SL0 sheath; **C.** The 5 F JR guide catheter and angioplasty insertion through SL0 catheter followed by a microcatheter. The mapping is performed connecting the proximal percutaneous coronary intervention (PCI) wire with electrophysiological system in unipolar mode (not presented in the picture). The contrast can be selectively administered to the small branch through a microcatheter after the PCI wire is removed; **D.** Replacement of a microcatheter using the "trapping technique" with angioplasty balloon; **E.** The contrast injection through over-the-wire (OTW) balloon; **F.** Ethanol injection through inflated OTW balloon according to the method described by Kreidieh et al. [8].

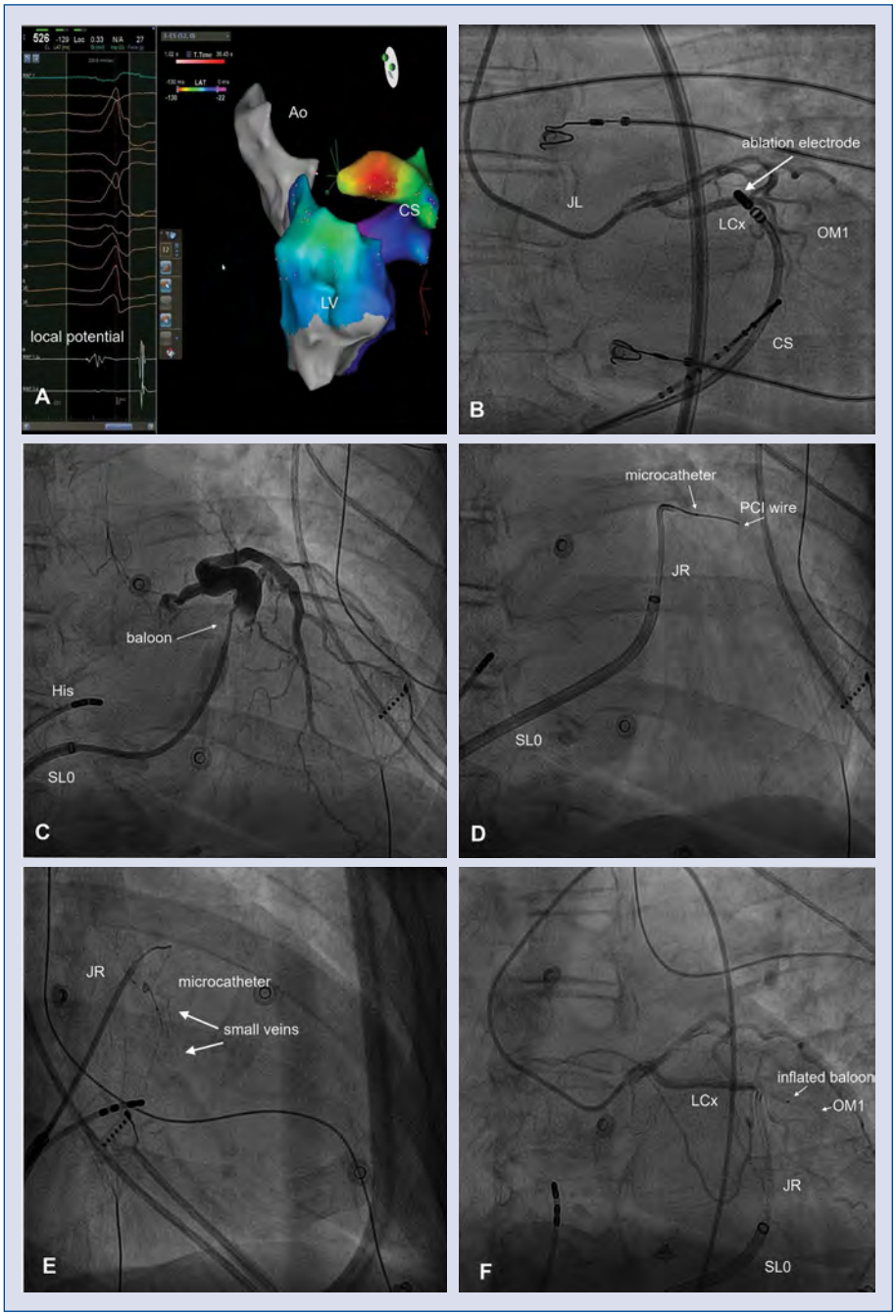

Figure 2. The important stages of ethanol transvenous ablation with telescopic coronary sinus cannulation technique after previously failed radiofrequency ablation (RFA); **A**. A 12-lead electrocardiogram of clinical VPC and the CARTO electroanatomical map presenting the earliest potentials within the distal part of coronary sinus (CS); **B**. The position of ablation electrode within CS. The "best" potential was recorded at the site of obtuse marginal branch (OM1). The RFA was not performed because of the high risk of arterial damage; **C**. The CS angiography performed with the use of SL0. The angiography clearly shows several potential branches for detailed mapping; **D**. The cannulation system consisted of SL0 and JR catheters enabling the introduction of a microcatheter and percutaneous coronary intervention (PCI) wire. The microcatheter creates the insulation of the PCI wire for recording unipolar signals and pacing from the distal part of the wire; **E**. After selecting the optimal site for ethanol ablation, the PCI wire can be removed and a small amount of contrast can identify the region supplied including possible collaterals; **F**. Presentation of location of inflated over-the-wire (OTW) balloon before ethanol injection together with coronary angiography. This picture presents the location of the potential site for ablation position very close to OM1 branch. Delivering a radio frequency application in this region could result in injury to OM1 branch while delivering the ethanol, though the vein dose is safe.

than the guidewire, there are two techniques for the exchange. In a "flushing technique", the inflator is connected to the microcatheter after it has been withdrawn and reaches the proximal part of the wire. A fast injection of saline with controlled pulldown ejects the wire from microcatheter leaving the distal part almost in place. In a "trapping technique", the angioplasty balloon is used to trap the angioplasty wire (Fig. 1D). The trapping of the wire can be obtained within the guide catheter or in the great cardiac vein depending on the anatomy. The standard semi compliant balloon (1.5 × 15 mm for JR or 2.5 × 15 mm for CS) is inserted through the JR catheter by the side of the microcatheter and advanced to the distal part of the catheter or to the great cardiac vein passing the tip of the microcatheter. Thereafter the balloon is inflated to trap the wire well against the JR or CS wall enabling safe removal of the microcatheter. The last stage is to insert the OTW balloon to a previously selected position (Fig. 1E, 2F). The wire is then removed, the balloon is inflated and a small amount of contrast is administered to visualize the drained region (Fig. 1F). An ethanol injection can be injected according to a technique described by Kreideih et al. [8].

The technique described was evaluated prospectively in 4 patients (17–65 years, 3 females) with LV summit ventricular tachycardia after 1–3 failed RFA. The CS was easily cannulated without complications in all patients and there were no technique related problems. The time for CS cannulation was 2–5 min, the time from CS intubation to contrast injection to venous branches ranged 17–29 min, and the time taken from selective venous angiography to first alcohol injection ranged from 28 to 31 min. The time from CS intubation to first ethanol injection ranged from 66 to 86 min. The mean fluoroscopy time of the procedure was 52 min (range 32–86 min) and the Air-Kerma dose 422 mGy (range 45–818 mGy) which included all stages of the procedure. The telescopic system was easy to control, allowed for rapid electrodes and catheter replacement. No obstacles or complications were noted during mapping or ablation therapy.

The described technique for transvenous ethanol ablation using 8 F SL0 catheter with 5 F guide catheter and microcatheter from the femoral vein is comfortable for both the patient and the cardiologist. All three components are important at each consecutive step of the procedure. The SL0 catheter helps to obtain safe and stable access to the CS with the ablation electrode and the balloon for performing angiography. The routine use of microcatheters is definitely more expensive than OTW balloons, but there are several benefits. They help exchange the angioplasty wire when the distal part has been deformed or a different wire or tip shape is required. The use of a microcatheter can reduce the number of OTW balloons and enables better unipolar mapping and allows deeper engagement of the wire for better support during OTW balloon insertion. It is possible that a routine use of femoral access with microcatheters for mapping and identification of the target site can be beneficial in time reduction, but this needs to be further investigated.

Conflict of interest: None declared

References

1. Yamada T, Yoshida N, Doppalapudi H, et al. Efficacy of an anatomical approach in radiofrequency catheter ablation of idiopathic ventricular arrhythmias originating from the left ventricular outflow tract. Circ Arrhythm Electrophysiol. 2017; 10(5): e004959, doi: 10.1161/CIRCEP.116.004959, indexed in Pubmed: 28500177.
2. Everett TH, Lee KW, Wilson EE, et al. Safety profiles and lesion size of different radiofrequency ablation technologies: a comparison of large tip, open and closed irrigation catheters. J Cardiovasc Electrophysiol. 2009; 20(3): 325–335, doi: 10.1111/j.1540-8167.2008.01305.x, indexed in Pubmed: 18803562.
3. Baman TS, Ilg KJ, Gupta SK, et al. Mapping and ablation of epicardial idiopathic ventricular arrhythmias from within the coronary venous system. Circ Arrhythm Electrophysiol. 2010; 3(3): 274–279, doi: 10.1161/CIRCEP.109.910802, indexed in Pubmed: 20400776.
4. Santangeli P, Marchlinski FE, Zado ES, et al. Percutaneous epicardial ablation of ventricular arrhythmias arising from the left ventricular summit: outcomes and electrocardiogram correlates of success. Circ Arrhythm Electrophysiol. 2015; 8(2): 337–343, doi: 10.1161/CIRCEP.114.002377, indexed in Pubmed: 25637596.
5. Baszko A, Telec W, Kałmucki P, et al. Bipolar irrigated radiofrequency ablation of resistant ventricular tachycardia with a septal intramural origin: the initial experience and a description of the method. Clin Case Rep. 2016; 4(10): 957–961, doi: 10.1002/ccr3.648, indexed in Pubmed: 27761246.
6. Futyma P, Wysokińska A, Sander J, et al. Bipolar endo-epicardial radiofrequency ablation of arrhythmia originating from the left ventricular summit. Circ J. 2018; 82(6): 1721–1722, doi: 10.1253/circj.CJ-17-0782, indexed in Pubmed: 29046505.
7. Baher A, Shah DJ, Valderrabano M. Coronary venous ethanol infusion for the treatment of refractory ventricular tachycardia. Heart Rhythm. 2012; 9(10): 1637–1639, doi: 10.1016/j.hrthm.2012.06.003, indexed in Pubmed: 22683748.
8. Kreidieh B, Rodríguez-Mañero M, Schurmann P, et al. Retrograde coronary venous ethanol infusion for ablation of refractory ventricular tachycardia. Circ Arrhythm Electrophysiol. 2016; 9(7): e004352, doi: 10.1161/CIRCEP.116.004352, indexed in Pubmed: 27406606.
9. Yamada T, Doppalapudi H, Maddox WR, et al. Prevalence and Electrocardiographic and Electrophysiological Characteristics of Idiopathic Ventricular Arrhythmias Originating From Intramural Foci in the Left Ventricular Outflow Tract. Circ Arrhythm Electrophysiol. 2016; 9(9): e004079, doi: 10.1161/CIRCEP.116.004079, indexed in Pubmed: 27625170.
10. Chen W, Yao Y, Zhang S, et al. Comparison of operator radiation exposure during coronary sinus catheter placement via the femoral or jugular vein approach. Europace. 2011; 13(4): 539–542, doi: 10.1093/europace/euq515, indexed in Pubmed: 21252193.

VIA MEDICA

IMAGE IN CARDIOVASCULAR MEDICINE

Cardiology Journal
2020, Vol. 27, No. 3, 316–317
DOI: 10.5603/CJ.2020.0081

ISSN 1897–5593

Silent plaque rupture in the left main stem assessed by optical coherence tomography

Yongcheol Kim[1], Byeong-Keuk Kim[2], Thomas W. Johnson[3], Sung-Jin Hong[2], Chul-Min Ahn[2], Jung-Sun Kim[2], Deok-Kyu Cho[1], Young-Guk Ko[2], Donghoon Choi[1], Myeong-Ki Hong[2], Yangsoo Jang[2]

[1]Division of Cardiology, Department of Internal Medicine, Yonsei University College of Medicine and Cardiovascular Center, Yongin Severance Hospital, Yongin, Republic of Korea
[2]Division of Cardiology, Severance Cardiovascular Hospital, Yonsei University College of Medicine, Seoul, Republic of Korea
[3]Department of Cardiology, Bristol Heart Institute, Bristol, United Kingdom

A 59-year-old man underwent primary percutaneous coronary intervention (PCI) for thrombotic total occlusion of his distal right coronary artery. Bystander disease was limited to an ambiguous lesion in the distal left main stem (LMS) with an intraluminal filling defect suggestive of a ruptured plaque. A staged inpatient assessment of the LMS was undertaken utilizing invasive physiologic and intravascular imaging assessments as distal flow in the left coronary system was preserved and symptoms had settled with index intervention (Fig. 1A, B; **Suppl. Video 1 and 2**). Evaluation of the LMS lesion by instantaneous wave-free ratio (iFR) and fractional flow reserve (FFR), 3 days following presentation, provided an iFR value of 0.95 and the hyperemic FFR value was 0.89. Optical coherence tomography (OCT) demonstrated a ruptured plaque without associated thrombus in the LMS with diffuse fibroatheroma with underlying necrotic core extending into the proximal left anterior descending artery (LAD) (Fig. 1C–F, **Suppl. Video 3**). Importantly, OCT generated a minimal lumen area (MLA) in the LMS of 8.73 mm^2 (Fig. 1G), with a MLA of 3.04 mm^2 in the proximal LAD segment. Therefore, based on the findings of the iFR/FFR and OCT assessment, it was concluded that the LMS plaque had stabilized following a previous rupture and in the absence of ischemia, elected to pursue a conservative strategy. At 3-month follow-up a treadmill test demonstrated good exercise tolerance (11.2 metabolic equivalents) without symptoms or electrocardiographic evidence of ischemia.

Although an acute phase of rupture plaque is defined by a disrupted fibrous cap, with or without thrombus, overlying a necrotic core, a definition of the chronic phase has, to date, not been well described [1]. The OCT is more accurate for detecting plaque characteristics due to its higher resolution, which is 10 times (10 μm) that of intravascular ultrasound [2]. The present case highlights the utility of OCT in the evaluation of ambiguous lesions, with the use of MLA to guide LMS intervention and detection of a smooth-edged, disrupted plaque devoid of thrombus and a necrotic core, is suggestive of a stabilized healed ruptured plaque.

Conflict of interest: None declared

References

1. Johnson TW, Räber L, di Mario C, et al. Clinical use of intracoronary imaging. Part 2: acute coronary syndromes, ambiguous coronary angiography findings, and guiding interventional decision-making: an expert consensus document of the European Association of Percutaneous Cardiovascular Interventions. Eur Heart J. 2019; 40(31): 2566–2584, doi: 10.1093/eurheartj/ehz332, indexed in Pubmed: 31112213.
2. Kim Y, Johnson TW, Akasaka T, et al. The role of optical coherence tomography in the setting of acute myocardial infarction. J Cardiol. 2018; 72(3): 186–192, doi: 10.1016/j.jjcc.2018.03.004, indexed in Pubmed: 29650398.

Address for correspondence: Byeong-Keuk Kim, MD, PhD, Division of Cardiology, Severance Cardiovascular Hospital, Yonsei University College of Medicine, 250 Seongsan-ro, Seodaemun-gu, Seoul 03722, Republic of Korea, tel: +82-2-2228-8460, fax: +82-2-2227-7732, e-mail: kimbk@yuhs.ac

Received: 16.03.2020 Accepted: 26.03.2020

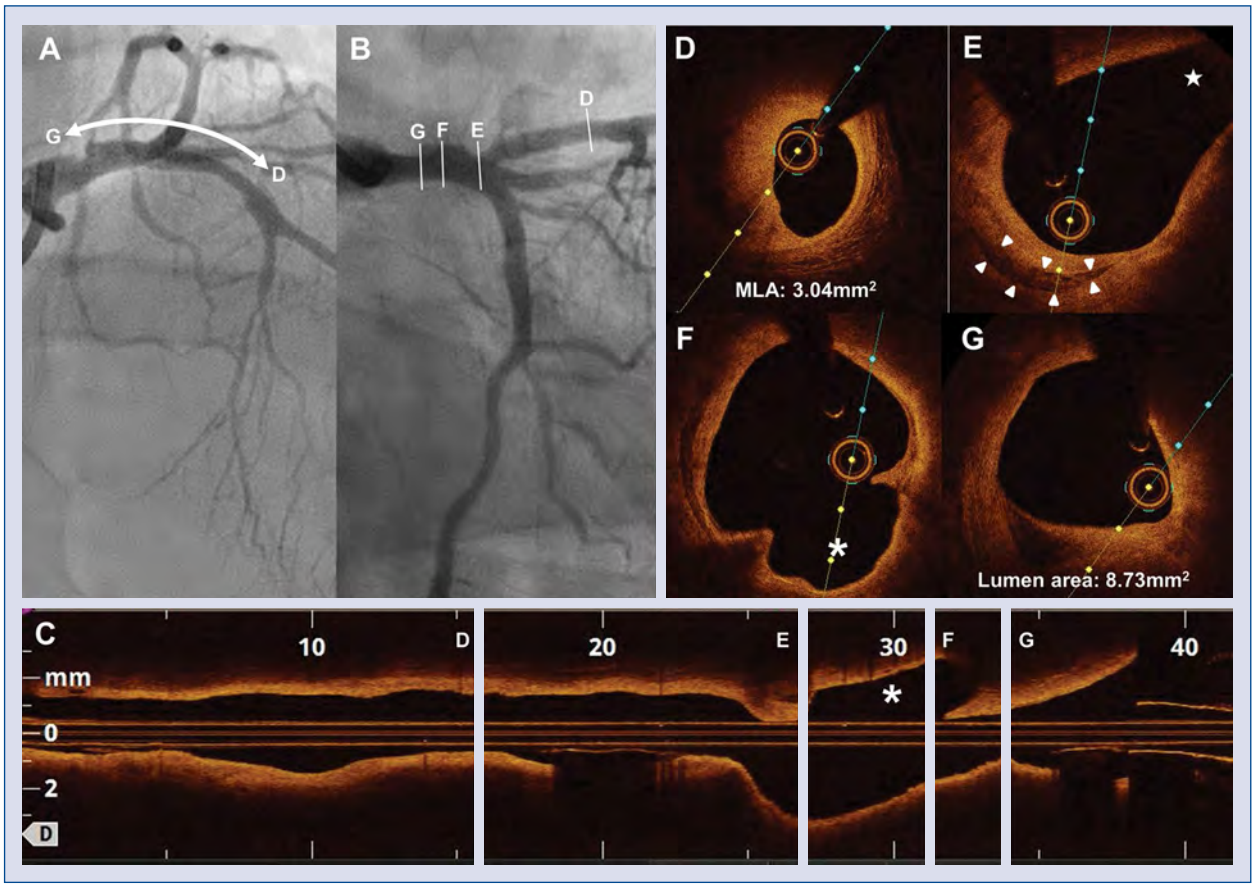

Figure 1. A, B. Angiographic assessment demonstrating mild stenosis with suspicious ruptured plaque in the left main stem (LMS); **C.** Longitudinal optical coherence tomography (OCT) imaging demonstrating a ruptured plaque space (asterisk); **D.** Minimal lumen area (MLA) of 3.04 mm^2 in the proximal left anterior descending artery; **E.** OCT, showing suspicious necrotic core (arrowheads) in the left main bifurcation (star: ostium of left circumflex artery; **F.** OCT demonstrating ruptured plaque space in the LMS; **G.** MLA of 8.73 mm^2 in the LMS.

VIA MEDICA

IMAGE IN CARDIOVASCULAR MEDICINE

Cardiology Journal
2020, Vol. 27, No. 3, 318–319
DOI: 10.5603/CJ.2020.0082

ISSN 1897–5593

Virtual fractional flow reserve and virtual coronary stent guided percutaneous coronary intervention

Fang-Yang Huang[1], Qi Liu[1], Xiao-Xiao Liu[2], Bin Ma[2], Ye Zhu[1]

[1]Department of Cardiology, West China Hospital, Sichuan University, Chengdu, China
[2]Shenzhen Keya Medical Technology Corporation, Shenzhen, China

Deep vessel (DV)-angio is a newly developed software utilizing machine learning methods to calculate virtual fractional flow reserve (vFFR) based upon coronary angiogram (CAG). Briefly, a supervised deep learning and neural net model is trained in advance from hundreds of cases to map the extracted three-dimensional vascular structures and the corresponding blood flow estimation. Furthermore herein, a virtual coronary stent (VCS) technology has been developed that simulates post-VCS coronary artery geometries and estimates corresponding vFFR.

A 70-year-old male patient with recurrent chest pain was scheduled to undergo CAG. CAG revealed a 90% luminal stenosis in distal right coronary artery (RCA) after intracoronary administration of nitrates (Fig. 1A). The left coronary artery is normal. Two orthogonal CAG cines were imported into the DV-angio that reconstructed the RCA as in Figure 1B. The vFFR was 0.78 in the distal RCA while an invasive FFR measured with the pressure wire was 0.75 (Fig. 1C). Then, the DV-angio modeled the targeted coronary artery after a simulated 3.5-mm × 24-mm stent was implanted, and estimated the post-VCS FFR to be 0.97 (Fig. 1D). These processes took about 4 min. After implanting the same stent as the simulated one at the stenosis site (Fig. 1E), the actual FFR was improved to 0.99 (Fig. 1F). The patient no longer experienced angina pectoris during follow-up.

The feasibility of VCS-guided percutaneous coronary intervention (PCI) was first reported herein, based on machine learning methods in a real-world case. As CAG allows ad hoc PCI after strategy determined, the CAG-based vFFR and VCS will have a great practical application foreground.

Fundings

The present study received grants from the National Key R&D Program of China (2017YFC0910004 and 2017YFB0702500), the National Natural Science Foundation of China (grant number: 81900258), the Sichuan Science and Technology Program (2020YFS0246), the China Postdoctoral Science Foundation Grant (2019M663521), the Post-Doctor Research Project, Sichuan University (2020SCU12029), and the Post-Doctor Research Project, West China Hospital, Sichuan University (2019HXBH016).

Conflict of interest: None declared

Address for correspondence: Ye Zhu, MD, Department of Cardiology, West China Hospital, Sichuan University, 37 Guoxue Street, Chengdu 610041, Sichuan, China, tel: +86-021-85422343, e-mail: zhuye1974@163.com

Received: 15.03.2020 Accepted: 11.04.2020

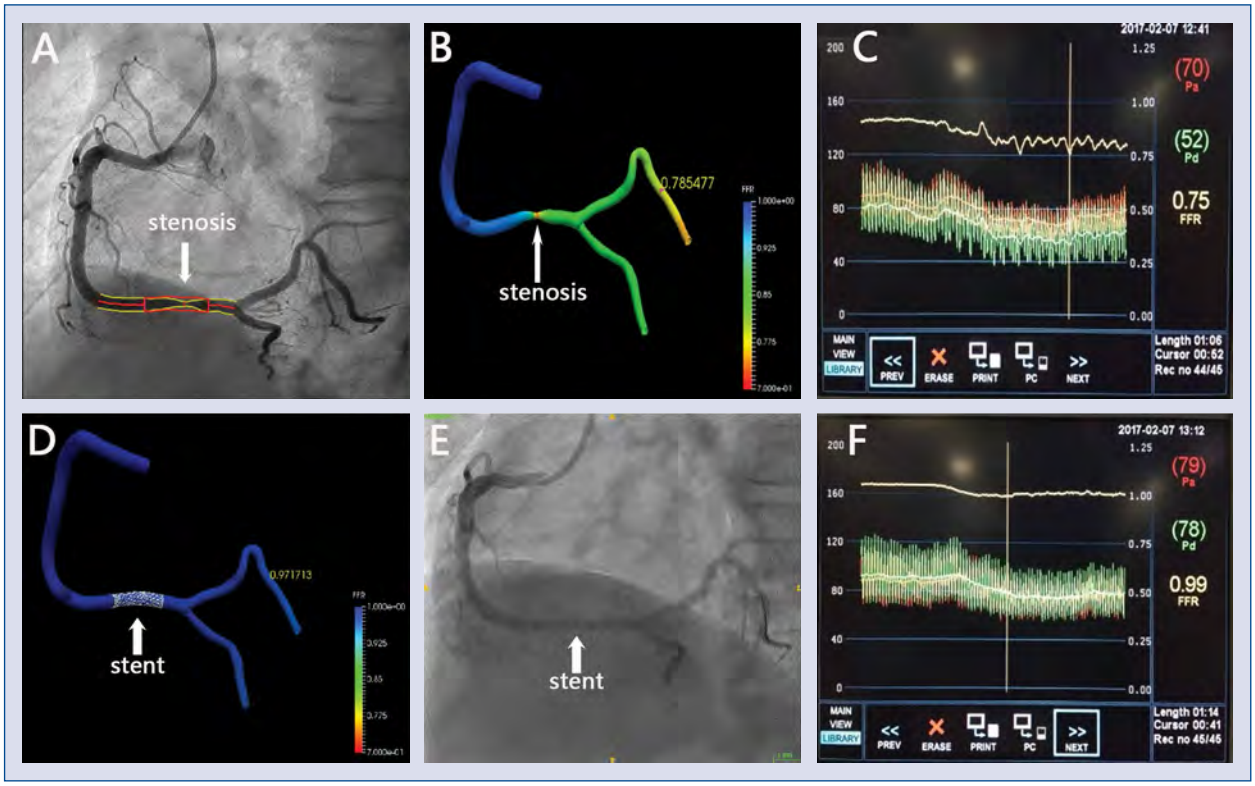

Figure 1. A. The right coronary angiogram was displayed; **B.** Deep vessel (DV)-angio reconstructed three-dimensional right coronary artery. A virtual fractional flow reserve (FFR) is estimated to be 0.78; **C.** The actual FFR was measured by pressure wire; **D.** The predicted DV-angio FFR, after a simulated 3.5-mm × 24-mm stent was implanted, was 0.97; **E.** The right coronary angiogram was displayed after implantation of a 3.5-mm × 24-mm stent; **F.** The true wire post-stent FFR was 0.99.

VIA MEDICA

IMAGE IN CARDIOVASCULAR MEDICINE

Cardiology Journal
2020, Vol. 27, No. 3, 320–321
DOI: 10.5603/CJ.2020.0083

ISSN 1897–5593

A case of drug-coated balloon treatment for two total occluded lesions in a patient with acute coronary syndrome

Song Lin Yuan[1, 2], Moo Hyun Kim[2], Scot Garg[3], Eun-Seok Shin[1]

[1]Division of Cardiology, Department of Internal Medicine, Ulsan Medical Center, Ulsan, South Korea
[2]Department of Cardiology, Dong-A University Hospital, Busan, South Korea
[3]East Lancashire Hospitals NHS Trust, Blackburn, Lancashire, United Kingdom

A 51-year-old man was admitted with worsening effort angina over a 1 month period. His only coronary risk factor was hypercholesterolemia. Cardiac enzymes including creatine kinase-MB and troponin I were normal. His electrocardiogram showed Q-waves in V_1 to V_4. The coronary angiograms showed a short left main with complete occlusions in the proximal left anterior descending (LAD) and left circumflex (LCX) artery (Fig. 1A–C). Revascularization options were discussed and the option to treat the lesions with drug-coated balloons (DCB) was decided. He was carefully assessed, and gave informed consent.

A guide wire successfully crossed the total occlusion of the LCX. Pre-dilatation was performed with a 1.5 × 15 mm balloon, followed by a 2.5 × × 15 mm non-compliant balloon up to 16 atm and finally a 2.5 × 30 mm DCB was inflated at 7 atm for 60 s. Then to the LAD lesion, pre-dilatation was performed with 1.5 × 15 mm balloon and a 3.0 × × 15 mm scoring balloon at 16 atm, and then finally a 3.5 × 20 mm DCB was inflated at 7 atm for 60 s. The final angiograms showed normal flow in both LAD and LCX with no significant dissection or residual stenoses (Fig. 1D–F).

Three months later, follow-up coronary angiography confirmed adequate patency of the DCB treated lesions and reassuringly the distal LCX and proximal LAD looked better (Fig. 1G–I). He remains symptom free, 13-month post-intervention.

After treatment with a DCB, it is possible that vessels will return to their original size over time, which is one of the greatest advantages of DCB treatment in total occluded lesions.

Conflict of interest: None declared

Address for correspondence: Eun-Seok Shin, MD, PhD, Division of Cardiology, Department of Internal Medicine, Ulsan Medical Center, Ulsan, South Korea, e-mail: sesim1989@gmail.com

Received: 3.04.2020 Accepted: 13.04.2020

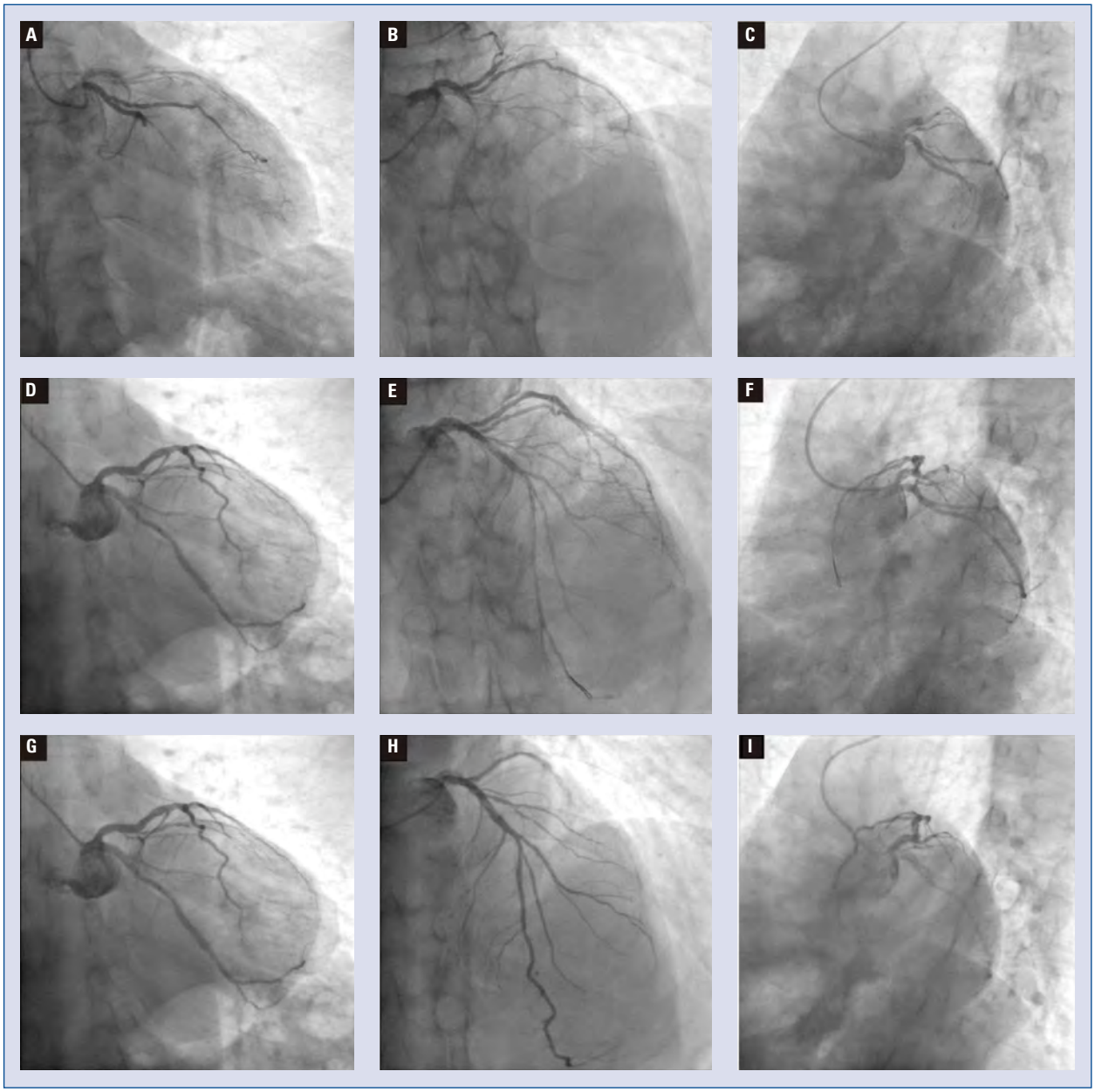

Figure 1. Coronary artery angiography; **A–C.** Before intervention; **D–F.** Right after treatment with a drug-coated balloon; **G–I.** Follow-up angiography at 3 months.

VIA MEDICA

IMAGE IN CARDIOVASCULAR MEDICINE

Cardiology Journal
2020, Vol. 27, No. 3, 322
DOI: 10.5603/CJ.2020.0084

ISSN 1897–5593

Aortic bioprothesis dehiscence in the context of a chronic endocarditis

Inês Almeida[1], Hélder Santos[1], Hugo Miranda[1], Mariana Santos[1], Catarina Sousa[1, 2], Joana Chin[1], Álvaro Laranjeira[3]

[1]Cardiology Department of Hospital Nossa Senhora do Rosário — Centro Hospitalar Barreiro-Montijo, Barreiro, Portugal
[2]Cardiovascular Center of the University of Lisbon, Lisbon School of Medicine, Lisbon, Portugal
[3]Cardiac Surgery Department of Hospital de Santa Marta — Centro Hospitalar Lisboa Central, Lisbon, Portugal

A 74-year-old woman carrier of an aortic bioprosthetic valve Trifecta St. Jude 21® implanted in 2013 in context of severe aortic stenosis was referred for a regular follow-up transthoracic echocardiogram. The patient was asymptomatic. Clinical examination revealed a systodiastolic murmur, grade IV/VI. Transthoracic echocardiogram showed a significant periprosthetic leak with rocking and expansion of the ascending aorta which was confirmed with transesophageal echocardiogram. It showed an aortic bioprosthetic valve with thickened leaflets, without images suggestive of vegetations, but there was evidence of an anechogenic free perivalvular space with flow inside and expansion during systole compatible with multiple pseudoaneurysms and a severe leak between 4 and 12 hours (Fig. 1A, B). The patient was proposed to undergo cardiac surgery. Blood cultures and microbiological exam of the excised valve were negative. During the procedure, an excision of the aortic bioprosthetic valve and the aortic root was made with enlarged surgical cleaning due to the presence of a false aneurysm down the prothesis suggestive of chronic endocarditis (Fig. 1C). A Freestyle® stentless porcine aortic root was successfully implanted. The post-operative period was uneventful.

Prosthetic valve endocarditis, 20–30% of all endocarditis', presents as dehiscence, fistula or pseudoaneurysm. A significant dehiscence of a prothesis with pseudoaneurysm formation is a rare complication that necessitates an urgent re-operation, given the high risk of spontaneous rupture, however it is particularly challenging due to the destruction of the aortic root and the need for complex repairs. The present case is notable as a complete asymptomatic presentation of pseudoaneurysm formation, demonstrating the role and importance of an specialized follow-up in these patients.

Conflict of interest: None declared

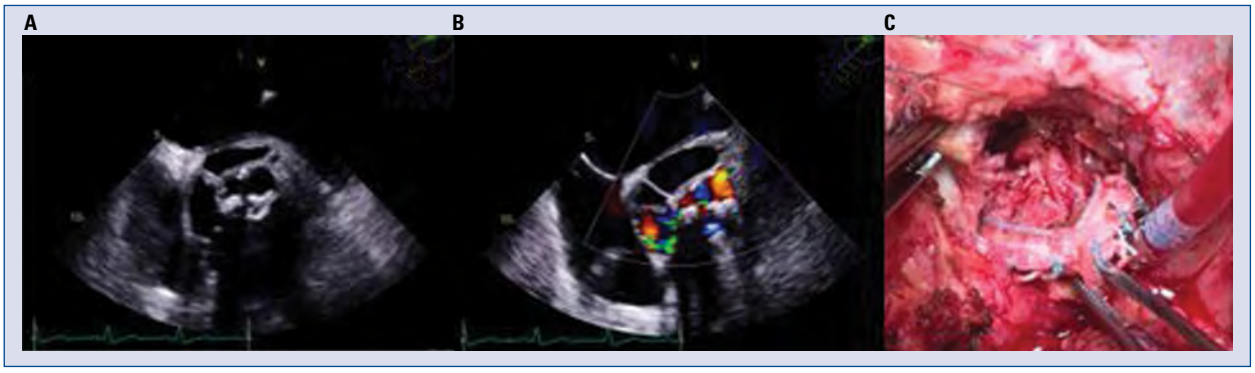

Figure 1. Transesophageal echocardiogram and surgical view of multiple pseudoaneurysms down the prothesis.

Address for correspondence: Dr. Inês Almeida, Avenida das Forças Armadas, 79C, 2834-003 Barreiro, Portugal, tel: +351 915186124, e-mail: inesalmeida91@gmail.com

Received: 29.02.2020 Accepted: 26.03.2020

VIA MEDICA

IMAGE IN CARDIOVASCULAR MEDICINE

Cardiology Journal
2020, Vol. 27, No. 3, 323–324
DOI: 10.5603/CJ.2020.0085

ISSN 1897–5593

Rare case of mitral annulus disjunction and noncompaction-like myocardium

Bryan E-Xin Tan[1], Mallory Balmer-Swain[2], Mohan Rao[2], Bipul Baibhav[2]

[1]Department of Internal Medicine, Rochester General Hospital, Rochester, NY, USA
[2]Sands Constellation Heart Institute, Rochester Regional Health, Rochester, NY, USA

A 74-year-old man presented to the cardiology office with exertional dyspnea. Transthoracic echocardiography showed mild left ventricular (LV) dilation, LV hypertrophy, LV ejection fraction 50%, mitral valve prolapse and bicuspid aortic valve. Stress echocardiography was nonrevealing. Coronary angiography showed non-obstructive coronary artery disease. Cardiac magnetic resonance imaging was performed, and showed a 9.1 mm atrial displacement of the posterior mitral valve leaflet at the hinge point during systole; the finding was consistent with mitral annulus disjunction (Fig. 1A, **Suppl. Video 1**). Cardiac magnetic resonance imaging also showed spongy/noncompacted myocardium in the LV, with a noncompaction-to-compaction ratio of 1.86 during end-diastole (Fig. 1B). Late gadolinium enhancement images did not show myocardial fibrosis or presence of LV thrombus. 24-hour Holter monitoring showed occasional premature ventricular complex, but no ventricular tachycardia.

Mitral annulus disjunction and LV noncompaction are rare arrhythmogenic cardiac anomalies. Mitral annulus disjunction is most commonly seen in patients with mitral valve prolapse. Mitral annulus disjunction distance > 8.5 mm, and myocardial fibrosis of LV papillary muscles and basal inferior wall are high risk features for ventricular arrhythmias. For patients with LV noncompaction, LV systolic impairment is associated with increased risk of sudden cardiac death. Competitive sports should be refrained in individuals with LV noncompaction and systolic impairment.

According to the current guidelines, implantable-cardioverter defibrillator is not indicated in patients with mitral annulus disjunction or LV noncompaction unless there is a history of sustained ventricular tachycardia, ventricular fibrillation, or aborted sudden cardiac death. To our best knowledge, this is the first reported case describing a patient with concomitant mitral annulus disjunction and LV 'spongy' noncompaction-like myocardium on cardiac magnetic resonance imaging.

Conflict of interest: None declared

Address for correspondence: Bryan E-Xin Tan, MD, 1425 Portland Avenue, Rochester, NY, 14621, USA, tel: +1(585)922-4365, e-mail: Bryan.Tan@rochesterregional.org

Received: 25.04.2020 Accepted: 5.05.2020

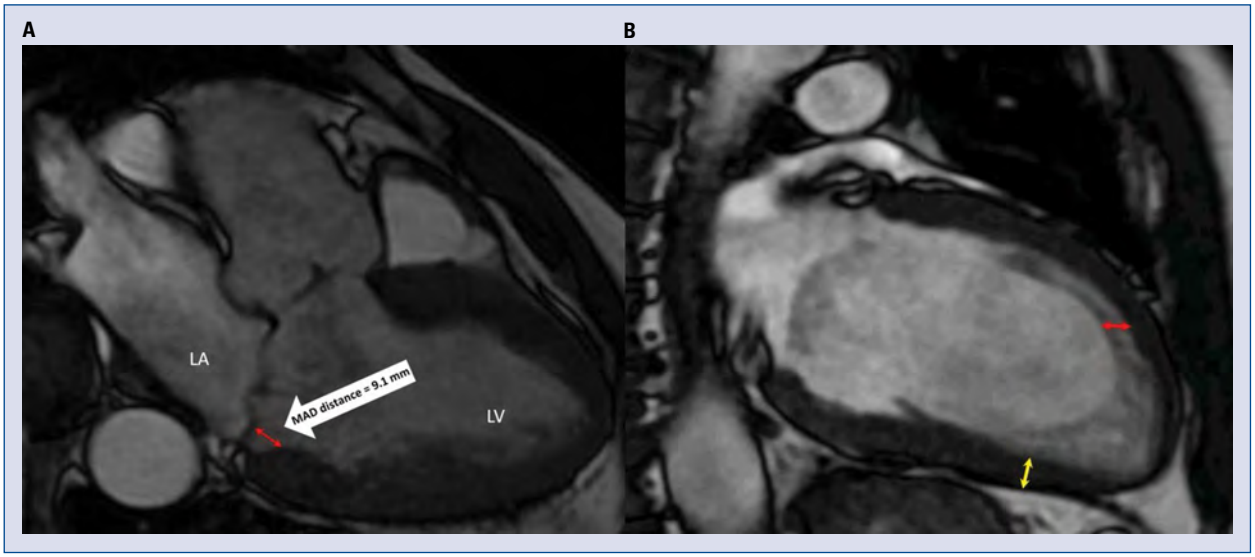

Figure 1. A. Cardiac magnetic resonance imaging (MRI) showed mitral annulus disjunction (MAD) with MAD distance of 9.1 mm during systole (red arrow); **B.** Cardiac MRI showed noncompacted myocardium at the apical cap, all apical segments, and mid-lateral wall with noncompacted to compacted myocardial thickness ratio of 1.86 during end-diastole. Red arrow — noncompacted myocardium; yellow arrow — compacted myocardium; LA — left atrium; LV — left ventricle.

VIA MEDICA

IMAGE IN CARDIOVASCULAR MEDICINE

Cardiology Journal
2020, Vol. 27, No. 3, 325–326
DOI: 10.5603/CJ.2020.0086

ISSN 1897–5593

Diagnosis of large, mobile thrombus in transit within a patent foramen ovale by echocardiography

Jong-Ho Nam, Jong-Seon Park

Division of Cardiology, Department of Internal Medicine, Yeungnam University Medical Center, Daegu, Republic of Korea

An 80-year-old woman was admitted for pulmonary embolism (PE; Fig. 1A), and deep vein thrombosis (DVT; Fig. 1B), and intravenous heparin was started. The next day, she was found to have right thumb motor weakness. Brain magnetic resonance imaging showed acute cerebral infarction of the left precentral gyrus, which is the hand motor area (Fig. 1C). Transthoracic echocardiography with contrast (Definity®) showed large, mobile masses in atria without contrast enhancement, suggesting thrombi (Fig. 1D–F, **Suppl. Video 1**). Transesophageal echocardiography visualized a thrombus traversing through a patent foramen ovale (PFO) from right to left atrium (Fig. 1G); agitated saline test demonstrated large right-to-left interatrial shunt (Fig. 1H). Surgical treatment was planned but follow-up echocardiography revealed that the thrombus size had decreased. Neurologic examination showed no neurologic deficit except previously observed right thumb motor weakness. After discharge and 3 months of follow-up under oral anticoagulant, there was no visible thrombus by transesophageal echocardiography. Considering paradoxical embolism and large right-to-left shunt, percutaneous transcatheter PFO closure was performed (Figulla Flex-II PFO Occluder®; Fig. 1I).

In the setting of PE and elevated pulmonary arterial pressure, foramen ovale can become patent and trap a thrombus during its passage from the right to the left atrium. This thrombus in transit, impending paradoxical embolism, is rare and has a high mortality rate. Therefore, it should be suspected in patients who have unexplained systemic embolisms complicating DVT and PE. In such cases, echocardiography helps diagnose a right-to-left interatrial shunt and visualizes a thrombus in transit within a PFO.

Acknowledgements

This work was supported by 2020 Yeungnam University Research Grant.

Conflict of interest: None declared

Address for correspondence: Jong-Seon Park, MD, PhD, Division of Cardiology, Department of Internal Medicine, Yeungnam University Medical Center, 170 Hyeonchung-ro, Nam-gu, Daegu, 42415, Republic of Korea, tel: +82-53-620-3847, fax: +82-53-621-3310, e-mail: pjs@med.yu.ac.kr

Received: 19.04.2020 Accepted: 17.05.2020

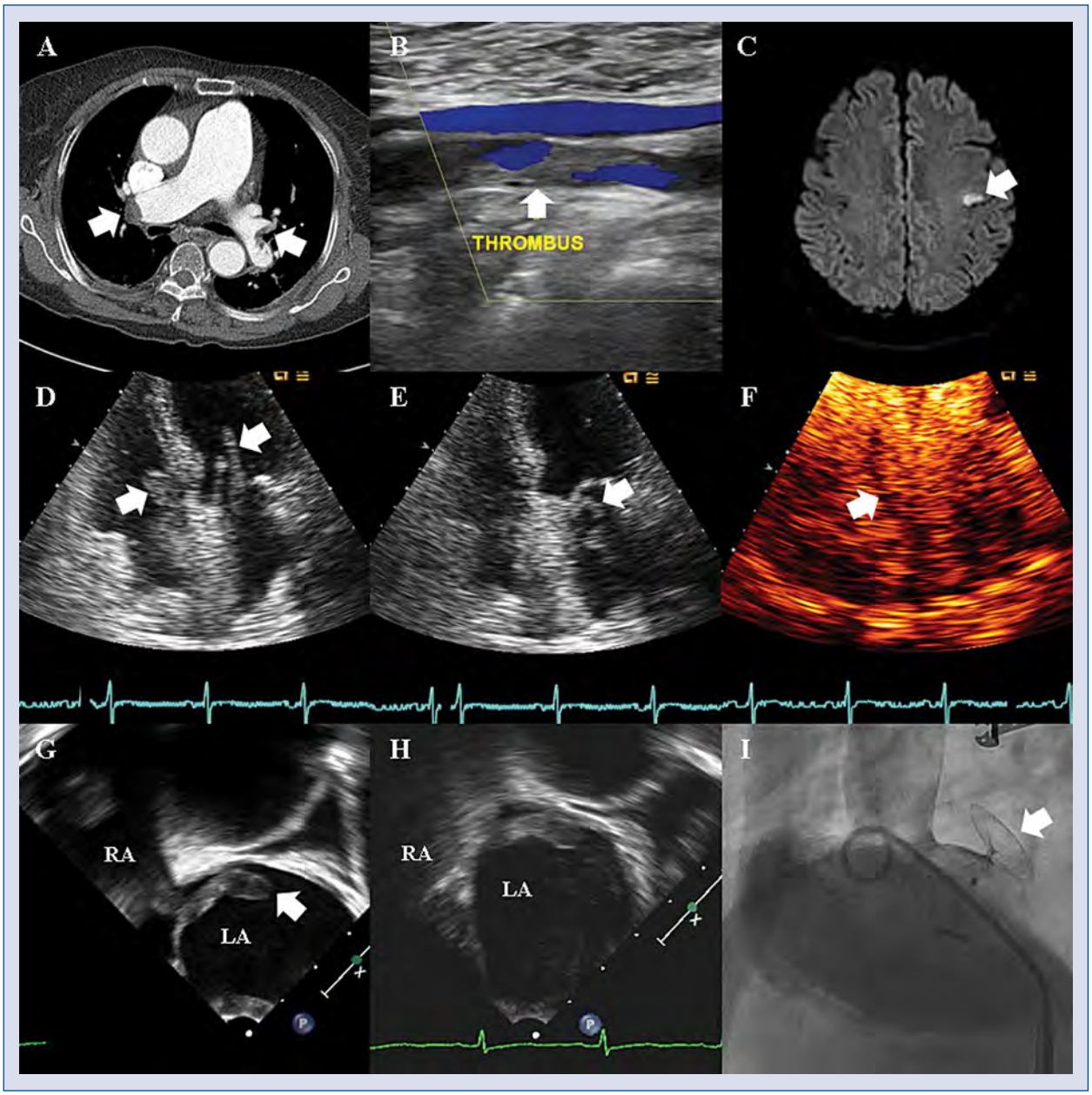

Figure 1. A. Chest computed tomography showing multiple filling defects (arrows) in both pulmonary arteries; **B.** Vascular duplex scan shows deep vein thrombosis (arrow) in the left popliteal vein; **C.** Brain magnetic resonance image showing acute cerebral infarction (arrow) of the left precentral gyrus; **D–F.** Apical 4-chamber transthoracic echocardiography shows large, mobile masses (arrows) in both atria at diastole (**D**) and systole (**E**), which were not enhanced by contrast (**F**); **G.** Mid-esophageal bicaval view of transesophageal echocardiography (TEE) shows a thrombus (arrow) in transit within the patent foramen ovale (PFO); **H.** Mid-esophageal bicaval view of TEE with agitated saline test confirming a large right-to-left shunt through the PFO; **I.** Fluoroscopy shows the transcatheter PFO occluder (arrow) placed successfully by intracardiac echocardiography and fluoroscopy; LA — left atrium; RA — right atrium.

VIA MEDICA

LETTER TO THE EDITOR

Cardiology Journal
2020, Vol. 27, No. 3, 327–328
DOI: 10.5603/CJ.a2020.0066

ISSN 1897–5593

Dilemmas in resuscitation of COVID-19 patients based on current evidence

Lukasz Szarpak[1], Kurt Ruetzler[2], Marek Dabrowski[3], Klaudiusz Nadolny[4], Jerzy R. Ladny[5], Jacek Smereka[6], Milosz Jaguszewski[7], Krzysztof J. Filipiak[8]

[1]Lazarski University, Warsaw, Poland; Polish Society of Disaster Medicine, Warsaw, Poland
[2]Departments of Outcomes Research and General Anesthesia, Anesthesiology Institute, Cleveland Clinic, Cleveland, Ohio, United States
[3]Chair and Department of Medical Education, Poznan University of Medical Sciences, Poznan, Poland
[4]Department of Emergency Medical Service, Higher School of Strategic Planning in Dabrowa Gornicza, Dabrowa Gornicza, Poland
[5]Clinic of Emergency Medicine, Medical University of Bialystok, Poland; Polish Society of Disaster Medicine, Warsaw, Poland
[6]Department of Emergency Medical Service, Wroclaw Medical University, Wroclaw, Poland; Polish Society of Disaster Medicine, Warsaw, Poland
[7]1st Department of Cardiology, Medical University of Gdansk, Poland
[8]1st Chair and Department of Cardiology, Medical University of Warsaw, Poland

This paper was guest edited by Prof. Łukasz K. Czyżewski

The authors of the present article read a recent article by Shao et al. [1] published in the Resuscitation Journal with interest. Indeed, since the beginning of the severe acute respiratory syndrome coronavirus 2 (SARS-CoV-2) epidemic, there have been 2,435,876 infected patients confirmed, with an observed level of mortality of nearly 8%. The study by Shao et al. [1] is of considerable importance as it is the first to present the survival of COVID-19 patients after in-hospital cardiac arrest. The authors both characterized the patients and compared a number of factors that may affect the return of spontaneous circulation, as well as 30-day survival.

In an extreme situation, such as a prevailing pandemic, extraordinary methods should be applied [2]. The decisions taken may often conflict with the general principle of "first do no harm" and with its intrinsic ethical values; however, medical personnel should take into account not only their patient, but also their own safety, as well as the safety of their other patients, families, and colleagues [3]. As in the case of SARS and MERS, the primary route of spreading COVID-19 is the droplet or direct contact pathway [4, 5]. It is worth remembering that HCoV-SARS, HCoV-MERS, and SARS-CoV-2 can also be transmitted via environmental vectors [6]. Therefore, when contacting a patient with suspected or, particularly, confirmed COVID-19, medical personnel should use personal protective equipment for aerosol generating procedures and all procedures regarding such a patient, including resuscitation, which should be performed in airborne infection isolation rooms.

Wang et al. [7] indicated that the time from the disease onset to death was shorter in people over 70 years of age compared with younger patients (11.5 and 20 days, respectively). Yang et al. [8] observed that in COVID-19 patients, comorbidities and diagnosed underlying diseases, including hypertension and respiratory system and cardiovascular diseases, may constitute risk factors for severe compared with the non-severe course of COVID-19. These results were confirmed in a study by Shao et al. [1], in which cardiac arrest

Address for correspondence: Lukasz Szarpak, Assoc. Prof. PhD, Lazarski University, ul. Świeradowska 43, 02–662 Warszawa, Poland, tel: +48 500186225, e-mail: lukasz.szarpak@gmail.com

Received: 28.04.2020 Accepted: 7.05.2020

in people over 60 years of age was associated with a higher risk of death; similarly, the risk of hypertension, the most common coexisting disease in this group, increased with age. The higher risk of death in the elderly with COVID-19 may be associated with impaired immune response, which is further reduced by the effect of coronavirus.

Shao et al. [1] also referred to two important issues. Firstly, patients with COVID-19 pneumonia should be monitored in intensive care units, which, compared with general wards, provide a higher chance of survival. Secondly, the survival of patients with non-shockable rhythms is below 0.8%; this, considered herein, is the most important concern. In this context, a question arises whether cardiopulmonary resuscitation should be conducted in each patient with COVID-19, exposing medical personnel and their closest associates, or, in the case of elderly patients with initial non-shockable rhythms, resuscitation should not be undertaken. The answer to this question should be established through discussions in individual therapeutic teams.

Conflict of interest: None declared

References

1. Shao F, Xu S, Ma X, et al. In-hospital cardiac arrest outcomes among patients with COVID-19 pneumonia in Wuhan, China. Resuscitation. 2020 [Epub ahead of print]; 151: 18–23, doi: 10.1016/j.resuscitation.2020.04.005, indexed in Pubmed: 32283117.
2. Dzieciatkowski T, Szarpak L, Filipiak KJ, et al. COVID-19 challenge for modern medicine. Cardiol J. 2020; 27(2): 175–183, doi: 10.5603/CJ.a2020.0055, indexed in Pubmed: 32286679.
3. Ruetzler K, Szarpak L, Filipiak K, et al. The COVID-19 pandemic — a view of the current state of the problem. Disaster Emerg Med J. 2020, doi: 10.5603/demj.a2020.0015.
4. Smereka J, Szarpak L, Filipiak K. Modern medicine in COVID-19 era. Disaster Emerg Med J. 2020, doi: 10.5603/demj.a2020.0012.
5. Szarpak L, Smereka J, Filipiak KJ, et al. Cloth masks versus medical masks for COVID-19 protection. Cardiol J. 2020; 27(2): 218–219, doi: 10.5603/CJ.a2020.0054, indexed in Pubmed: 32285928.
6. Smereka J, Szarpak L. The use of personal protective equipment in the COVID-19 pandemic era. Am J Emerg Med. 2020 [Epub ahead of print], doi: 10.1016/j.ajem.2020.04.028, indexed in Pubmed: 32305157.
7. Wang W, Tang J, Wei F. Updated understanding of the outbreak of 2019 novel coronavirus (2019-nCoV) in Wuhan, China. J Med Virol. 2020; 92(4): 441–447, doi: 10.1002/jmv.25689, indexed in Pubmed: 31994742.
8. Yang J, Zheng Ya, Gou Xi, et al. Prevalence of comorbidities in the novel Wuhan coronavirus (COVID-19) infection: a systematic review and meta-analysis. Int J Infect Dis. 2020 [Epub ahead of print]; 94: 91–95, doi: 10.1016/j.ijid.2020.03.017, indexed in Pubmed: 32173574.